Optimal Power Flow and Pricing Mechanism for Bipolar DC Distribution Grids

Robin Guarnotta

Master of Science Thesis

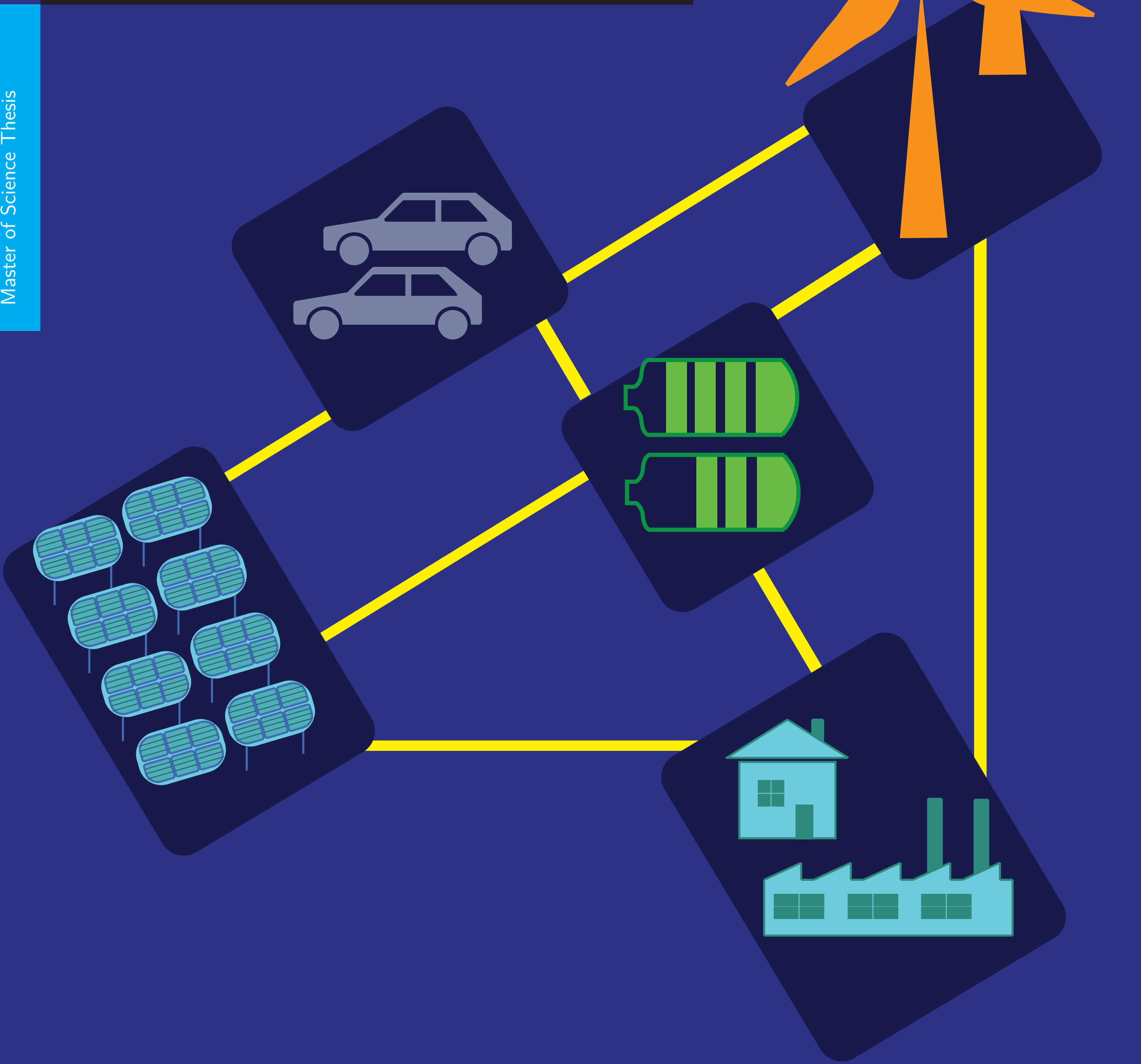

TU Delft Delft University of Technology

Challenge the future

Optimal Power Flow and Pricing Mechanism for Bipolar DC Distribution Grids

by

Robin Guarnotta

Master of Science

in EWI

For the degree of Mater of Science in Sustainable Energy Technology
at the Delft University of Technology

To be defended publicly on Tuesday November 15, 2016 at 14:00.

Supervisor:	Dr. ir. L.M. Ramirez Elizondo
Advisor:	L.J. Mackay
Thesis committee:	Prof. dr. Eng. P. Bauer
	Dr. ir. L.M. Ramirez Elizondo
	Dr. ir. M. Cvetkovic

Delft University of Technology

Acknowledgments

I would like to thank my PhD supervisor Laurens Mackay for this opportunity and his support throughout my thesis. His guidance and motivation were valuable from the beginning to the end of the project. Thanks to him I acquired many new skills and knowledge about the planning and optimization of electrical networks.

I would also like to mention that the core of the model, Chapter 3, is the result of a collaboration with Laurens MacKay, Anastasios Dimou and German Morales-Espania. Laurens formulated the power flow equations while Anastasios founded that basis of the model in GAMS as well as the interface required for the input data. The modeling expertise of German Morales-Espania has proved to be very useful to develop a robust model.

Finally, I would like to thank my family for their support during the entire duration of my thesis. Without them I would not be where I stand today. A warm thank you to my close friends for their presence.

Robin Guarnotta

Abstract

The fast advances of renewable energy technologies lead to an increasing amount of distributed energy resources. Most are inherently DC or have a DC link which re-opens the AC vs. DC distribution systems discussion. The deployment of Distributed Generators (DG) units and Energy Storage System (ESS) at the consumption level presents opportunities and challenges. Low Voltage Direct Current (LVDC) distribution systems can potentially increase power quality, reliability and efficiency. As opposed to AC grids, it offers the possibility of meshing distribution grids to increase the amount of paths without converting voltage to a higher or lower levels. Additionally, the affordability of DG and storage units promotes market participation from prosumers. As a result new market models based on real-time pricing could encourage the use of energy when available as well as revealing investment opportunities with regards to renewable sources or ESS in an effort to increase reliability. Distribution grids are expected to be more subject to congestions as a consequence of the rising penetration of DG and electric vehicles. A market closely linked to the physics of distribution systems should be developed to reflect congestions and losses in electricity prices.

The main contribution of this master thesis is twofold, an Optimal Power Flow (OPF) specifically designed for bipolar DC distribution grids is presented and used to construct a locational pricing mechanism. In comparison to unipolar DC distribution grids, the bipolar configuration offers twice the power capacity while the total losses remain the same if the system is balanced. Instead of the traditional formulation in terms of power, the power flow is modeled in terms of voltages and currents, it is subject to the physical limitations of the network. The grid is thus modeled following circuit physical laws guaranteeing an exact OPF for which the solution is always physically feasible. Using this methodology the utilization of renewable energy sources is optimized and the system's production cost minimized. Electricity prices, or Locational Marginal Prices (LMP), are directly obtained from the OPF for each location in the network. It follows that the losses and congestions are reflected in these prices. LMP can differ from the positive to negative polarity if the system is asymmetrical or in the presence of partial congestion. When large asymmetrical loading occurs, LMP were found to be negative which can be interpreted as an incentive to balance the grid. Furthermore, nodal prices can be used as indicators to reflect financial motivations to better utilize DG units.

In Chapter 4, the model is extended to a multi-period problem enabling the control of ESS. Using demand, solar and wind profiles the OPF and LMP are computed for each period to allow for energy management and a better utilization of renewable energies. Demand side management is incorporated in the model by assigning an indicator reflecting the willingness of users to purchase electricity. Under the assumption that renewable energies have a zero marginal cost of production, electricity prices are derived from the demand side and loads are shedded according to the willingness indicator and the energy availability. Using a series of examples the role of storage in alleviating electricity prices is shown. In Chapter 5 the model is further developed as a design tool able to site and size ESS in an effort to maximize the utilization of renewable energies and to manage congestions. The price of storage units is used to reflect the investment cost of ESS. Using mixed-integer programming the optimal location and capacity of storage are obtained. However, this approach results in physically impossibilities as the optimal battery size most often do not match with the capacity of commercially available batteries. The model should be improved to find an optimal feasible solution.

Developing countries are interesting due to their poor electrical infrastructure. The barriers to move towards DC systems is lower which offers the opportunity to leapfrog AC distribution. In Chapter 6 a case study based on a district of a village in Senegal is used to assess the validity of the model. The case study is divided in three sub-cases to demonstrate the impact of asymmetries as well as the role of storage. Finally the last part of the thesis presents a business model for the commercialization of a bipolar DC microgrids for rural electrification in developing countries. Such system has never been implemented in the context of access to electricity. The technology and pricing mechanisms are believed to be key assets to contribute to the social welfare of remote communities.

Contents

List of Figures

List of Tables

ACRONYMS

ABC Model Anchor-Business-Community Model.

AC Alternating Current.

AC OPF Alternating Current Optimal Power Flow.

DC Direct Current.

DC OPF Direct Current Optimal Power Flow.

DERM Distrbuted Energy Resource Management System.

DG Distributed Generators.

DLMP Distribution Locational Marginal Prices.

ESS Energy Storage System.

GSF Generation Shift Factor.

HVAC High Voltage Alternating Current.

HVDC High Voltage Direct Current.

KCL Kirchhoff's current law.

LF Marginal Loss Factor.

LMP Locational Marginal Prices.

LVAC Low Voltage Alternating Current.

LVDC Low Voltage Direct Current.

OPF Optimal Power Flow.

PV Phovoltaic.

RE Renewable Energies.

SHS Solar Home Systems.

Nomenclature

Indices

k	Time periods
m	Nodes of the bipolar network
n	Alias of m. Nodes of the bipolar network
s	Sources, loads and ESS conneced across a pair of nodes. Used to differentiate multiple generators, loads or ESS connected across the same pair of nodes

Sets

$(m,n) \in \mathscr{G}$	Pair of nodes connecting defined branches/distribution lines
$(m,n) \in \mathscr{P}$	Pair of nodes connecting at least one generator, load or ESS
$(m,n,s) \in \mathscr{F}$	ESS connected to a pair of nodes for which capacity is defined by a parameter
$(m,n,s) \in \mathscr{L}$	Generators and loads connected to a pair of nodes
$(m,n,s) \in \mathscr{V}$	ESS connected to a pair of nodes for which capacity is defined by a parameter. Used for optimal size and placement of ESS
$\mathscr{B} = \mathscr{F} \cup \mathscr{V}$	All fixed and variable ESS connected to a pair of nodes
$\mathscr{N} = \mathscr{N}_{+} \cup \mathscr{N}_{-} \cup \mathscr{N}_{\mathrm{N}}$	All nodes of the bipolar grid
$\mathscr{S} = \mathscr{L} \cup \mathscr{F} \cup \mathscr{V}$	Generators, loads or ESS connected to a pair of nodes
$m,n \in \mathscr{N}$	Nodes of the bipolar grid
$m,n \in \mathscr{N}_{+}$	Positive polarity nodes
$m,n \in \mathscr{N}_{\mathrm{N}}$	Neutral polarity nodes
$m,n \in \mathscr{N}_{-}$	Negative polarity nodes

Parameters

$\eta^{\mathrm{ESS}}_{m,n,s}$	Charging and discharging ESS efficiency
$\eta^{\mathrm{S}}_{m,n,s}$	Solar panels conversion efficiency
$\Pi^{\mathrm{ESS}}_{m,n,s}$	Investment cost of variable capacity ESS [\$/Wh]
$\Pi^{\mathrm{S}}_{m,n,s}$	Marginal cost of generators and loads [\$/Wh]
$A^{C}_{m,n}$	Cross section area of distribution cables [m^2]
$A^{S}_{m,n,s}$	Area of solar panels [m^2]
$E^{\mathrm{ESS}}_{m,n,s,\max}$	Maximum energy content of fixed ESS (ESS capacity) [Wh]
$E^{\mathrm{ESS}}_{m,n,s,\min}$	Minimum energy content of fixed ESS [Wh]
$G_{m,n}$	Branch conductance [Ω^{-1}]

$I^{\mathrm{S}}_{m,n,s,k,\max}$	Maximum current of generators, loads and ESS [A]
$I^{\mathrm{S}}_{m,n,s,k,\min}$	Minimum current of generators, loads and ESS [A]
$I_{m,n,\max}$	Maximum branch current [A]
$I_{m,n,\min}$	Minimum branch current [A]
$P^{\mathrm{S}}_{m,n,s,k,\max}$	Maximum power of generators, loads and ESS [W]
$P^{\mathrm{S}}_{m,n,s,k,\min}$	Minimum power of generators, loads and ESS [W]
$S^{\mathrm{ESS}}_{m,n,s,\max}$	Maximum capacity of variable ESS [Wh]
$S^{\mathrm{ESS}}_{m,n,s,\min}$	Minimum capacity of variable ESS [Wh]
$U_{+,\max}$	Maximum node voltage for positive pole [V]
$U_{+,\min}$	Minimum node voltage for positive pole [V]
$U_{-,\max}$	Maximum node voltage for negative pole [V]
$U_{-,\min}$	Minimum node voltage for negative pole [V]
$U_{\mathrm{N},\max}$	Maximum node voltage for neutral conductor [V]
$U_{\mathrm{N},\min}$	Minimum node voltage for neutral conductor [V]

Variables

$\lambda^{\mathrm{I}}_{m,k}$	LMP for node m in terms of current [$/Ah]
$\lambda^{\mathrm{P}}_{m,n,k}$	LMP for node pair m,n in terms of power [$/Wh]
$b_{m,n}$	Binary variable indicating location of variable capacity ESS
$c^{\mathrm{I}}_{m,k}$	Current injection cost at node m [$]
$c^{\mathrm{P}}_{m,n,k}$	Power injection cost between nodes m,n [$]
$e_{m,n,s,k}$	Energy content of ESS [Wh]
$i^{\mathrm{S}}_{m,n,k}$	Current of all generators connected across a set of nodes [A]
$i^{\mathrm{S}}_{m,n,s,k}$	Current of sources, generators output a negative current (−) and loads output a negative current (+) [A]
$i_{m,k}$	Current at node m, going from the source layer to the resistive network [A]
$i_{m,n,k}$	Current of a branch connecting node pair m,n [A]
$p^{\mathrm{S_{charge}}}_{m,n,s,k}$	Charging power of ESS (+) [W]
$p^{\mathrm{S_{discharge}}}_{m,n,s,k}$	Discharging power of ESS (−) [W]
$p^{\mathrm{S}}_{m,n,s,k}$	Current of sources, generators output a negative current (−) and loads output a negative current (+) [W]
$s_{m,n,s}$	Capacity of variable ESS [Wh]
$u_{m,k}$	Voltage of node m [V]

I

OPF for Bipolar DC Distribution Grids

1

INTRODUCTION

The end of the 19th century witnessed a debate which outcome dictated the standards of power transmission and distribution. The War of Currents opposed Thomas Edison to George Westinghouse, respectively promoting Direct Current (DC) and Alternating Current (AC). AC won the battle and became the worldwide standard for electrical power systems. The main reason that dictated this choice was mainly the invention of AC transformers capable of adjusting voltages and reducing line losses [9]. The growing use of poly-phase AC machines, relying on fossil energies, as an alternative to DC machines also contributed to the global acceptance of AC systems for generation, transmission and distribution [10]. However, these reasons are nowadays less obvious and not coherent with progresses in power electronic and energy generation. Indeed, the main disadvantage of AC networks is their inability to ensure reliable power supplies in the presence of distributed energy resources.

1.1. WHY LVDC?

INDUSTRIES RELYING ON DC SYSTEMS

Although AC transmission and distribution systems dominate, DC electrical networks have some applications in which DC is preferred. Currently High Voltage Direct Current (HVDC) is being used for long distance transmission [11]. Above the break-even distance losses and costs associated with DC lines are lower [12, 13]. Data centers have sensible loads that cannot be interrupted, some rely on DC networks to gain in stability. Furthermore, DC is widely used in the automotive industry to distribute energy to electric equipments in vehicles. Lastly for the operation of isolated systems the aerospace and telecom industries have adopted DC systems for their reliability at low costs [10, 14].

ADVANTAGES OF LVDC

Low Voltage Direct Current (LVDC) for distribution and residential purposes is becoming more and more accepted and it makes sense. The advantages of such distribution systems outweighs all of the above mentioned reasons that led to AC. A comparative representation of the two competing systems is represented in Figure 1.1 [1]. Switching to LVDC significantly decreases the number of conversions in consumer's devices, Renewable Energies (RE) and Energy Storage System (ESS). Higher efficiencies are obtained due to the absence of reactive power, skin effects and AC/DC conversions [15].

The invention of the power transistor has been a milestone achievement in electronics. It allowed for the transformation of DC voltages and initiated progresses made in computers and communication [9]. Consumer electronic devices rely on DC and are nowadays more and more equipped with DC/DC converters instead of AC transformers. These appliances first rectify the current to DC before adjusting voltage values.

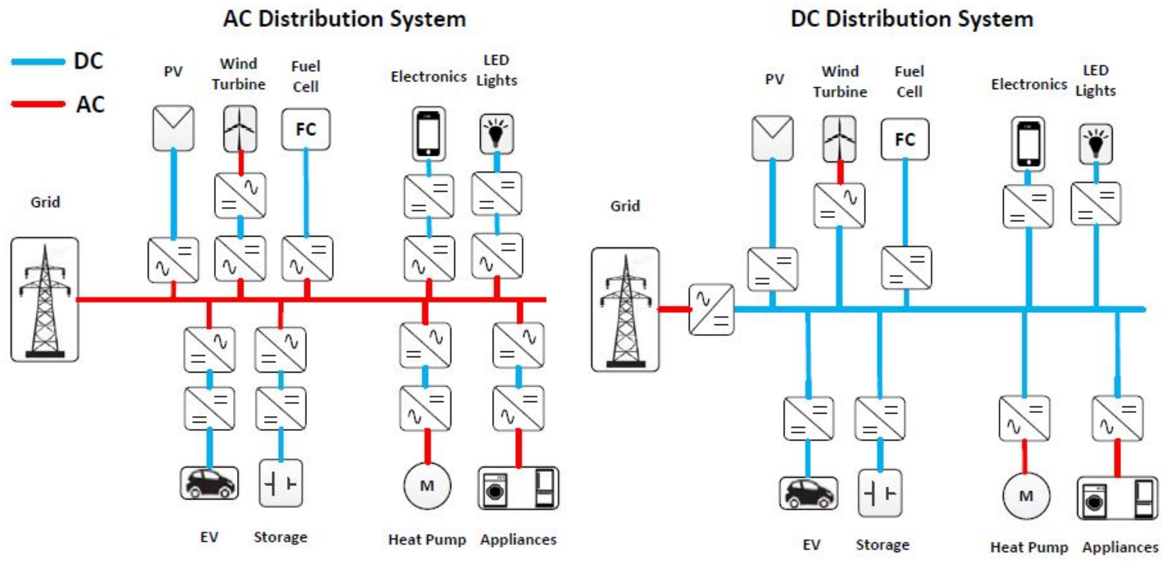

Figure 1.1: AC and DC distribution systems comparison including conversion steps for different loads and sources by Rodriguez *et al.* [1].

As opposed to older devices, sizes, weights and costs are considerably reduced [13]. It also offers a good reason to switch to LVDC which would allow to by-pass the rectification step and lower power losses. Additionally, decreasing the number of components in devices improve their reliability. Already many loads in a building are DC loads [1, 10], electric vehicle will most likely increase this value.

DC ready devices are essential to ensure a transition towards LVDC. Appliances must have the ability to operate normally under such conditions. Devices able to function on both AC and DC would guarantee a smooth transition. However, the rectification step should be by-passed [16]. Several studies assess the compatibility of appliances in a DC network [16, 17]. Typical residential loads were tested such as lighting systems, devices with an external adapter (e.g. notebook computer), devices with built-in switching mode supply (e.g. TV set), motor drives (e.g refrigerators, air conditioning). All of these appliances operated correctly when tested in an LVDC network. In most cases, integrated DC/DC converter do not need to be resized [18]. The limiting factor is the devices' voltage ratings rather than by-passing the AC/DC converter. The ability of internal components to handle wide voltage ranges depends on the devices itself. Network standards should be decided according to these ratings. Therefore, in theory most devices are DC ready and should be able to operate correctly in LVDC operation.

Power consumption of consumer's electronic is constantly decreasing. Many devices are now powered using USB ports. It is foreseen that building and residences will most likely host DC networks, hence the amount of AC/DC converters would considerably decrease [19]. The recent introduction of the USB Type-C connector and new power delivery standards provides the necessary requirements to introduce LVDC networks. Up to 100W can be delivered, devices with higher power requirements such as computers or TV sets can rely on USB charging. Additionally, USB Type-C connectors enables Internet connection and data transfer [20].

The rise of RE in our energy mix is a considerable incentive to LVDC. Most renewable resources (e.g. photovoltaic, fuel cells) and ESS (e.g. batteries, electrical vehicles) are inherently DC. Even wind turbines which naturally generate an alternating current could benefit from a DC distribution system. A DC link is in any case used to decouple rotation and grid frequency. Integrating RE in an AC grid requires a conversion step from DC to AC. In addition to losses associated to rectification, grids are not designed to fully utilize RE. LVDC could act as a driver towards a greener energy mix.

Barriers to the Implementation of LVDC

Why is LVDC not implemented? The transition is large and delicate, mainly because networks are designed according to AC criteria. The costs associated to replacing an AC distribution network to DC are large, most especially in developed countries were access to electricity is established since a long time. However, there are opportunities in large cities were the network is close to reach full capacity and in developing countries were no AC network is in place. Emerging nations have the opportunity to leapfrog AC distribution. Although many devices are DC compatible, the industry standards still rely on AC, we observe a chiken-and-egg problem. Quoting Mackay *et al.*, "*The lack of available DC devices hinders the implementation of small DC grids while the lack of DC grids prevents manufacturers from building DC devices*" [19]. Standardization is primordial, several agencies such as Emergence Alliance, European Telecommunications Comission, IEEE, IEC and others are working on it [1]. Such standard or state-of-the-art should include faster protection schemes. Indeed protection for LVDC is technical issue that is still to be tackled in order to guarantee safety.

1.2. Rethinking the System

High capital costs (e.g. power plants, long distance transmission lines) and high energy prices due to our dependency on fossil fuels constraint our energy system [21]. Considering the aging infrastructure and global warming awareness, it is the right time to rethink our structure and meet the growing energy demand. Distributed generation offer an attractive solution, especially due to competing prices of RE. Here the key elements of the transition towards networks adapted to the penetration of DG are discussed.

Meshed Grids for the Integration of DG

Rethinking our architecture is key to make the most out of DG. Traditionally networks are radial and follow a top-down vertical structure starting from centralized generators and stepping down to lower voltages to finally feed our residential appliances. Consequently, power flows are unidirectional. Radial structures have proved to be efficient and reliable in absence of DG, moreover the operation of such networks is relatively simple and economical [22]. The balance between demand and supply is managed at the supply side where the energy output is either increased or decreased. Such architecture are not adapted for the integration of RE based DG as they would most likely suffer from unstable voltage profiles and poor control over local generation [23].

A transition towards meshed architecture is expected as it can facilitate the penetration of DG. Increasing the interconnections between DG in a distribution system present multiple advantages. It can reduce overall losses, ameliorate the voltage profiles and increase reliability as well as flexibility [22, 24]. Most importantly, it can result in a better balance of power flows by increasing the number of paths that power can take in an effort to limit congestions and system failures. Meshed architectures are thus inevitable to efficiently enhance power flow capacities in distribution networks [24, 25].

Smart Grids and ESS for the Integration of DG

In traditional systems power generators are on the transmission level and often far from demand centers, the power flow is inherently unidirectional. Disturbances on the load side are harder to manage for operators, the system is passive. The greater deployment of DG on the low and medium voltage level should change how these disturbance can be addressed thanks to enhanced control of DG [21]. By increasing the interconnection of DG, power flows can be bidirectional and generation can be locally managed by power controllers, the system becomes active.

The smart grid concept as emerged as a consequence of the rise of RE. It enables active management of the network using digital technologies to manage the energy flow from DG to meet the electricity demand at any given time [26]. It will inevitably allows to coordinate capacities between the different elements of the network. Developing these grids is currently a priority for the energy sectors, already many companies and energy utilities are working together to deviate from the traditional power systems. For the deployment of smart grids the following technologies play a key role: power electronics for generation control and information, communication and control technologies for the network operation [26, 27]. In such a grid, the optimization of resources is achieved by connecting all the agents using information, communication and control. It enables the optimization of RE by storing and allocating power to ESS and variable loads in an effort to reduce the impact of intermittency. Moreover, the access of real-time data is a key element to the energy market as it enables active market participation and dynamic pricing [21]. Implementing demand response protocols such as load shedding in case of under voltage makes networks more stable [18]. Another advantage of such grids is the ability for each voltage level to function alone regardless of faults of different levels, reliability is improved.

Energy storage is a key element in future electricity networks. It solves the intermittency limitation of RE and increase the variability in generation and demand. Hence, it can contribute to the flexibility of grids [26, 27]. While Phovoltaic (PV) panel generate during hours of sunlight most of the energy is consumed at night. Batteries are the energy buffers needed to adjust mismatch between supply and demand [19]. ESS also serve has a voltage and frequency stabilizer [28]. Storage systems could play a role at any level, from the devices level to the distribution level. In residences batteries increase the system efficiency [1]. By storing energy during peak production when prices are low and using this energy during peak consumption consumers save money and reduce stresses on the network at times when it is the most sensible.

The rise of electric vehicles will most likely impact the energy system of the future. Given that charging stations' availability is expected to increase, electric vehicles can act as a mobile storage system enabling a new approach to energy management. Smart grids and electric vehicles have the ability to interact with each other. Traditionally the interaction is from the grid to the vehicle (G2V) where vehicles consume energy from the network to charge their batteries. However, another possible interaction is from the vehicle to the grid (V2G) where electricity is withdrawn from the vehicle's battery to the grid. In other words, electric vehicles can act as mobile DG that might partially satisfy the demand of energy intensive workplace during the day. It is foreseen that the deployment of electric cars can help reducing the cost of energy [26, 27].

1.3. LVDC STANDARDIZATION AND CONFIGURATIONS

VOLTAGE STANDARDS

Standardization is truly needed to encourage development of LVDC microgrids. Currently there are no voltage standards and different voltages are used in certain applications. In the telecommunication industry, off-grid stations rely on -48V [19]. Although operating a system under 24V or 48V is advantageous since batteries and small devices can directly be connected to the grid without converters it makes the system rigid. It causes circulating currents and controlling voltages at common bus is nearly impossible [9]. Furthermore, small voltage levels (e.g. 12V, 24V, 48V) are inefficient for larger networks with high power and long distances.

Higher voltage values for distribution network are preferred. A value between 350V and 400V is expected to be standardized for LVDC [19]. Most researches converge to 380V as it matches industry standard for consumer electronics, it is also the level used in data centers. At this level we obtain the best efficiency gain over AC [9]. The current in 380V is 61% the real current in 230V AC and conduction losses are 36% of the AC network [29]. Thus, using this voltage cables can be made smaller and cheaper. Similarly to the European AC distribution network operating at 230V, a DC distribution grid of 380V with converter stepping down the voltage for appliances is envisioned. DC architectures relying on this level are in development and should be soon implemented [9].

NETWORK CONFIGURATION

Different arrangements for DC distribution networks are considered. Power can either be distributed in a monopolar, unipolar and bipolar configuration. In monopolar systems use a high voltage conductor and a ground return. This set-up is mostly used for HVDC, however it is prohibited in some countries due to the potential risks of corrosion induced by ground current. It is common to operate such system with a negative polarity to reduce the corona effect [21]. Although it is the simplest and most cost effective arrangement, due to safety consideration monopolar LVDC is not the preferred setup.

In the unipolar configuration, the current flows between the positive and negative conductors while the bipolar configuration consists of two connectors with opposite polarities (positive and negative) and a ground return line. There are several advantage of using this arrangement. When loaded symmetrically the current is the same in both poles the neutral current is then zero and the system is safer. Loads can be connected in two different configurations, they can be connected between either of the polarity and the ground return or between both polarities in which case transmission capacity is increased [2]. Voltage level can be reduced while being able to connect appliances with larger power requirement between the two poles. The system becomes safer, line losses are halves and the cables are cheaper since less copper is required [30]. In case of a fault in one line energy can still be supplied making the system more reliable [1, 31]. However, complications might arise due to asymmetrical loading [32]. Devices with the ability to connect between one or the other polarity could thus be made available.

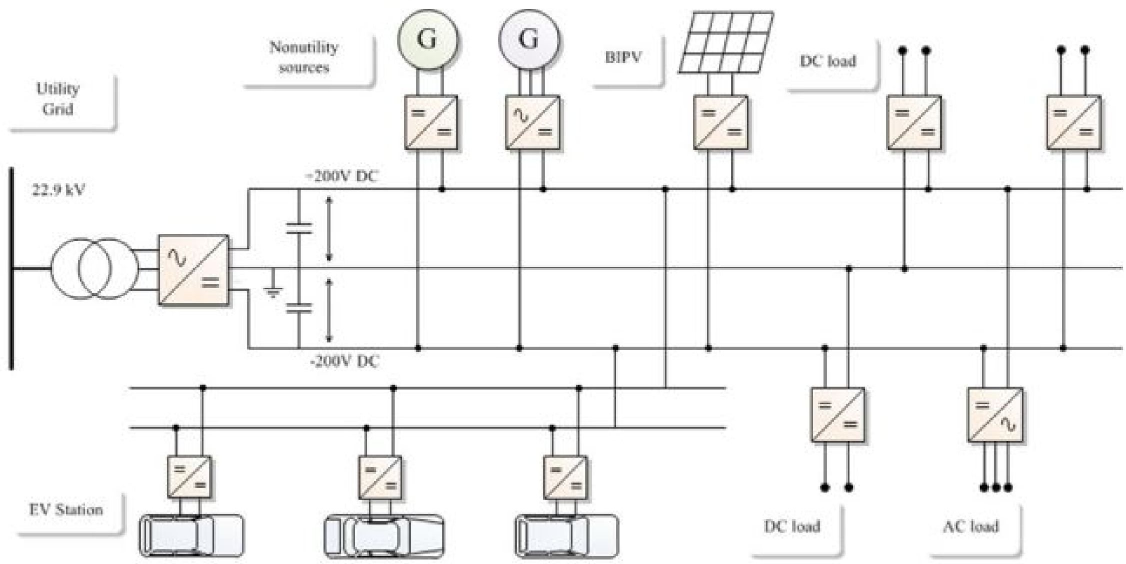

Figure 1.2: LVDC bipolar configuration for microgrid and building application by Byeon *et al.* [2].

1.4. LOCATIONAL MARGINAL PRICES AND THE MAXIMIZATION OF DG AND ESS UTILIZATION

The rise and availability of renewable energies will shape the energy market of the future. Current systems only consider supply side management. DG add an extra degree of freedom by enabling demand side participation to the energy balance. The market should change towards a prosumer market where the end-user act as a producer and consumer. The best option to effectively shift is by implementing smart microgrids where power management on the distribution level is enhanced by recent advances in controls. Electronic controllers in conjunction with sensors and information processing should be used to optimize power systems in an effort to decrease electricity prices.

Pricing can be used as a mechanism to ensure efficient utilization of DG and ESS. Monetary value of electricity can serve as a control signal to efficiently use the network [33]. If electricity prices are interconnected with the system topology, digital communication is envisioned to play a role in the high speed control of controllers to manage power flows. An efficient market structure should be implemented in order to provide incentives to the deployment of RE, ESS and smart loads in an effort to increase grid reliability and social welfare.

Real time pricing, or dynamic pricing, has proved to increase the economic efficiency of electric networks and introduces fairest price to buyers and sellers [34]. Using this approach based on time, demand and supply can be matched more precisely. Locational Marginal Prices (LMP) is an accurate real time pricing approach that takes location into consideration by providing prices locally in a system [33]. The method considers the marginal cost, cost of delivering an additional unit of power, at a specific bus. Taking location into account inherently considers the system topology in the computation of prices, this market approach reflect truest and more accurate real time costs. The implications of using LMP in a distribution network can be essential to the optimization of distribution grids by:

- Maximizing the utilization of distributed resources and storage
- Decreasing energy spending of users
- Including network topology to reflect losses and line congestion in the cost of electricity
- Creating incentives to invest in DG and ESS at the most suited locations
- Decreasing peak capacity of the system and reducing investment costs by preventing oversizing of components

1.5. OBJECTIVES AND RESEARCH QUESTIONS

1.5.1. OBJECTIVES

LVDC networks are promising solutions to assist the deployment of renewable DG, with that comes the concept of prosumers. The idea of prices based on real time operation of the grid is essential to the well being of the network. Adding an additional degree of freedom using locational pricing allows prices to be closely related to the system topology. Bipolar DC networks for electricity distribution is a relatively new concept. The research on power flows in such network is limited and it mostly relies on AC systems. Therefore the objective of this thesis is twofold. This research first investigates how power flows in DC distribution networks can be modeled considering bipolarities and asymmetrical loading. Intermittency of RE can mainly be addressed using ESS, therefore the model developed should be time dependent in order to match demand and supply at any time. Secondly, the OPF method is implemented to optimize grid operations while generating a dynamic prices at every location in the network. Using LMP a cost reflecting the cost losses and line constraints is emitted in an effort to reveal investment opportunities to increase the reliability of the network while minimizing the social welfare. Furthermore, in case of energy scarcity loads should be prioritized to direct power where it is the most needed, it is thus important to incorporate a demand-response mechanism in the model.

The availability of DG is increasing, distribution grids are thus prone to expand through time and should not be self-limiting. In other words, the network should be able to incorporate new producers and/or consumers. Flexibility of microgrids is an important parameter that will be taken in consideration. Moreover, a large portion of the world does not have access to energy. Electricity is a primordial need to ensure the development and ameliorate quality of life. Few developing countries have transmission and distributions networks making access to energy one of the most urging problem. Progress in PV and the economy of scale afford the possibility to electrify rural areas at a reasonable cost. Developing nations have the opportunity to leapfrog the traditional energy system to directly transit to LVDC microgrids. A case study is used to evaluate the validity of the OPF model for the case of a small to medium isolated community in a developing country. Based on a specific generation and load profiles the power flow is analyzed in an effort to reveal investment incentives.

OPF in conjunction with LMP is believed to be an efficient tool capable of improving energy management within distribution networks. The last section of this thesis aims at formulating a business plan for the deployment of bipolar DC microgrids in developing countries. The technology is based on the OPF algorithm developed thoughout this thesis. This theoretical business consists in the development of smart meters enabling load prioritization by assigning a price of electricity to each loads reflecting the willingness of consumers to purchase electricity.

The research objectives are summarized as such:

- Formulating a power flow specifically for bipolar DC distribution networks

- Developing an OPF algorithm based on the power flow model in an effort to maximize the utilization of RE based DG and ESS
- Based on the OPF approach, develop a functional model with pricing mechanisms that incorporates the network constraints and demand-response
- Develop a first approach to the find the optimal size and location of ESS
- Assess the validity of the model using a case study focusing on a small to medium community in a developing country
- Develop a plan to turn this model into business

1.5.2. RESEARCH QUESTIONS

1. What is the most suitable approach to formulate a power flow dedicated to bipolar DC distribution networks?
   (a) How can this model incorporate network constraint and topologies?
   (b) How can this model be formulated in relation to time in order to model ESS?
2. Using the OPF, what is the most suitable approach to develop a pricing mechanism to optimize the operation of bipolar DC distribution grids while minimizing system costs?
   (a) With respect to the network topology, how can line congestions and losses be incorporated in the price structure?
   (b) How should costs function be formulated for the different generators and/or loads in an effort to enable demand-response?
   (c) In case of asymmetrical loading, how can the price structure reveal incentives to balance the loading in a bipolar network?
   (d) How can this model reveal investment opportunities in an effort to maximize the utilization of RE and ESS?
3. Using OPF, how can the system be optimized by finding the location and size of ESS?
4. What are business opportunities and how can this model be turned into a business?

1.6. PUBLICATIONS

This thesis explores concepts that have not been investigated in previous researches. The main contribution to science is the novelty of the power flow model with regards to LVDC networks. Additionally, the OPF is used to compute the economic dispatch in bipolar grids with asymmetrical loading. Lastly, the LMP method serves as a dynamic pricing mechanism that reflects the grid operation while providing economical incentive to increase the reliability of the grid. Based on this thesis a conference paper has been published [35]:

Laurens Mackay, Anastasios Dimou, Robin Guarnotta, German Morales-Espania, Laura Ramirez-Elizondo
Pavol Bauer *Optimal Power Flow in Bipolar DC Distribution Grids with Asymmetric Loading*,
in IEEE ENERGYCON 2016, Vol.0 (2016) p. 5.

Two additional journal articles are planned. The first article is an extension of the conference paper. The second article will demonstrate how the model can include energy storage and demand-side management using a multi-period approach.

2

Optimal Power Flow and Locational Marginal Prices: A Review

This section is a literature review of the main different types of OPF. The OPF as a method to solve for the economic dispatch is first introduced. The role of LMP as the dynamic pricing mechanism is explained. Originally used in transmission networks, LMP are believed to be the building block of electricity markets for distribution networks [33, 34]. The OPF is traditionally used in AC transmission networks where losses have less of an impact on the locational electricity prices. As a result, most of the literature is centered around OPF for AC transmission systems, mainly the exact AC OPF and its simpler form the DC OPF. These formulations with corresponding LMP formulation are explained in Section 2.3.1-2.3.4. As of now, there is no preferred formulation for distribution systems. Finally, although the literature is limited, OPF and pricing mechanisms specifically developed for DC networks are discussed in the last sections.

2.1. The Economic Dispatch and OPF

Transmission and distribution networks are composed of a set of generators responsible for power production in an effort to meet the loads requirements at any time. Managing electricity to satisfy demand while considering the economic impact is the role of network operators. The concept of interconnecting grid operation and generation costs is termed *Economic Dispatch*. The generation is dispatched among generators based on their commitment level and their operational cost. Satisfying the energy balance at any time is crucial to the stability and reliability of the grid, doing it at the lowest cost result in lower electricity prices. Solving the economic dispatch problem in a short amount of time is essential given that loading and generation are time dependent, especially when electricity is supplied from RE.

OPF is a tool capable of solving the economic dispatch to enable control of a power system. The methodology was first formulated by Carpentier in 1962 and is still used in power markets [37]. The OPF combines an economic dispatch and a power flow specific to a network into a single program. The model was originally developed for AC networks and is named the Alternating Current Optimal Power Flow (AC OPF). It is a set of equations containing real and reactive flows as well as voltage magnitudes and phase angles [38]. The main challenge in the application of the OPF for power systems and markets is related to convergence due to the nonlinearity of power balances. In large and complex systems optimality is not guaranteed [39]. Furthermore, the process can be time consuming depending on the system.

The configuration and operation of generators impact spatial and temporal patterns of production, transmission and electricity use [40]. Therefore, both time and location should be taken in consideration by the market. The notion of time is linked to the constantly changing energy demand, production have to be adjusted accordingly which inherently changes the economic dispatch and energy prices. Network topology and generator characteristics constrain electricity transmission, models should thus include these physical properties to reflect more accurate prices. Three electrical characteristics affect transmission and distribution [40]: losses, line capacity and natural flows. The amount of power at the beginning of line differs from the power received at the end of the line, the difference is caused by losses and depends on the cable, its length and the efficiency of interconnected power electronic elements. The capacity of transmission lines limits power flows, cables are rated for a certain capacity, exceeding this threshold can cause damages. Finally, power flows in the network depend on the system properties, it is impossible to directly allocate electrical flows among transmission lines. For instance, when a generating unit is connected to two lines, the amount of power flowing through one line or the other cannot be directly controlled.

These physical laws affect the price of energy with regards to space. Transmission capacity limits power flows and in some situation can lead to congestion in the network, when a line is at its full capacity and exceeds its thermal limits. In this situation, it is obvious that more power cannot flow through this branch [38]. In deregulated market, it opposes perfect competition making the market inefficient and possibly rises the value of the OPF's global objective. The problem is illustrated in Figure 2.1 with a simple two bus network, a generator and a load are connected to each bus. In the absence of a line limit, generator 1 can produce 400 MW at a cost of 5 $/h. However in the presence of a line limit, generator 1 cannot satisfy the load at bus 2, it will produce 250 MW and the rest of the energy will be provided by the most expensive source, generator 2. The total generation cost will be 2750 $ as opposed to 2000 $ in the absence of a line limit.

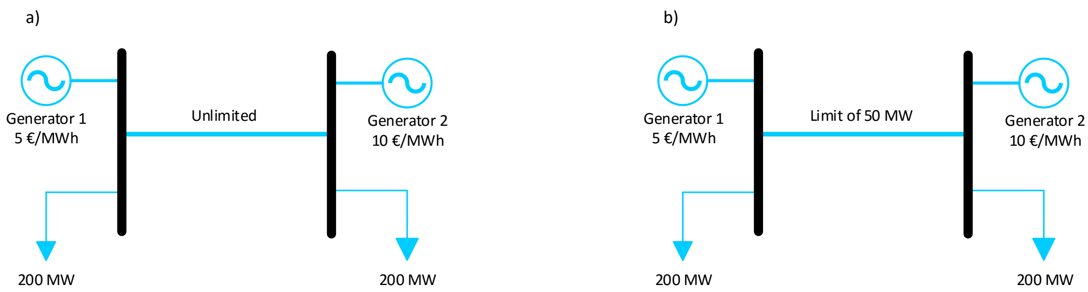

Figure 2.1: Line congestion example in a simple two bus network a) non-congested b) congested

2.2. THE ROLE OF LMP

In a larger network, congestion management is inevitable to ensure that supply matches demand at the lowest cost. One option to deal with congestions is using LMP [38, 40–42]. Also termed *Spot Prices* or *Nodal Prices*, LMP were first introduced by Schweppe *et al.* and represent the least cost to provide the next increment of demand at a bus by considering network constraints [43]. LMP are traditionally used to manage congestion in transmission networks using the Direct Current Optimal Power Flow (DC OPF), a simplified version of the AC OPF, see Section 2.3.2. Electricity prices are used as signals when a transmission or distribution line is constrained [39]. LMP are directly obtained as a dual variables of the OPF of the nodes' balance of energy equality constraints, a price for each node is therefore obtained. The correctness of LMP depends on the functions defining the OPF. For convex problems, the Karush–Kuhn–Tucker conditions (first order condition for a solution to optimal) hold true and LMP are correct [44].

Spot prices incorporate the cost of the energy source and transmission constraints. In the context of a lossless network with no transmission constraint the price is the same for each node. This is termed the *equal-lambda generation dispatch*, adding line losses and limits results in different nodal prices [42]. In the presence of congestions, there will always be a at least one source that is marginal while the rest would either be operating at their maximum or minimum output. Consequently, the LMP for each marginal unit is equal to its marginal cost of operation or offer price [44]. The LMP will be obtained as a linear function of the cost of the marginal unit, the losses and congestions.

The instability of electricity market imposed by variable demand profiles lead to LMP with high volatilities and uncertainties. Breaking down LMP into its different components and relating them to the network topology is a solution to increase stability. They can be used to provide signals to ameliorate the network and financial decisions. LMP are traditionally composed of three parts, namely the energy term, loss term and congestion term. The energy term is the same for all the nodes, it depends on the reference node [44]. The loss term represents marginal losses. It can be expressed using a nodal loss sensitivity factor which is computed with respect to a reference node for which the factor is 0. Finally, the congestion term expresses the cost associated with congestions at the node, it is obtained as a linear combination of the dual variables associated with active transmission constraints [42]. LMP is the most popular tool for congestion management in many electricity markets worldwide. In combination with the Financial Transmission Rights (FTR), the congestion term of LMP is used as a mechanism to hedge against congestion. In the presence of capacity limits on transmission lines, LMP inevitably lead to a surplus of funds collected by the grid operator. Under the FTR the congestion fund is distributed to the FTR holder [44].

Furthermore, according to Heydt *et al.* real-time pricing at the distribution level can increase the economic efficiency. LMP can reflect fairest prices to the buyer and seller [33, 34]. In distribution networks, spatial and temporal considerations cannot be omitted, especially in the presence of DG. LMP as a mean for real-time pricing reflects both factors and inherently the truest cost [40]. Using LMP to formulate a pricing mechanism could lower consumer's electricity bills and decrease the need to plan for larger peak capacities [45]. Dynamic pricing could also contribute to the system reliability as spot prices increase in the presence of a congestion which inherently lead to a decrease in demand at locations where the network is at its maximum distribution capacity.

Although LMP have been used widely, some of the properties of LMP are not well understood. The practical issues of real markets to use locational based prices are related to: 1) the exactness of the models used to solve the economic dispatch, unit commitment and LMP calculations 2) addressing infeasibilities 3) interpretation of LMP and its components [44].

2.3. OPF FOR AC NETWORKS

TRANSMISSION NETWORKS

Two main OPF were developed for AC networks, specifically for transmission. The first OPF were formulated directly from the AC power flow equations. However, the non-linearity of these equations considerably increase the complexity of the problem. As a result the economic dispatch may not be correct, divergence may occur. To increase the reliability of the economic dispatch an approximation of the AC OPF has been developed, the DC OPF. It should be emphasized that the DC OPF is by no mean dedicated to DC networks, it is a simpler version of the AC OPF for which the power flow is expressed by a set of linear equations. Its name originate from the fact that only active power is considered. In addition to its convex form, it can be up to 60 times faster than the AC OPF, an essential requirement for enhanced market operations [41]. Its simplicity, high speed and convergence robustness makes it the most suitable model for softwares dedicated to electricity markets [38, 42].

Both models have been used to derive LMP [39]. Although, the DC OPF is preferred to compute the economic dispatch it comes with its own inconvenient. The assumptions used to linearize the model omit losses in the transmission lines. From an economic dispatch point view it is acceptable as the losses in transmission networks have a smaller impact as in distribution networks. However, it also means that the losses are naturally not incorporated in LMP. Moreover, the formulation of the DC OPF does not allow for the decomposition of the LMP into its three terms, namely the energy, congestion and losses terms. Consequently, different versions of the OPF exist for which LMP can be decomposed [39].

DISTRIBUTION NETWORKS

As mentioned earlier, the AC OPF and DC OPF were originally designed for transmission systems rather than distribution systems. Merging the two levels is complex mainly caused by the system size and different constraints that needs to be taken in consideration [46]. For the reasons stated above, the DC OPF is the preferred method to compute the economic dispatch and derive LMP. However, the assumptions made in this model are not applicable to distribution networks. It assumes a constant voltage at all buses. On a distribution level variation in voltage can significantly affect the operation of the grid. Indeed, voltage control should be part of the planning a distribution network, DG can lead to large variation in voltage with respect to power generation [47]. In a situation where too many generators are located next to each other the grid network could abnormally rise to levels that would affect stability and security. Moreover, on the distribution level both the active and reactive power needs to be considered as well as voltage angles. Consequently, the DC OPF cannot be used when considering distribution networks. A noticeable difference in the economic dispatch can be observed between the two methods when applied to a distribution network, the AC OPF is thus the preferred OPF [27]. The disadvantages of this model are the same as for the transmission system, namely non-linearity leading to non-convexity requiring convexification and relaxation steps as well as a high degree of complexity leading to longer computation time [48, 49]. Although some alternatives have been developed to reformulate the AC OPF into a convex optimization problem, as of now there are no linearized OPF specifically designed for distribution networks [50, 51].

The AC OPF and LMP have been used in some publications as a placement technique of DG and ESS in distribution grids. In these papers, LMP for distribution networks are termed Distribution Locational Marginal Prices (DLMP). DLMP are essentially the same as LMP, their formulation may vary depending on the objective function. It can be used as a mean to determine appropriate location of DG by comparing prices at different buses as a function of time [47, 52, 53]. Similarly to transmission systems, it is also a tool to mitigate congestions [54, 55]. DLMP can be formulated to encourage the utilization of renewable energies [33, 46, 56–58]. DLMP have also been used to avoid voltage problems as a result of unbalanced distribution [59]. Storage allocation and dynamics based on nodal prices by adding specific constraints in the OPF has also been studied [60]. In [61], DLMP are studied as a mean to alleviate the congestion problems that might occur as a result of the deployment of electric vehicles.

The economic dispatch and DLMP are obtained from the original non-convex AC OPF, only the formulation of DLMP vary. However, this method is not deemed adequate as the computation time is a burden, especially when a high penetration of DG is considered [62]. Moreover, given the time dependency of RE the OPF needs to be computed more frequently [50]. Therefore, this methodology is argued to be non-scalable and not optimal for clearing algorithms [49].

2.3.1. AC OPF

OPF FORMULATION

The AC OPF, originally formulated by Carpentier, provides an exact power flow that considers both active and reactive power in addition to phase angles. It relies on a set of nonlinear algebraic equations. The active and reactive power flowing out of node m are respectively expressed as follow in (2.1)-(2.2) [39, 63]. Where u_m, u_n, θ_m and θ_n denotes the voltage magnitudes and angles at node m and n. $G_{m,n}$ and $\beta_{m,n}$ denotes the conductance and susceptance of branch (m,n).

$$p_m = \sum_{l=1} u_m u_n \left(G_{m,n}\cos(\theta_m - \theta_n) + \beta_{m,n}\sin(\theta_m - \theta_n)\right) \tag{2.1}$$

$$q_m = \sum_{l=1} u_m u_n \left(G_{m,n}\sin(\theta_m - \theta_n) - \beta_{m,n}\cos(\theta_m - \theta_n)\right) \tag{2.2}$$

The problem is first constrained by the equality constraints, or energy balances, representing the active and reactive power flows at each node. The active power balance is a function of the power p_m flowing out of a node, the sum of active power p_m^{G} injected by generators at this node and the active power p_m^{D} consumed by a load at this node. The reactive power balance is a function of the power q_m flowing out of a node, the sum of reactive power q_m^{G} injected by generators as this node and the reactive power q_m^{D} consumed by a load at this node. The steady state condition is formulated as such [64]:

$$p_m^{\mathrm{G}} - p_m^{\mathrm{D}} - p_m = 0 \tag{2.3}$$

$$q_m^{\mathrm{G}} - q_m^{\mathrm{D}} - q_m = 0 \tag{2.4}$$

The resistance $R_{m,n}$ and reactance $X_{m,n}$ are the source of transmission losses and are modeled as part of the power flow from node m to node n. The real and reactive flows are denoted by $p_{m,n}$ and $q_{m,n}$ (2.5-2.6). (2.7) expresses the power flow magnitude, $f_{m,n}$, in branch (m,n). This values is subject to an inequality constraint defining the upper and lower transmission limits [39].

$$p_{m,n} = \frac{\left[u_m^2 - u_m u_n \cos(\theta_m - \theta_n)\right] R_{m,n} + \left[u_m u_n \cos(\theta_m - \theta_n)\right] X_{m,n}}{R_{m,n}^2 + X_{m,n}^2} \tag{2.5}$$

$$q_{m,n} = \frac{\left[u_m^2 - u_m u_n \cos(\theta_m - \theta_n)\right] X_{m,n} + \left[u_m u_n \cos(\theta_m - \theta_n)\right] R_{m,n}}{R_{m,n}^2 + X_{m,n}^2} \tag{2.6}$$

$$f_{m,n} = \sqrt{p_{m,n}^2 + q_{m,n}^2} \tag{2.7}$$

The objective, (2.8), is to seek for the minimum production cost of the system. Each generator is attributed a cost function reflecting fixed and operating expenses. C_m^{G} is the production cost of a generator located at node m. The problem is bounded by upper and lower limits representing generators active and reactive power outputs (2.11-2.12), power flows in branches (2.13) and voltage magnitudes (2.14). The full formulation of the OPF is given as such:

$$\begin{aligned}
\min \quad & \sum_m C_m^{\mathrm{G}}(p_m^{\mathrm{G}}) && (2.8)\\
\text{s.t.} \quad & p_m^{\mathrm{G}} - p_m^{\mathrm{D}} - p_m = 0 && (2.9)\\
& q_m^{\mathrm{G}} - q_m^{\mathrm{D}} - q_m = 0 && (2.10)\\
& P_{\min}^{\mathrm{G}} \leq p_m^{\mathrm{G}} \leq P_{\max}^{\mathrm{G}} && (2.11)\\
& Q_{\min}^{\mathrm{G}} \leq q_m^{\mathrm{G}} \leq Q_{\max}^{\mathrm{G}} && (2.12)\\
& F_{\min} \leq f_{m,n} \leq F_{\max} && (2.13)\\
& U_{\min} \leq u_m \leq U_{\max} && (2.14)
\end{aligned}$$

LMP

The Lagrange function, or Lagrangian, of the above AC OPF and its constraints , is expressed as follow:

$$\begin{aligned}
\mathscr{L} = & \sum_m C_m^{\mathrm{G}}(p_m^{\mathrm{G}}) && \text{Operation cost of generators}\\
& - \sum_m \lambda_m \left(p_m^{\mathrm{G}} - p_m^{\mathrm{D}} - p_m\right) && \text{Active power balance constraint}\\
& - \sum_m \pi_m \left(q_m^{\mathrm{G}} - q_m^{\mathrm{D}} - q_m\right) && \text{Reactive power balance constraint}\\
& - \sum_m \hat{\tau}_m \left(P_{\max}^{\mathrm{G}} - p_m^{\mathrm{G}}\right) && \text{Generator real power output upper constraint}\\
& - \sum_m \check{\tau}_m \left(p_m^{\mathrm{G}} - P_{\min}^{\mathrm{G}}\right) && \text{Generator real power output lower constraint}\\
& - \sum_m \hat{\omega}_m \left(Q_{\max}^{\mathrm{G}} - q_m^{\mathrm{G}}\right) && \text{Generator reactive power output upper constraint}\\
& - \sum_m \check{\omega}_m \left(q_m^{\mathrm{G}} - Q_{\min}^{\mathrm{G}}\right) && \text{Generator reactive power output lower constraint}\\
& - \sum_m \hat{\mu}_{m,n} \left(F_{\max} - f_{m,n}\right) && \text{Power flow in branches upper constraint}\\
& - \sum_m \check{\mu}_{m,n} \left(f_{m,n} - F_{\min}\right) && \text{Power flow in branches lower constraint}\\
& - \sum_m \hat{\psi}_m \left(U_{\max} - u_m\right) && \text{Voltage upper constraint}\\
& - \sum_m \check{\psi}_m \left(u_m - U_{\min}\right) && \text{Voltage lower constraint}
\end{aligned}$$

Where π_m, λ_m, $\hat{\tau}_m$, $\check{\tau}_m$, $\hat{\omega}_m$, $\check{\omega}_m$, $\hat{\mu}_{m,n}$, $\check{\mu}_{m,n}$, $\hat{\psi}_m$ and $\check{\psi}_m$ are the dual variables for each constraint. LMP represent a demand increase of one unit, thus the marginal cost at each bus can be calculated by taking the partial derivative of the Lagrangian function with respect to p_m^{D}. It follows that the LMP of each node is the dual variable, λ_m, associated to the active power balance [39, 65]:

$$LMP_m = \frac{\partial \mathscr{L}}{\partial p_m^{\mathrm{D}}} = \lambda_m \tag{2.15}$$

The non-linearity of the model has an impact on the exactness of LMP. The product of bus voltages in addition to sin and cos power functions increase the complexity of the optimization problem. As a result, problems are often not convex leading to a duality gap [66–68]. In other words, the optimal value of the OPF do not coincides with the values of dual variables, we say that the problem has a non zero duality gap [69]. In a non convex problem, the Lagrangian variables only guarantee a locally optimal solution. Guaranteeing that the problem is convex to obtain a global optimal solution is therefore essential in order to derive correct Lagrangian multipliers and LMP. With regards to AC OPF, the problem has to go through a convexification and relaxation processes to improve the exactness of LMP [70].

2.3.2. DC OPF

The DC OPF is a simplified, linearized, version of the AC OPF. Its main characteristic is that it focuses on active power and ignores reactive power. Its faster time of computation and robustness have made it the most deployed manner of solving economic dispatch problem and computing LMP [38]. Additionally, the model does not suffer has much from duality gap, it is the preferred manner to derive LMP [71]. The DC OPF has many formulations, here the standard DC OPF is explained and LMP are obtained from the Lagrangian, this formulation does not allow for the decomposition of nodal prices. Alternate formulations have been developed allowing the decomposition of LMP in its three components, namely the energy, loss and congestion term. These variations are presented in Section 2.3.3 and 2.3.4.

OPF Formulation

DC OPF omits reactive power flow equations (2.2, 2.4, 2.6 and 2.12) from the optimization problem. Three main assumptions are used to simplify the AC OPF formulation [39, 41, 63, 72, 73]. 1) The resistance of branch $R_{m,n}$ is negligible in comparison to reactance $X_{m,n}$. The resistance of all branches is set to 0. Given this assumption it follows that $G_{m,n} = 0$ and $\beta_{m,n} = {}^{-1}/_{X_{m,n}}$. 2) The voltage magnitude at each node is equal to the nominal voltage. Given this assumption $u_m u_n = u_0^2$ where V is the nominal voltage. 3)The voltage angle difference $\theta_m - \theta_n$ across any branch (m,n) is so small that $\cos(\theta_m - \theta_n) = 1$ and $\cos(\theta_m - \theta_n) = \theta_m - \theta_n$. These assumptions were judged to be acceptable in cases where the branch power flows is not too high, voltage profile is relatively flat and the ratio of a branch resistance to reactance is less than 0.25 [74]. For these reasons this power flow can be applied to transmission networks, however the voltage profile of distribution networks is more sensitive and the $R_{m,n}/X_{m,n}$ ratio is often high [50]. Combining these assumptions lead to the following branch power flows equations [63]:

$$p_{m,n} = U^2 \frac{(\theta_m - \theta_n)}{X_{m,n}} \tag{2.16}$$

$$q_{m,n} = \frac{(U^2)}{X_{m,n}} - \frac{(U^2)}{X_{m,n}} = 0 \tag{2.17}$$

$$f_{m,n} = \sqrt{p_{m,n}^2 + q_{m,n}^2} = p_{m,n} \tag{2.18}$$

From (2.17) we conclude that the reactive power flow will not be part of the problem which simplifies the power flow magnitude which is now equal to the real power flow (2.18). Moreover, U is a constant and same at all nodes, the problem is now linear and the operating voltage inequality is removed from the set of constraints. The full DC OPF is formulated as such:

$$\min \quad \sum_m C_m^{\mathrm{G}}(p_m^{\mathrm{G}}) \tag{2.19}$$

$$\text{s.t.} \quad p_m^{\mathrm{G}} - p_m^{\mathrm{D}} - p_m = 0 \tag{2.20}$$

$$P_{\min}^{\mathrm{G}} \leq p_m^{\mathrm{G}} \leq P_{\max}^{\mathrm{G}} \tag{2.21}$$

$$F_{\min} \leq f_{m,n} \leq F_{\max} \tag{2.22}$$

LMP

The Lagrange function of the above AC OPF and its constraints , is expressed as follow:

$$\begin{aligned}
\mathscr{L} = &\sum_m C^{\mathrm{G}}_m(p^{\mathrm{G}}_m) \quad \text{Operation cost of generators}\\
-&\sum_m \lambda_m \left(p^{\mathrm{G}}_m - p^{\mathrm{D}}_m - p_m\right) \quad \text{Active power balance constraint}\\
-&\sum_m \hat{\tau}_m \left(P^{\mathrm{G}}_{\max} - p^{\mathrm{G}}_m\right) \quad \text{Generator real power output upper constraint}\\
-&\sum_m \check{\tau}_m \left(p^{\mathrm{G}}_m - P^{\mathrm{G}}_{\min}\right) \quad \text{Generator real power output lower constraint}\\
-&\sum_m \hat{\mu}_{m,n} \left(F_{\max} - f_{m,n}\right) \quad \text{Power flow in branches upper constraint}\\
-&\sum_m \check{\mu}_{m,n} \left(f_{m,n} - F_{\min}\right) \quad \text{Power flow in branches lower constraint}
\end{aligned}$$

Similarly to the AC OPF, nodal prices are equal to the the dual variable associated to the active power balance (2.23) [39]. Although the computational speed is augmented and the problem is less subject to divergence, this formulation has three major drawbacks. First, the model does not include voltage variation between nodes making it less safe, the only active security limit is the transmission constraint. Second, line losses are not considered in the model and consequently they are not part of the LMP. As opposed to the AC OPF, when the network is congestion free the nodal price at each node will be the same. Including losses is challenging due to the quadratic relationship between line loss and flow [38, 75]. Thermal losses in cables are inevitable, they should thus be reflected in LMP. Lastly, the LMP cannot be decomposed into different terms, the marginal cost of energy and marginal cost of congestion cannot be differentiated [39, 76].

$$LMP_m = \frac{\partial \mathscr{L}}{\partial p^{\mathrm{D}}_m} = \lambda_m \tag{2.23}$$

2.3.3. DC OPF WITHOUT LOSSES

The role of LMP decomposition is crucial for congestion management and should be taken into consideration to calculate congestion rents [77]. Also called the merchandising surplus, the congestion rent is the rent paid to the grid operator given that each load pays its nodal price for its consumption and each generator is paid the nodal price for its production [77, 78]. Therefore, a model enabling the analysis of nodal prices is needed. LMP can be decomposed into the marginal energy term and congestion term by using Generation Shift Factor (GSF). GSF maintain linearity and superposition properties of the DC OPF while being able to optimize for congestion [38]. The purpose of these factors is to relate branch power flow to net power injection. As defined by Liu *et al.*, it measures the change in power flow on a branch (m,n) when one power unit change in generation occurs at bus m compensated by a withdrawal of one power unit at the reference bus [39]. In other words, it gives the flow on a transmission line from a source node to a sink node [38, 79]. GSF on a line (m,n) due to a change in injection at bus m can be expressed as such:

$$GSF_{m,n-m} = \frac{\partial f_{m,n}}{\partial p_m} \tag{2.24}$$

Where $f_{m,n}$ is the flow on line (m,n) with respect to bus m and p_m is the net injection at bus m. Note that the number of shift factors is equal to the number of lines multiplied by the number of nodes. The GSF values depend on the choice of reference bus. It can be computed using information from the network topology where B^{-1} is the inverse of B (the imaginary part of Y bus matrix), $X_{m,n}$ is the reactance of line (m,n), a is the sending bus and b is the receiving bus [80, 81]:

$$GSF_{m,n-m} = \frac{B^{-1}_{a,m} - B^{-1}_{b,m}}{X_{m,n}} \tag{2.25}$$

OPF FORMULATION

This DC OPF formulation is referred in the literature as the lossless DC OPF [82]. The optimization follows a linear model that optimizes the energy and congestion price. The optimization problem is formulated as follow [75, 80, 83, 84]:

$$\min \quad \sum_m C_m^{\mathrm{G}}(p_m^{\mathrm{G}}) \tag{2.26}$$

$$\text{s.t.} \quad \sum_m p_m^{\mathrm{G}} - \sum_m p_m^{\mathrm{D}} = 0 \tag{2.27}$$

$$F_{m,n,\min} \le \sum_m GSF_{m,n-m} \cdot \left(p_m^{\mathrm{G}} - p_m^{\mathrm{D}}\right) \le F_{m,n,\max} \tag{2.28}$$

$$P_{\min}^{\mathrm{G}} \le p_m^{\mathrm{G}} \le P_{\max}^{\mathrm{G}} \tag{2.29}$$

The power balance is maintained at the node and is now expressed as the sum of power inflow and outflow at node m. The generators operation constraint is the same as in the previous formulation. Finally, the congestion constraint is now expressed as function of GSF.

LMP

The benefit of using GSF is the ability to decompose LMP. In the AC OPF and standard DC OPF, LMP were directly derived from the active power balance constraint as λ_m. In this approach nodal prices are the sum of two terms: the energy component (LMP^{E}) and the congestion component (LMP^{C}) [39, 76]. In a simple 3 bus example Liu *et al.* demonstrate that using this approach leads to the same LMP as in the standard DC OPF for each node. The added value of using shift factors for grid operators is the congestion term, LMP_m^{C} which can be interpreted as the congestion rent or congestion charge [77]. It should be noted that the definition of the GSF requires the selection of a reference node, also called slack node. Consequently in this model the energy component is in fact the price of energy at the slack node, λ_m changes upon a change in the location of the reference node [73]. Moreover, losses are not considered in this system the difference in the price between each node is only caused by congestions, ergo there is no real need of splitting the LMP as such [44]. However, this is not valid anymore if losses are included. In this case GSF are used to dissociate prices differences caused by congestions and losses as in Section 2.3.4.

$$LMP_m^{\mathrm{E}} = \lambda_m \tag{2.30}$$

$$LMP_m^{\mathrm{C}} = \sum_{m,n} \left(-\hat{\mu}_{m,n} + \check{\mu}_{m,n}\right) \cdot GSF_{m,n-m}) \tag{2.31}$$

$$LMP_m = LMP_m^{\mathrm{E}} + LMP_m^{\mathrm{C}} \tag{2.32}$$

2.3.4. DC OPF WITH LOSSES

Using the above formulation allows for the differentiation of the marginal energy costs from the marginal congestion costs, however losses are not modeled. Some approaches exists where losses are included in the standard DC OPF formulation nonetheless they do not always lead to proper results [38]. An approach considering losses in the optimization process such that these losses are minimized is needed. This formulation should allow for a loss term (LMP^{L}) in the total LMP.

Losses can be approximated for each individual branch using a piece-wise linear approximation [44]. The key to consider the marginal cost of losses in DC OPF are Marginal Loss Factor (LF) and Marginal Delivery Factor (LF). Mathematically, they are expressed as such [75, 80, 81, 83–85]:

$$DF_m = 1 - LF_m = 1 - \frac{\partial p_{\mathrm{Loss}}}{\partial p_m} \tag{2.33}$$

Where LF_m is the Marginal Loss Factor at bus k, DF_m is the Marginal Delivery Factor at bus k, and p_m is the net injection at bus k. p_{Loss} is the total loss in the system, it is a function of $f_{m,n}$ and the line resistance ($R_{m,n}$) as expressed in equation 2.34. Therefore, LF can be expressed as a function of GSF [75, 76] (2.35). Note that the LF can be either positive or negative. This implies that for a positive factor an increase of injection at bus

m may increase the system cost or may decrease the system cost if negative.

$$p_{\text{Loss}} = \sum_{m,n} f_{m,n}^2 * R_{m,n} \tag{2.34}$$

$$\begin{aligned}\frac{\partial p_{\text{Loss}}}{\partial p_m} &= \frac{\partial}{\partial p_m}\left(\sum_{m,n} f_{m,n}^2 * R_{m,n}\right) \\ &= \sum_{m,n} \frac{\partial}{\partial p_m}\left(f_{m,n}^2 * R_{m,n}\right) \\ &= \sum_{m,n} R_{m,n} \cdot 2 f_{m,n} \cdot \frac{\partial f_{\text{m,n}}}{\partial p_m} \\ LF_m &= \sum_{m,n} 2 \cdot R_{m,n} \cdot GSF_{m,n-m} \cdot \left(\sum_{n} GSF_{m,n-n} \cdot p_n\right)\end{aligned} \tag{2.35}$$

OPF FORMULATION

The DC OPF with losses can be formulated in different manners. One common formulation that incorporates losses in the power balance multiplies LF with the power injection [41, 42, 75, 83, 86]. Note that sometimes in literature the term p_{Loss} is referred as offset, an estimate of the total system losses [75].

$$\min \quad \sum_{m} C_m^{\text{G}}(p_m^{\text{G}}) \tag{2.36}$$

$$\text{s.t.} \quad \sum_{m} DF_m \cdot p_m^{\text{G}} - \sum_{m} DF_m \cdot p_m^{\text{D}} + p_{\text{Loss}} = 0 \tag{2.37}$$

$$F_{m,n,\min} \leq \sum_{m} GSF_{m,n-m} \cdot \left(p_m^{\text{G}} - p_m^{\text{D}}\right) \leq F_{m,n,\max} \tag{2.38}$$

$$P_{\min}^{\text{G}} \leq p_m^{\text{G}} \leq P_{\max}^{\text{G}} \tag{2.39}$$

LMP

Using this methodology the decomposition of LMP is straightforward and results in three components: an energy term, a congestion term and a loss term [75]. The loss component should be termed the marginal loss component, moreover it is important to highlight that this term do not reflect the cost of physical losses. Litvinov claims that the price of physical losses in this model is undefined and that assigning a price to physical losses using LMP is impossible [44]. As a matter of fact, similarly to congested networks, when losses are approximated in the model it results in a surplus. When losses and transmission line capacity limits are introduced, it results in a loss revenue and congestion revenue funds. Both the loss sensitivities, LF, and the power flow sensitivities, GSF, depend on the location of the reference node. Consequently, changing the slack node changes the distribution of money between congestion and loss funds. As explained in the previous sections, the congestion fund is distributed to the FTR holders. In some markets, the loss revenue is allocated to the loads. However, the allocation of this revenue is based on the wrong assumption that physical losses are the nature of the fund [44].

$$LMP_m^{\text{E}} = \lambda_m \tag{2.40}$$

$$LMP_m^{\text{L}} = LMP_m^{\text{E}}(DF_m - 1) = \lambda_m(DF_m - 1) \tag{2.41}$$

$$LMP_m^{\text{C}} = \sum_{m,n} \left(-\hat{\mu}_{m,n} + \check{\mu}_{m,n}\right) \cdot GSF_{m,n-m} \tag{2.42}$$

$$LMP_m = LMP_m^{\text{E}} + LMP_m^{\text{L}} + LMP_m^{\text{C}} \tag{2.43}$$

2.4. OPF FOR DC NETWORKS

OPF FOR DC TRANSMISSION NETWORKS

Transmission networks in the world mostly rely on AC technologies. Many transmission systems have reached their capacity limits in Europe and North America. Grids need to be upgraded to plan for the increase in electricity consumption. Additionally, the penetration of RE in an effort to expand the energy mix using onshore or offshore solar and wind parks requires network enhancements [87]. The development of HVDC technologies has lead to many proposal for future extensions of HVAC networks. Moreover, HVDC has some advantages in comparison to HVAC such as high controllability and reduction costs due to lower losses [88].

The extension of transmission grids using HVDC result in hybrid networks where HVDC lines are connected to HVAC lines, generally using voltage source converter. Consequently, for these systems power flow models need to combine power equations for HVDC grid, HVAC grid and for the power station. Several authors addressed the topic of optimal power flows for such systems but there is no literature about LMP in HVAC/HVDC networks [87, 89–92]. The AC OPF is often used for the AC part of the grid and the modeling of the conversion stations is presented in [90]. With regards to the HVDC side in [87, 89, 93], the power flow is modeled in terms of power using Ohm's law and Joule. For unipolar configurations the power flowing through a line (m,n) is given by (2.44) [89]. For bipolar configuration the power is multiplied by a factor of 2 (2.45) [87, 93, 94].

$$p_{m,n} = \frac{u_m(u_n - u_m)}{R_{m,n}} \tag{2.44}$$

$$p_{m,n} = 2\frac{u_m(u_n - u_m)}{R_{m,n}} \tag{2.45}$$

OPF FOR DC DISTRIBUTION NETWORKS

Here, the literature about OPF for LVDC distribution networks is reviewed. There are very few studies that cover power flows for this specific application. Only two publications were judged to be relevant. The first one proposes a formulation for OPF in DC networks [95]. The other one discusses the use of a voltage dependent pricing mechanism as a mean to generate nodal prices and compute the economic dispatch of DC radial microgrids [96].

In their publication, Gan and Low seek to solve for optimal power flows in direct current networks using a second-order cone programming as a mean of relaxation of the non-convex problem. The OPF approach is specifically meant to be adapted to DC networks unlike the DC OPF which is a simplification meant to be used in AC systems. In this study the power flow is modeled following circuit laws, namely Ohm's law, current balance and power balance. By substituting Ohm's law in the power balance equation the following power equation is used to model the power flow where $Y_{m,n}$ is the admittance [95]:

$$p_m = u_m \sum_n (u_m - u_n)\, G_{m,n} \tag{2.46}$$

(2.46) leads to a non-convex constraint in the optimal power flow formulation. Gan and Low proceed to relaxation of the problem using second-order cone programming. It has been observed that two sufficient conditions for exact relaxation are required. Following their observation that two sufficient conditions for exact relaxation are required, the authors propose a modified OPF formulation with an exact relaxation. Note that the validity of this model to compute nodal prices is not discussed.

A voltage dependent price mechanism is discussed by Mackay *et al.*. The power flow and unit commitment is controlled by voltage levels which inherently consider losses. Each DG is assigned a price and voltage-power curve and follows a droop slope. When a source's threshold voltage is reached, it starts injecting power in the grid. This method is a simple way to determine the economic dispatch of a microgrid without solving any optimization problem. Convergence is not an issue which makes this methodology modular and robust. However, this methodology has multiple disadvantages. Line constraints are not included, thus congestion management is not considered. Only radial networks are addressed, however for the reasons mentioned in Chapter 1 meshed LVDC distribution networks are favorable to ensure optimal operation and full utilization of DG. Asad and Kazemi developed an approach different of the OPF to compute the economic dispatch of a DC microgrid. The method is based on the same voltage dependent pricing, the methodology is termed the *Optimal DC Power Sharing* method and is used to generate nodal prices. The formulation is proper to DC radial microgrids. The price, Λ, at a receiving node m is derived from the ratio of the voltage between an emitter and receiver node as such [96]:

$$\Lambda_n = \frac{u_m}{u_n}\Lambda_m \tag{2.47}$$

2.5. CONCLUSION

From the literature, it is clear that the OPF is used as the main tool to compute the economic dispatch in both transmission and distribution networks. The dominance of AC networks motivated many studies on OPF for such systems. Moreover, there is a common agreement that LMP are an efficient method for market clearing. However, accurate prices can only be obtained if the problem is convex, linear OPF are thus preferred. As of today, most researches focused on AC transmissions grids, however the recent deployment of RE will inevitably change the energy sector resulting in a growing adoption of HVDC. More studies should be oriented towards market clearing mechanisms using LMP for hybrid HVAC/HVDC grids. Concerning LVAC networks, no OPF other than the AC OPF has been formulated. Solving for the economic dispatch may result in long computation times and LMP may be subject to divergence. Alternatives are needed to ensure an efficient deployment of DG at this level. With regards to the scope of this work, vary few studies focus on DC distribution networks. The limited amount studies on the topic reveal that there is currently no standard OPF and LMP formulation applicable to such grids. Moreover, combining pricing mechanisms with DC bipolar networks that may be subject to asymmetries is a novel idea that has never been researched before.

3

Optimal Power Flow and Locational Marginal Prices for Bipolar DC Distribution Grids

In this chapter a method is proposed to solve the OPF and derive LMP in DC bipolar distribution grids. The model is the result of a collaboration with Laurens Mackay and Anastasios Dimou. Laurens formulated the power flow equations and Anastasios founded the basis of the model in GAMS as well as the interface required for the input. Along with finalizing the power flow model on GAMS, my main contribution is the formulation of the OPF to solve for the economic dispatch and LMP. Overall the main contribution to science is the formulation of the OPF in terms of current and voltages. Usually, as reported in Chapter 2, OPF are formulated in terms of power. The main reasons why power flows equations are formulated in terms of current are the following:

- In Chapter 2, OPF methods for AC and DC distribution grids are reviewed. AC distribution networks rely on the AC OPF, however there are no standard method for DC distribution networks.
- The power flow modeling approach based on current rely on Kirchhoff's current law (KCL) and Ohm's law, an exact power flow is guaranteed and the solution is always physically feasible.
- These physical laws are linear. As opposed to the AC OPF, power flow is subject to a completely linear set of equations. The optimization process is easier and less subject to convergence.
- The main benefit of using an exact power flow based on linear equations is the possibility to develop a pricing mechanism closely linked to the network topology.

In this chapter, the method used to model DC power flow is discussed. A formulation of the OPF problem is proposed along with the optimization methodology used to obtain current based LMP. Using these variables power based LMP are derived. The validity of the model is then demonstrated using different case studies consisting of sources and loads for bipolar DC networks with either radial or mesh configurations. Finally, the effects of the network and sources constraints on the locational prices are explained. The model discussed in this chapter assumes a single time period one hour. The multiple periods formulation is introduced with energy storage in Chapter 4.

3.1. Linear Model for Exact Power Flow in Bipolar DC Distribution Grids

The exact power flow represented in terms of current is modeled using two layers: grid layer and sources/load layer. These superposed layered are illustrated in Figure 3.1. Each layer is composed of its own set of equations and are interconnected thanks to a common variable: the node current, i_m.

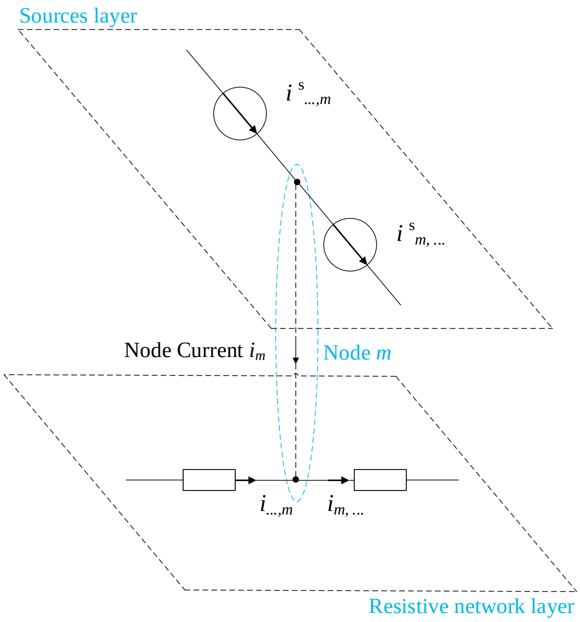

Figure 3.1: Grid representation with respect to layers representing sources and resistive network. The node current i_m connects both layers at each node

3.1.1. MODELING OF THE GRID

The bottom layer is the resistive network, it can be interpreted as distribution lines connecting sources and loads in the grid. Using voltage and current as variables, losses are modeled linearly by considering the DC voltage magnitude differences between nodes and the line resistance (3.1) [98]. The network consists of nodes in set $\mathcal{N}$ and its subsets used to differentiate nodes located on the positive conductor ($\mathcal{N}_+$), the neutral conductor ($\mathcal{N}_\mathrm{N}$) and the negative conductor ($\mathcal{N}_-$). The current flowing through a branch between node m and n in $\mathcal{G}$ is expressed as $i_{m,n}$. In the model, we define the node current as the algebraic sum of the currents flowing in the branches connected to node m [35].

$$i_{m,n} = G_{m,n}(u_m - u_n) \qquad \forall (m,n) \in \mathcal{G} \tag{3.1}$$

$$i_m = \sum_{n|(m,n)\in\mathcal{G}} i_{m,n} - \sum_{n|(m,n)\in\mathcal{G}} i_{n,m} \qquad \forall m \in \mathcal{N} \tag{3.2}$$

3.1.2. MODELING OF SOURCES AND LOADS

In a unipolar grid, sources and loads can only be connected between the positive and neutral conductor. However, in bipolar grids three configurations are possible: between the positive and neutral conductors, between the neutral and negative conductor or between the positive and negative conductor. These different configurations lead to asymmetries between currents flowing through the positive and negative conductors, a current is thus forced in the neutral conductor. Therefore, a ground plan cannot be assumed, a single node is designated as an ideal ground point. A bipolar network is termed symmetric when sources and loads are exactly the same between the positive and negative polarity. In this configuration no current flows through the neutral conductors. Loads are modeled as sources with positive current injection, no distinction is made between sources and loads within the model, the same variable is used for both. The proposed formulation suggests that sources have a negative current output while loads have a positive current output. It is worth-mentionning that formulating the problem in terms of current and voltages allows for the compute the power flows in the the neutral conductor, this variable could not be obtained if the problem was formulated in terms of power.

It is important to make a distinction between the set $\mathcal{S}$, $\mathcal{P}$ and $\mathcal{L}$. In Chapter 4, storage units are introduced and modeled as sources, therefore the power flow also applies to ESS. Set $\mathscr{S}$ groups all the sources or ESS referred by the index s and connected to nodes (m,n). Set $\mathscr{P}$ groups all the sources or ESS connected between the same set of nodes (m,n). However with regards to the cost function and constraints discussed in the next sections, it is essential to differentiate sources from batteries, therefore set $\mathscr{L}$ gathers all the sources referred by the index s and connected to nodes (m,n).

The top layer of Figure 3.1 represents the sources layer. Sources are connected between a pair of nodes (m,n) and defined by a third index, s. Each source is thus numbered which allows for the connection of multiple sources between the same nodes. An example is provided in Figure 3.2. The current of a source is denoted as $i^{\mathrm{S}}_{m,n,s}$ for all $(m,n,s)\in\mathscr{S}$. By summing the currents of sources and loads connected between the same set of nodes a net current is obtained for all pair of node $(m,n)\in\mathscr{P}$ between which at least one source is connected (3.3). Similarly to the previous section, the node current is the algebraic sum of the net current connected to node m (3.4). Together with (3.1)-(3.4) constitute the power flow model.

$$i^{\mathrm{S}}_{m,n} = \sum_{s|(m,n,s)\in\mathscr{S}} i^{\mathrm{S}}_{m,n,s} \qquad \forall(m,n)\in\mathscr{P} \tag{3.3}$$

$$i_m = \sum_{n|(n,m)\in\mathscr{P}} i^{\mathrm{S}}_{n,m} - \sum_{n|(n,m)\in\mathscr{P}} i^{\mathrm{S}}_{m,n} \qquad \forall m\in\mathscr{N} \tag{3.4}$$

The combination of (3.2) and (3.4) essentially represents Kirchhoff's current law. The node current, i_m, is the element interconnecting both layers. If no current is injected or extracted due to the presence of a source or load connected to node m, the node current will be zero. However, if current is injected or extracted due to the presence of a source or load connected to node m, the node current will be equal to the total balance of current injected and extracted at this node [35]. (3.2) is therefore the equality constraint of the OPF.

By considering voltages magnitude difference the power generated or consumed by each source is computed and denoted by $p^{\mathrm{S}}_{m,n,s}$ (3.5). It is important to realize that this equation is not part of the power flow, it is only use to generate a price mechanism in energy terms (Wh). With respect to the type of programming used to derive LMP, it is important to mention that this equation is the only one non-linear.

$$p^{\mathrm{S}}_{m,n,s} = (u_m - u_n)\cdot i^{\mathrm{S}}_{m,n,s} \qquad \forall(m,n,s)\in\mathscr{S} \tag{3.5}$$

3.1.3. COMBINING THE GRID AND SOURCE LAYERS

In this section the naming conventions are explained to avoid confusion in the further examples and case studies. Figure 3.2 shows a simple radial bipolar network composed of 9 nodes. The node current i_m is the link between the resistive and sources layer. In all cases indexes start from 0, we have $m0, m1, m2$... and $s0, s1, s2$....

The resistive network is composed of the three conductors with different polarities. The black arrows are used as a convention to name branch currents variables, it is not used to illustrate in which direction current is flowing. For example, the current flowing in line connected between note 3 and 4 is named $i_{3,4}$. Therefore, $i_{3,4}$ is positive if the current is flowing from node 3 to 4 and negative if the current is flowing from node 4 to 3.

Sources are always connected between two different polarities. In the case where a source inject a positive or negative current in a node, the node current will be non-zero. However, if no positive or negative current is injected in the node, it will only be considered in the modeling of grid (3.2) and its value will be zero. As mentioned in Section 3.1.2, sources and loads are modeled in the same way. In schematic 3.2, black arrows represent sources while red arrows represent loads. The arrows are also used as a naming convention, only the sign of $i^{\mathrm{S}}_{m,n,s}$ determines whether it is a source or a load. Sources are always named from top to bottom. If it is connected on the positive pole, m represents the node of the positive polarity and n represents the node of the negative polarity. Similarly if a source is connected on the negative pole, m represents the node of the neutral polarity and n represents the node of the negative polarity. The same is applicable for sources directly connected from the positive to negative pole. Since source 1 is a generator, $i^{\mathrm{S}}_{3,0,1}$ is negative, on the other hand source 7 is a load, $i^{\mathrm{S}}_{2,8,7}$ is positive.

The model allows for multiple sources to be connected across the same nodes. It allows to use only two nodes

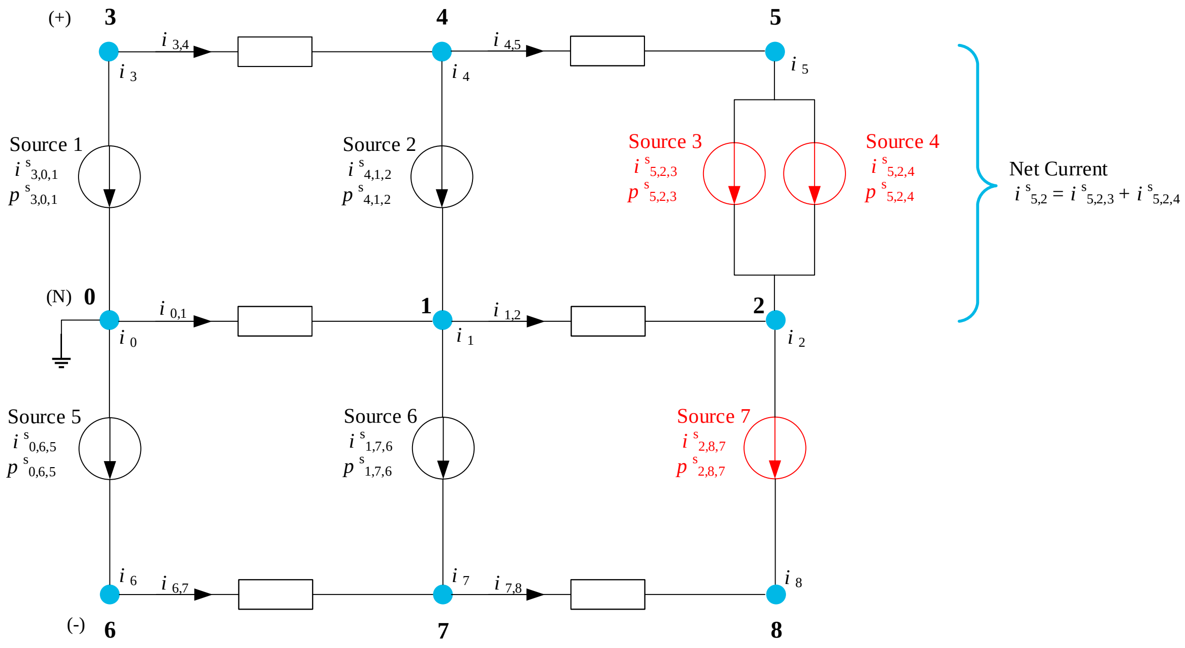

Figure 3.2: Bipolar network representation with corresponding variables

to easily include nanogrids such as houses for which resistive losses are negligible. In Figure 3.2, two loads are connected in parallel between node 2-5. The resultant current across these nodes, , $i^{\mathrm{S}}_{5,2}$, is given by (3.3).

3.1.4. NETWORK CONSTRAINTS

Unlike transmission networks, distribution networks are sensible to changes in voltage magnitudes. Voltage in the positive, neutral and negative network are constrained between an acceptable percentage of the nominal voltage (3.6)-(3.8). Additionally, as discussed in the Chapter 2, lines have thermal limits that should not be reached in order to maintain the well-being and safety of the grid. To guarantee sustainable operation the constraint is set by restraining the branch current to a range deemed acceptable (3.9). Note that this constraint is responsible for congestions.

$$U_{\min} \leq u_m \leq U_{\max} \qquad \forall m \in \mathcal{N}_+ \tag{3.6}$$

$$U_{\min} \leq -u_m \leq U_{\max} \qquad \forall m \in \mathcal{N}_- \tag{3.7}$$

$$U_{\mathrm{N},\min} \leq u_m \leq U_{N,\max} \qquad \forall m \in \mathcal{N}_{\mathrm{N}} \tag{3.8}$$

$$I_{m,n,\min} \leq i_{m,n} \leq I_{m,n,\max} \qquad \forall (m,n) \in \mathcal{G} \tag{3.9}$$

$$I^{\mathrm{S}}_{m,n,s,\min} \leq i^{\mathrm{S}}_{m,n,s} \leq I^{\mathrm{S}}_{m,n,s,\max} \qquad \forall (m,n,s) \in \mathcal{L} \tag{3.10}$$

$$P^{\mathrm{S}}_{m,n,s,\min} \leq p^{\mathrm{S}}_{m,n,s} \leq P^{\mathrm{S}}_{m,n,s,\max} \qquad \forall (m,n,s) \in \mathcal{L} \tag{3.11}$$

DG and loads, cannot exceed a given parameter. This limit can be set in terms of current or power enabling the simulation of constant power and constant current loads (3.10)-(3.11). Both constraints can also be set simultaneously for a same source. For generators a range of operation is assigned for which $I^{\mathrm{S}}_{m,n,s,\min}$, $I^{\mathrm{S}}_{m,n,s,\max}$, $P^{\mathrm{S}}_{m,n,s,\min}$ and $P^{\mathrm{S}}_{m,n,s,\max}$ have to be smaller or equal to zero. For loads these parameters have positive values. Fixing a load to a constant value is done by setting the upper limit equal to the lower limit (3.12)-(3.13).

$$i^{\mathrm{S}}_{m,n,s} = I^{\mathrm{S}}_{m,n,s,\min} = I^{\mathrm{S}}_{m,n,s,\max} \qquad \forall (m,n,s) \in \mathcal{L} \tag{3.12}$$

$$p^{\mathrm{S}}_{m,n,s} = P^{\mathrm{S}}_{m,n,s\min} = P^{\mathrm{S}}_{m,n,s\max} \qquad \forall (m,n,s) \in \mathcal{L} \tag{3.13}$$

Together (3.6)-(3.11) form a set of constraints that take into account the network topology. They either apply to positive poles ($\mathcal{N}_+$), neutral conductor ($\mathcal{N}_{\mathrm{N}}$), negative poles ($\mathcal{N}_-$), pairs of nodes connected to a branch ($\mathcal{G}$)

or to all generators or loads ($\mathscr{L}$) [35]. All of these constraints are linear except for the inequality representing constant power sources' limits since $p^{\mathrm{S}}_{m,n,s}$ is itself the product of two variables.

3.2. OPF FOR BIPOLAR DC DISTRIBUTION GRIDS

The above power flow model designed for bipolar DC bipolar distribution grids provide the necessary framework to satisfy the supply-demand balance while considering the network topology. Using these sets of equations, an optimization problem aiming at minimizing the system generation cost is formulated. The objective is constrained by the exact power flow model and physical properties such as power losses, voltage and limits, generation capacities and natural power flows.

3.2.1. SOLVING FOR THE ECONOMIC DISPATCH

Although the model is formulated in terms of current and voltages, electricity is priced in terms of energy. A marginal cost is assigned to each source, $\Pi^{\mathrm{S}}_{m,n,s}$, and expressed in [$/Wh]. It is therefore necessary to compute the energy generated or consumed by all sources $\in \mathscr{L}$ to then calculate the generation cost of each source (3.5). Note that (3.5) only applies to $\mathscr{L}$ and not $\mathscr{S}$, ESS introduced in the next chapter are always operated at a marginal cost of 0 $/Wh, consequently they should not be included in the cost function. A time period Δt is defined to compute the amount of energy generated or consumed. Throughout the report the time period is taken as 1 hour.

$$c^{\mathrm{P}}_{m,n,s} = p^{\mathrm{S}}_{m,n,s} \cdot \Pi^{\mathrm{S}}_{m,n,s} \cdot \Delta t \qquad \forall (m,n,s) \in \mathscr{L} \tag{3.14}$$

The system cost is expressed as the algebraic sum of the generation cost of sources and loads. In the litterature, most often sources are described by a positive value, the economic dispatch is computed by minimizing the objective function. The formulatin of this model implies that sources inject a negative current. The economic dispatch is thus obtained by maximizing the objective function subject to the network's constraints (3.1) – (3.11). The optimization problem is formulated as follow:

$$\begin{aligned} \max \quad & \sum_{(m,n,s)\in\mathscr{L}} c^{\mathrm{P}}_{m,n,s} \\ \text{s.t.} \quad & (3.1) - (3.11) \end{aligned} \tag{3.15}$$

Solving the economic dispatch using the objective function (3.15) inherently allows for the computation of node voltages, node currents and branch currents with respect to the network topology.

3.2.2. SOLVING FOR LMP

The multiplication of two variables in (3.5) makes the problem bilinear, a special case of quadratic programming for which the problem may not be convex. Non-convex problems suffer from a weak duality between the objective function and constraints. The optimal value of problems with non zero duality gap does not coincide with the value of dual variables [69]. Lagrangian values only guarantee a locally optimal solution. Therefore, Lagrangian multipliers of quadratic problems cannot be used to interpret LMP as opposed to linear problems for which the duality gap is small. Extracting nodal prices from the optimization problem described by (3.15) and subject to (3.1) – (3.5) is achievable if the problem is linearized. LMP are retrieved from the dual variables of the equality constraint (3.4).

Similarly to the approach presented by O'Neill *et al.*, the OPF is computed using a three steps process relying on two types of programming. The purpose of this methodology is to solve the economic dispatch using quadratic programming and remove non-linearities using linearization (3.5). The problem is then solved with linear programming and dual variables are finally interpreted as LMP. Each step relies on a different power and objective function as indicated in Table 3.1.

	Programming type	Power Function	Objective function
Step 1	Quadratic (QCP)	$p^{S}_{m,n,s} = i^{S}_{m,n,s}\,(u_m - u_n)$	$\sum_{(m,n,s)\in\mathscr{L}} p^{S}_{m,n,s}\cdot\Pi^{S}_{m,n,s}\cdot\Delta t$
Step 2	Linear (LP)	$p^{S}_{m,n,s} = i^{S^*}_{m,n,s}\,(u_m - u_n) + i^{S}_{m,n,s}\,(u^*_m - u^*_n) - i^{S^*}_{m,n,s}\,(u^*_m - u^*_n)$	$\sum_{(m,n,s)\in\mathscr{L}} p^{S}_{m,n,s}p^{S}_{m,n,s}\cdot\Pi^{S}_{m,n,s}\cdot\Delta t + \sum_{m\in\mathscr{N}} \epsilon\cdot\mid u_m - u^*_m\mid$
Step 3	Linear (LP)	$p^{S}_{m,n,s} = i^{S^*}_{m,n,s}\,(u_m - u_n) + i^{S}_{m,n,s}\,(u^*_m - u^*_n) - i^{S^*}_{m,n,s}\,(u^*_m - u^*_n)$	$\sum_{(m,n,s)\in\mathscr{L}} p^{S}_{m,n,s}\cdot\Pi^{S}_{m,n,s}\cdot\Delta t$

Table 3.1: Three steps approach with corresponding power functions and objective functions used to derive LMP from OPF.

STEP 1: SOLVING THE ECONOMIC DISPATCH USING QCP

The problem is first solved using the bilinear equation (3.5), an optimal point is found by the non-linear solver. Under the assumption that this point is a maximum (the production cost is minimized by maximizing the algebraic sum of the cost of all generators given that they output a negative power), the economic dispatch is obtained and defined by of u_m and $i^{S}_{m,n,s}$ for all $m\in\mathscr{N}$ and all $(m,n,s)\in\mathscr{S}$. The other variables are computed accordingly.

STEP 2: LINEARIZATION AND THE PROXIMITY TERM

These values are used as fixed points to proceed to the linearization of the power function. From now on, u^*_m and $i^{S^*}_{m,n,s}$ denote the points obtained from step 1. They are used as given points to find a linear approximation while u_m and $i^{S}_{m,n}$ remain as variables in the linear optimization problem. Following Taylor series the power function is linearized around the given points u^*_m and $i^{S^*}_{m,n,s}$ as such:

$$p^{S}_{m,n,s} = i^{S^*}_{m,n,s}\,(u_m - u_n) + i^{S}_{m,n,s}\,(u^*_m - u^*_n) - i^{S^*}_{m,n,s}\,(u^*_m - u^*_n) \qquad \forall (m,n,s)\in\mathscr{S} \tag{3.16}$$

If the problem has a unique solution, after solving the OPF using the linearized power formula in conjunction with linear programming u_m and $i^{S}_{m,n}$ should have the same values as u^*_m and $i^{S^*}_{m,n}$. Depending on the scenarios, OPF problems may have multiple solutions leading to the same global objective. After linearizing the problem, in some cases a difference in the economic dispatch has been observed between the quadratic and linear problem while the global objective stayed the same. It suggests that multiple solutions are available. When the results varied from the two types of programming, it resulted in wrong LMP. In order to effectively generate nodal prices using dual variables, the quadratic and linear solvers have to find the same optimal points [100]. To guarantee that both solvers return the same optimum a proximity term is added to the objective function. The solver now maximizes the cost function as well as the voltage difference between u^*_m and u_m where ϵ is a value that is very close to zero but different from zero. The proximity term guarantee that u_m equals to u^*_m. The objective function becomes:

$$\max \sum_{(m,n,s)\in\mathscr{L}} p^{S}_{m,n,s}\cdot\Pi^{S}_{m,n,s}\cdot\Delta t + \sum_{m\in\mathscr{N}} \epsilon\cdot\mid u_m - u^*_m\mid \tag{3.17}$$

STEP 3: SOLVING FOR LMP BY USING LP AND REMOVING THE PROXIMITY TERM

LMP reflect the marginal cost of supplying the next increment of energy at every node. The proximity term in the objective function can have an impact on these prices. To ensure accurate LMP, the term has to be removed from the objective function. In GAMS when solving an optimization problem a basis is formed where information about the problem and its solution are stored. A basis created by a solver can easily be passed on to another model as long as these models are similar. It essentially ease the optimization process for the solver as it contains prior information about the optimal point. It is often used to compare models. Under the assumption that multiple solutions can lead to same global objective and to guarantee the same results from step 2 to 3, the basis of the second step created by the LP solver is passed on to the third step. As a result, u_m and $i^{\mathrm{S}}_{m,n,s}$ are the same and the LMP are accurate. The linear optimization problem now has the same objective function but is now subject to equation (3.16) instead of (3.5):

$$\begin{aligned} \max \quad & \sum_{(m,n,s)\in\mathscr{L}} p^{\mathrm{S}}_{m,n,s} \cdot \Pi^{\mathrm{S}}_{m,n} \cdot \Delta t \\ \text{s.t.} \quad & (3.1) - (3.4) \\ & (3.6) - (3.11) \\ & (3.16) \end{aligned} \tag{3.18}$$

In the literature referred in Chapter 2, LMP are expressed in terms of power. Indeed, in the AC OPF, nodal prices are obtained from the Lagrange multipliers of the power balance. In DC OPF, prices are obtained as the combination of the power balance dual variable, the loss term derived from power factors and the congestion term derived from dual variable of line limits. The implication of formulating the power flow in terms of current is reflected in LMP inherently expressed in terms of current as the power balance is substituted by the KCL. The marginal price at each node is denoted by λ^{I}_m for which the unit is \$/Ah. This term is directly obtained as the marginal value of 3.2 in step 3 after solving for the OPF.

Nevertheless, LMP can be translated in terms of \$/Wh by considering all set of nodes where at least one source is connected. It is important to note that a price, $\lambda^{P}_{m,n}$, is obtained for all $(m,n) \in \mathscr{P}$ and not for all $(m,n,s) \in \mathscr{S}$. Nodal prices depend on a set of nodes, not on a specific source. Using the power function (3.5) and considering that the LMP of the reference node is the cheapest and nearest available source, LMP are derived as follows:

$$c^{\mathrm{I}}_m = \lambda^{I}_m \cdot i^{\mathrm{S}}_{m,n} \qquad \forall m \in \mathscr{N} \tag{3.19}$$
$$i^{\mathrm{S}}_{m,n} = -i^{\mathrm{S}}_{n,m} \qquad \forall (m,n) \in \mathscr{P} \tag{3.20}$$
$$c^{\mathrm{P}}_{m,n} = c^{\mathrm{I}}_m + c^{\mathrm{I}}_n \qquad \forall (m,n) \in \mathscr{P} \tag{3.21}$$
$$= (\lambda^{\mathrm{I}}_m \cdot i^{\mathrm{S}}_{m,n}) + (\lambda^{\mathrm{I}}_n \cdot i^{\mathrm{S}}_{n,m}) \qquad \forall (m,n) \in \mathscr{P} \tag{3.22}$$
$$= i^{\mathrm{S}}_{m,n} \cdot (\lambda^{\mathrm{I}}_n - \lambda^{\mathrm{I}}_m) \qquad \forall m,n \in \mathscr{P} \tag{3.23}$$
$$\lambda^{\mathrm{P}}_{m,n} = \frac{c^{\mathrm{P}}_{m,n}}{(u_m - u_n) \cdot i^{\mathrm{S}}_{m,n}} = \frac{\lambda^{\mathrm{I}}_m - \lambda^{\mathrm{I}}_n}{u_m - u_n} \qquad \forall (m,n) \in \mathscr{P} \tag{3.24}$$

In (3.21) it is shown that the cost, $c^{\mathrm{P}}_{m,n}$, of injecting power into the resistive network at nodes m and n is equal to the cost c^{I}_m and c^{I}_n of injecting and extracting the respective current at those two nodes. The energy based LMP between those two nodes can be derived by (3.24). Which in the end is equal to the difference of current LMP divided by the voltage difference of the nodes.

3.3. THE MARGINAL LOSS COMPONENT IN LMP

As explained in Chapter 2, LMP are composed of the energy, loss and congestion terms . How to derive the loss component by hand is not exactly clear. Losses are modeled linearly (3.1) in the model, however losses are also indirectly defined quadratically, $p^{\mathrm{Loss}} = i^2_{m,n}/G_{m,n}$. Traditionally in power flows where voltages are assumed constant, the losses from a power flow, $F_{m,n}$, are obtained as $a_{m,n}F^2_{m,n}$. The average loss is given by $a_{m,n}F^2_{m,n}/F_{1,2} = a_{m,n}F_{m,n}$. In Section 2.3.4, the LMP loss term is expressed as the marginal loss rate or the change in system losses due to a change in generation. According to calculus, this rate is obtained as the derivative of the total losses where $\partial a_{m,n}F^2_{m,n}/\partial F_{m,n} = 2 \cdot a_{m,n}F_m$, [101]. It follows that the the marginal loss rate is approximately twice as much as the average loss rate [101, 102]. The difference between the different loss rates is expressed graphically in Figure 3.3b where the loss rates are the slope of the linear graph [103].

A simple example composed of two sources is used in this section to better explain how losses are incorporated into LMP. Summing the total generation cost with the cost of consumption result in a surplus. The LMP

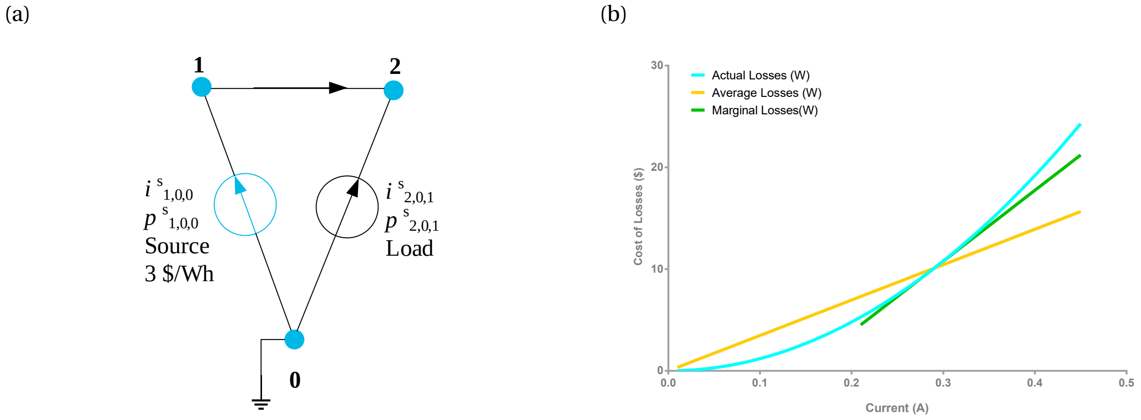

Figure 3.3: 3-nodes unipolar examples where the source is represented in blue and the load in black (Figure 3.3a). Losses are only occurring in line connecting node 1 to node 2. Assuming a time step of one hour, the load consumes 100 Wh. Figure 3.3b is a graphical representation of the cost of losses as a function of the power flow through a line.

obtained from the simulation for Source $s0$ and $s1$ are respectively 3 $/Wh and 3.20 $/Wh. Considering that LMP is the electricity price to be paid by the user to cover the cost of the energy consumption, the sum of the production cost and customer payment is expected to be equal to zero. In OPF where losses are not considered, the cost of generation and the cost paid by the consumer always balance. However in this case it results in a payment surplus of 10.55$ for a load of 100 Wh. Ergo, it suggests that the surplus is caused by the losses and that the cost paid by the user is more than the actual cost of losses in the network.

$$\pi^{S}_{1,0,1} \cdot p^{S}_{1,0,0} \cdot \Delta t + \lambda^{P_{2,0,1}} \cdot p^{S}_{2,0,1} \cdot \Delta t = -103.29 \cdot 3.00 + 100.00 \cdot 3.20 = 10.55 \quad \$ \tag{3.25}$$

For a load consuming 100 Wh, the generator approximately produces 0.29 A for a period of one hour, equivalent to 103.29 Wh. The excess energy, 3.29 Wh, is lost in the distribution line. Therefore, in this scenario the cost of physical losses is equal to $3\$ \cdot 3.29Wh = 9.87\$$. This cost is also obtained from the actual losses in Figure 3.3b for the given current output. As explained in Section 2.3.4, the loss component of LMP do not reflect the cost of physical losses but rather marginal losses [44]. Given that the energy component is equal to 3 $/Wh it follows that the loss component is equal to 0.20 $/Wh. This cost covers the physical losses and generate a revenue. The surcharge, 10.55$, is almost equal to the actual cost of losses which suggests that the marginal loss rate is obtained from the derivative of total losses. Consequently the total cost paid by the consumer is approximately twice as much as the actual cost of losses. It is noteworthy to remark that the surplus is not exactly equal to the cost of losses which implies that the customer pays slightly more than twice the cost of losses. The reasons why this occurs may be that the power flow does not assume constant voltages.

3.4. SIMULATION EXAMPLES

In this section a few simple examples are used to demonstrate the validity of the model. A simple non-meshed configuration is first used to highlight the working principles and possibilities of the model. For the reasons stated in Chapter 1, bipolar networks are used, however it is important to mention that the model can also be applied to unipolar networks. An additional example is provided to show the different configurations in which sources can be connected. Finally, an example of simple mesh grid is provided. In all cases generators can be seen as diesel generators for which a variable cost representing the fuel cost is assigned. Simulations are performed using GAMS and CONOPT is the preferred solver for both quadratic and linear programming [104].

3.4.1. NON-MESHED BIPOLAR LVDC NETWORK WITH UNIQUE SOURCE CONFIGURATION

Figure 3.4 shows a network consisting of 12-nodes connected by a positive, neutral and negative conductor. Sources are connected across the neutral conductor and the positive or negative pole only. Note that for simplification, multiple sources across the same pair of nodes is not considered in these cases. Four ideal sources represent DG producing variable outputs and four ideal sources represent different loads for which the power consumed is conventionally positive and fixed to a specific value as in (3.12)-(3.13). The simulation only consider one time period, for simplification the time step is set to one hour.

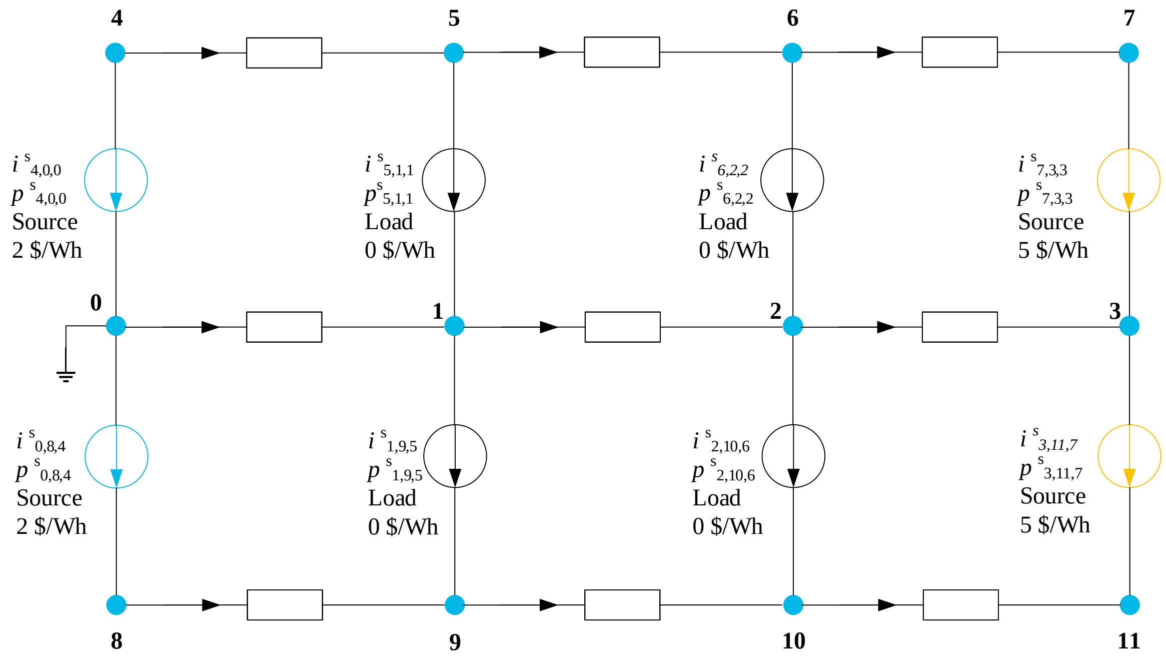

Figure 3.4: Case 1, 2 and 3: Network topologies used in the simulation examples. Inexpensive generators are denoted in blue, expensive generators in yellow and loads in black.

Three cases configured as in Figure 3.4 are presented in which both symmetric and asymmetric loading between the positive and negative polarity are simulated. The effect of generation capacity, lines' conductance and capacity on LMP is examined. Note that sources can either be subject to a current or power constraints, it gives the possibility to model loads as constant power or constant current. In the following examples loads are modeled as constant power, they are fixed to a specific power level. In Tables A.1, A.3 and A.6 the upper and lower bounds of generators and fixed limits of loads are displayed for all cases. Line capacities and conductance are displayed in Tables A.2, A.4 and A.7. The network is grounded at node 0 and voltage constraints with respect to each conductor are as follows where nodes $[4,5,6,7] \in \mathcal{N}_+$, $[8,9,10,11] \in \mathcal{N}_-$ and $[0,1,2,3] \in \mathcal{N}_\mathrm{N}$:

$$340 \leq u_m \leq 360 \qquad \forall m \in \mathcal{N}_+ \tag{3.26}$$

$$340 \leq -u_m \leq 360 \qquad \forall m \in \mathcal{N}_- \tag{3.27}$$

$$-10 \leq u_m \leq 10 \qquad \forall m \in \mathcal{N}_\mathrm{N} \tag{3.28}$$

CASE 1: THE ROLE OF LOSSES ON LMP

This case seeks to demonstrate how losses through distribution cables are incorporated into LMP. To do so, the network is configured symmetrically. All parameters and limits are set equal for both polarities. To allow unconstrained operation of DG, the upper capacity of the cheapest sources exceed the total loading of the grid. Furthermore, branches are not limited by the amount of current that can flow through them. The line resistance is the same in all conductors of different polarities. However, the resistance in branches with the following conductance $G_{5,6}$, $G_{1,2}$ and $G_{9,10}$ is larger. Resistance vary as function of distance, increasing the resistance at this location can be seen as longer distribution cables. In other words no constraints is activated.

Looking at Table 3.2, it is clear that only the cheapest generators produce power, note that they operate below their maximum capacities. This is why no current is flowing in branches connecting node 6-7, 2-3 and 10-11. Consequently voltages are the same in these sets of nodes. Due to symmetry, there is no current flowing in the neutral conductor. This is the preferred scenario in a bipolar network, the absence of a current in the ground line effectively reduces system losses. Generators $p^S_{4,0,0}$ and $p^S_{0,8,4}$ generate more than the loads consume, they have to make up for power losses in cables.

With regards to LMP, prices in between each node where a source is connected are derived from the marginal cost of the cheapest generators, 2 \$/Wh. The variation in prices is only caused by power losses, as a result LMP increase as a function of the distance/resistance from the operating sources. Consequently the larger resistances in connecting branches at the center of the network lead to a larger price difference. This is expressed by the much higher nodal prices $\lambda^P_{6,2}$ and $\lambda^P_{2,10}$. No price difference is seen between nodes on the right side as no current is flowing in the lines. It can be concluded that using LMP as a tool to price electricity takes losses into consideration. In distribution grids losses cannot be omitted and customers should be charged for the additional power supply require to satisfy loads.

Outputs	Generation Units[W]				Generation Units [A]				LMP [\$/Wh]			
	$p^S_{4,0,0}$	$p^S_{5,1,1}$	$p^S_{6,2,2}$	$p^S_{7,3,3}$	$i^S_{4,0,0}$	$i^S_{5,1,1}$	$i^S_{6,2,2}$	$i^S_{7,3,3}$	$\lambda^P_{4,0}$	$\lambda^P_{5,1}$	$\lambda^P_{6,2}$	$\lambda^P_{7,3}$
Case 1	-206.71	100.00	100.00	0.00	-0.57	0.28	0.29	0.00	2.00	2.07	2.21	2.21
Case 2	-173.10	100.00	100.00	-29.15	-0.48	0.28	0.28	-0.08	2.00	2.08	5.04	5.00
Case 3	-172.35	100.00	100.00	-28.04	-0.48	0.28	0.28	-0.08	2.00	1.98	5.03	5.00
	$p^S_{0,8,4}$	$p^S_{1,9,5}$	$p^S_{2,10,6}$	$p^S_{3,11,7}$	$i^S_{0,8,4}$	$i^S_{1,9,5}$	$i^S_{2,10,6}$	$i^S_{3,11,7}$	$\lambda^P_{0,8}$	$\lambda^P_{1,9}$	$\lambda^P_{2,10}$	$\lambda^P_{3,11}$
Case 1	-206.71	100.00	100.00	0.00	-0.57	0.28	0.29	0.00	2.00	2.07	2.21	2.21
Case 2	-204.80	100.00	100.00	0.00	-0.57	0.28	0.29	0.00	2.00	2.06	2.09	2.11
Case 3	-300.00	100.00	200.00	-14.78	-0.83	0.29	0.59	-0.04	4.41	4.75	5.01	5.00

Table 3.2: Case 1, 2 and 3: Outputs of simulations with generation level of each source in terms of power and current and LMP formulated in term of power for set of node connecting at least one source are displayed.

CASE 2: THE ROLE OF CONGESTIONS ON LMP

This case demonstrates how congestion impact network operations and LMP when a branch current constraint is introduced in the grid. Similarly to the previous example, the operational capacity of inexpensive generators, $p^S_{0,8,4}$ and $p^S_{4,0,0}$, exceed the total loading. To properly compare the effect of a congestion, the loading within the network is symmetrical and the resistance is set to the same value in each line. A current limit $I_{5,6,\max}$ of 0.2 A is implemented. Note that this is not a realistic case, otherwise $I_{1,2,\max}$ and $I_{9,10,\max}$ would most likely be limited as well. Operating ranges are determined by cable properties, in a bipolar configuration lines connecting the equivalent nodes in the different polarities should use identical cables of approximately the same length. Here the constraint is only applied to $I_{5,6,\max}$ in order to compare nodal prices of the positive and negative polarity. It prevents $i^S_{4,0,0}$ from fully feeding loads $i^S_{5,1,1}$ and $i^S_{6,2,2}$.

The upper limit imposed on the line between node 5-6 forces generator $p^s_{7,3,3}$ to supplement the inexpensive generator $p^s_{4,0,0}$ to satisfy Load $p^s_{6,2,2}$. On Table 3.3 it can be seen that the current $i_{5,6}$ is at its maximum, a congestion is occurring. The negative value of $i_{6,7}$ indicates that current is flowing from node 7 to 6. Although the grid is loaded symmetrically, the congestion induce a current in the neutral conductor as a result in the different behaviors of generator in the positive and negative polarity.

The effect of this constraint on LMP is displayed in Table 3.2. As opposed to the previous example, nodal prices are not the same in the two polarities. $\lambda^P_{6,2}$ and $\lambda^P_{7,3}$ reveal that the next increment of energy at these locations will be supplied by the most expensive sources due to the congestion. These prices are indeed closer to $\Pi^S_{7,3,3}$. On the other hand, $\lambda^P_{4,0}$ and $\lambda^P_{5,1}$ show that across these nodes energy supply is not affected by the congestion and prices are derived from $\Pi^S_{4,0,0}$. Looking at the negative polarity, all prices are derived from the inexpensive unconstrained generator. Therefore, congestion can cause asymmetries in bipolar grids resulting in different prices in each polarity. The impact of the congestion is clearly reflected when LMP are expressed in terms of current (Table 3.3).

Outputs	Branch Current [A]			Node Voltage [V]				LMP [$/Wh]			
	$i_{4,5}$	$i_{5,6}$	$i_{6,7}$	u_4	u_5	u_6	u_7	λ^{I}_4	λ^{I}_5	λ^{I}_6	λ^{I}_7
Case 1	0.57	0.29	0.00	360.00	354.26	342.58	342.58	-720.0	-732.0	-758.3	-758.1
Case 2	0.48	0.20	-0.08	360.00	355.19	353.19	354.01	-724.2	-740.2	-1786.2	-1782.3
Case 3	0.48	0.20	-0.08	360.00	355.21	353.21	353.99	-675.1	-691.2	-1810.6	-1806.8
	$i_{0,1}$	$i_{1,2}$	$i_{2,3}$	u_0	u_1	u_2	u_3	λ^{I}_0	λ^{I}_1	λ^{I}_2	λ^{I}_3
Case 1	0.00	0.00	0.00	0.00	0.00	0.00	0.00	0.00	0.00	0.00	0.0
Case 2	0.09	0.08	0.08	0.00	-0.88	-1.74	-2.56	-4.2	-0.08	4.1	0.0
Case 3	0.36	0.35	0.03	0.00	-3.55	-7.00	-7.35	44.2	18.9	1.7	0.0
	$i_{8,9}$	$i_{9,10}$	$i_{10,11}$	u_8	u_9	u_{10}	u_{11}	λ^{I}_8	λ^{I}_9	$\lambda^{\mathrm{I}}_{10}$	$\lambda^{\mathrm{I}}_{11}$
Case 1	-0.57	-0.29	0.00	-360.00	-354.26	-342.58	-342.58	720.0	732.3	758.1	758.1
Case 2	-0.57	-0.29	0.00	-360.00	-354.31	-351.45	-351.45	715.7	727.5	733.5	733.5
Case 3	-0.83	-0.55	0.04	-360.00	-351.67	-346.21	-346.64	1630.3	1671.3	1698.7	1696.5

Table 3.3: Case 1, 2 and 3: Outputs of simulations with branch, node currents and corresponding LMP formulated in terms of current for each node for which a source is connected to.

CASE 3: THE ROLE OF CAPACITY CONSTRAINTS ON LMP

In Case 1 and 2 the impact of losses and congestion on LMP were investigated. Case 3 demonstrates the third component that can affect nodal prices, namely capacity constraint. The effect of having both congestion and sources working at full capacity is shown. The line constraint is setup on the same branch, $I_{5,6,\max}$, as Case 2. In order to force the inexpensive generator, $p^{\mathrm{s}}_{0,8,4}$, to its full capacity an asymmetry is introduced by raising load $p^{\mathrm{s}}_{2,10,6}$ to 200 W.

With regards to the negative polarity, the inability of unit $p^{\mathrm{s}}_{0,8,4}$ to supply the increase in demand forces $p^{\mathrm{s}}_{3,11,7}$ to participate in the demand-supply balance. All LMP values on this side of the network are closer to the marginal cost of the most expensive generator. Indeed, the inexpensive Source $p^{\mathrm{s}}_{0,8,4}$ is at its boundary, the next increment of energy cannot be expected from this generator. An interesting observation is that $\lambda^{\mathrm{P}}_{3,11}$ and $\lambda^{\mathrm{P}}_{2,10}$ are equal and slightly higher than $\Pi^{\mathrm{S}}_{3,11,7}$ while $\lambda^{\mathrm{P}}_{1,9}$ and $\lambda^{\mathrm{P}}_{0,8}$ are both lower. At first it looks counter intuitive. However, it should be noted that both $i_{8,9}$ and $i_{9,10}$ are flowing from right to left and $i_{10,11}$ is flowing from left to right. This is due to the flow in the positive pole. These prices reveal that increasing the power consumption between either node 8-0 and 1-9 would decrease system losses. As the load at these locations is increased $\lambda^{\mathrm{P}}_{1,9}$ and $\lambda^{\mathrm{P}}_{0,8}$ get closer to $\Pi^{\mathrm{S}}_{3,11}$. The same phenomena is observed in the positive pole where $\lambda^{\mathrm{P}}_{5,1}$ is lower than the marginal cost $\Pi^{\mathrm{S}}_{4,0,0}$. Due to the presence of the current in the negative conductor and if $p^{\mathrm{s}}_{5,1,1}$ would be incremented by one unit, generator $p^{\mathrm{s}}_{4,0,1}$ would have to produce less than one unit to satisfy this load. As a result we obtain LMP with lower values than the marginal cost of generators.

3.4.2. NON-MESHED AND MESHED BIPOLAR LVDC NETWORK WITH MULTIPLE SOURCE CONFIGURATIONS

Two networks are proposed to demonstrate how physical laws govern power flows and impact LMP. In these examples, nodal prices are determined by the circuit configuration rather than generator and line capacities.

As a result LMP may greatly differ from the marginal costs of generators. Two cases are studied, Case 4 illustrated in Figure 3.5a is a non-meshed network composed of sources with different configurations and Case 5 illustrated in 3.5b is a meshed bipolar network. Similarly to the previous examples Δt is set to one hour and voltage limits are given by equations (3.26)-(3.28). The rest of the parameters are displayed in Appendix A.

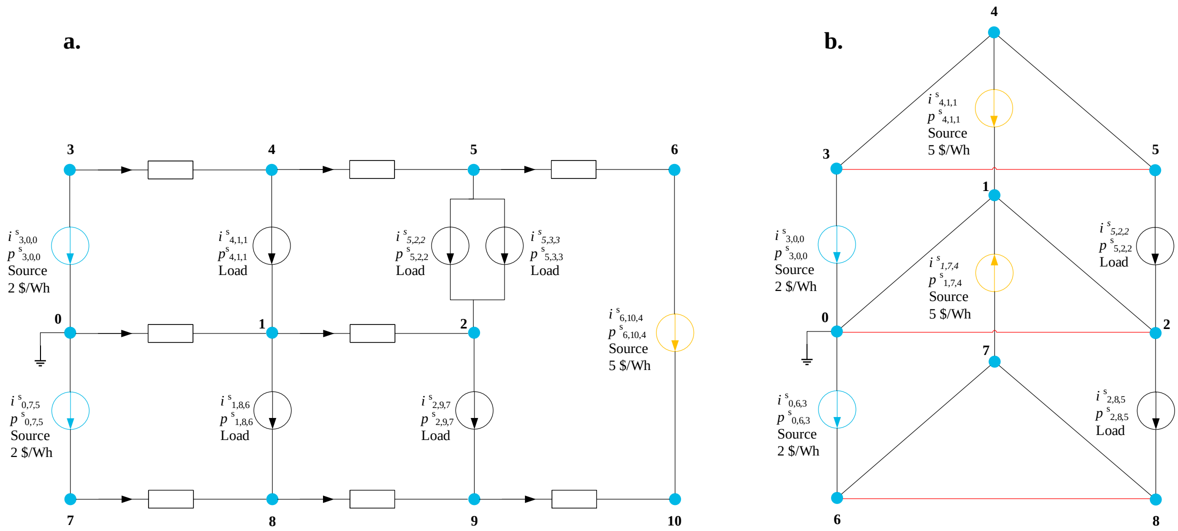

Figure 3.5: Case 4.1-5: Network topologies used in the simulation examples. Figure 4.1a refers to case 6.1, 6.2 & 6.3, Figure 4.1b refers to case 7. Inexpensive generators are denoted in blue, expensive generators in yellow, loads in black and line congestion in red.

Case 4: The role of Sources Configuration on LMP

The network in Figure 3.5a consist of 11-nodes connected by a positive, neutral and negative conductor where $[3,4,5,6] \in \mathcal{N}_{+}$, $[7,8,9,10] \in \mathcal{N}_{-}$ and $[0,1,2] \in \mathcal{N}_{\mathrm{N}}$. Sources are setup using three different configurations. As in the previous examples they can be connected to the neutral conductor and the positive or negative conductor. A set of nodes $(m,n) \in \mathcal{P}$ can also have multiple sources as in between node 2-5. Moreover, the model offer the possibility to fully exploit the advantages of bipolar grids by allowing a source to be directly connected from the positive to negative pole. Larger loads and generator units can thus benefit from a large Δu for higher power generation or consumption. Two subcases, 4.1 and 4.2, are used to measure the impact of this source configuration on the power flow and LMP. Three ideal sources represent DG producing variable power outputs and five sources represent constant power loads. The economic dispatch and corresponding LMP are displayed in Table 3.4 and the node currents, branch currents and $\lambda^{\mathrm{I}}_{m,n}$ are available in Table A.5.

No congestion occur in Case 4.1, however the inexpensive generator $p^{\mathrm{s}}_{3,0,0}$ is operating at its maximum capacity forcing the expensive generator $p^{\mathrm{s}}_{6,10,4}$ to activate to satisfy the loads located in the positive pole. The presence of a source connected to the positive and negative conductor changes the behavior of power flows in comparison to previous cases. In Case 1-3, the positive and negative side of the network could be interpreted as independent from each other resulting in LMP derived from the marginal price of the generators in their respective poles. Here $p^{\mathrm{s}}_{6,10,4}$ directly connects conductors with opposite polarities, the negative and positive side of the network cannot operate independently anymore if $p^{\mathrm{s}}_{6,10,4}$ is activated.

The impact of this source configuration is reflected on $\lambda^{\mathrm{P}}_{3,0}$, $\lambda^{\mathrm{P}}_{4,1}$ and $\lambda^{\mathrm{P}}_{5,2}$. At these location nodal prices are much higher than 2\$/Wh or 5\$/Wh. Source $p^{\mathrm{s}}_{3,0,0}$ is operating at its maximum capacity, therefore it cannot respond to an increment in either of the load in contact with the positive conductor. That can be seen in Case 4.2 in which the load $s3$ is incremented by one power unit in caparison to Case 4.1. Although the inexpensive source $p^{\mathrm{s}}_{0,7,5}$ is not operating at its upper bound circuits laws prohibit it from participating to the supply-demand balance when $p^{\mathrm{s}}_{6,10,4}$ is active. A raise in the power production at this location to supply an increment of one unit at either $p^{\mathrm{s}}_{4,1,1}$, $p^{\mathrm{s}}_{5,2,2}$ or $p^{\mathrm{s}}_{5,2,3}$ inherently induce a decrease in the power production of $p^{\mathrm{s}}_{0,7,5}$. Consequently, $p^{\mathrm{s}}_{6,10,4}$ has to provide more than one power unit so that KCL is satisfied at all nodes. Such behavior explains why LMP of the positive side are much higher than $\Pi^{\mathrm{S}}_{3,10,4}$. Using $\lambda^{\mathrm{P}}_{3,0}$ and $\Pi^{\mathrm{S}}_{3,10,4}$ it can be deduced that for an increment of one unit in either load of the positive polarity, $p^{s}_{6,10,4}$ has to roughly provide 2 unit of power. This is reflected in the outputs of Case 4.2 in Table 3.4. The power produced by $p^{s}_{0,7,5}$ decrease from 93.91 W to 92.83 W while the power produced by $p^{s}_{6,10,4}$ increase from 214.181 W to 216.312 W. Nodal prices of the positive polarity are thus a combination of the marginal cost of production of both generators. The difference in cost upon an increment of unit of $s3$ is computed analytically in (3.29). Note that this cost difference is not exactly the same as in Table 3.4, the difference is caused by extra losses that are not taken into account in the below formula:

$$\lambda^{\mathrm{P}}_{5,2} = [5 \cdot (216.31 - 214.18) - 2 \cdot (93.91 - 92.83)] \cdot 1\mathrm{h} = 8.49 \quad \$ \tag{3.29}$$

Outputs	Generation Units[W]				Generation Units [A]				LMP [$/Wh]		
	$p^{\mathrm{S}}_{3,0,0}$	$p^{\mathrm{S}}_{4,1,1}$	$p^{\mathrm{S}}_{5,2,2}$	$p^{\mathrm{S}}_{5,2,3}$	$i^{\mathrm{S}}_{3,0,0}$	$i^{\mathrm{S}}_{4,1,1}$	$i^{\mathrm{S}}_{5,2,2}$	$i^{\mathrm{S}}_{5,2,3}$	$\lambda^{\mathrm{P}}_{3,0}$	$\lambda^{\mathrm{P}}_{4,1}$	$\lambda^{\mathrm{P}}_{5,2}$
Case 4.1	-200.00	100.00	100.00	100.00	-0.556	0.284	0.289	0.289	7.638	8.156	8.517
Case 4.2	-200.00	100.00	100.00	101.00	-0.556	0.284	0.289	0.292	7.640	8.163	8.524
	$p^{\mathrm{S}}_{0,7,5}$	$p^{\mathrm{S}}_{1,8,6}$	$p^{\mathrm{S}}_{2,9,7}$	–	$i^{\mathrm{S}}_{0,7,5}$	$i^{\mathrm{S}}_{1,8,6}$	$i^{\mathrm{S}}_{2,9,7}$	–	$\lambda^{\mathrm{P}}_{0,7}$	$\lambda^{\mathrm{P}}_{1,8}$	$\lambda^{\mathrm{P}}_{2,9}$
Case 4.1	-93.91	100.00	100.00	–	-0.274	0.292	0.289	–	2.000	1.834	1.659
Case 4.2	-92.83	100.00	100.00	–	-0.271	0.292	0.289	–	2.000	1.832	1.656
	$p^{\mathrm{S}}_{6,10,4}$	–	–	–	$i^{\mathrm{S}}_{10,6,4}$	–	–	–	$\lambda^{\mathrm{P}}_{10,6}$	–	–
Case 4.1	-214.18	–	–	–	-0.307	–	–	–	5.000	–	–
Case 4.2	-216.31	–	–	–	-0.310	–	–	–	5.000	–	–

Table 3.4: Case 4.1 and 4.2: Outputs of simulations with generation level of each source in terms of power and current and LMP formulated in term of power for set of node connecting at least one source are displayed.

CASE 5: THE ROLE OF MESHED CONFIGURATION ON LMP

This example is used to assess the validity of the proposed model for meshed grids. The simplest meshed layout is shown in Figure 3.5b. The network is comprised of 9 nodes for which $[3,4,5] \in \mathcal{N}_{+}$, $[6,7,8] \in \mathcal{N}_{-}$ and $[0,1,2] \in \mathcal{N}_{\mathrm{N}}$. Sources are all connected to the neutral conductor and there is only one source for each $(m,n) \in \mathcal{P}$. Line constraints $I_{3,5,\max}$, $I_{0,2,\max}$ and $I_{0,8,\max}$ are set to 0.1 A. In meshed network natural power flows dictate where power flows to. For example, when a generating unit is connected to two power lines it is impossible to directly allocate electrical flows among these lines. In this case, given that all $G_{m,n}$ are the same, 2/3 of the power generated by the generator will flow through the shortest path and the remaining third will flow through the longest path. Using the same layout two sub-cases, namely 5.1 and 5.2, are used to demonstrate how natural flows can affect nodal prices. The economic dispatch and corresponding LMP are displayed in Table 3.5 and the node currents, branch currents and $\lambda^{\mathrm{I}}_{m,n}$ are available in Table A.8.

In Case 5.1, symmetrical loading is implemented and a current constraints limit flows between nodes 3-5, 0-2 and 6-8. As a result, the inexpensive generators $p^{s}_{3,0,0}$ and $p^{s}_{0,6,3}$ cannot provide the power required by the loads. Moreover, cheap generators are indirectly constrained by natural flows. Although, they have sufficient capacity to satisfy both loads current cannot be forced to flow through lines $i_{3,4}$, $i_{4,5}$, $i_{6,7}$ and $i_{7,8}$. Since resistances are equivalent in all branches, if 0.1 A can flow through $i_{3,5}$ and $i_{6,8}$ only 0.05 A can flow through $i_{3,4}$, $i_{4,5}$, $i_{6,7}$ and $i_{7,8}$. However, as can be seen in Table 3.5 the loads consume roughly 0.28 A, the expensive generators $p^{s}_{4,1,1}$ and $p^{s}_{1,7,7}$ are forced to operate. As a consequence of natural flows in the network, the maximum contribution of $p^{s}_{3,0,0}$ and $p^{s}_{0,6,3}$ is rather small in comparison to $p^{s}_{4,1,1}$ and $p^{s}_{1,17,7}$.

LMP at generator's location are equal to the marginal costs of production as they are not operating at their boundaries. However, nodal prices at the loads are much higher than any $\Pi^{\mathrm{S}}_{m,n,s}$. These prices is the consequence of both the mesh configuration and the line constraints. Similarly to Case 4, $\lambda^{\mathrm{P}}_{5,2}$ and $\lambda^{\mathrm{P}}_{2,8}$ are derived from the price of the marginal cost of generators. An increment of one unit in the Load $p^{s}_{5,2,2}$ is implemented in Case 5.2. From Table 3.5 it can be seen that due to the natural flows the next increment of power has to be provided by the expensive generator $p^{s}_{4,1,1}$. To satisfy physical laws the output of $p^{s}_{3,0,0}$ is decreased when compared to its output in Case 5.1. Ergo, an increase of unit at the load obliges the expensive generator to increase its output level by roughly 2 units while the cheapest generator decreases its output level by roughly 1 unit. Nodal prices at the load locations are a combination of these two factors as described in (3.30). Note that the difference between the difference in production computed analytically and the $\lambda^{P}_{5,2}$ from the model outputs is caused by the losses that are not taken into account in (3.30).

$$\lambda^{P}_{5,2} = [5 \cdot (95.03 - 93.00) - 2 \cdot (7.48 - 6.47)] \cdot 1\text{h} = 8.13 \quad \$ \tag{3.30}$$

Outputs	Generation Units[W]			Generation Units [A]			LMP [$/Wh]		
	$p^{S}_{3,0,0}$	$p^{S}_{4,1,1}$	$p^{S}_{5,2,2}$	$i^{S}_{3,0,0}$	$i^{S}_{4,1,1}$	$i^{S}_{5,2,2}$	$\lambda^{P}_{3,0}$	$\lambda^{P}_{4,1}$	$\lambda^{P}_{5,2}$
Case 5.1	-7.48	-93.00	100	-0.021	-0.258	0.279	2.000	5.000	8.106
Case 5.2	-6.472	-95.03	101	-0.018	0.26	0.28	2.000	5.000	8.110
	$p^{S}_{0,6,3}$	$p^{S}_{1,7,4}$	$p^{S}_{2,8,5}$	$i^{S}_{0,6,3}$	$i^{S}_{1,7,4}$	$i^{S}_{2,8,5}$	$\lambda^{P}_{0,6}$	$\lambda^{P}_{1,7}$	$\lambda^{P}_{2,8}$
Case 5.1	-7.48	-93.00	100	-0.021	-0.258	0.279	2.000	5.000	8.106
Case 5.2	-7.48	-92.99	100	-0.021	-0.258	-0.279	2.000	5.000	8.105

Table 3.5: Case 5.1 and 5.2: Outputs of simulations with generation level of each source in terms of power and current and LMP formulated in term of power for set of node connecting at least one source are displayed.

4

Modeling Energy Storage Systems

In this chapter energy storage is introduced to the OPF. ESS are essential in environments where energy availability is intermittent. To fully utilize these resources, namely wind and solar energy, battery have to be used for peak shaving. Balancing the energy supply-demand throughout the day or even longer time frames. Storage is thus time dependent and the energy content of storage units depend on the previous time period. So far we only considered single time period cases for which Δt is set to one hour. The model has to be adjusted to a multi-period model enabling control of ESS. Moreover, the system can be made more realistic by including time dependent solar or wind profiles. The impact of storage on LMP is investigated through different case studies. Up to now, the cost was assigned on the generator side and considered to be an operational cost representing fuel consumption. The concept of renewable energy with zero marginal cost is considered and a cost assigned on the load side is introduced to reflect user's willingness to consumer energy. It also enables demand-responce mechanisms.

4.1. Multi-period Power Flow for Bipolar Distribution Grids with ESS

4.1.1. Multi-Period Modeling of the Grid and Sources

Power flow equations presented in Section 3.1 have to be adjusted for the multi-period approach. A new index defining time periods is introduced to solve for the OPF at every step. Periods are denoted by k and assigned as such $k0, k1, k2$... Variables that were expressed in terms of two or three indexes, (m,n) or (m,n,s), now have an additional time component. Note that only $G_{m,n}$ is time independent as line resistance is only defined by the network topology. The grid layer is now modeled using (4.1) and (4.2), the source layer is modeled using (4.3) and (4.4). The power term is expressed in (4.5).

$$i_{m,n,k} = G_{m,n}(u_{m,k} - u_{n,k}) \qquad \forall (m,n) \in \mathcal{G}, \qquad k \in \mathcal{K} \tag{4.1}$$

$$i_{m,k} = \sum_{n|(m,n)\in\mathcal{G}} i_{m,n,k} - \sum_{n|(m,n)\in\mathcal{G}} i_{n,m,k} \qquad \forall m \in \mathcal{N}, \qquad k \in \mathcal{K} \tag{4.2}$$

$$i^{S}_{m,n,k} = \sum_{s|(m,n,s)\in\mathcal{S}} i^{S}_{m,n,s,k} \qquad \forall (m,n) \in \mathcal{P}, \qquad k \in \mathcal{K} \tag{4.3}$$

$$i_{m,k} = \sum_{n|(n,m)\in\mathcal{P}} i^{S}_{n,m,k} - \sum_{n|(n,m)\in\mathcal{P}} i^{S}_{m,n,k} \qquad \forall m \in \mathcal{N}, \qquad k \in \mathcal{K} \tag{4.4}$$

$$p^{S}_{m,n,s,k} = i^{S}_{m,n,s,k} * \left(u_{m,k} - u_{n,k}\right) \qquad \forall (m,n,s) \in \mathcal{S}, \qquad k \in \mathcal{K} \tag{4.5}$$

With regards to inequality constraints, most remain unchanged as they depend on the network topology rather than time. Voltage limits are constant throughout the whole simulation and so are the branch current limits. However, generation capacities are set to be time dependent and correlated to the renewable energy profiles. In the case of solar energy, the upper panels' capacity limits in terms of power can be set as a function of the irradiance given that an efficiency and size is predefined. Simultaneously, the upper current capacity limit of a solar panel is independent from time and set accordingly to the panel's specification sheet. Concerning loads, time dependency allows for load fluctuation with reference to time. The inequality constraint for multi-period simulation are as follow:

$$U_{\min} \leq u_{m,k} \leq U_{\max} \qquad \forall m \in \mathcal{N}_+, \qquad k \in \mathcal{K} \tag{4.6}$$
$$U_{\min} \leq -u_{m,k} \leq U_{\max} \qquad \forall m \in \mathcal{N}_-, \qquad k \in \mathcal{K} \tag{4.7}$$
$$U_{\mathrm{N},\min} \leq u_{m,k} \leq U_{N,\max} \qquad \forall m \in \mathcal{N}_{\mathrm{N}}, \qquad k \in \mathcal{K} \tag{4.8}$$
$$I_{m,n,\min} \leq i_{m,n,k} \leq I_{m,n,\max} \qquad \forall (m,n) \in \mathcal{G}, \qquad k \in \mathcal{K} \tag{4.9}$$
$$I^{\mathrm{S}}_{m,n,s,\min} \leq i^{\mathrm{S}}_{m,n,s,k} \leq I^{\mathrm{S}}_{m,n,s,\max} \qquad \forall (m,n,s) \in \mathcal{S}, \qquad k \in \mathcal{K} \tag{4.10}$$
$$P^{\mathrm{S}}_{m,n,s,k,\min} \leq p^{\mathrm{S}}_{m,n,s,k} \leq P^{\mathrm{S}}_{m,n,s,k,\max} \qquad \forall (m,n,s) \in \mathcal{S}, \qquad k \in \mathcal{K} \tag{4.11}$$

4.1.2. MODELING OF ENERGY STORAGE SYSTEMS

The modified power flow model described by (4.1)-(6.3) now support energy storage units. ESS are modeled as sources, they behave as generators during discharge and as loads during discharge. Thus, $p^{\mathrm{S}}_{m,n,s,k}$ is positive while charging and negative while discharging. The energy content of ESS during time period k depends on the energy content and the energy stored or extracted in/from the unit during the previous time period (4.13). This is calculated by integrating power flows going in and out of batteries over time. The conversion efficiency factor is considered by introducing two variables, $p^{\mathrm{S,charge}}_{m,n,s,k}$ and $p^{\mathrm{S,discharge}}_{m,n,s,k}$, respectively subject to $\eta^{charge}_{m,n,s}$ and $\eta^{discharge}_{m,n,s}$. The round-trip efficiency is the product of both [105]. In this model it is assumed that these efficiencies are set equal and constant in time. The power variable, $p^{\mathrm{S}}_{m,n,s,k}$, is the link between the ESS model and the above power flow model. The power flowing in or out an ESS is obtained from (4.14). The energy content, $e^{\mathrm{S}}_{m,n,k}$, is set to 0 for the first time period k_0.

$$e^{\mathrm{S}}_{m,n,s,k_0} = 0 \qquad \forall (m,n,s) \in \mathcal{F}, \tag{4.12}$$
$$e^{\mathrm{S}}_{m,n,s,k} = e^{\mathrm{S}}_{m,n,s,k-1} + p^{\mathrm{S,charge}}_{m,n,s,k-1} * \eta^{\mathrm{ESS}}_{m,n,s} * \Delta t + p^{\mathrm{S,discharge}}_{m,n,s,k-1} * \frac{1}{\eta^{\mathrm{ESS}}_{m,n,s}} * \Delta t \qquad \forall (m,n,s) \in \mathcal{F}, \qquad k \in \mathcal{K} \tag{4.13}$$
$$p^{\mathrm{S}}_{m,n,s,k} = p^{\mathrm{S,charge}}_{m,n,s,k} + p^{\mathrm{S,discharge}}_{m,n,s,k} \qquad \forall (m,n,s) \in \mathcal{F}, \qquad k \in \mathcal{K} \tag{4.14}$$

A set of inequality constraints bound the variables introduced in (4.12)-(4.14). The energy content, $e^{\mathrm{S}}_{m,n,k}$, represent how much energy is available within a given storage unit. The amount of energy that can be stored is thus limited by the size of the battery. In this chapter, as opposed to Chapter 5 where the size of the storage can be set a variable, the storage capacity is a parameter defined as $E^{\mathrm{ESS}}_{m,n,s,\max}$. The lower limit, $E^{\mathrm{ESS}}_{m,n,s,\min}$, has to be greater than 0 Wh. Note that the problem is not formulated in terms of state of charge as it would result in an additional non-linear equation, however a minimum energy content in the storage can be assigned individually to each battery. The inequality constraint imposed on $e^{\mathrm{S}}_{m,n,k}$ is expressed by (4.15). A maximum and minimum limit bounds $p^{\mathrm{S,discharge}}_{m,n,s,k}$ and $p^{\mathrm{S,charge}}_{m,n,s,k}$, it forces the power to be negative during discharge and positive during charge.

$$E^{\mathrm{ESS}}_{m,n,s,\min} \leq e^{\mathrm{S}}_{m,n,s,k} \leq E^{\mathrm{ESS}}_{m,n,s,\max} \qquad \forall (m,n,s) \in \mathcal{F}, \qquad k \in \mathcal{K} \tag{4.15}$$
$$p^{\mathrm{S,charge}}_{m,n,s,k} \geq 0 \qquad \forall (m,n,s) \in \mathcal{F}, \qquad k \in \mathcal{K} \tag{4.16}$$
$$p^{\mathrm{S,discharge}}_{m,n,s,k} \leq 0 \qquad \forall (m,n,s) \in \mathcal{F}, \qquad k \in \mathcal{K} \tag{4.17}$$

Modeling storage units using two variables, $p^{\mathrm{S,charge}}_{m,n,s,k}$ and $p^{\mathrm{S,discharge}}_{m,n,s,k}$, is equivalent to considering two sources either injecting or extracting current from the grid. The above formulation do not prevent these sources to operate simultaneously which would result in physical infeasibilities. Batteries can either charge or discharging at a given time. This problem is avoided if two conditions are respected, the round-trip efficiency has to be less than 1 and the marginal cost on sources has to be positive. Minimizing the production cost implies that the minimum for a time period only occurs when $p^{\mathrm{S,charge}}_{m,n,s,k} = 0$ during charging and $p^{\mathrm{S,discharge}}_{m,n,s,k} = 0$ during discharging. Therefore, an optimal solution will only be found when the battery is either charging or discharging [105].

4.2. MULTI-PERIOD OPF WITH ESS IN BIPOLAR DISTRIBUTION GRIDS

In a single-period context, as presented in Chapter 3, the OPF is computed for a unique period. The economic dispatch is computed for this time step only as no information is given about future time periods. For a multi-period problem where no storage units is implemented the same will occur as there are no interaction between periods. However, when storage is implemented energy can be stored from one time period to the other. For instance, if energy is cheap and exceed demand during a certain time it can be stored and used for a cheap price during periods where energy is not available or expensive.

4.2.1. SOLVING FOR THE ECONOMIC DISPATCH

In the presence of ESS, the OPF is not solved for each time period but for all time periods. It is important to highlight that all time periods are solved simultaneously to efficiently plan for storage usage while maximizing the utilization of intermittent resources such as solar or wind energy. This approach is different from algorithm relying on a loop for which decisions are only based on the previous time step. Solving for all time periods at once allows for the minimization of the production cost from the start to the end of the simulation. It also means that information about renewable energy and load profiles must be known in advance. Cost is then minimized for the whole system from the initial to the last time step. The objective have to be changed accordingly by summing the total cost over time (4.18). The multi-period optimization problem with the bilinear power function (4.5) is as follows where the minimization of the production is obtained as maximization problem given that generators have negative outputs. Note that only the cost of sources part of $\mathscr{L}$ is taken into account in the production cost. It is assumed that batteries have no marginal cost and that investment costs for DG or ESS should not be part of LMP.

$$
\begin{aligned}
\max \quad & \sum_{k} \sum_{(m,n,s)\in\mathscr{L}} p^{\mathrm{S}}_{m,n,s,k} \cdot \Pi^{\mathrm{S}}_{m,n,s} \cdot \Delta t \qquad\qquad \forall k \in \mathscr{K} \qquad (4.18)\\
\text{s.t.} \quad & (4.1) - (4.11)\\
& (4.12) - (4.17)
\end{aligned}
$$

4.2.2. SOLVING FOR LMP

All of the equations added to the OPF in Section 4.1.2 are linear, hence there is no multiplication of variables. However, the storage model rely on the quadratic term $p^{\mathrm{S}}_{m,n,s,k}$, consequently these equations depend on a quadratic term. Linearizing the problem is thus all the more important. Consequently LMP are solved following the same steps as in Chapter 3. The objective functions and power functions of the three steps are in Table 4.1. These functions are now in terms of time. LMP are obtained using the same methodology described by equations (3.19)-(3.24) with time dependent variables $c^{\mathrm{I}}_{m,k}$, $c^{\mathrm{P}}_{m,n,k}$, $\lambda^{I}_{m,k}$ and $\lambda^{P}_{m,n,k}$.

4.3. MODELING RENEWABLE ENERGIES

The rise of RE in distribution grids and microgrids is imminent. Solar or wind energies have an impact on the way energy is produced and consumed as it will inevitably increase the amount of DG. In combination with ESS, sustainable energies enable local energy production and allows grid/microgrid user to move away from centralized energy supply. As of now energy is produced using finite resources, a fuel that partially constitute the marginal cost of production dictates the price of electricity. In distribution grids or microgrids relying on diesel generators, the cost of energy is derived from an operation costs, mainly fuel and labor. In the model this cost is defined by $\Pi^{\mathrm{S}}_{m,n,s}$, as seen in the cases of Chapter 3, it contributes to the energy term of LMP.

	Programming type	Power Function	Objective function
Step 1	Quadratic (QCP)	$p^{S}_{m,n,s,k} = i^{S}_{m,n,s,k} \cdot (u_{m,k} - u_{n,k})$	$\sum_{k} \sum_{(m,n,s)\in\mathscr{L}} p^{S}_{m,n,s,k} \cdot \Pi^{S}_{m,n,s} \cdot \Delta t$
Step 2	Linear (LP)	$p^{S}_{m,n,s,k} = i^{S^*}_{m,n,s,k} \left(u_{m,k} - u_{n,k}\right) + i^{S}_{m,n,s,k} \left(u^*_{m,k} - u^*_{n,k}\right) - i^{S^*}_{m,n,s,k} \left(u^*_{m,k} - u^*_{n,k}\right)$	$\sum_{k} \sum_{(m,n,s)\in\mathscr{L}} p^{S}_{m,n,s,k} \cdot \Pi^{S}_{m,n,s} \cdot \Delta t + \sum_{m\in\mathscr{N}} \epsilon \cdot \lvert u_{m,k} - u^*_{m,k} \rvert$
Step 3	Linear (LP)	$p^{S}_{m,n,s,k} = i^{S^*}_{m,n,s,k} \left(u_{m,k} - u_{n,k}\right) + i^{S}_{m,n,s,k} \left(u^*_{m,k} - u^*_{n,k}\right) - i^{S^*}_{m,n,s,k} \left(u^*_{m,k} - u^*_{n,k}\right)$	$\sum_{k} \sum_{(m,n,s)\in\mathscr{L}} p^{S}_{m,n,s,k} \cdot \Pi^{S}_{m,n,s} \cdot \Delta t$

Table 4.1: Three steps approach with corresponding power functions and objective functions used to derive LMP from OPF with time dependency.

Renewable energy have zero marginal cost, the energy generated is extracted from the environment in the form of solar radiation or wind. Moreover, these generators can operate on their own and maintenance costs are minimal. It can be converted to electricity by anyone owning a solar panel or wind turbine for no cost, translating to $\Pi^{S}_{m,n,s} = 0$ \$/Wh. In a network strictly relying on renewable energy, electricity is then free. However, the amount of energy available is limited by the amount of distributed generators and intermittency. For example, solar energy is only available during day time for which there is a restricted amount of sun peak hours. Similarly loads fluctuate throughout the day, in the distribution grids loading is generally lower during day time and higher during night time leading to a mismatch of production and consumption. Energy storage play a key role by capturing the excess energy at times where it is abundant and redistributing at times where it is scarce. The amount of DG and ESS determine how much energy is available in the network when it is needed the most. If both conditions are satisfied the price of electricity will inherently be zero for all nodes. If the energy from RE is abundant the marginal cost of losses is inherently 0 \$/Wh. However, if there is not enough energy part of the network will not be fed, the price of electricity is then derived from fuel based generators.

In cases where loading exceed the available energy and a demand-response mechanism needs to be implemented. Maintaining the balance between demand and supply is enabled from the generation and consumption side. Power should be distributed accordingly to how much consumers are willing to pay to use electricity. Such system can be seen as a bidding system where highest bidder buy energy up to its bidding price. This notion is primordial in such network in order to maintain electricity distribution to loads that are deemed primordial.

A demand-response mechanism is incorporated in the model by introducing marginal prices on the load side and by allowing load shedding. Assigning a positive $\Pi^{S}_{m,n,s}$ for loads reflect the willingness to pay in order to avoid power interruptions, it can also be seen as a way to prioritize loads [106]. Load shedding can be implemented using an on/off binary variable or by allowing loads to operate within a given range [107]. Here, the latter option is implemented, it is therefore assumed that loads are adjustable. For examples, it allows lighting appliances to deem when they are not functioning at their rated power.

The impact of assigning a marginal cost on the load side is reflected on LMP. Given that the amount of energy available from RE or ESS is insufficient, the economic dispatch depends on the marginal prices of loads and diesel generators. If the operating cost of these generators is sufficiently low to fulfill all the loads, LMP will directly be derived from this price as in Chapter 3. However, if this is not the case load shedding will occur. Loads with the highest $\Pi^{S}_{m,n,s}$ are prioritized, consequently these loads will be fulfilled to the detriment of loads with lower $\Pi^{S}_{m,n,s}$. LMP will be obtained from the marginal price of the shedded loads.

In order to model RE sources while enabling load shedding parameters cannot be set as in Chapter 3. These changes are expressed in Table 4.2. With regards to PV panels, the marginal cost is set to 0 $/Wh. As opposed to diesel generators for which the capacity is time dependent, the operational limits of PV panels depend on irradiance. Consequently, these limits should be time dependent and expressed as a function of the irradiance (R_k), panel's area ($A_{m,n,s}$) and conversion efficiency ($\eta^{\mathrm{S}}_{m,n,s}$). Similarly, in order to implement load profiles the operating limits of loads should also be time dependent. To enable load shedding a positive marginal price must be assigned to the loads, it reflects the willingness to purchase electricity. Additionally the consumption rate of sources should be able to vary. The upper boundary of loads represents the optimal consumtion rate while the lower boundary is the lowest consumption rate guaranteeing the operation of the load. Setting $P^{\mathrm{S}}_{m,n,s,k,\min}$ to 0 W is equivalent to shutting down the load. Given that sources inject a negative current while loads inject a positive current, the solver inherently maximizes the demand at the smallest possible cost. In other words, each load attempts to reach its higher limit.

PV Panels	Load Shedding
$\Pi^{\mathrm{S}}_{m,n,s} = 0$	$\Pi^{\mathrm{S}}_{m,n,s} > 0$
$P^{\mathrm{S}}_{m,n,s,k,\max} = -R_k \cdot A_{m,n,s} \cdot \eta^{\mathrm{S}}_{m,n,s}$	$P^{\mathrm{S}}_{m,n,s,k,\max} > P^{\mathrm{S}}_{m,n,s,k,\min}$
$P^{\mathrm{S}}_{m,n,s,k,\min} = 0$	$P^{\mathrm{S}}_{m,n,s,k,\max} \leq 0$

Table 4.2: Marginal prices and operating limits of PV generators and loads.

4.4. SIMULATION EXAMPLES

These cases seek to illustrate the behavior of LMP as a consequence of power flows constrained by batteries' capacities. A simple irradiance and load profile is implemented. An arbitrary value is assigned to $P^{\mathrm{S}}_{m,n,s,k,\max}$ in the following examples. The irradiance and area of the solar panels are not taken into consideration yet. PV panels can only operate up to a certain level during time $k0$ and $k1$ while the upper limit of loads is set constant throughout the simulation. These profiles are shown in Figure B.1. The impact of battery sizes is evaluated in Case 6.1 and 6.2. The role of marginal costs in relation with user's willingness to use electricity is assessed in Case 6.3 leading to load shedding. The consequences of asymmetrical networks with sources connected between the positive and negative poles is explained in Case 7.

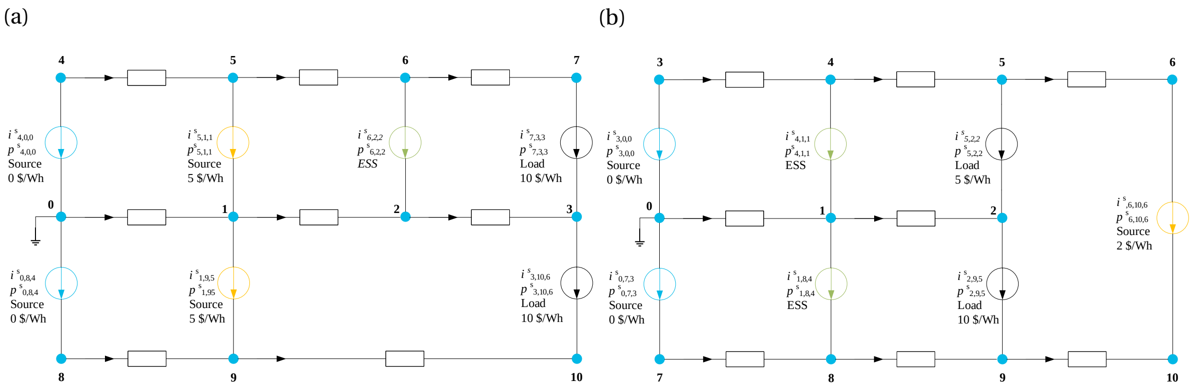

Figure 4.1: Case 6.1-7: Network topologies used in the simulation examples. Figure 4.1a refers to case 6.1, 6.2 & 6.3, Figure 4.1b refers to case 7. PV panels are denoted in blue, diesel generators in yellow, ESS in green and loads in black.

4.4.1. THE ROLE OF ESS CAPACITY AND LOAD SHEDDING

The network in Figure 4.1a consist of 11-nodes with asymmetric loading where only one source is connected to a same set of nodes. Two ideal sources represent PV panels with a marginal cost of 0 $/Wh and varying maximum output to account for varying irradiance. The other two sources operate at a fixed marginal cost and represent diesel/backup generators. To show the role of storage on electricity prices the positive side of the network has a storage unit while the negative side doesn't. Generators satisfy two loads with shedding possibilities. Line capacities and conductance are the same for all conductors and no congestions are simulated. The operating range with respect to time steps are displayed in Table B.1. The network is grounded at node 0 and voltage constraints are similar to the examples in the previous chapter where nodes $[4,5,6,7] \in \mathcal{N}_+$, $[8,9,10] \in \mathcal{N}_-$ and $[0,1,2,3] \in \mathcal{N}_\mathrm{N}$. Simulation with four time steps are carried out from $k0$ to $k3$. PV energy is only available from $k0$ to $k1$. In the presence of storage units the price of electricity is given by the amount of energy solar energy available, size of the batteries and the willingness of user to purchase electricity.

Power flows are visually represented in Figure 4.1a, the exact outputs are in Table B.2. Bars above the horizontal axis symbolize loads or the battery during its charging state while bars below the horizontal axis symbolize generators or the battery during its charging state. Finally the state of charge of the battery at the beginning of each period across the pair of node 6-2 is shown in Figure B.2. At the end of each simulation, $k3$, the battery is empty.

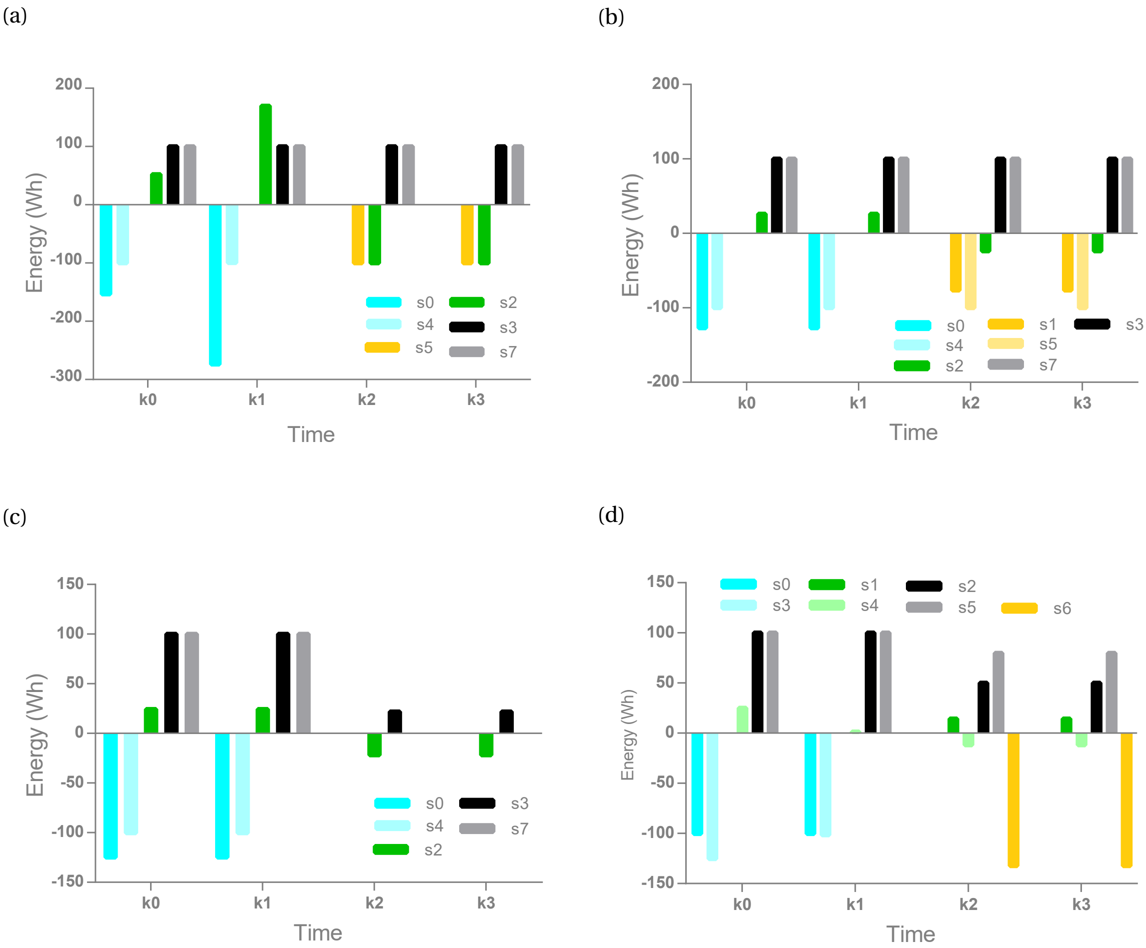

Figure 4.2: Case 6.1-7: Power output of sources with PV panels represented in blue, sources with marginal cost in yellow and ESS in green. Figures 4.2a-4.2c and 4.2d-5.3e respectively represent Cases 6.1-6.3 and 7.

CASE 6.1: UNCONSTRAINED OPERATION OF PV PANELS AND ESS

This example relies on a network where neither the generators nor the battery are constrained. The storage unit is large enough to store enough energy from PV panels so that the supply-demand balance is satisfied at all time. During $k0$ and $k1$, the ESS between nodes 6-2 is charged, it acts as a load for which $p^{\mathrm{S}}_{6,2,2,0}$ and $p^{\mathrm{S}}_{6,2,2,1}$ are positive. Energy is stored and redistributed later when the sun is not shining. The power withdrawn from the solar panel on the positive side of the network is higher than the maximum output of loads $p^{\mathrm{S}}_{7,3,3,0}$ and $p^{\mathrm{S}}_{7,3,3,1}$. In other words, the overall supply exceed the demand. One could expect $p^{\mathrm{S}}_{4,0,0,0}$ and $p^{\mathrm{S}}_{4,0,0,1}$ to be equal but the marginal cost of this generator is null, hence losses do not affect LMP during these time steps. Consequently multiple solutions are available, the same LMP will be obtained regardless of how much power is generated during $k0$ and $k1$ as long as the battery contain enough energy for the next time periods. Electricity is thus available at no marginal cost and LMP are close to 0\$/Wh during all time steps. The reason why nodal prices slightly differ from 0 during $k2$ and $k3$ is due to the asymmetry between the positive and negative polarity. For the pair of nodes located on the left side of the storage unit, an increment in loading will increase the current flowing through the neutral conductor, losses will thus slightly increase. On the right side of the storage unit, the price is slightly negative meaning that an increase in the loading will decrease the current flowing in the neutral conductor and consequently losses will decrease. These marginal cost are non-zero because the lower side of the network is partially fed by a diesel generator during $k2$ and $k3$. A negative LMP is interpreted as a payment from the grid operator to the consumer. This phenomena is explained in further details in Case 7.

Looking at the negative side of network, the absence of battery is reflected in nodal prices during time periods where PV panels are unable to function. $\Pi^{\mathrm{S}}_{7,3,3}$ and $\Pi^{\mathrm{S}}_{3,10,6}$ are set higher than $\Pi^{\mathrm{S}}_{5,1,1}$ and $\Pi^{\mathrm{S}}_{1,9,5}$ so that the user willingness to consume power is higher than the highest generation cost. Ergo, diesel generators are activated as the price on the load side is higher than the operating cost of $p^{\mathrm{S}}_{1,9,5}$. Under these conditions LMP are derived from $\Pi^{\mathrm{S}}_{1,9,5}$. The difference in prices from a pair of nodes to the other is caused by losses in the conductors.

In conclusion, if generators with no marginal costs exceed the demand and batteries are large enough, energy is then available for free. In the absence of batteries, energy is only free when solar panels are operating, otherwise nodal prices are derived from the marginal cost of the next least expensive and unconstrained generator given that its cost is lower than the cost applied on the load side.

CASE 6.2: CONSTRAINED OPERATION OF THE ESS

An OPF constrained by an ESS capacity is implement in this case. The battery is not large enough to store enough energy from PV panels to satisfy loads at time step $k2$ and $k3$. As seen in Figure B.2, the unit is charged to its full capacity. Similarly to the previous example, the marginal cost $\Pi^{\mathrm{S}}_{5,1,1}$ is lower than $\Pi^{\mathrm{S}}_{7,3,3}$ enabling loads to function at their upper limit. Generator $p^{\mathrm{S}}_{5,1,1}$ is activated to supplement the power provided by the storage. Inherently, nodal prices for $k2$ and $k3$ are derived from $\Pi^{\mathrm{S}}_{5,1,1}$. The differences in prices is caused by losses.

CASE 6.3: LOAD SHEDDING

In the previous examples LMP are formulated as a function of generators' marginal costs by enabling user to withdraw as much power as they need from sources. Here, loads are assigned a price lower than diesel generators and solar panels cannot produce enough to fully charge the ESS. Loads are limited by the limited supply of solar energy as opposed to the storage's capacity. Additionally, the high price $\Pi^{\mathrm{S}}_{5,1,1}$ prohibit users from consuming as much power as they would like.

As seen in Table 4.3, under these conditions load $p^{\mathrm{S}}_{7,3,3}$ is shedded during $k2$ and $k3$ and the available cheap energy is fully utilized. Consequently, electricity prices in between nodes in the positive side of the network are derived from $\Pi^{\mathrm{S}}_{7,3,3}$. For $k2$ and $k3$, $\lambda^{\mathrm{P}}_{7,3}$ is equal to the marginal cost $\Pi^{\mathrm{S}}_{7,3,3}$. The rest of nodes have very close and equal values, the difference is caused by the asymmetry resulting in a current flowing through the neutral conductor. A symmetrical case would have resulted in LMP all equal to 7 \$/Wh. Therefore, if an additional load with a marginal cost higher than $\Pi^{\mathrm{S}}_{7,3,3}$ were to be connected anywhere in the positive polarity it would be prioritized and no power would be fed to $p^{\mathrm{S}}_{7,3,3}$.

$$\lambda^{\mathrm{P}}_{6,2,0} = \lambda^{\mathrm{P}}_{6,2,1} = \frac{\lambda^{\mathrm{P}}_{7,3,2}}{\eta^2} = \frac{7}{0.95^2} = 6.31 \quad \$/\mathrm{Wh} \tag{4.19}$$

At time $k0$ and $k1$ nodal prices are also obtained from $\Pi^{\mathrm{S}}_{7,3,3}$, the difference is caused by the round-trip effi-

	Case 6.1				Case 6.2				Case 6.3			
	$\lambda^{P}_{4,0,k}$	$\lambda^{P}_{5,1,k}$	$\lambda^{P}_{6,2,k}$	$\lambda^{P}_{7,3,k}$	$\lambda^{P}_{4,0,k}$	$\lambda^{P}_{5,1,k}$	$\lambda^{P}_{6,2,k}$	$\lambda^{P}_{7,3,k}$	$\lambda^{P}_{4,0,k}$	$\lambda^{P}_{5,1,k}$	$\lambda^{P}_{6,2,k}$	$\lambda^{P}_{7,3,k}$
$\Pi^{S}_{m,n,s}$	0	5	–	10	0	5	–	10	0	10	–	7
k0	0.00	0.00	0.00	0.00	0.00	0.00	0.00	0.00	6.23	6.27	6.31	6.34
k1	0.00	0.00	0.00	0.00	0.00	0.00	0.00	0.00	6.23	6.27	6.31	6.34
k2	0.01	0.01	0.00	-0.01	4.99	5.00	5.01	5.02	6.99	6.99	6.99	7.00
k3	0.01	0.01	0.00	-0.01	4.99	5.00	5.01	5.02	6.99	6.99	6.99	7.00
	$\lambda^{P}_{0,8,k}$	$\lambda^{P}_{1,9,k}$	$\lambda^{P}_{3,10,k}$	–	$\lambda^{P}_{0,8,k}$	$\lambda^{P}_{1,9,k}$	$\lambda^{P}_{3,10,k}$	–	$\lambda^{P}_{0,8,k}$	$\lambda^{P}_{1,9,k}$	$\lambda^{P}_{3,10,k}$	–
$\Pi^{S}_{m,n,s}$[\$/W]	0	5	10	–	0	5	10	–	0	10	7	–
k0	0.00	0.00	0.00	–	0.00	0.00	0.00	–	0.00	-0.01	-0.04	–
k1	0.00	0.00	0.00	–	0.00	0.00	0.00	–	0.00	-0.01	-0.04	–
k2	4.99	5.00	5.04	–	5.00	5.00	5.02	–	10.00	10.00	9.99	–
k3	4.99	5.00	5.04	–	5.00	5.00	5.02	–	10.00	10.00	9.99	–

Table 4.3: Case 6.1, 6.2 and 6.3: LMP in terms of power for set of node connecting at least one source are displayed.

ciency of the battery. Indeed, in order to feed power to the load 7-3 during the last two periods the ESS has to go through a charging and discharging state. The relation between prices from one time period to the other is expressed in (4.19). $\lambda^{P}_{6,2,0}$ and $\lambda^{P}_{6,2,1}$ are used as basis to compute the rest of nodal prices for which the difference is explained by losses. If a load with marginal cost higher than $\lambda^{P}_{m,n,0}$ and $\lambda^{P}_{m,n,1}$ were to be connected in the network at this time it would be prioritized to the detriment of $p^{S}_{7,3,3}$ even though its price might be smaller than $\Pi^{S}_{7,3,3}$. It would result in less losses and better utilization of the solar energy as no power would be loss upon charging and discharging the battery.

Looking at the lower side of the network, the absence of a battery results in different prices. Similarly to the previous examples solar energy cannot be fully utilized, user only benefit from renewable resources during $k0$ and $k1$. LMP are either 0 or negative. A negative nodal price can be interpreted as a payment to the user if loading is incremented by one unit at these locations as it would cause a decrease in losses These prices are caused by the asymmetry within the network. No power is fed to $p^{S}_{7,3,3}$ during $k2$ and $k3$, the only available generator has an operational cost higher to what customer are willing to pay. Prices in the network are then derived from $\Pi^{S}_{5,1,1}$.

4.4.2. ASYMMETRICAL LOADING WITH SOURCES CONNECTED FROM THE POSITIVE TO NEGATIVE CONDUCTOR

The configuration of sources and ESS in combination with asymmetries can have a direct impact on LMP. Case 7 is used to demonstrate a scenario where nodal prices are highly negative. Similarly to the previous cases of this chapter. The network in 4.1b consists of 10-nodes with asymmetrical loading. Two ideal sources represent PV panels with a marginal cost of 0 \$/Wh and connected to the positive and negative pole. The third source is a diesel generator with a marginal cost of 2 \$/Wh connected between the positive and negative conductor. The loads have different marginal costs, the high priority load is located on the negative pole. During $k0$ and $k1$ the loading is symmetrical, however during $k2$ and $k3$ there is a large asymmetry between the two loads. $p^{S}_{5,2,2,k}$ is much lower than $p^{S}_{2,9,5,k}$. Finally two batteries with limited capacities of 25 Wh are connected to both poles. The generation and load profiles are shown in Table B.3. The network is grounded at node 0 and voltage constraints are the same as in the previous examples. Finally, PV panels can only operate during the first two time steps and the batteries are not large enough to satisfy any of the loads during $k2$ and $k3$. The OPF is represented graphically in Figure 4.2d.

At the beginning of the simulation, $k1$ and $k2$, the same behavior is observed as in Case 6. The PV panels are generating enough energy to feed both loads to their upper limit. However, the power output during the first time step are not equal, $s3$ is used to charge the ESS $s5$ while the battery on the positive pole is left empty. Since power is available and generators are not constrained the nodal prices for these periods are equal to 0 $/Wh.

During $k3$ and $k4$ solar energy is scarce, the diesel generators is thus activated to feed both loads. The asymmetry and the connection configuration of the generator result in load shedding. The load with the highest priority, $s5$, is shedded while the load with the lowest priority, $s2$, is operating at its upper limit. It suggests that the network topology and the asymmetry limit power flows in the network. Generator $s6$ is not connected to the neutral conductor, as a result the two polarities cannot operate independently as seen in cases where generation is balanced. The current flowing through $s5$ is limited by $s2$. Therefore, the current flowing through load $s5$ can only be increased by increasing the current flowing through $s2$. Consequently, the energy consumption of the load with the lowest priority has to be maximized in order to increase the power of the load with the highest priority. The upper limits $P^{\mathrm{S}}_{5,2,2,2}$ and $P^{\mathrm{S}}_{5,2,2,3}$ only allows the load connected between node 2-9 to consume 79.83 Wh.

The behaviors of ESS is rather interesting. During $k2$ and $k3$, the battery on the positive polarity is charging while the battery on the negative pole is discharging. The Storage Unit $s1$ essentially acts as a load while $s4$ acts as a source. In such a way, the current flowing through the neutral conductor is increased resulting in a larger current through the load with the highest priority. It is even more surprising that the power stored in $s1$ is generated from a diesel generator with a non-zero operational cost. It suggests that the batteries can also have a role in balancing the network in case of asymmetrical loading and generation. The consumption rates $p^{\mathrm{S}_{2,1,5,2}}$ and $p^{\mathrm{S}_{2,1,5,2}}$ could even be increased by charging the $s1$ to its maximum energy content. However, the charging rate at that location is also limited by the consumption rate of $s2$.

The consequences of unbalanced generation and asymmetrical loading result in highly negative prices. In order to fulfill the power requirements of the high priority loads on the negative side, the loading of the positive pole has to be increased. LMP for sources connected between the positive and neutral conductor are negative. An increment of one unit at these locations lead to both a decrease in generation and an increase in consumption of the shedded load. Negative nodal prices can be interpreted as a payment from the grid operator to the consumers. In this scenario LMP provide an incentive to balance the grid.

Case 7							
	$\lambda^{\mathrm{P}}_{3,0,\mathrm{k}}$	$\lambda^{\mathrm{P}}_{4,1,\mathrm{k}}$	$\lambda^{\mathrm{P}}_{5,2,\mathrm{k}}$	$\lambda^{\mathrm{P}}_{0,7,\mathrm{k}}$	$\lambda^{\mathrm{P}}_{1,8,\mathrm{k}}$	$\lambda^{\mathrm{P}}_{2,9,\mathrm{k}}$	$\lambda^{\mathrm{P}}_{6,2,\mathrm{k}}$
$\Pi^{\mathrm{S}}_{\mathrm{m,n,s}}$	0	–	5	0	–	10	2
k0	0.00	0.00	0.00	0.00	0.00	0.00	0.00
k1	0.00	0.00	0.00	0.00	0.00	0.00	0.00
k2	-6.39	-6.41	-6.43	9.96	9.97	10.00	2.00
k3	-6.39	-6.41	-6.43	9.96	9.97	10.00	2.00

Table 4.4: Case 7: LMP in terms of power for set of node connecting at least one source are displayed.

5

Optimal Sizing and Placement of ESS

Within the context of DG, optimal size and location is essential to the maximization of RE resources' utilization. As seen in Chapter 4, storage reduces the problem of intermittency and increase the availability of energy at times where solar or wind energy is scarce. Consequently, electricity prices are significantly lower. So far only ESS with a defined capacity and placement were considered. In this chapter, the battery model is further developed as a design tool to maximize the utilization of sustainable energies by optimizing the size and siting of energy storage units. The method seeks to find a solution to the technical and economical trade-off. Thus, minimizing production cost is accomplished by determining ESS capacities and location while considering natural power flows, losses and current limits. Apart from guaranteeing a better use of DG, it is also a congestion management strategy [108–110]. This new version of the OPF can either be used to design distribution networks or reveal investment opportunities. The optimal size of ESS is calculated by setting the capacity as variable and optimal placement is obtained by using additional constraints and mixed integer programming. It is important to mention that the methodology proposed is a first approach to solving for battery location and sizes. The optimal capacity obtained from the model is constrained between a range, therefore the optimal size of storage in most cases do not match the capacity of commercially available batteries. The model could be further improved by using mixed-integer programming and integer variables instead of binary variables.

5.1. Modeling ESS with Variable Size and Location

The grid and source model do not differ from the previous chapter. It is defined by (4.1)-(4.11). Only the storage model is modified. The ability to simultaneously model ESS with capacity set as a parameter and ESS with optimized capacity was deemed important, therefore a distinction need to be made. Storage units are organized in three set of nodes: set $\mathscr{F}$ defines all ESS for which capacity is a parameter, set $\mathscr{V}$ defines all ESS for which capacity is a variable and set $\mathscr{B}$ is the union of $\mathscr{F}$ and $\mathscr{V}$. Using these sets different constraints and equations are applied accordingly in an effort to model an OPF with ESS with a fixed capacity and ESS with a variable capacity.

5.1.1. Optimal ESS Size

Storage units with sizes set by the user are modeled as in Chapter 4. However, the storage model has to be adjusted to include variable capacity ESS. To optimize the size of storage units the capacity is now set as variable and denoted by $s^{\mathrm{ESS}}_{m,n,s}$. The energy content $e^{\mathrm{S}}_{m,n,s,k}$ only has a lower bound and (4.15) becomes:

$$E^{\mathrm{S}}_{m,n,s,\min} \le e^{\mathrm{S}}_{m,n,s,k} \qquad \forall (m,n,s) \in \mathscr{V}, \qquad k \in \mathscr{K} \tag{5.1}$$

In the upcoming case study no minimum state of charge are considered, $E^{\mathrm{S}}_{m,n,s,\min}$ has a value of 0 Wh. The absence of an upper limit essentially means that any battery connected across two nodes part of $\mathscr{V}$ can store as much as it needs to decrease the production cost. The amount of energy available in a battery now only depends on the capacity of DG and the marginal costs set on both generators and sources. It implies that the optimal storage size of an ESS is equal to largest value assigned to $e^{\mathrm{S}}_{m,n,s,k}$ throughout the sumulation. In (5.2), the lower bound of $s^{\mathrm{ESS}}_{m,n,s}$ is defined as the largest $e^{\mathrm{S}}_{m,n,s,k}$ obtained for a given k.

$$s^{\mathrm{ESS}}_{m,n,s} \geq e^{\mathrm{S}}_{m,n,s,k} \qquad \forall (m,n,s) \in \mathscr{V}, \qquad k \in \mathscr{K} \tag{5.2}$$

Notice that the variable $s^{\mathrm{ESS}}_{m,n,s}$ does not have an upper limit, it can take any value higher or equal to $e^{\mathrm{S}}_{m,n,s,k}$. In order to guarantee an optimal $s^{\mathrm{ESS}}_{m,n,s}$ an investment cost, $\pi^{\mathrm{ESS}}_{m,n,s}$, in terms of \$/Wh is applied to the variable capacity storage unit. This cost represent the investment that needs to be made to install a storage unit at a specified location. Including this investment cost in the cost function essentially reveals if investing in a battery will decrease the production cost as opposed to no battery. It also prevent $s^{\mathrm{ESS}}_{m,n,s}$ from taking a value larger than the highest $e^{\mathrm{S}}_{m,n,s,k}$.

5.1.2. OPTIMAL ESS LOCATION

Sources, loads and ESS locations are characterized by a set of two nodes declared in the input data. Nodes and connecting branches define the network and constitute the base for the OPF. It is therefore not possible to define a location as a variable. The strategy adopted to determine the ideal placement of ESS rely on the optimal storage model formulated in the above section. By assigning multiple storage units with a variable capacity at different location in the network the optimal sizes of these units is returned for all sites.

Under the assumptions that variable capacity storage units are declared at multiple locations in the network, the solver will output an $s^{\mathrm{ESS}}_{m,n,s}$ for each unit. Given that line constraints, losses and natural power flows are part of the OPF it is unlikely that any of the variable storage unit will have a capacity of 0 kWh. On the contrary, it is more likely that all ESS will have an optimal capacity that can range from very small to very large. Commercially available ESS for distribution network have given sizes that cannot be exceeded. An optimal solution with units for which $s^{\mathrm{ESS}}_{m,n,s}$ is not within this range is inherently infeasible. For example, a solution featuring storage units with capacities of 1 Wh does not make sense.

To prevent such problem from occurring mixed-integer programming is employed. Each set of node part of $\mathscr{V}$ is assigned binary variable, $b_{m,n,s}$. A binary variable equal to 0 symbolizes that no unit should be installed at this location and 1 represents the opposite. An additional inequality constraint is implemented, its role is to bound $s^{\mathrm{ESS}}_{m,n,s}$ to a realistic capacity range. A binary variable $b_{m,n,s}$ will only be given a value of 1 if its optimal size is within the range or if a capacity equal to either one of the limits participates to the minimization of the production cost. It results in inequality constraints expressed as in (5.3) and (5.4). If an optimal battery size is not within these limits its capacity will be 0 Wh and no storage will be allocated to this location.

$$s^{\mathrm{ESS}}_{m,n,s} \leq S^{\mathrm{S}}_{m,n,s,\max} \cdot b_{m,n,s} \qquad \forall (m,n,s) \in \mathscr{V}, \qquad k \in \mathscr{K} \tag{5.3}$$

$$s^{\mathrm{ESS}}_{m,n,s} \geq S^{\mathrm{S}}_{m,n,s,\min} \cdot b_{m,n,s} \qquad \forall (m,n,s) \in \mathscr{V}, \qquad k \in \mathscr{K} \tag{5.4}$$

Although (4.12) still holds, it needs to be applied to all ESS $\in \mathscr{B}$.(4.13) and (4.14) need to be adjusted accordingly to ensure that ESS for which the binary variable is zero do not participate to the OPF. For all ESS $\in \mathscr{V}$, the binary variable is thus multiplied to both variables $p^{\mathrm{S,charge}}_{m,n,s,k}$ and $p^{\mathrm{S,discharge}}_{m,n,s,k}$. If no ESS is assigned the energy content at any time will be zero (5.6) and there no power will flow in or out (5.8). For all ESS $\in \mathscr{F}$, the energy content and power output of the unit is obtained as in Chapter 4 using (5.7) and (5.9).

$$e^{\text{S}}_{m,n,s,k_0} = 0 \qquad \forall(m,n,s) \in \mathscr{B}, \tag{5.5}$$

$$\begin{aligned} e^{\text{S}}_{m,n,s,k} = e^{\text{S}}_{m,n,s,k-1} + b_{m,n,s} \cdot p^{\text{S,charge}}_{m,n,s,k-1} * \eta_{m,n,s} * \Delta t + \\ b_{m,n,s} \cdot p^{\text{S,discharge}}_{m,n,s,k-1} * \frac{1}{\eta_{m,n,s}} * \Delta t \end{aligned} \qquad \forall(m,n,s) \in \mathscr{V}, \quad k \in \mathscr{K} \tag{5.6}$$

$$e^{\text{S}}_{m,n,s,k} = e^{\text{S}}_{m,n,s,k-1} + p^{\text{S,charge}}_{m,n,s,k-1} * \eta^{\text{ESS}}_{m,n,s} * \Delta t + p^{\text{S,discharge}}_{m,n,s,k-1} * \frac{1}{\eta^{\text{ESS}}_{m,n,s}} * \Delta t \qquad \forall(m,n,s) \in \mathscr{F}, \quad k \in \mathscr{K} \tag{5.7}$$

$$p^{\text{S}}_{m,n,s,k} = b_{m,n,s} \cdot p^{\text{S,charge}}_{m,n,s,k} + b_{m,n,s} \cdot p^{\text{S,discharge}}_{m,n,s,k} \qquad \forall(m,n,s) \in \mathscr{V}, \quad k \in \mathscr{K} \tag{5.8}$$

$$p^{\text{S}}_{m,n,s,k} = p^{\text{S,charge}}_{m,n,s,k} + p^{\text{S,discharge}}_{m,n,s,k} \qquad \forall(m,n,s) \in \mathscr{F}, \quad k \in \mathscr{K} \tag{5.9}$$

Inequality constraints defined by (4.15)-(4.17) also have to be adjusted and applied to the right sets. They become:

$$E^{\text{ESS}}_{m,n,s,\min} \leq e^{\text{S}}_{m,n,s,k} \leq E^{\text{ESS}}_{m,n,s,\max} \qquad \forall(m,n,s) \in \mathscr{F}, \qquad k \in \mathscr{K} \tag{5.10}$$

$$p^{\text{S,charge}}_{m,n,s,k} \geq 0 \qquad \forall(m,n,s) \in \mathscr{B}, \qquad k \in \mathscr{K} \tag{5.11}$$

$$p^{\text{S,discharge}}_{m,n,s,k} \leq 0 \qquad \forall(m,n,s) \in \mathscr{B}, \qquad k \in \mathscr{K} \tag{5.12}$$

Using this approach a storage unit with variable capacity can be connected between any set of nodes with a different polarity. When combined with a new cost function that considers ESS investment costs, only ESS for which the capacity is between the upper and lower limit while maximizing the utilization of renewable energy are placed in the network.

5.2. MULTI-PERIOD OPF WITH OPTIMAL ESS SIZING AND PLACEMENT IN BIPOLAR DISTRIBUTION GRIDS

The economic dispatch is solved in the same way as in Chapter 4, the optimization process is centralized and information about the grid and all future time steps is taken into account to solve the OPF for all time period at once. Therefore, the minimization of the production cost is obtained by maximizing the sum of the cost of production of each sources given that generators produce a negative power.

5.2.1. SOLVING FOR THE ECONOMIC DISPATCH

To solve for optimal ESS size a new cost function is used. In the original storage model no costs were assigned to storage, it is assumed that storage units are already purchased and their cost of operation is zero. However, solving for optimal storage capacities implies that these batteries are currently inexistent. ESS represent a large part of the capital cost in a distributed network, a trade-off exist between the investment cost of new storage units and their contribution with regards to the total production cost. This investment cost needs to be added to the objective function and be formulated in terms of capacity. It guarantees that only storage units that contributes to the minimization of the production cost are assigned a capacity. The economic dispatch is obtained by solving the following optimization problem:

$$\max \quad \sum_{k} \sum_{(m,n,s)\in\mathscr{S}} p^{\text{S}}_{m,n,s,k} \cdot \Pi^{\text{S}}_{m,n,s} \cdot \Delta t + \sum_{(m,n,s)\in\mathscr{V}} e^{\text{S}}_{m,n,s,k} \cdot \Pi^{\text{ESS}}_{m,n,s} \qquad \forall k \in \mathscr{K} \tag{5.13}$$

$$\begin{aligned} \text{s.t.} \quad & (4.1) - (4.11) \\ & (5.1) - (5.12) \end{aligned} \tag{5.14}$$

The binary variables in (5.3)-(5.8) imply that the problem is a mixed-integer problem, it cannot be solved using the same solvers as in Chapter 3 and 4. The optimization process is now termed mixed-integer quadratic constrained problem (MIQCP) and the solver eligible for this application are BONMIN, COUENNE and BARON [104]. It is important to highlight that solving mixed-integer problem is a more complicated process, the number of possibilities is larger. Inherently the computation time is longer than the initial problem. However, solving for optimal size and location should only be done occasionally to improve the network. As opposed to the methodology explained in the previous chapters, this procedure should not be used to compute the economic dispatch for grid control, it would be inefficient.

5.2.2. SOLVING FOR LMP

The presence of an additional term in the objective function is to the detriment of the derivation of LMP. Indeed the investment cost is now reflected in the cost of increasing the energy demand at a specific location. In this model it is assumed that the investment cost should not be incorporated in the price of electricity. The investment decision should be taken by either the grid users or the system operator. This model is originally designed for micrograds in developing countries, therefore if a consumer decides to purchase a battery the investment cost will not be reflected in electricity prices. However, it will eventually benefit the user itself and an overall better utilization of renewable energies.

In order to prevent the investment cost of ESS from affecting LMP an additional step needs to be added. Nodal prices are now derived using four steps. First the economic dispatch is solved using mixed-integer programming and the optimization problem in 5.2.1. The OPF is obtained as well as optimal battery locations and battery sizes, the results are assumed to be correct. Before proceeding to the second step the capacity of each ESS for which storage units connected between nodes part of $\mathscr{V}$ is fixed by equating the optimal capacity $s^{\mathrm{S}}_{m,n,s}$ to the parameter $E^{\mathrm{ESS}}_{m,n,s,\max}$ (5.15). In order to model ESS according to (4.12)-(4.17), all ESS $\in \mathscr{V}$ should now be considered as part of $\mathscr{F}$:

$$E^{\mathrm{ESS}}_{m,n,s,\max} = s^{\mathrm{ESS}}_{m,n,s} \qquad \forall (m,n,s) \in \mathscr{V}, \qquad k \in \mathscr{K} \tag{5.15}$$

$$\mathscr{F} = \mathscr{F} \cup \mathscr{V} \tag{5.16}$$

During the second step, the optimization problem is solved using the same approach as in Chapter 4. The optimal ESS are now considered as storage units with capacities defined by a parameter. The economic dispatch is solved again but the investment cost of storage units is now omitted from the cost function. The objective is therefore different. The change in problem type, from MIQCP to QCP, prohibit us from keeping the same basis. As a result, the OPF may vary from step 1 to step 2. However, it does not mean that the results obtained in either step is wrong. The presence of multiple time periods may result in problems with multiple solutions. In order to verify that an equivalent but different solution is obtained in step 2 a quick check can be performed by computing the production cost in step 1 by excluding ESS investment costs.

The last two steps are then equivalent to the methodology in Chapter 4. Linearization is performed the same way and the proximity term is used to guarantee that the economic dispatch obtained in step 3 do not vary from the objective of step 2. Lastly the basis of step 3 is used in step 4 where the proximity term is omitted from the objective function. All the steps with corresponding cost function are displayed in Table 5.1. The complete formulation of each step is in Appendix B.1 and C.

5.3. SIMULATION EXAMPLES

Simulation examples are used to assess the validity of the model and its purposes. Three types of case studies are carried out. Simple 12-nodes bipolar networks are implemented with different parameters between the positive and negative side of network for comparison purposes. Case 8 is used to demonstrate how the optimal size of an ESS is computed. By varying the parameters and by comparing the two polarities the impact of the capacity range and the investment costs on the storage capacity is demonstrated. In Case 9, multiple ESS are connected in parallel to generators and loads. The aim is to illustrate how the optimal siting of a storage unit can be obtained. Finally in Case 10, the role of variable ESS for congestion management is validated by imposing current constraints to connecting branches. The current limits and conductance of each lines are in Table C.1.

	Programming type	Power Function	Objective function
Step 1 C.1	Mixed-Integer Quadratic (MIQCP)	$p^{\mathrm{S}}_{m,n,s,k} = i^{\mathrm{S}}_{m,n,s,k} \cdot (u_{m,k} - u_{n,k})$	$\sum_k \sum_{(m,n,s)\in\mathscr{S}} p^{\mathrm{S}}_{m,n,s,k} \cdot \Pi^{\mathrm{S}}_{m,n,s} \cdot \Delta t + \sum_{m,n,s\in\mathscr{V}} e^{\mathrm{S}}_{m,n,s,k} \cdot \Pi^{\mathrm{ESS}}_{m,n,s}$
Step 2 B.1	Quadratic (QCP)	$p^{\mathrm{S}}_{m,n,s,k} = i^{\mathrm{S}}_{m,n,s,k} * (u_{m,k} - u_{n,k})$	$\sum_k \sum_{m,n,s} p^{\mathrm{S}}_{m,n,s,k} \cdot \Pi^{\mathrm{S}}_{m,n,s} \cdot \Delta t$
Step 3 B.1	Linear (LP)	$p^{\mathrm{S}}_{m,n,s,k} = i^{\mathrm{S}*}_{m,n,s,k} (u_{m,k} - u_{n,k}) + i^{\mathrm{S}}_{m,n,s,k} \left(u^*_{m,k} - u^*_{n,k}\right) - i^{\mathrm{S}*}_{m,n,s,k} \left(u^*_{m,k} - u^*_{n,k}\right)$	$\sum_k \sum_{(m,n,s)\in\mathscr{S}} p^{\mathrm{S}}_{m,n,s,k} \cdot \Pi^{\mathrm{S}}_{m,n,s} \cdot \Delta t + \sum_{m\in\mathscr{N}} \epsilon \cdot \mid u_{m,k} - u^*_{m,k} \mid$
Step 4 B.1	Linear (LP)	$p^{\mathrm{S}}_{m,n,s,k} = i^{\mathrm{S}*}_{m,n,s,k} (u_{m,k} - u_{n,k}) + i^{\mathrm{S}}_{m,n,s,k} \left(u^*_{m,k} - u^*_{n,k}\right) - i^{\mathrm{S}*}_{m,n,s,k} \left(u^*_{m,k} - u^*_{n,k}\right)$	$\sum_k \sum_{(m,n,s)\in\mathscr{S}} p^{\mathrm{S}}_{m,n,s,k} \cdot \Pi^{\mathrm{S}}_{m,n,s} \cdot \Delta t$

Table 5.1: Four steps approach with corresponding power functions and objective functions used to derive LMP from OPF.

5.3.1. THE ROLE OF CAPACITY RANGES AND INVESTMENT COSTS

The role of investment costs in combination with the capacity range of variable ESS is reflected in Case 8. All sub-cases are based on the bipolar network shown in Figure 5.1a. PV panels can produce enough energy to satisfy the loads throughout the simulation in the presence of storage units. Note that the willingness to purchase electricity is higher than the marginal cost of the diesel generator. Therefore, if batteries are not large enough the backup generators will be activated and load shedding won't occur. To understand the impact of capacity ranges and investment costs, parameters very from one sub-case to the other. Respective capacity ranges and investment costs are displayed in Table 5.2. The energy generated and consumed during each time steps as well as the state of charge of ESS are displayed in Figures 5.3a-5.3c, for details refer to Table C.2. LMP are reported in Table 5.3.

Cases	ESS Cost [$/Wh]		Capacity Range [Wh]		Optimal Capacity [Wh]	
	$\pi^{\mathrm{ESS}}_{6,2,2}$	$\pi^{\mathrm{ESS}}_{2,10,6}$	$\mathrm{S}^{\mathrm{S}}_{6,2,2}$	$\mathrm{S}^{\mathrm{S}}_{2,10,6}$	$\mathrm{S}^{\mathrm{ESS}}_{6,2,2}$	$\mathrm{S}^{\mathrm{ESS}}_{2,10,6}$
Case 8.1	1	1	600–1000	100–1000	600.00	528.25
Case 8.2	5	1	600–1000	100–500	0.00	500.00
Case 8.3	1	4.8	100–1000	100–1000	586.26	386.39

Table 5.2: Case 8.1, 8.2 & 8.3: Investment costs, upper/lower limits and optimal capacity of variable ESS.

CASE 8.1 & 8.2

The impact of capacity ranges is assessed in Cases 8.1 and 8.2 for which the upper and lower limits of storage sizes vary from the positive to negative side of the network. Variable batteries connected between nodes 6-2 and 2-10 have the same investment costs and the unit on the negative conductor has a wider range. As a result, $s^{\mathrm{ESS}}_{2,10,6}$ is unconstrained, its value lies between $S^{\mathrm{S}}_{2,10,6,\max}$ and $S^{\mathrm{S}}_{2,10,6,\min}$. It can be concluded that a

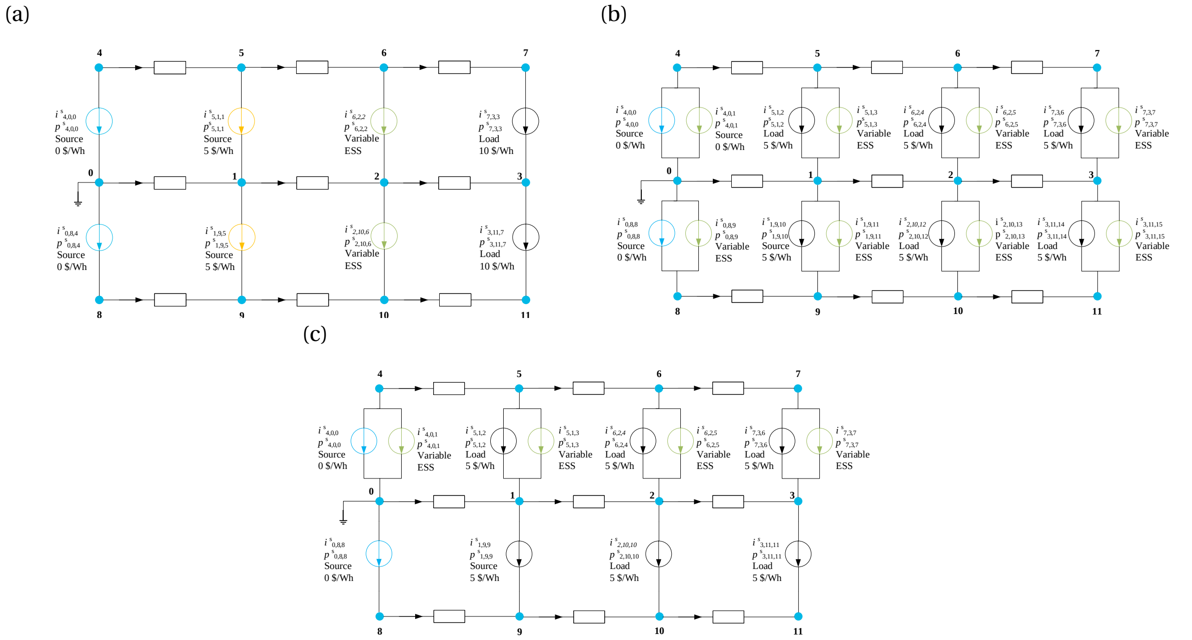

Figure 5.1: Case 8.1-10: Network topologies used in the simulation examples. Figure 5.1a refers to Case 8.1, 8.2 & 8.3, Figure 5.1b refers to Case 9.1 & 9.2 and Figure 5.1c refers to Case 10. PV panels are denoted in blue, diesel generators in yellow, ESS in green and loads in black.

capacity of 529.25 Wh is the optimal size allowing for the maximization of the PV panel, $p^{\mathrm{S}}_{0,8,4,k}$, utilization. Inherently the state of charge of that unit reaches its maximum at the end of the second time period. A smaller ESS would require the activation of the expensive generator $p^{\mathrm{S}}_{1,9,5,k}$ leading to rise in the production cost and a larger unit would increase the investment cost while not being utilized to its maximum. Notice that the solar panel is not operating at its upper bound, more energy can be harvested to provide the next increment of energy. Ergo, LMP are all 0 \$/Wh on this side of the network.

The loading and parameters with respect to the generation units are the same, thus the optimal size of batteries are expected to be the same. However, the lower limit $S^{\mathrm{S}}_{6,2,2,\min}$ is set higher than 529.25 Wh. The closest value that $s^{\mathrm{ESS}}_{6,2,2}$ can take is equal to its lower bound. Here the investment cost $\pi^{\mathrm{ESS}}_{6,2,2}$ is sufficiently small so that a capacity of 600 Wh at this location result in a lower objective as opposed to activating the expensive generator $p^{\mathrm{S}}_{5,1,1,k}$. In Figure C.1, it can be seen that the battery is never at its maximum. Similarly to the upper part of the network, the storage unit is large enough to satisfy the supply-demand balance using cheap energies, consequently LMP are all 0 \$/Wh.

To highlight the impact of ESS investment costs on storage allocation the irradiance and load profile in Case 8.2 are the same as in Case 8.1. In Case 8.2 the investment cost assigned to the ESS connected between nodes 6-2 is larger, consequently no battery is assigned at this location. Investing in a storage unit with a capacity of 600 Wh is at the detriment of the production cost, it is more advantageous to active the diesel generator instead. No battery is allocated at this location and LMP are now derived from the marginal cost $\pi^{\mathrm{S}}_{5,1,1}$. Additionally the higher limit $S^{\mathrm{S}}_{2,10,6,\max}$ is set to 500 Wh. The capacity of unit $s^{\mathrm{ESS}}_{2,10,6}$ cannot be assigned its optimal capacity as opposed to Case 8.1. The utilization of renewable energies is limited, nodal prices vary accordingly during the time period when $p^{\mathrm{S}}_{1,9,5,k}$ is in use.

CASE 8.3

In this case the load profile is changed, two peaks are simulated where demand exceeds generation. During the time period $k1$ and $k2$, the energy demand is respectively 250 Wh and 500 Wh. Loads do not consume energy during the remaining time steps. The aim of this simulation is to illustrate a trade-off between production cost and investment cost. The upper and lower limit of the storage units in both polarities are the same and set to guarantee unconstrained operations of the ESS. However, $\pi^{\mathrm{ESS}}_{2,10,6}$ is larger than $\pi^{\mathrm{ESS}}_{6,2,2}$.

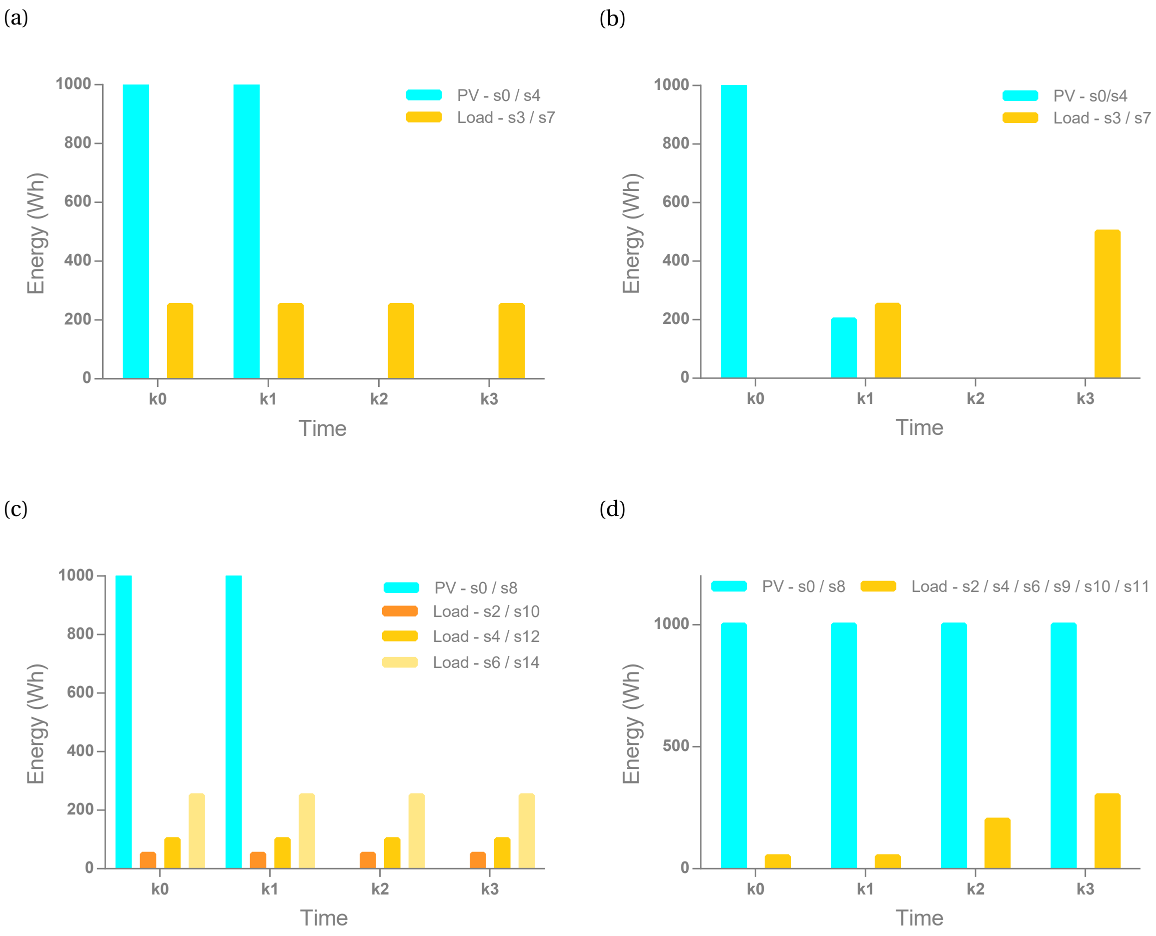

Figure 5.2: Irradiance and load profiles for cases 8.1 & 8.2 (5.2a), case 8.3 (5.2b), case 9.1 & 9.2 (5.2b) and case 10 (5.2d).

The effect of the difference in investment cost is reflected in the capacities of storage units. Looking at the positive side of the network where the investment cost is low, $s^{\text{ESS}}_{6,2,2}$ has the capacity to store all the energy necessary to deliver energy during $k1$ and $k2$. Investing in an ESS with sufficient capacity is less expensive than supplying the load with the most expensive generator, the storage is thus sized with respect to highest peak in demand. Nodal prices for the positive pole are close to 0 \$/Wh, the small variations are due to the current flowing in the neutral conductor.

On the other hand the ESS connected between the pair of node 2-10 has a smaller capacity. For the given investment cost $\pi^{\text{ESS}}_{2,10,6}$, the break-even capacity is 386.39 Wh. Increasing the size of Storage Unit $s^{\text{ESS}}_{2,10,6}$ would result in higher cost in comparison to supplying the next increment of energy with the diesel generator $p^{\text{S}}_{1,9,5,k}$. Nodal prices for the negative pole are derived from $\pi^{\text{S}}_{1,9,5}$. During the first time period, the PV panel is not operating at its maximum, the price of electricity is consequently 0 \$/Wh. However, during the second time period $p^{\text{S}}_{0,8,4,k}$ is at its upper limit, the next increment of energy will be supplied by the most expensive generator. During the rest of the simulation an increase of energy cannot be satisfied by the battery, prices are also derived from $\pi^{\text{S}}_{1,9,5}$.

5.3.2. The Role of Capacity Ranges for Optimal Location

In Cases 9.1 and 9.2, a simple scenario where a storage unit with variable capacity is connected between each pair of nodes of different polarity is implemented. The aim is to demonstrate how the network needs to be setup in order to find the appropriate location of ESS. Note that a connection between the positive and

	Case 8.1				Case 8.2				Case 8.3			
	$\lambda^{P}_{4,0,k}$	$\lambda^{P}_{5,1,k}$	$\lambda^{P}_{6,2,k}$	$\lambda^{P}_{7,3,k}$	$\lambda^{P}_{4,0,k}$	$\lambda^{P}_{5,1,k}$	$\lambda^{P}_{6,2,k}$	$\lambda^{P}_{7,3,k}$	$\lambda^{P}_{4,0,k}$	$\lambda^{P}_{5,1,k}$	$\lambda^{P}_{6,2,k}$	$\lambda^{P}_{7,3,k}$
$\Pi^{S}_{m,n,s}$	0	5	–	10	0	5	–	10	0	5	–	10
k0	0.00	0.00	0.00	0.00	0.00	0.00	0.00	0.00	0.00	0.00	0.00	-0.02
k1	0.00	0.00	0.00	0.00	0.00	0.00	0.00	0.00	0.04	0.02	0.00	0.00
k2	0.00	0.00	0.00	0.00	5.00	5.00	5.08	5.12	0.00	0.00	0.00	0.00
k3	0.00	0.00	0.00	0.00	5.00	5.00	5.08	5.12	0.02	0.01	0.00	-0.04
	$\lambda^{P}_{0,8,k}$	$\lambda^{P}_{1,9,k}$	$\lambda^{P}_{2,10,k}$	$\lambda^{P}_{3,11,k}$	$\lambda^{P}_{0,8,k}$	$\lambda^{P}_{1,9,k}$	$\lambda^{P}_{2,10,k}$	$\lambda^{P}_{3,11,k}$	$\lambda^{P}_{0,8,k}$	$\lambda^{P}_{1,9,k}$	$\lambda^{P}_{2,10,k}$	$\lambda^{P}_{3,11,k}$
$\Pi^{S}_{m,n,s}$	0	5	–	10	0	5	–	10	0	5	–	10
k0	0.00	0.00	0.00	0.00	0.00	0.00	0.00	0.00	0.00	0.00	0.00	0.00
k1	0.00	0.00	0.00	0.00	0.00	0.00	0.00	0.00	4.95	5.00	5.05	5.11
k2	0.00	0.00	0.00	0.00	5.00	5.00	4.97	5.00	4.56	4.56	4.56	4.56
k3	0.00	0.00	0.00	0.00	5.00	5.00	4.97	5.00	4.99	5.00	5.05	5.18

Table 5.3: Case 8.1, 8.2 & 8.3: LMP in terms of power for set of node connecting at least one source are displayed.

negative conductor is also possible. The network is bipolar and parameters are completely symmetric. It consists of only one generator, a PV panel with enough capacity to satisfy all the loads if a storage of sufficient size is available. Loads have the same marginal cost reflecting the user-willingness to consume electricity. Note that no diesel generators is available in the network. As a result load shedding will only occur if the batteries have insufficient capacities. To make sure that no such things is happening the investment costs of ESS are kept low.

The main difference between the two cases is related to the capacity range that is attributed to storage units. In Case 9.1, the units are given a wide range to guarantee unconstrained operation. As a result, values attributed to $s^{ESS}_{m,n,s}$ reflect the optimal capacities that will lead to the least losses. However, these values can be unrealistic by either being too small or too large. Five batteries are allocated with equal capacity from one polarity to the other. Sizes range from 55.53 Wh to 526.30 Wh. It is interesting to observe that the largest units are sited between nodes 7-3 and 3-11 where loads consume the most energy as it limits distribution losses. Notice that more ESS are assigned to the positive pole than the negative pole. However, the total storage capacity in both polarities is the same. It suggests that multiple solutions are available.

In Case 9.2, the model is made more realistic by adjusting the minimum size to a much larger value. The minimum storage capacity is set to 500 Wh, consequently only two storage units are allocated as opposed to five. In Figure C.3 the power outputs of PV panels are displayed, a difference is observed between the two scenarios. The energy produced in the latter case is slightly higher while the energy consumed by the loads is the same. It suggests that the narrower range imposed on $s^{ESS}_{m,n,s}$ leads to more losses. Therefore, although ESS capacities in Case 9.1 may be deemed unrealistic, they lead to a better exploitation of distributed generators. With regards to nodal prices, in both cases the next increment of energy at any time period can be supplied by the cheap generators. Note that they are not functioning at their maximum capacity. LMP are thus 0 \$/Wh at any location and time.

To conclude, the optimal location of batteries can be obtained by declaring an ESS with variable capacity between every nodes of different polarity in a network. Imposing capacity ranges allows to return a solution that is physically feasible with respect to the commercially available batteries. Omitting these ranges inevitably result in the allocation of an ESS at every location where storage units are declared. One of the disadvan-

Cases	Capacity Range [Wh]				Optimal Capacity [Wh]			
	$S^{S}_{4,0,1}$	$S^{S}_{5,1,3}$	$S^{S}_{6,2,5}$	$S^{S}_{7,3,7}$	$s^{ESS}_{4,0,1}$	$s^{ESS}_{5,1,3}$	$s^{ESS}_{6,2,5}$	$s^{ESS}_{7,3,7}$
Case 9.1	0–1000	0–1000	0–1000	0–1000	0.00	55.53	260.28	526.30
Case 9.2	500–1000	500–1000	500–1000	500–1000	0.00	0.00	0.00	842.92
Case 10	300–1000	300–1000	300–1000	300–1000	0.00	0.00	0.00	454.80
	$S^{S}_{0,8,9}$	$S^{S}_{1,9,11}$	$S^{S}_{2,10,13}$	$S^{S}_{3,11,15}$	$s^{ESS}_{0,8,9}$	$s^{ESS}_{1,9,11}$	$s^{ESS}_{2,10,13}$	$s^{ESS}_{3,11,15}$
Case 9.1	0–1000	0–1000	0–1000	0–1000	0.00	0.00	315.92	526.30
Case 9.2	500–1000	500–1000	500–1000	500–1000	0.00	0.00	0.00	842.92
Case 10	–	–	–	–	–	–	–	–

Table 5.4: Case 9.1, 9.2 & 10: Upper/lower limits and optimal capacity of variable ESS.

tage of this method is the computation time, indeed mixed-integer quadratically constrained programming is significantly more demanding in terms of amount of operation that the solver needs to go through. For larger and more complex networks, allocating an ESS with variable capacity may not practical. To ease the computation process only a limited amount of pair of nodes may be selected.

5.3.3. OPTIMAL ESS CAPACITY AND LOCATION FOR CONGESTION MANAGEMENT

The network simulated in Case 10 consists of two solar panels with a constant upper limit throughout the simulation. Three loads are connected to the positive and negative pole. The load profile is the same for both polarities and loading increase as a function of time. A battery with variable capacity is connected in parallel with every loads from the positive side of the network while no storage unit is connected to the negative side. So far variable ESS where used to balance the mismatch between energy supply and demand. In this case there is enough energy during each time period to directly supply the loads without a battery. However, a line constraint is introduced on $i^{S}_{4,5}$, $i^{S}_{0,1}$ and $i^{S}_{7,8}$. A maximum current of 1.5 A can flow through these lines. The aim of this example is to demonstrate how storage units with variable capacities can be used for congestion management. The economic dispatch is displayed in Table C.4.

On the negative side of the network where no storage is declared, loads are operating at their maximum output during the first two time steps when the energy demand is relatively low. The electrical flow in the the lines with a current limit is below the upper bound. However, a congestion is observed during $k2$ and $k3$ due to an increase in loading. Loads $p^{S}_{2,10,10,2}$, $p^{S}_{2,10,10,3}$ and $p^{S}_{3,11,10,3}$ cannot be fed enough power as result of the constraint imposed on branch $i^{S}_{7,8,k}$. During the last two time steps, these branches are operating at their upper limit. Consequently, loads are operating below their desired output. Nodal prices derived for $k0$ and $k1$ are all 0.00 \$/Wh as no constraint is activated. However, as explained in the previous chapter when load shedding occur LMP are derived from the price assigned to loads. Prices during the last two periods are all based on $\pi^{S}_{2,10}$ and $\pi^{S}_{3,11}$ except for $\lambda^{P_{0,8,2}}$ and $\lambda^{P_{0,8,3}}$. This pair of nodes is located before the congestion and power is available at a marginal cost of zero, inherently the LMP is 0.00 \$/Wh.

Looking at the upper side of the network, ESS with a variable capacity are connected between each pair of node on the positive and neutral conductor and a rather wide capacity range is assigned. As can be seen from Table C.4, the algorithm takes the line limit of branch 4-5 in consideration by allocating a storage unit between node 7 and 3. The battery takes advantage of the lower loading during $k0$ and $k1$ to charge. The charging rate is limited by the branch constraint, therefore the ESS cannot charge at a rate that would cause the branch current $i^{S}_{7,8,k}$ to exceed a current of 1.5 A. The energy stored during these time steps is then redistributed at times where loading increase. As a result, every loads can operate at their desired output throughout the

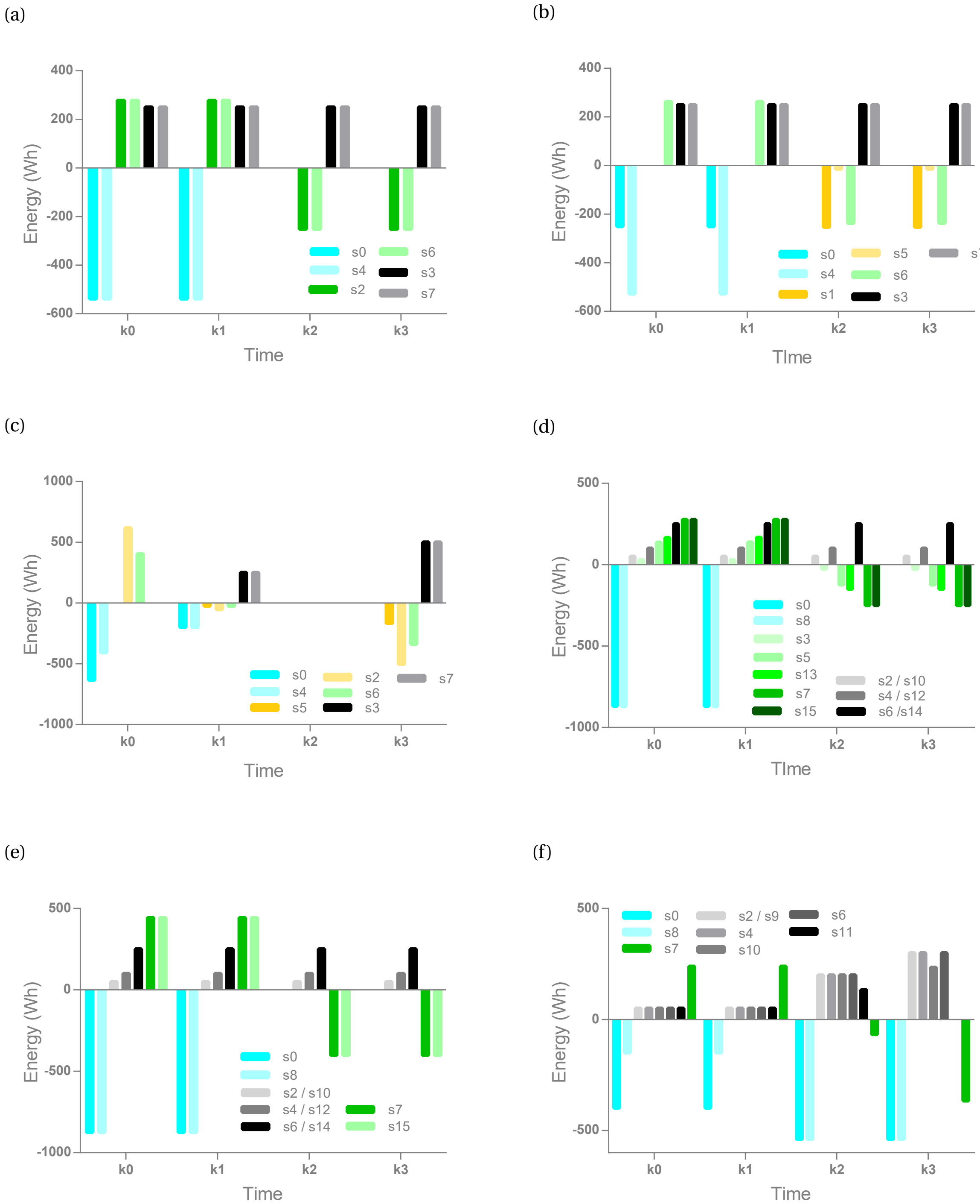

Figure 5.3: Case 8.1-10: Power output of sources with PV panels are represented in blue, diesel generators in yellow, ESS in green and loads in black. Figures 5.3a-5.3c, 5.3d-5.3e and 5.3f respectively represent Cases 8.1-8.3, 9.1-9.2 and 10.

simulation. Since the marginal cost $\pi^{S}_{4,0}$ is small, the most economical scenario is to use this generator until the line limit is reached, the branch current $i^{S}_{4,0,2}$ and $i^{S}_{4,0,2}$ is thus 1.5 A. Given the investment cost of storage and its capacity range it is cheaper to invest in only one ESS. In the absence of load shedding all LMP are obtained from $\pi^{S}_{4,0}$ and the difference is caused by the current flowing in the neutral conductor.

	Case 9.1				Case 9.2			
	$\lambda^{P}_{4,0,k}$	$\lambda^{P}_{5,1,k}$	$\lambda^{P}_{6,2,k}$	$\lambda^{P}_{7,3,k}$	$\lambda^{P}_{4,0,k}$	$\lambda^{P}_{5,1,k}$	$\lambda^{P}_{6,2,k}$	$\lambda^{P}_{7,3,k}$
k0	0.00	0.00	0.00	0.00	0.00	0.00	0.00	0.00
k1	0.00	0.00	0.00	0.00	0.00	0.00	0.00	0.00
k2	0.00	0.00	0.00	0.00	5.00	5.00	5.08	5.12
k3	0.00	0.00	0.00	0.00	5.00	5.00	5.08	5.12
	$\lambda^{P}_{0,8,k}$	$\lambda^{P}_{1,9,k}$	$\lambda^{P}_{2,10,k}$	$\lambda^{P}_{3,11,k}$	$\lambda^{P}_{0,8,k}$	$\lambda^{P}_{1,9,k}$	$\lambda^{P}_{2,10,k}$	$\lambda^{P}_{3,11,k}$
k0	0.00	0.00	0.00	0.00	0.00	0.00	0.00	0.00
k1	0.00	0.00	0.00	0.00	0.00	0.00	0.00	0.00
k2	0.00	0.00	0.00	0.00	5.00	5.00	4.97	5.00
k3	0.00	0.00	0.00	0.00	5.00	5.00	4.97	5.00

Table 5.5: Case 9.1 and 9.2: LMP in terms of power for set of node connecting at least one source are displayed.

	Case 10							
	$\lambda^{P}_{4,0,k}$	$\lambda^{P}_{5,1,k}$	$\lambda^{P}_{6,2,k}$	$\lambda^{P}_{7,3,k}$	$\lambda^{P}_{0,8,k}$	$\lambda^{P}_{1,9,k}$	$\lambda^{P}_{2,10,k}$	$\lambda^{P}_{3,11,k}$
k0	0.00	0.00	0.00	0.00	0.00	0.00	0.00	0.00
k1	0.00	0.00	0.00	0.00	0.00	0.00	0.00	0.00
k2	0.00	0.04	0.01	0.00	0.00	4.89	4.97	5.00
k3	0.00	0.02	0.00	0.00	0.00	4.94	5.00	5.01

Table 5.6: Case 10: LMP in terms of power for set of node connecting at least one source are displayed.

5.4. CONCLUSION

To conclude, this algorithm has for main purpose to maximize the use of renewable energies by finding the most appropriate location and size of storage to balance supply and demand in the presence of intermittency. Additionally, it can be used to manage congestions that can occur as a result of varying load profiles and lines' current limits. The presence of a storage unit can prevent congestions when loading exceed the line capacities. Batteries can be charged at times when loading is smaller and discharge when loading increase. This algorithm can be used by system operators as a preventive tool to improve users' benefits without changing the topology of the network.

It should be mentioned that this model is a first approach to finding the appropriate location and size of batteries. The main disadvantage is the infeasibility of the results. Indeed, the size of an ESS is constrained by the range defined by $S^{S}_{m,n,s,\max}$ and $S^{S}_{m,n,s,\max}$. The optimal capacity of the battery could be any value between these two capacities. It follows that finding a commercially available battery of the exact same capacity is unlikely. The model could be improved if a fixed value is assigned instead of a range, in short if $S^{S}_{m,n,s,\max} = S^{S}_{m,n,s,\max}$. By proceeding as such the capacity of a commercially available battery could serve as a fixed limit. If integer variables are used instead of binary variables, the amount of batteries of that capacity could be obtained for a given location. In case storage at a specific location do not improve the global objective, the integer variable will naturally be 0.

6

Case Study

Around 1.3 billion of people in the world do not have access to electricity. The challenge of supplying economically viable services to promote electrification of rural areas is inevitable. For the reasons stated previously in this report bipolar DC distribution networks have many advantages in comparison to AC distribution systems. The potential to transit from LVAC to LVDC is considerable. Developing countries offer an excellent opportunity to leapfrog AC distribution networks. The amount of studies on OPF for bipolar DC distribution systems is limited. Moreover, there are no research that combines this type of network with LMP in an attempt to formulate a pricing mechanism both adapted to the network topology and promoting the maximization of RE resources' utilization. The OPF algorithm is implemented in a case study based on a rural area in Senegal, it aims at formulating a price mechanisms relying on consumer's willingness to purchase electricity. The impact of the network topology and availability of solar energy on LMP is also demonstrated. Nodal prices reveal to be an appropriate tool to reduce asymmetries and reveal investment opportunities that maximize the use of DG while benefiting consumers.

The case study is divided in three sub-cases to illustrate different behaviors. In the first case the PV plant is directly connected between the positive and negative conductor while in the second case half of the panel are connected between the positive and neutral conductor, the other half is connected between the neutral and negative conductor. A noticeable difference in the utilization of RE is observed. In the third case the method for optimal sizing and siting of ESS is implemented. It reveals to be a useful tool for grid operators to establish a balance between the positive and negative pole and to increase the utilization of renewable DG.

6.1. Netork Topology

The network is based on a satellite imagery of the village of Godiba in Senegal, see Appendix D.1. A district consisting of three streets with nearby agricultural activities was selected for the implementation of an off-grid DC bipolar microgrid. To assess the validity of the model with regards to the maximized utilization of DG a PV plant was hypothesized. The bipolar network is illustrated in Figure 6.1, it includes 15 installations defined as houses, schools, health centers, PV plants and agricultural sites.

The microgrid is composed of 80 nodes, the positive, neutral and negative conductor are respectively represented by nodes $[27-53] \in \mathcal{N}_+$, $[0-26] \in \mathcal{N}_\mathrm{N}$ and $[54-80] \in \mathcal{N}_-$. As in the previous examples, voltage constraints are given by (3.26)-(3.28) and the grounded node is 0. Distribution lines are sized proportionally to the satellite image of Godiba where the connection from one street to the is approximately 500m, the PV plant and the agricultural site are respectively located 1000m and 500m from the closest streets. Given the size of the microgrid relatively small cables were chosen. The cross sectional area of lines in the street, to the PV plant and to the agricultural site are 10, 25 and 50mm^2. The electrical conductance is computed as in (6.1)-(6.2) where L denotes the length of a cable, A its surface area and the specific capacity, ρ, is set to $2.65\mathrm{e}{-8}\ \Omega\cdot\mathrm{m}$ for all cables. Current limits are set as in (3.9) and a relatively low value of -10A and 10A was

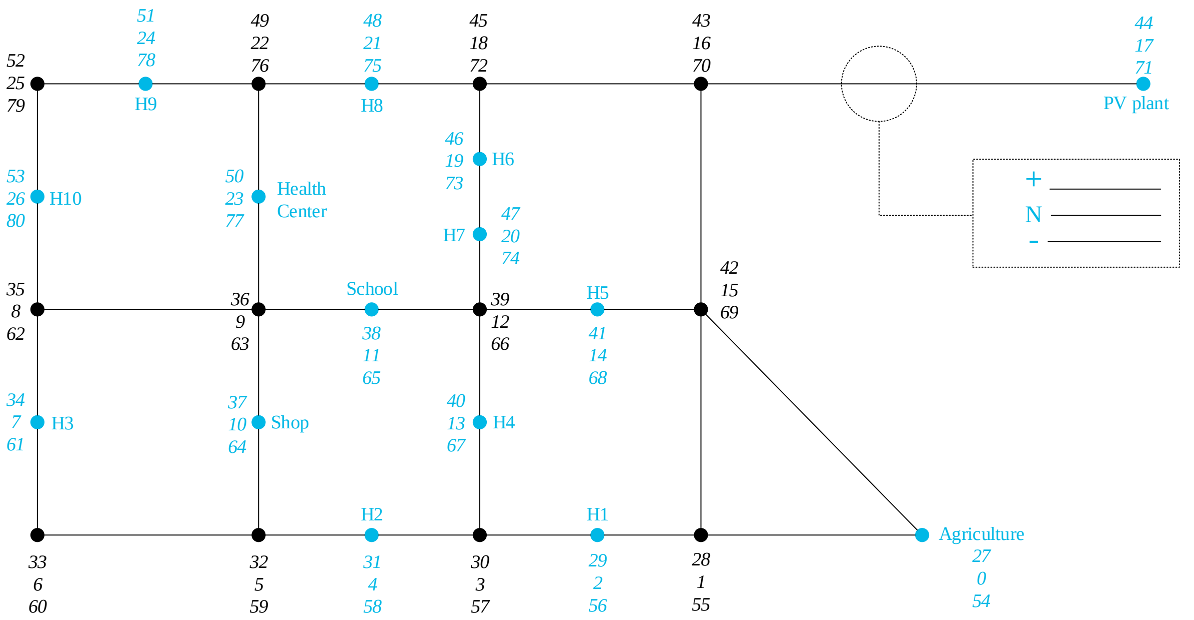

Figure 6.1: Schematic of the simulated microgrid. For ease of representation the neutral, positive and negative conductors are represented as one line. Sources are represented in blue and buses in black with their corresponding indexes.

assigned to $I_{m,n,\min}$ and $I_{m,n,\max}$ in order to cause congestions.

$$R_{m,n} = \frac{\rho_{m,n} \cdot L_{m,n}}{A_{m,n}} \qquad \forall (m,n) \in \mathcal{G} \tag{6.1}$$

$$G_{m,n} = \frac{1}{R_{m,n}} \qquad \forall (m,n) \in \mathcal{G} \tag{6.2}$$

Three sub-case studies are proposed with different sources. Case 1, 2 and 3 have respectively 69, 70 and 79 sources representing generators, loads and ESS. Sources are only connected between pairs of nodes that define an installation. Each installation has multiple sources connected in parallel as illustrated in Figure 3.2. In short, households, shops, health centers... are considered to be nanogrids with negligible power losses. Loads with large power outputs are directly connected between the negative and positive poles, they benefit from a large Δu which reduces the amount of current that needs to be generated for a given power to be produced. This configuration is used in the first and third case to connect PV panels, diesel generators, ESS and loads from the PV plant and agricultural site. In the second case the PV plant and ESS connection type is changed, two storage units are connected from the positive to neutral and negative to neutral conductors. The cumulative capacities of these batteries is equal to the capacity of the ESS in the former case, therefore the total storage capacity remains unchanged. The purpose is to reflect the role of connection configurations of generating sources on LMP. The rest of the sources are uniform in all cases and are either connected between the positive to neutral pole or between the neutral to negative pole. The configuration and index of each source is given in Tables D.1 and D.3. Finally, in third case variable ESS are defined at different locations to solve for optimal location and size. The difference between the three cases is illustrated in Table 6.1.

6.2. LOADS AND RESOURCES ESTIMATIONS

In rural villages the demand for electricity is low in comparison to urban areas. The load assessment for Godiba is based on previous studies from Sen and Bhattacharyya. The electricity demand is classified in five categories: domestic use, commercial activities, community activities, health services and agricultural activities. In Table D.4 each category with the corresponding loads are indicated. For each load the power requirement is specified as well as the usage time per day. To obtain a load profile with a mismatch between energy demand and supply loads were strategically distributed throughout the day. Lights, fans, radios and

	Case Study 1	Case Study 2	Case Study 3
Network Topology	Same	Same	Same
Generation Capacity	Same	Same	Same
Installation's L0ading	Same	Same	Same
Configuration of loads	Same	Same	Same
Configuration of sources	All PV panels and ESS from the PV plant are connected between the positive and negative conductors	The generation and storage capacities of the PV plant are the same as in Case 1. However, the ESS are connected to the positive pole and the other half is connected to the negative pole. The total storage capacity is the same as in Case 1	Same as Case 1
Optimal Location and Size of ESS	No	No	Yes

Table 6.1: Difference between the three sub-cases

charging devices are used during the night while fans are used during the day when the outside temperature is hot. Fridge are modeled as constant loads and pumps operate during the day. In order to reveal different LMP behaviors the electricity demand of pumps during the first and second day differs. Asymmetrical loading is introduced by the pump located in the health center from $k12$ to $k14$ and a congestion is caused by the pumps used for agricultural activities from $k34$ to $k36$. Figure 6.3b reflects the loading for each time period with respect to the configuration type, this graph reveals loading asymmetries.

In this model it is assumed that loads have a variable outputs. Note that in reality not all the loads have the ability to do so. To demonstrate the role of load shedding in a network the minimum power, $P^{\mathrm{S}}_{m,n,s,k,\mathrm{min}}$, is set to 0 W for all loads and their maximum power, $P^{\mathrm{S}}_{m,n,s,k,\mathrm{max}}$, is indicated in Table D.4. Moreover, a marginal cost reflecting the willingness of user to purchase electricity is attributed to each load. These prices were chosen without doing any background research about the economical situation in this area. Here, fridges and water pumps are given the highest priority while domestic loads are given a lower priority.

Diesel generators and PV panels are the two types of generator considered. The microgrid contains five DG as indicated in Table D.5. To assess the energy production from PV panel irradiance data was obtained from SoDa's website[1] at the location of Godiba. The solar energy assessment is simplified by assuming a surface area of 1m^2 per panel and an efficiency of 15%. Using (6.3) the maximum power production is expressed by $P^{\mathrm{S}}_{m,n,s,k,\mathrm{min}}$ since generators have negative power outputs. The limit is the product of the panel efficiency (η^{PV}), the irradiance (R_k) and the area of the panels ($A_{m,n,s}$), it is obtained for each time period as indicated in (6.3). To simulate different behaviors the irradiance profile of the second day is increased by 20% with respect to the first day. In Figure 6.3a the maximum amount of energy that can be generated from PV panels is expressed and compared to the demand profile. As explained in Chapter 4 the marginal cost of PV panels is set to 0 \$/Wh while the marginal cost of diesel generators is 1\$/Wh.

$$P^{\mathrm{S}}_{m,n,s,k,\mathrm{max}} = R_k \cdot A_{m,n,s} \cdot \eta^{\mathrm{S}}_{m,n,s} \qquad \forall m,n,s,k \in \mathscr{S} \tag{6.3}$$

The total amount of energy that can be produced from PV panels exceeds the total energy demand and inter-

[1] http://soda-is.com

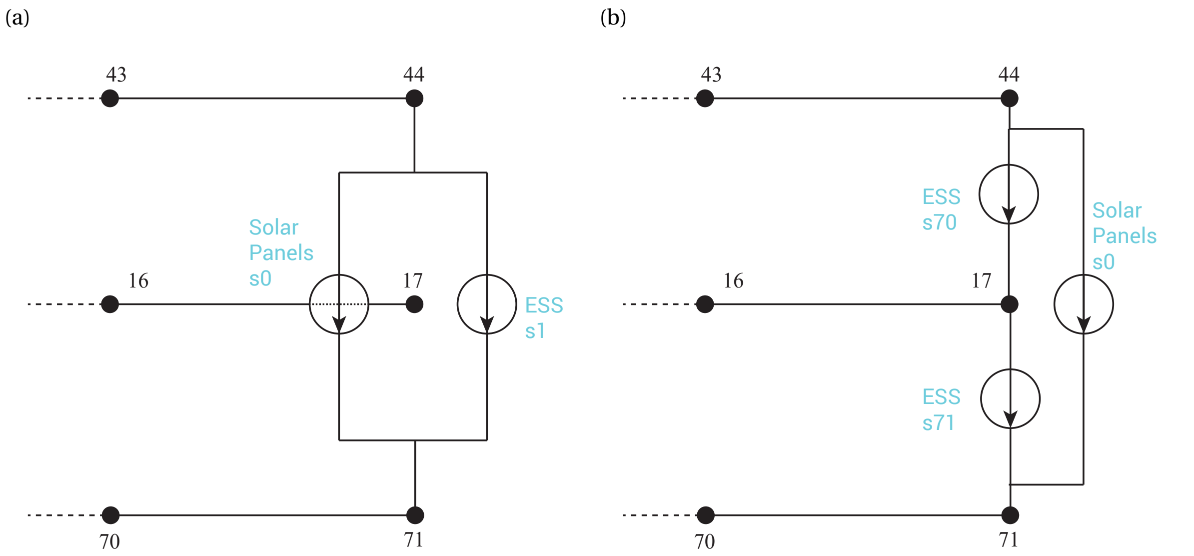

Figure 6.2: Figure 6.3a illustrates PV plant configuration used in Case 1 and 3. Figure 6.3b illustrates PV plant configuration used in Case 2.

mittency occurs during certain time periods when solar energy is scarce. An ESS is placed at the PV plant but its capacity is not large enough to store enough energy to redistribute it at the times when PV panels cannot produce. The capacity was strategically chosen to cause a demand-response phenomena from the load side. The first and second case studies only rely on this storage unit while in the third case study optimal sizing and placement of batteries is implemented.

6.3. CASE STUDY 1

The results of the first case study are discussed in this section. As shown in Figure 6.5b, the behavior of LMP varies throughout the simulation. The exact values of nodal prices are displayed in Tables D.6-D.8. In the following sections LMP are explained with respect to the power flows and network topology. The exact values of each source's power output for every time periods is available in Tables D.9-D.18. In this case, the configuration of the main generators (directly from the positive to negative conductors) limits power flows and the utilization of RE.

SOLAR ENERGY SCARCITY AND EMPTY ESS: k0-k7

The energy content of the battery is set to 0 Wh during the first time step, no minimum state of charge is implemented. Batteries are thus empty at the beginning of the simulation. Additionally, $k0$ is the time step between 12AM to 1AM, as a result solar energy is not available until $k7$. The diesel generators $s2$ and $s5$ are the only sources that can supply energy during this interval. The demand is constant and consists of two fridges located in the health center and the shop, their marginal prices are higher than the generators'. Consequently, the energy delivered to the sources is equal to their upper limits and the same outputs are obtained from $k0$ to $k6$. The diesel generators have the same cost of operation, therefore the difference in the energy produced by $s2$ and $s5$ is a consequence of the network topology. The generator located at the PV plant is farther away from the loads, to limit losses its output is thus lower than $s5$.

As no other cheaper option is possible, LMP are directly derived from $\pi^S_{44,71,2}$ and $\pi^S_{27,54,5}$. The effect of losses and location of the active loads on the prices is relatively small, however a difference is observed between the positive and negative polarity for which the average nodal prices are respectively 1.01 and 0.99 \$/Wh. For locations where $\lambda^{\mathrm{P}}_{m,n,k}$ is lower than 1 \$/Wh it implies that less than one unit needs to be generated by the generators if an increment of one unit is implemented anywhere in the negative polarity. Although the

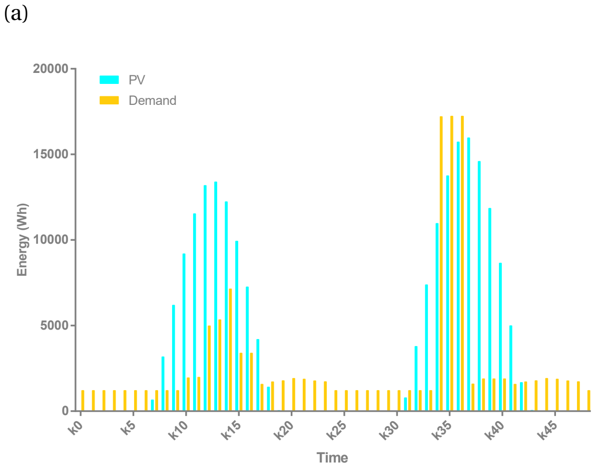

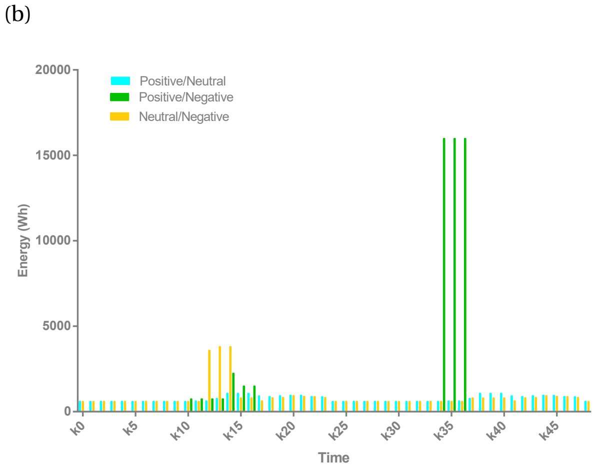

Figure 6.3: Figure 6.3a illustrates the total PV profile and electricity demand for the village of Godiba. Figure 6.3b illustrates the total loading per connection configuration.

loading of the positive and negative pole is equal, the network topology causes asymmetrical power flows. All diesel generators are directly connected from the positive to negative conductors which explains why the positive pole has LMP higher than 1$/Wh while the negative pole has LMP lower than 1$/Wh. If these generators were to be connected to the neutral conductor nodal prices of the positive and negative pole would all be above 1$/Wh and the price variation between each location is a result of thermal losses.

The loading of $k7$ is the same as in the previous time periods. However, solar energy is available which enables the use of PV panels. Solar panels $s0$, $s29$ and $s59$ are operating at their full capacity given the small irradiance. The energy generated is not sufficient to satisfy loads $s29$ and $s56$. However, it is enough to allow the deactivation of the diesel generator located at the PV plant. Only the closest backup generator $s5$ compensates for the lack of solar energy. Inherently, the production cost during this time step is lower as in the previous periods and as opposed to $k0$-$k6$ more power is generated from DG located at the PV plant than the agricultural sites. Since the marginal cost of PV panels is 0 $/Wh the marginal cost of losses caused by these generators is also 0$/Wh. It is important to notice that the storage is not charging which suggests that there is no better utilization of the DG. Indeed solar power is used to supply the loads with the highest priority. Moreover from Figure 6.5a it can be seen that the ESS is fully charged during $k18$, the last time period when solar power is available.

Since all PV panels are operating at their boundary the next increment of energy can only be supplied by the diesel generator, most likely from $s5$ to limit thermal losses in conductors. Inherently, nodal prices are close to 1$/Wh and the difference is caused by losses and the different locations of both loads. A difference is also observed between the positive and negative pole where the average LMP of the positive side is 0.99$/Wh and the average LMP of the negative side is 1.01$/Wh. DG $s29$ and $s59$ are respectively connected to the negative and positive pole, however they are both constrained. The difference in nodal prices from one side of the network to the other is thus explained by the connection type of $s5$.

RELYING ON SOLAR ENERGY: k8-k9 / k32-k33 / k37-k38 / k42 / k44 / k46-k48

During these time periods LMP are all equal to 0 $/Wh. It suggests that the energy consumed is obtained from solar resources and that all loads are operating at their boundary $P^{S}_{m,n,s,k,\max}$. Such prices can be obtained under different conditions. As in $k9$, it can occur if a PV panel is not operating at its maximum output. Ergo, the next increment of energy can be obtained at no cost. LMP be can also be equal to 0 $/Wh in situations where all PV panels are operating at their full capacity. In such a case, the energy produced is used to satisfy all the loads and the remaining energy is fed to a storage unit. The next increment of energy is thus obtained for free and the energy used to charge the battery decreases by one unit. That can only happen if the energy used to charge the battery can be obtained during other time periods when electricity supply from PV panels exceeds demand. This scenario is observed during $k8$. Lastly, nodal prices of 0 $/Wh are obtained at times where solar energy is not available under the condition that the energy content of the ESS is large enough to feed every loads. This occurs towards the end of the simulation for $k44$ and $k46$-$k48$.

ASYMMETRICAL LOADING: k12-k14 / k15-k17 / k39-k41 / k43 / k45

As indicated in Figure 6.3b, loading in the network is highly asymmetric from $k12$ to $k14$. The demand in the negative pole drastically exceeds the demand in the positive pole. The asymmetry is caused by the water pump $s57$ located in the health center. The difference in loading is reflected in the voltage of nodes $n27$ and $n71$, both constrained to their lower boundary. Consequently, the voltage drop Δu in the negative pole is maximized in an effort to increase power outputs $p^{\mathrm{S}}_{m,n,s,k}$. On the contrary, the voltage drop of the positive pole is minimized to force higher currents to flow through the conductors. These two phenomenas lead to larger power outputs between the neutral and negative conductors. Note that this power flow behavior is a direct consequence of having the PV panel with the largest capacity connected between the positive and negative pole. A similar behavior is observed as in Example 7 from 4

Consequently all the the loads located on the upper side of the network, regardless of their marginal costs, are consuming as much power as they can in order to increase the current flowing through the positive and negative conductors which inherently boosts the power consumption of loads connected on the lower side. Reciprocally, on the negative side of the network all the loads with a marginal price lower than $\pi^{S}_{23,77,57}$ are turned-off in order to increase the power consumptions of the loads with the highest priorities. The PV panel connected between the positive and neutral conductor, $s59$, is not activated as opposed to PV panel connected between the neutral and negative conductor, $s29$, which operates at its maximum capacity. In such a way the power available in the negative polarity is augmented. Despite these efforts to increase the power between the neutral and negative conductor, the high priority loads $s23$ and $s59$ cannot be fully satisfied. Given that the amount of solar energy exceeds loading during these time periods it can be concluded that load shedding of the negative pole occurs as a result of the asymmetry between the two polarities.

The difference in load shedding between the two sides of the network is expressed on the LMP. On the positive side, prices are negative which implies that the next increment at these locations will result in a payment from the grid operator to the consumers. In other words, by increasing the loading on the positive side of the network by one unit, an extra unit will automatically be consumed by the high priority loads of the negative pole, $s23$ and $s59$. By increasing any load on the positive pole, the extra unit produced by generator $s0$ will lead to an increase in consumption of approximately two units. LMP of sources connected between the positive and neutral conductors have an average value of -2.09, -2.08 and -2.06 $/Wh. A negative price is an incentive to increase electricity consumption to balance the loading of the two polarities. These nodal prices are derived from the marginal cost of the loads for which the power consumption is constrained by the asymmetry. In this case loads $s23$ and $s59$ have a marginal cost of 2$/Wh. LMP of the negative side of the network are also derived from this value, the average nodal prices are slightly lower that $\pi^{S}_{23,77,57}$, the difference is caused by the losses and sources' locations.

From $k15$ to $k17$ and $k39$ to $k41$ a similar behavior is observed, although this time the asymmetry is smaller and occurs due to a higher loading on the positive side of the network. The lower imbalance between the two polarities causes load shedding of sources from the positive pole with a marginal cost 0.5 $/Wh, namely fans and computers. Every loads from this pole with marginal cost lower than 0.5 $/Wh are naturally not active. Reciprocally, every loads from the negative pole are operating at their maximum capacities. Similarly to the previous time steps, both positive and negative nodal prices are obtained and derived from the shedded loads. The negative side has negative LMP while the positive side has positive LMP. The same phenomena occurs in $k43$ and $k45$ where load shedding occurs for loads with lower priorities.

LIMITED AMOUNT OF SOLAR ENERGY: k18

This time step is another case where load shedding occurs. There is no major asymmetry in the network, the difference in power requirement between the positive and negative side is only 70 W. Solar energy is available in smaller quantities and the total energy that can be generated from PV panels is smaller than the demand. Moreover, the ESS was fully charged during the last time period. The state of charge at the beginning of $k18$

is thus equal to 1. The best way to utilize the energy generated from $s0$, $s29$ and $s59$ is to distribute it to loads with the largest marginal prices. During this time periods fridges $s23$ and $s56$ have the highest priority and the renewable DG can generate enough power to fully satisfy them. However, the remaining energy is not enough to fulfill the power requirements of loads with the second highest priority, namely lights. Only a limited amount of lighting appliances are operating at their upper boundary, the rest are either consuming a smaller amount of energy or turned-off. Diesel generators are not activated as their marginal cost is larger than any other loads.

LMP are derived from the pair of nodes where load shedding occurs. Therefore, $\lambda^{\mathrm{P}}_{56,2,18}$ and $\lambda^{\mathrm{P}}_{44,71,18}$ are equal to 0.75 $/Wh. The rest of the nodes have nodal prices that are either slightly higher or lower as a consequence of the network topology.

THE ROLE OF ESS: k19-k31

The power flow observed in this interval is similar to k0-k6. In the absence of solar power, from $k20$ to $k30$, energy can only be supplied by the diesel generators or the ESS. Although the battery is fully charged at $k19$, its capacity is not large enough to feed every loads in the network. As a matter of fact its energy content is too small to guarantee the supply of high priority loads $s23$ and $s56$. It discharges uniformly $k20$ to $k30$ and the closest diesel generators, $p^{\mathrm{S}}_{54,2,5}$, is used as complementary generators. Consequently, loads for which the marginal cost, $\pi^{\mathrm{S}}_{m,n,s}$ is lower than $\pi^{\mathrm{S}}_{54,2,5}$ are shut down. THe power flow is slightly different during $k19$ and $k31$ as solar energy is available in small quantities. LMP are similar to $k18$, they are obtained from the operating cost of the diesel generators. The topology of the network causes nodal prices of the negative side of the network to be slightly higher than 1 $/Wh while the negative side have prices slightly lower than 1 $/Wh.

CONGESTED NETWORK: k34-k36

The impact of congestion on LMP is demonstrated from $k34$ to $k36$. As shown in Figure 6.3b, the network loading is considerably higher during these periods and there are no major asymmetries as the largest loads, $s3$ and $s4$ are connected from the positive to negative conductor. Only the PV plant can generate enough energy. Therefore, $s0$, $s1$ and $s2$, has the potential to feed the grid with enough current as the rest of the DG are considerably smaller . However, the current that needs to flow through branches $i_{43,44}$ and $i_{70,71}$ exceeds the current limits of these lines. Consequently, the electricity production from the PV plant generators is curtailed to 10 A. The rest of DG are not contributing to the congestion but their outputs is not sufficient to reach the demand-supply balance. Load shedding occurs for loads with high priorities such as pumps and fridges while loads with smaller marginal costs are turned off.

The maximum amount of power produced in the microgrid is reached. Therefore, the next increment of energy can only be provided at the detriment of the loads currently consuming power. LMP are derived from $\pi^{\mathrm{S}}_{27,54,3}$, $\pi^{\mathrm{S}}_{27,54,4}$ and $\pi^{\mathrm{S}}_{10,64,23}$, the marginal cost of loads that are not operating at their desired output as a consequence of the congestion. Depending on sources' locations in the network nodal prices vary. LMP are higher than 2 $/Wh if the next increment of power at a location causes an increase in losses in comparison to the current OPF. Reciprocally, if the the next increment of power at a location decreases the system losses its nodal price is lower than 2 $/Wh.

6.4. CASE STUDY 2

This case study is based on the exact same network and parameters. The only difference from case 1 is the connection type of the battery located in the PV plant. In the previous example the main contributors to power distribution were connected between the positive and negative poles. As it can be seen in the LMP, this configuration can be a burden to the grid operation in the presence of excessive asymmetries. Here $s70$ and $s71$ are both connected to the neutral conductor. The former contributes to the energy supply of the positive pole while the latter contributes to the energy supply from the negative pole.

The change of configuration has a beneficial effect on the economic dispatch. The objective is higher in comparison to the first case, from 181,506.6 $ to 194,005.3 $, which translates into less load shedding. For instance, from $k12$ to $k13$ in the negative pole high priority loads were shedded while low priority loads were turned off in consequence of the limited flows caused by the asymmetry in combination with generators connected from the positive to negative conductor. Here, ESS $s70$ and $s71$ are charged at different rates during the previous time steps. Naturally, Battery $s71$ connected to the negative pole has a higher state of charge. Starting from $k12$, when the asymmetry is large, the energy from that battery is discharged to feed the intensive load of the negative loads. Water pump $s57$ is still shedded as in case 1, however it can consume considerably more energy. It is now limited by the carrying capacity of the cables connecting the PV plant to the microgrid, $i_{70,71}$ is operating at its boundaries. If this cable had the capacity to carry more current all the loads will be satisfied an no load would be shedded. Notice the change in LMP for these time periods. The prices on the negative side of the network are derived from the shedded load and are thus close to 2 $/Wh, the water pump's marginal cost. In the previous case study LMP were highly negative which suggested that load shedding occurred as consequence of asymmetries, here nodal prices for that pole are nearly 0 $/Wh. Although at some location slightly negative prices are observed, it conveys that the two poles are able to operate independently from each other. Such power flows translate into higher current and voltage deviation in the neutral conductor.

A similar behavior is observed during the intervals where load shedding was caused by asymmetrical loading, namely $k15$-$k17$, $k39$-$k41$, $k43$ and $k45$. In case 1, low priority loads were shedded as the power flows were limited by both loading asymmetries and generators connected from the positive to negative conductor. In this example, we notice that implementing power generators on the positive and negative poles allows for the neutral currents and voltages to compensate for the asymmetry. As a result no loads are being shedded as there is enough solar energy available and batteries have sufficient capacities for most time periods. LMP are inherently all equal to 0 $/Wh as the next increment can be supplied directly or indirectly from the solar panels. It's only during $k18$ that there is not enough energy which explains why the nodal prices are derived from the marginal cost of the loads with the highest priority that cannot be fully satisfied. In other terms, this configuration do not only decrease electricity prices in the network, it also increase the utilization of PV panels. The power generated from the PV panels with respect to the total amount of energy that can be generated is 49 %, a 13 % increase from case 1.

6.5. CASE STUDY 3

Optimal sizing and placement of ESS is implemented in this case study. The network is the same as in the first case study, hence the only storage units has a fixed capacity and is located in the PV plant with a connection from the positive to negative pole. The limitation of this connection is demonstrated in Sections 6.3 and 6.4. The capacity of the only storage unit is not large enough to satisfy all the loads using solar energy. The modified OPF described in Chapter 5 is applied and multiple storage units with a variable capacity constrained by a range defining a maximum and minimum size are declared at different location in the network. To ease the solving process, only 12 variable ESS are declared. Half are connected from the positive the neutral conductor and half are connected from the neutral to negative conductor. The price and capacity constraints were chosen arbitrarily, they do not rely background researches. The investment cost is set to 0.5 $/Wh and the lower and upper capacity limits are 2,000 Wh and 8,000 Wh.

The simulation results are displayed in Table 6.2, only two locations were deemed optimal for the implementation of ESS. The capacity of the units are almost the same and neither is equal to the capacity limits. It can be concluded that the size of the batteries are optimal given the availability and loading of the grid for the two days simulated. These batteries are placed at the same location, more or less in the center of the network and close to the large loads of the agricultural site. The central position of these ESS lead to less losses in comparison to other alternative listed in Table 6.2. Note that each storage unit is connected to a different pole, similarly as in the second case study, it enables a better utilization of DG and prevents unbalances in power distribution between the positive and negative poles. The amount of energy generated from the panels with respect to the total amount of energy that be generated is 61.46 %, a 41.89 % increase from case 1.

In the first case study, high LMP were caused by asymmetries, congestions and intermittency in combination with undersized storage units. In the second case, it was demonstrated that LMP are much lower if generators

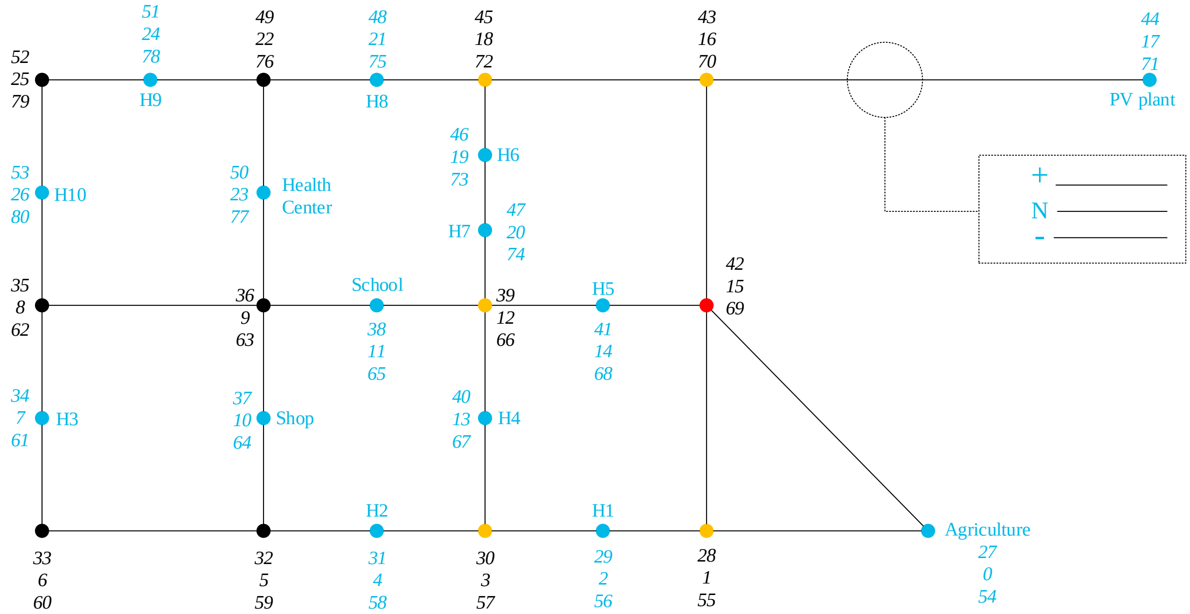

Figure 6.4: Schematic of the simulated microgrid. The nodes represented in red and yellow represents the locations where where ESS with variable capacities are declared. The node is red is the most optimal location where a storage should be implemented.

are connected to each pole. The same phenomena is observed in this case. As shown in Figure 6.5f, during the time intervals when LMP were both negative and positive, a consequence of asymmetries, prices are now 0 \$/Wh. In the previous cases, the intermittency and the lack of storage units were reflected in the nodal prices from $k19$ to $k31$. Increasing the storage capacity allows for a maximized utilization of the loads during these time steps, consequently LMP are also 0 \$/Wh. Notive that not all the batteries are reach their full capacity before $k19$, moreover solar panels are not operating at their maximum output from $k10$ to $k19$. The next increment of energy at any location from $k19$ to $k31$ can be obtained from solar energy. It is only at the beginning of the simulation that electricity prices of the positive and negative poles are non-zero, indeed solar energy is not available and batteries are empty. The next increment of energy can only be provided at the marginal price of diesel generators.

Although it is not displayed in the nodal prices of the positive and negative pole, the congestion from $k34$ to $k35$, lines $i_{27,28}$ and $i_{43,44}$ are still congested. In this case the congestion cannot be solved by increasing the system storage capacity. The demand of the irrigation and water pump of the agricultural site is too high in comparison to the capacity of distribution cables. Figure 6.5f only displays prices for the positive and negative side of the network, however a price is also obtained for sources connected across the positive and negative conductor. The LMP at the agricultural site, $\lambda^{P}_{27,54}$, is equal to 2 \$/Wh which indicates that loads at this location are shedded. The rest of the prices in the network are close to 0 \$/Wh, indeed the next increment of energy anywhere else can be provided by the storage units $s78$ and $s79$. During this time interval, LMP are either slightly higher or lower than 0 \$/Wh as an increment in energy will affect the power flows in the whole network. Consequently, loads $s3$ and $s4$ will either benefit or be penalized depending on where the increment takes place. LMP from $k34$ to $k35$ are displayed in Tables D.19.

6.6. CONCLUSION

It can be concluded that LMP are highly sensitive to the network topology as they reflect distribution losses, congestions and asymmetries. For each time step nodal prices of the same pole have more or less the same value, the small difference from one pair of node to another is caused by the thermal losses in the conductors. On such a scale losses are minimal and their effect on electricity prices is almost negligible. However, in large networks where distances from DG are higher the difference may affect prices to a larger extent. It could potentially lead to load shedding if losses cause LMP to be greater than the consumers' willingness to

Cases	ESS Cost [$/Wh]		Capacity Range [Wh]		Optimal Capacity [Wh]	
	$s^{ESS}_{39,12,70}$	$s^{ESS}_{12,66,71}$	$s^{ESS}_{45,18,72}$	$s^{ESS}_{18,72,73}$	$s^{ESS}_{30,3,74}$	$s^{ESS}_{3,57,75}$
$\pi^{ESS}_{m,n,s}$	1	1	1	1	1	1
$\mathrm{S}^{\mathrm{S}}_{\mathrm{m,n,s}}$	2,000–8,000	2,000–8,000	2,000–8,000	2,000–8,000	2,000–8,000	2,000–8,000
$\mathrm{s}^{\mathrm{ESS}}_{\mathrm{m,n,s}}$	0.00	0.00	0.00	0.00	0.00	0.00
	$s^{ESS}_{43,16,76}$	$s^{ESS}_{16,70,77}$	$s^{ESS}_{42,15,78}$	$s^{ESS}_{15,69,79}$	$s^{ESS}_{28,1,80}$	$s^{ESS}_{1,55,81}$
$\pi^{ESS}_{m,n,s}$	1	1	1	1	1	1
$\mathrm{S}^{\mathrm{S}}_{\mathrm{m,n,s}}$	2,000–8,000	2,000–8,000	2,000–8,000	2,000–8,000	2,000–8,000	2,000–8,000
$\mathrm{s}^{\mathrm{ESS}}_{\mathrm{m,n,s}}$	0.00	0.00	7,059.97	6,999.40	0.00	0.00

Table 6.2: Investment costs, upper/lower limits and optimal capacity of variable ESS.

purchase electricity.

Different cases of load shedding were demonstrated for which a simple analysis can be used to reveal their nature and possibly suggest operation and investment decisions. Load shedding occurs as a consequence of intermittency when all PV panels are operating at their full capacity or if ESS reach its maximum capacity. The price of electricity is thus obtained from the marginal cost of loads that have to adjust their energy consumption. To prevent such event from happening, the grid operator or consumers could increase the availability of energy by purchasing additional DG and/or storage units.

A similar strategy can be adopted to prevent congestions. Indeed networks are congested if generation or consumption are centralized rather than spread out. For instance in this case study most of the power is produced at the PV plant. Consequently, the distribution line making the connection to the grid is congested when loading increase. Investing in DG or ESS could provide a better distribution of the produced energy. It is worth mentioning that congestion may also be the direct consequence of undersized distribution cables. In the examples provided, even in the presence of additional storage unit the congestion persists. It suggests that the congestion can be only be avoided through the replacement of the distribution lines or by increasing the amount DG.

Lastly, the sources' configuration plays an essential role on power flows and LMP. In order to demonstrate the downsides of having generators and loads connected from the positive to the negative conductors, the main contributors to power generation and consumption were configured accordingly in case 1. In the presence of asymmetrical loading natural power flows limit the availability of electricity on the poles with higher loading even though DG or lines are not constrained. The presence of negative prices is an indicator of asymmetries that can be interpreted as an investment opportunity. Load shedding can be decreased by connecting additional DG or ESS from the positive or negative pole to the neutral conductor as implemented in the second case study. Additionally, the ability of LMP to be negative benefits the grid by giving an incentive to increase the consumption to establish a balance between the negative and positive pole. In essence by incorporating the grid topology to the model the pricing mechanism enhance the utilization of RE and operation of the grid.

(a)

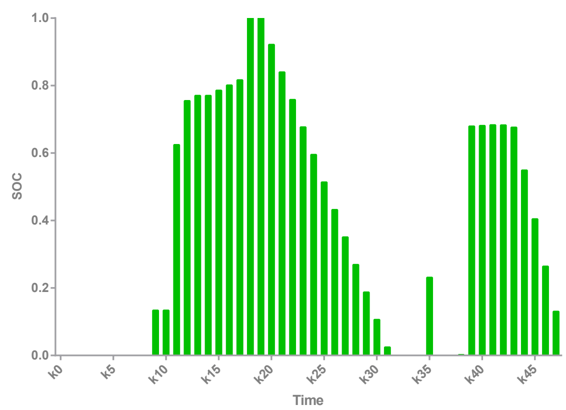

(b)

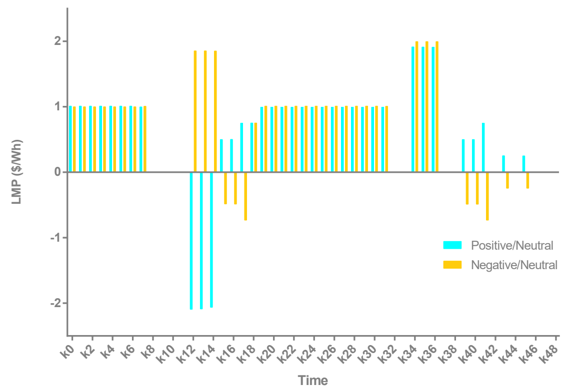

(c)

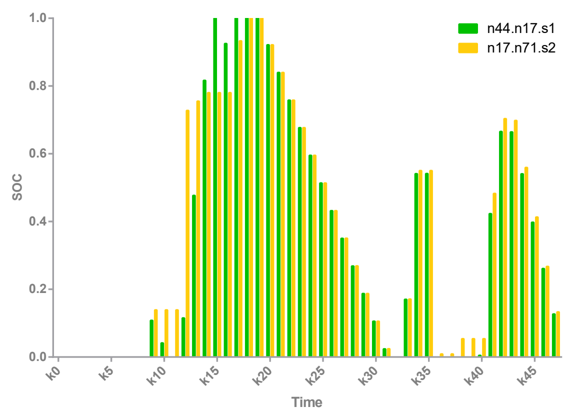

(d)

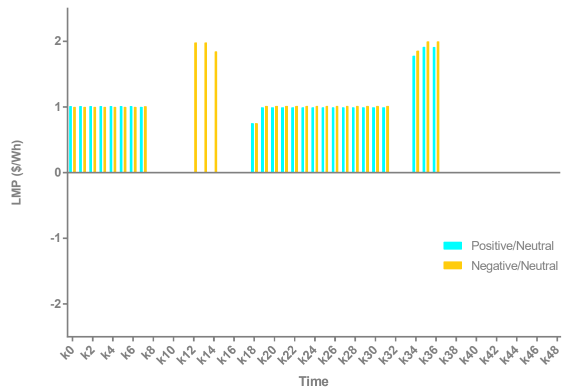

(e)

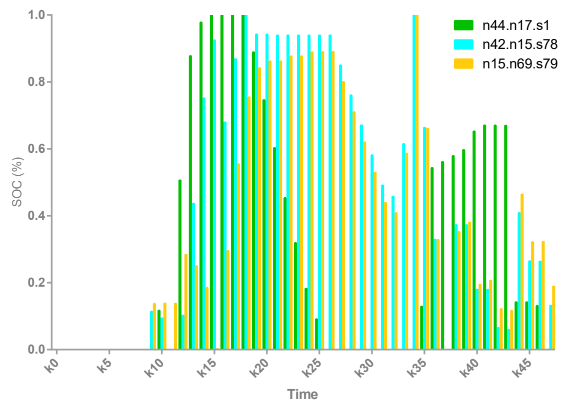

(f)

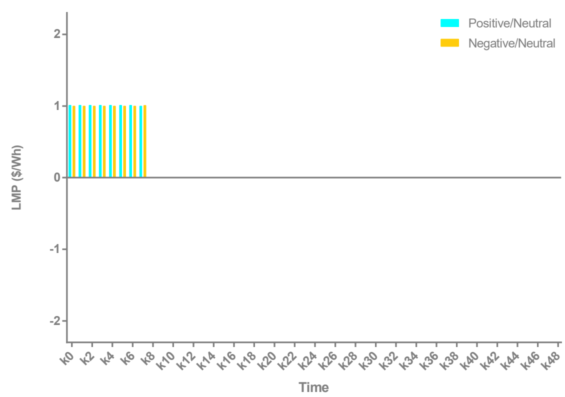

Figure 6.5: Figure 6.5b illustrates the average LMP from the positive and negative pole. Figure 6.5a illustrates the ESS state of charge at the beginning of each time period.

7

Conclusion and Future Work

7.1. Conclusion

The model developed throughout this thesis is a novel approach to tackle the control of bipolar DC distribution grids. As of now, the research on power flows for DC distribution grids is limited as opposed to AC systems. In this work, the formulation of the power flow is strictly developed for DC networks and do not rely on the already existing formulation of AC power flows. Consequently, formulating the power flow in terms of current and voltages in a linear manner enables an exact power flow where voltages are not fixed and losses can be expressed linearly using Ohm's law. Decomposing the power flow into a network and source layer interconnected by a variable representing the node current has never been done before. In general the equality constraints of OPF problems is based on the power balance between sources and loads, using this variable now enables the equality constraint to be formulated in terms of current. If only constant current sources are implemented the optimization problem is thus exact and losses are modeled linearly as opposed to AC OPF and DC OPF.

Incorporating a power variable has been the main challenge of this project, it was deemed essential as it serves several purpose. Firstly, most loads and sources are generally constant power sources. Secondly, electricity pricing is in terms of energy. Thirdly, the capacity content of batteries is also in energy terms. Deriving the power produced or consumed by generators and loads is inevitable for the last two purposes. The power term is obtained from a bilinear equation, a special case of quadratic programming. It is a burden as the problem essentially becomes of the quadratic form and convexity is not guaranteed. Consequently, the economic dispatch obtained may be a global or local optimum and LMP cannot be assumed to reflect electricity prices. To ensure correct nodal prices a strategy has been developed where the problem is solved in multiple steps. The economic dispatch is obtained from the quadratic problem, the solution is then linearized around these points and solved a second time to obtain valid LMP. The methodology is more complex and explained in further details in Chapters 3 and 4.

In short, the model has a dual purpose. It outputs the economic dispatch and generate prices at every location in the network. In essence, it can be used by grid operators as a control and pricing tool that guarantees an exact power flow and prices that are closely correlated to the network topology. The possibility to define the location and characteristics of distribution cables essentially result in prices that incorporate both losses and congestions. When combined with the defined placement of sources, the physical rules that dictate power flows are also included in LMP. The effect of natural power flows on electricity prices is highlighted in several examples from Chapters 3-6.

The OPF support both unipolar and bipolar distribution grids. Bipolar grids are particularly interesting as it can decrease distribution losses while offering the ability to incorporate sources with large power outputs if they are connected between the positive and negative pole. Additionally, they are more reliable than unipolar grid as the positive and negative polarity can operate as one network in case of failure of either pole. The amount of studies on power flows in bipolar DC grids is rather limited. Asymmetrical loading is likely to occur in such networks, understanding the behavior of the grid under this condition is essential. Using the case studies, the operation of the grid with asymmetrical loading has been demonstrated. In case of loading asymmetries, the neutral conductor is used to compensate power flows from one pole to another. Indeed power flows are not limited under the condition that the neutral conductor is carrying a current that is within its limits and that voltages of positive and negative poles are not constrained simultaneously to their upper or lower limits. In addition to asymmetrical loading, asymmetries due to sources' configurations were deemed a main contributor to the reliability of the grid. In cases in which production from one pole drastically exceed the production from the other pole, or when the system mainly rely on generators connected from positive to neutral conductors, the grid becomes unstable and failure could occur. Coupling these behaviors with LMP resulted in interesting observations. Indeed, LMP reflect asymmetries in a way where they can be interpreted as incentives to establish a balance between the negative and positive poles. To a larger extent analyzing these prices can reveal investment opportunities to increase the reliability of the network.

The maximization of RE resources' utilization has been implemented by assigning a zero marginal cost to these units while assigning a marginal cost to loads. A demand response mechanisms is inherently implemented when loads are given the ability to change their energy consumption regime. By proceeding as such, the case study demonstrated that the power output of solar panels is enhanced given the demand and the topology of the grid. Moreover, the price assigned to each load is interpreted as the willingness of consumers' to purchase energy. Electricity prices are thus a function of both the marginal costs on the generation and consumption side. The modeling approach of RE and load prioritization is particularly useful in developing countries where incomes are limited. Under the assumption that installations are equipped with meters with the ability to assign a marginal cost on each loads give users the flexibility to set their priorities at any given time. Moreover, important loads such as for hospitals or shops are guaranteed to have access to electricity. It is worth mentioning that in such system every generator or storage unit contribute to the amelioration of the social welfare. Therefore, unless implemented there is no local control of the operation of its own solar panel or ESS, the power generated or stored in batteries cannot be privatized, it is inherently used to contribute to minimization of the total production cost. The control is centralized given that every component of the network is known. In other words, the model developed can be used by grid operators to control the grid and derive electricity prices for each time period. The short computation allows for the grid operator to solve for the economic dispatch to adapt to change in irradiance.

Finally, the model can also be used as a tool to determine the optimal placement and size of ESS to enhance the utilization of renewable energy based DG with respect to an investment cost. This version of the model is based on mixed-integer programming and ideal batteries are constrained by a minimum and maximum capacity. However, there is no need to solve for the optimal size and placement of ESS repetitively, it can only be done once using previous irradiance data.

7.2. FUTURE WORK

The OPF method enables control of DC distribution microgrid in a way that has never been done before, however it is not flawless. As mentioned above, one of the main challenge was the nonlinearity imposed by the power term. Although the equations governing the power flow are linear, convexity is not guaranteed as a consequence of the power equations. Non-convex problems imply that the solution obtained may be a local rather than a global optimum. In the methodology developed it is assumed that the solution obtained is the global optimum. The model could be improved by ensuring that the problem is convex.

As seen in Chapter 3, LMP are obtained from a model that has been linearized around the solution obtained from quadratic programming. Some cases have been observed where the results from the linear programming deviate from the original solution. To remedy to this issue a proximity term has been implemented, its purpose is to decrease the gap between node voltages in the quadratic and linear program. Although this strategy works most of the time, there are still cases where the two solutions deviate from each other especially when multiple constraints are active at the same time. A special attention should be given to this problem in order to make sure that the economic dispatch obtained with the linear programming does not change from the original solution.

With respect to electricity prices, LMP are directly obtained as dual variables of the optimization problem. Therefore, it is not possible to decompose them into their components, namely the energy term, losses term and congestion term. More research should be undertaken to assess how LMP are computed. For instance as explained in Chapter 3, nodal prices in which only the energy and losses term are reflected result in an surplus. The reasons leading to this surplus should be given more attention, as well as its allocation.

The model could be improved by increasing the complexity in an effort to better represent physical limitations. PV panels are modeled in a very simple manner which result in an estimation in the potential power produced. The model could be made more realistically if inclination angles and other meteorological factors were taken into account. The same holds true for ESS, the physical limitation of batteries are not reflected in this model. For instance, charging rates and minimum state of charge are not implemented. Addtionally, loads can only be switched on and fixed (non-sheddable) or given a range of operation to simulate flexible loads. Loads that can only be turned on or turned off are not supported in the model. Similarly to the optimal ESS location mixed-integer programming is needed to incorporate such loads. This programming method is much longer than non mixed-integer programming. The program should be optimized for computational speed in an effort to enable a periodic economic dispatch to control the grid.

Finally, in Chapter 5 a methodology is proposed to solve for the optimal placement and sizing of batteries in an effort to maximize the utilization of RE. Mixed-integer programming is employed, the ESS capacity is bounded by a minimum and maximum capacity that represent feasible capacity range. However, the solution may lead to a storage unit for which the capacity lay between these limits, it is unlikely that commercial battery with the same capacity exist. The model could be improved by introducing an integer variable as opposed to a binary variable. By setting the lower and upper limit equal to each other, the capacity of commercial battery could be implemented. The solution would then result in the amout of batteries of this capacity that are needed at a specific location to improve the grid reliability.

II

Turning the Model into a Business

8

Bipolar DC Microgrids: A Solution to Rural Electrification

The technology described in this chapter is a solution to address the access to energy inequality in developing countries. Although most cities in developing nations have distribution grids, there are still many places that do not have access to electricity. Establishing a connection to the transmission grid to provide energy to rural areas is often seen as a non-viable solution. Investment costs related to the expansion of the grid, transmission lines and increase in capacity, are in most cases too high. Renewable Energies (RE) can play an essential role in the electrification of rural areas, energy can be produced at a lower marginal cost in comparison to diesel generators and investment costs are much lower.

The solution proposed here is a bipolar DC microgrid that can easily be expanded to cope with incremental development of rural villages. The microgrid infrastructure comes with an energy management system guaranteeing the microgrid's reliability while maximizing the utilization of RE as well as demand-side management. A smart meter specifically developed for bipolar DC microgrids is capable of prioritizing appliances to allocate energy where it is needed the most in case of shortage. Finally, real time prices are obtained from the energy management system. These prices can be used by the system operator to charge consumers, as an incentive to balance the bipolar grids in case of asymmetries and as an investment indicator to enhance the reliability of the microgrid. In comparison to other microgrid solution dedicated to rural electrification, the novelty of this system rely in the bipolarity of the grid and on the real time prices reflecting the fairest price of electricity for users, it aims at increasing the affordability for remote communities. In short, the system proposed is a solution that intends to increase the access to energy by providing an infrastructure, its control and economical tools for its operation.

8.1. Technology Description

The solution proposed is a microgrid that enables the generation and distribution of electricity in off-grid installations. It is a system composed of different technologies namely Distributed Generators (DG), loads, Energy Storage System (ESS), connecting cables, electrical components (e.g. switches and transformers), control algorithms, communication devices, smart meters... Many of these technologies are already developed and available on the market. The novelty of the solution is related to use of DC, instead of AC, in a bipolar configurations. Using DC conversion losses are reduced, moreover solar panels which are expected to be the main energy contributors are naturally a DC technology, the conversion step is thus skipped. In addition to unipolar grids (a positive and negative conductor), bipolar grids have a neutral conductor, the advantage of this configuration is twofold. First, it increases the power possibilities. Small devices can be connected between the positive pole and neutral or between the neutral and negative pole. Larger loads can benefit from twice the voltage drop if they are directly connected between the positive and negative pole. Secondly, it offers twice the power transfer capacity in comparison to unipolar grids, while only one conductor is added. The voltage rating of the system remain the same as does the total losses given that the system is balanced. Using this configuration, the grid can include small loads such as households and larger loads from industrial activities.

The system is illustrated in Figure 8.1. A central generation site based on solar energy is implemented and sized according to the local demand. The available power is monitored and distributed to the loads while the excess energy is collected in batteries and redistributed during times where solar energy is scarce. The power house is equipped with a management system that controls the power flows in the microgrid and enables demand-response based on the customers' willingness to purchase power. The system also enables decentralized generation to increase the capacity in case of expansion, it also enables entrepreneurs to purchase solar panels to generate an income. The bipolar configuration is especially useful for larger load centers, or anchor loads. In Chapter 10 the economic role of these loads is explained.

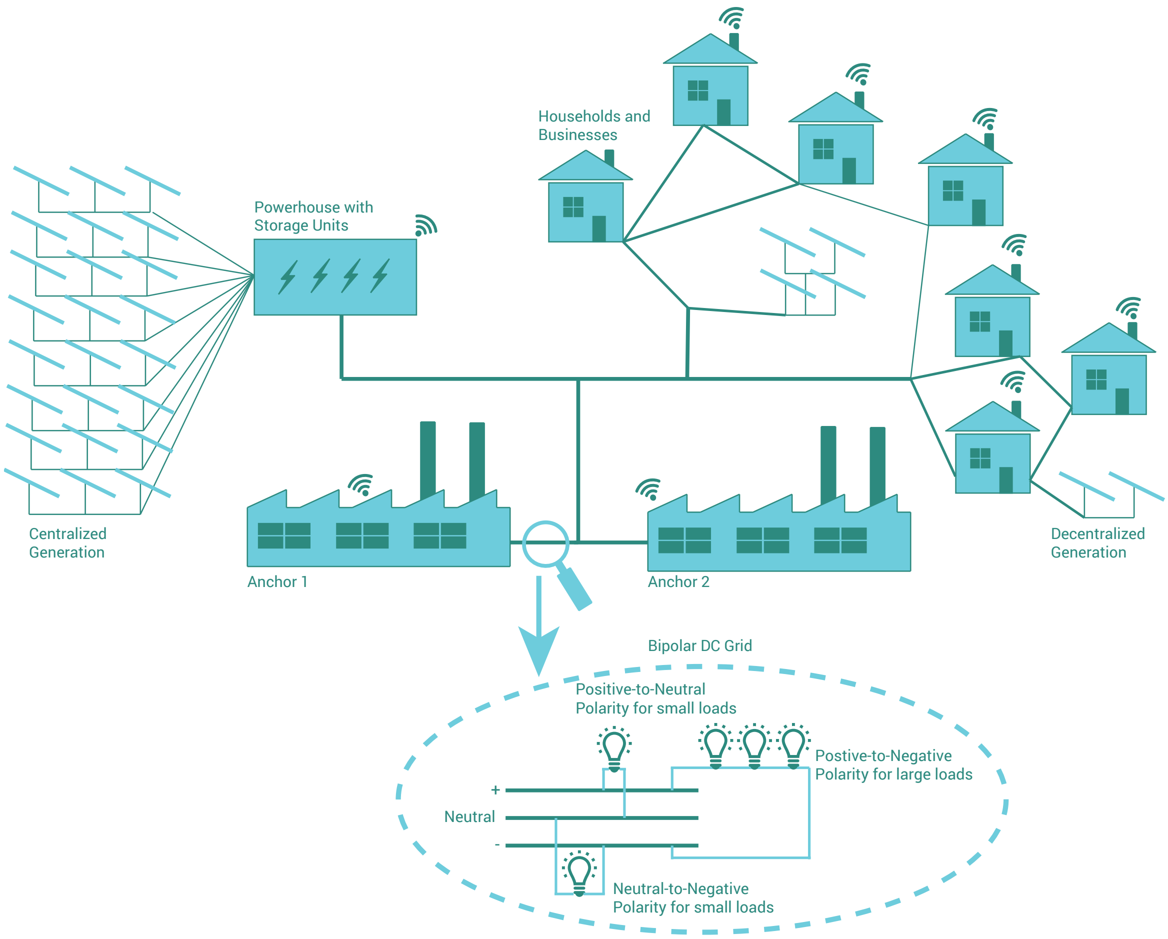

Figure 8.1: Illustration of a bipolar DC microgrids for a community with nearby anchor loads.

The algorithms used in AC or DC unipolar grids to compute the economic dispatch and power flows cannot be applied to bipolar DC microgrids. A new approach is needed to manage energy from DG based on RE in an effort to satisfy the demand at a minimal cost and ensure the reliability of the grid. This management method is termed Distrbuted Energy Resource Management System (DERM). Depending on RE implies that the energy supply can be limited, a demand-response mechanism is required to prioritize critical loads over non-critical loads. This mechanism can be enabled by implementing smart meters capable of prioritizing loads, such smart meter is part of the solution. The innovative DERM and smart meters are discussed in the following sections.

8.1.1. DERM

The model described in Chapter 3-5 can be interpreted as a DERM. Its main purpose is to enable active distribution management to coordinate RE and DG. DERMs are commonly used by utilities to control and increase the flexibility to better cope with the penetration of RE. The resources that can be taken into account vary, e.g. solar and wind generation, ESS, eletrical vehicles, fuel cells... In short, DERMs are closely related to the microgrid controller. It is the interface that manages sources and loads within a distribution grid or microgrid, it dispatches operational commands in an effort to meet an objective. On the other hand, the controller enables the dispatch by controlling the hardware such as opening/closing switches, adapting generation levels... DERMs can have different level of complexities depending on their capabilities. Fulfilling all of these tasks is not a requirements, however some are primordial. The DERM developed in this study has the following abilities:

1. Manage DG: Assess the availability and capacity of DG periodically to cope with the constantly changing availability of RE. Using the Optimal Power Flow (OPF) method, power flows are computed in an effort to minimize the total system production cost. The OPF is computed on a multi-period basis to allow for the planning of ESS.
2. Distribution Network Modeling: The complete topology of the distribution grids, namely the location and characteristics of electrical components, connecting branches is taken into account to enable accurate dispatch and simulation of power flows. Characteristics include the configuration of sources and loads with respect to their polarity and their operational ranges. Information regarding the loads are obtained using a smart meter and a communication protocol with the DERM.
3. Bulk Renewable Integration: With regards to developing countries, it is expected that the local generation and consumption is subject to rapid changes as a result of development. The program is flexible, the simulated network can easily be adapted to cope with changes such as new DG, distribution lines, loads, ESS...
4. Coordinate Demand-Side Management (DSM): Different loads can be incorporated in the model depending on the definition of their upper and lower limit. Non-sheddable loads and flexible loads are supported, however the program needs to be adjusted to model sheddable loads that can only be turned on or turned off. An indicator reflecting consumers' willingness to consumer electricity is used for load prioritization and demand-side management.
5. Dynamic pricing: A marginal cost is given as a parameter for each source and load. For sources this cost symbolizes the generators' costs of operation. For loads it represent the willingness of consumer to purchase electricity. It also enables load prioritization and demand-side management. Locational Marginal Prices (LMP) are used a financial tool to tariff electricity. It reflects the fairest price in an effort to increase affordability.
6. Microgrid Optimization: Locations in the network can be selected as potential sites for ESS. Using the investment cost of ESS and previous load and solar energy profile the software has the ability to identify the locations and size of ESS that would contribute to a better utilization of RE.

ENERGY MANAGEMENT

The solution proposed is specifically designed for DC distribution networks either in a unipolar or bipolar configuration. Therefore, it should be noted that AC power is in no way supported by the algorithm. Consequently, this technology can only be used in DC networks. As opposed to the traditional ways of computing economic dispatches, this model makes use of Ohm's law and the KCL. An exact power flow formulated in terms of voltages and currents is guaranteed, the solution obtained is thus always physically feasible. This formulation is a novel approach to model load flows, moreover it allows the use of the OPF method in DC bipolar networks, a novelty in the field. The program aims at minimizing the total system production cost. Given that DG based on RE have a lower marginal cost of operation than diesel generator, the use of RE is inherently maximized. The main purpose of the energy management algorithm is to periodically compute the OPF to enable the control of the microgrid. The fast computation time of the model allows for small time intervals between each period to better allocate resources and satisfy the demand.

Optimal Storage Location and Size

On top of resource management, the DERM has a functionality enabling optimal storage location and sizing of ESS. Using mixed-integer programming as described in the Chapter 5, different locations in the networks can be set-up as potential sites for the implementation of a storage units. The network operator can tune a capacity range for storage unit depending on the capacity of commercially available batteries. Based on the investment cost of batteries and on the load and solar energy profiles, the energy management system has the ability to return the locations and capacity of ESS that would result in a better utilization of RE and/or more reliable microgrids. As opposed to the energy management algorithm, this functionality is slow. Consequently, this task is designed to be ran occasionally and not periodically. Moreover, to better optimize the system on the long run this functionality should be computed based on the load and sun profiles of the previous weeks or months.

Embedded Real-Time Prices

Other than computing the economic dispatch and controlling power flows in the network, the software incorporates a pricing mechanism. Using LMP, the price of electricity is obtained periodically at every location in the network. The price expressed is obtained from the dual solution of the OPF, it represents the cost of supplying an extra unit of energy at any location. The marginal cost obtained incorporates the marginal cost of operating generators, the cost of congestion if any and the marginal cost of losses.

In bipolar networks, energy delivery can be limited by asymmetries between the negative and positive polarity or by an unbalanced configuration of generators. In short an asymmetry occurs when there is more loads connected to the positive or negative polarity, see Figure 8.1. Asymmetries can have a negative effect on the reliability of the grid, it can limits power transfer. The pricing mechanism developed reflect these unbalances and provide economical incentives to improve power distribution in the grid. Such a mechanism has never been implemented before.

Real time prices can be used for multiple purposes. First, from the software and smart meters the grid operator has all the necessary information to assess the tariff that should be charged to each consumers based on its consumption and the payment to be made to producers based on the energy produced and the marginal cost of production. Secondly, the real time prices can reflect inefficiencies of the microgrid. For example a large fluctuation in prices from one location to another can suggest that a line is often congested. In other words, real time prices can reflect investment opportunities to increase energy availability. Thirdly, when loading asymmetries occurs (loading of pole exceed the loading of the other pole) prices in the opposite poles will be quite different. The prices of the pole with the lowest loading will be lower than prices on the other pole. It encourages user to adjust their appliances' connection configuration in an effort to balance the grid.

Demand Side Management

Demand side management is incorporated in the DERM using sheddable loads. Depending on the nature of the load it can be either ON/OFF or it can operate within a given range of operation (e.g. LED). When solar energy is scarce, the software can control which loads should be shedded depending on their importance. Loads are prioritized using a price indicator assigned by users to each loads. The price indicator is not to be confused with the price at which consumers purchase energy, it represents the maximum price that users are willing to pay for electricity with respect to each appliances. In other words, it is a willingness indicator. Loads for which the price indicator is set high will be prioritized over loads for which the price indicator is lower. In short, sheddable loads will be turned off if their price indicator, or the willingness to purchase electricity, for this load is higher than the current cost of electricity at this location. Inversely, the load will be turned-off if its cost is lower than the current price of electricity at this location. The same occurs for flexible loads except that they can operate below their optimal rating depending on their price indicator and availability of energy. To summarize loads are shedded based on their importance when there is not enough energy to supply each load or when the price of electricity is higher than the price indicator of an appliance.

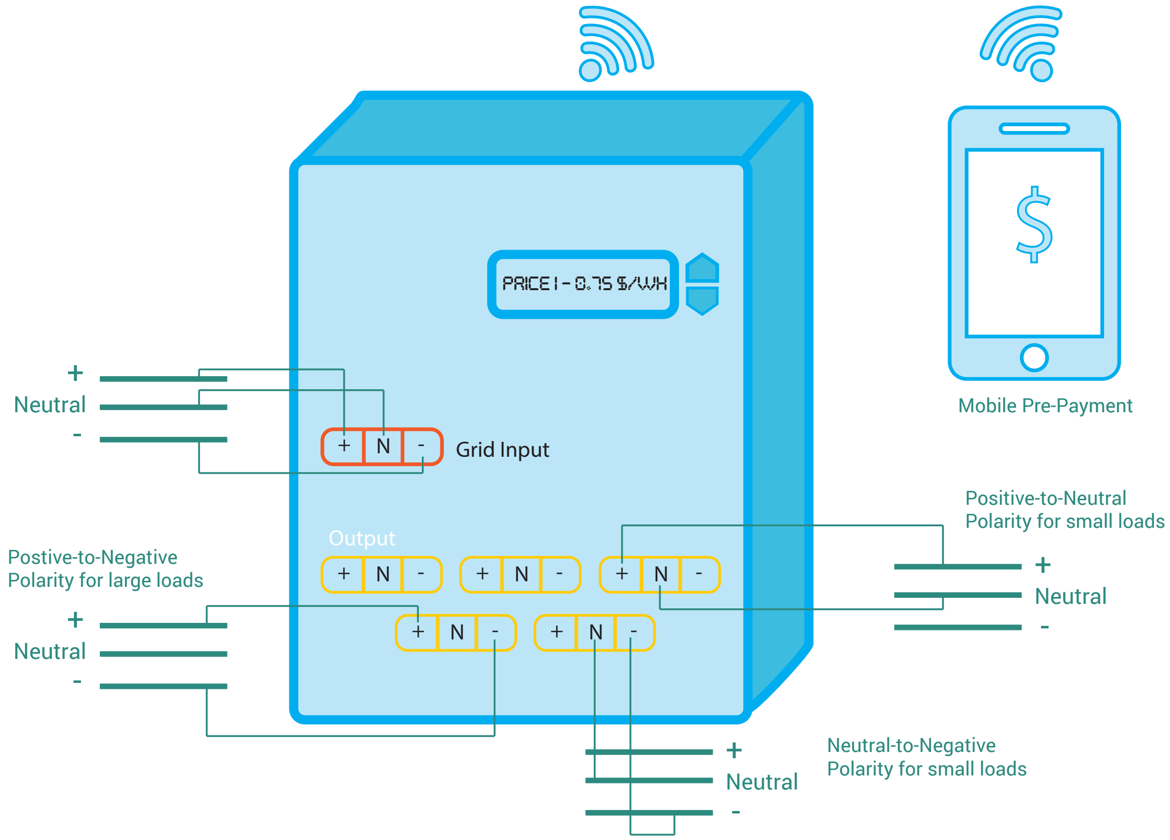

Figure 8.2: Smart meter capable of five load prioritization.

8.1.2. SMART METERS CAPABLE OF PRIORITIZING LOADS

The purchasing power in developing countries is relatively low. Users should have the option to set a limit to the price at which they are willing to purchase electricity. A smart meter enabling both the users to input a price indicator for loads and communication with the DERM enables demand-side management. The smart meter designed is connected to the grid using three sockets for the positive, neutral and negative conductors. Assigning a price indicator to every load is too complex, it would require an output circuit for each load. The system is thus limited to five price indicators. Consequently, there are five output circuits. Each circuit has three sockets enabling the user to connect loads to the positive pole, negative pole or directly between the positive and neutral conductor. Using five prioritization, users can ideally have two price indicators for the positive and negative pole and a price indicator for larger loads connected between the positive and negative conductor. Price indicators are directly inputed by the user using the LCD display.

The two-way communication between meters and the grid operator is used. Price indicators and consumption data are communicated to the grid operator and real-time electricity prices, LMP, at the meter location are sent to each smart meter. Based on these factors and the availability of energy, the DERM controls power flows in the grid. The amount of energy consumed is metered and communicated to the grid operator, consumers are charged according to the dynamic prices of electricity. Additionally, using the smart meter users can set a limit to their monthly energy expenditure. A pre-payment method is used to guarantee the payment from users. Using mobile payment methods available in developing countries, users can top up their meter up to a certain limit. The information is automatically transfered to the smart meter. Once this limit, when the account runs out of money, is reached loads are automatically shedded.

To summarize the characteristics of the smart meter are the following:

1. Interface the grid with loads
2. Support bipolar grids and allows for three connection configurations: Positive/Neutral, Neutral/Negative and Positive/Negative. Connection configurations can easily be adjusted by the user to encourage symmetric loading.
3. User can prioritize its loads using five price indicators reflecting the willingness of the consumer to purchase electricity for each category.
4. Wireless communication of loads' consumption and price indicators with DERM.
5. User can set a limit to their monthly energy expenditure using the pre-payment mobile method.

8.1.3. Other Technologies Involved

The DERM and the smart meter described in the above sections are the novelty of the system. In addition to these two innovative products, the solution proposed rely on other technologies necessary for power production, power distribution and grid operation. It is difficult to establish a list all of the components in a DC microgrid. However the main components are the following:

1. Generation: Generators are responsible for the production of power. Depending on the type of generators different types of technologies are needed to ensure the interface with grids. PV panels are connected to the grid using a DC/DC converters. Diesel generators produce alternating currents, they are connected to the grid using acrshortdc/DC. ESS are used to store energy at times when supply is higher than then demand. They are controlled by a charge controller which limit the rate at which electric current is added to or drawn from the batteries.
2. Distribution: Electricity is distributed in the network using distribution cables. For bipolar DC distribution grids, three DC conductors are needed.
3. Control: The control of the microgrid is operated from a central servers to which the generation and consumption data is sent to. The server operates the microgrid controller and the DERM.

8.1.4. Assumptions

The solution described in the above sections is not fully developed yet. More development is needed in certain domains to guarantee the operation of bipolar DC microgrids. With regards to the infrastructure, the technology rely on the availability of certain components specific to bipolar distribution networks. Concerning the softwares, the DERM should be further develop to incorporate additional functionalities essential to the optimization of energy resources. The business plan presented in Chapter 10 is based on the following assumptions:

1. Cables and sockets: DC networks in a bipolar configuration is a rather new in the sector of distribution networks. It requires a different type of wires, there is currently no standards. Additionally, DC connectors enabling the connection of currently existing appliances should be available and allow for the three connection configurations possible in bipolar grids.
2. Safety: Protection is one of the main barrier to the deployment of DC distribution networks. The solution currently do not consider fault detection.
3. Communication: Currently no communication protocol enabling communication between the DERM, smart meters and other components exists. The energy management system cannot operate without it, the business plan assumes that the technology is already developed and integrated in the DERM.
4. Weather forecasting: Planning of DG in an effort to decrease electricity prices by maximizing the utilization of RE depends on the availability of RE and on the consumption profiles. To better manage DG a mechanism able to forecast solar energy potential is needed.

8.2. COMPETING RURAL ELECTRIFICATION SOLUTIONS

GRID EXPANSION

Supplying electricity to remote locations can be done by expanding existing grids. New transmission and distribution lines should be installed to connect villages to the closest power plant. Generally, in developing countries the reach of the transmission grids is geographically limited resulting in large distances from communities. Even if the costs of fossil fuels or nuclear energy are omitted, the capital investment required to expand the traditional centralized is often too large. Such investment cannot be recovered due to the lack of purchasing power and low average income level. Expanding the grid is in most cases not a viable option [111].

SOLAR HOME SYSTEMS

Solar Home Systems (SHS) are individual household-scale energy system generally composed of solar panels, batteries and charge controllers. In most cases, these systems are DC and the energy provided is limited to the size and amount of PV modules installed per house. It is used in cases where the energy consumption is relatively low as most SHS only have one solar panel. Therefore, SHS as a mean of rural electrification depends on number of homes as there is a threshold capacity where it becomes more viable to add another house to a microgrid rather than investing in an additional SHS [112].

In contrast to microgrids which are interconnected systems integrating multiple sources, loads and ESS, SHS are independent from each other and no connection is established between one home to another. SHS should be sized for peak load, it has been observed that it often results in a low utilization ratio. On the other hand, microgrids have multiple power flow possibilities leading to a higher utilization of resources. Additionally, microgrids are more flexible as it can support different generation sources to enhance power reliability [113].

AC MICROGRIDS

As of now most microgrids are designed using AC. The familiar configuration of electrical grids led to the development of AC microgrids. These systems distribute power using AC. Consequently, AC/DC and AC/AC converters are needed to cope with frequency, phase angles and voltage levels of PV panels, diesel generators and loads.

In the context of rural electrification, PV is regarded as the main energy source in a microgrid for the availability of solar resources in most developing countries, the low cost of solar modules and the modularity and ease of transport of panels. Secondly, the majority of appliances in these developing nations are DC appliances, namely lighting, cell phone and fans. When compared to AC microgrids, solar based DC microgrids can contribute to a cost reduction of approximately 20% [113]. These costs reduction come from improved power conversion efficiencies. The improvement of solar based DC microgrids are illustrated in Figure E.1. In AC systems ESS there is constant power loss due to the fact that ESS are DC appliances. These losses do not occur in a DC microgrid. The majority appliances are DC, in a solar based AC network two conversion steps are needed (from DC to AC and from AC to DC). The conversion step occurring at the end-use appliances is not needed in DC microgrids. Inverters are generally sized according to the peak power load expected. Undersizing inverters inevitably lead to a system failure, expanding the microgrid incrementally becomes challenging. Furthermore, an inverter's efficiency is at its highest when operating between 80%-90% of its rated capacity. Consequently, efficiencies suffer when the power demand is below the peak.

On th other hand, DC microgrids come with some disadvantages that may act as a barrier to the deployment of such systems. Protection in DC networks is more complex than in AC, there is a need for more research in the field of protection systems [114]. Improved fault detection and protection system are needed to ensure safety and reliability [115]. Furthermore, although some loads are DC compatible, there are still a wide range of appliances that are exclusively designed for AC.

In general the benefits of DC microgrids outweigh the disadvantages, it is clear that system performances and efficiencies lead to an higher affordability of DC microgrid. However, despite these advantages the microgrid market for rural electrification tend towards AC microgrids as a result of the long history of AC power systems. A lock-in effect limits the deployment of DC microgrids despite their advantages [116].

UNIPOLAR DC MICROGRIDS

There are two main configuration in DC transmission and distribution networks, unipolar and bipolar systems. The unipolar system has two conductors, consequently one voltage level via energy is distributed. Every source or loads are connected to this voltage level. The implementation is easier and it requires less power electronics.

In addition to the positive and negative conductor, bipolar grids have a neutral conductors. It results in three voltage profiles, from the positive to neutral, from the neutral to negative and from the positive to negative. The transmission capacity in a bipolar network is larger in comparison to the unipolar topology, about twice as much [35]. Furthermore, for a balances network the total losses remain the same. The multiple selective voltage level is regarded more suitable in the presence of RE and DG [117]. Moreover, bipolar networks are more reliable as it can operate in a unipolar mode if a fault is detected in one of the pole

COMPARATIVE ANALYSIS OF COMPETING TECHNOLOGIES

Figure 8.3 compares the different options for rural electrification as a function of community size and unsubsidized cost of electricity. With regards to grid expansion, it can be seen that the cost function associated with the electrification via grid expansion increases at a larger rate than any other technologies with respect to the system size. This option only makes sense if communities are large and densely populated. It follows that rural electrification is most of the time associated with middle to small size communities. On the other hand, for SHS the cost as a function of communities sizes is almost a linear function with a relatively low rate. The price of electricity associated with this technology is rather high, these stand alone systems are competitive when communities are very small and not densely populated. In most of the case, they are only used to power lighting appliances of single households. The electrification slightly denser communities via SHS is not a cost efficient solution [7]. Microgrids, termed mini-grids in Figure 8.3, are the most cost efficient when it comes to electrifying middle size communities. Furthermore, from a development perspective these systems also enhance local development of communities. As opposed to SHS, microgrids have a higher distribution capacities allowing the presence of larger loads for refrigeration, food processing, water pumping and construction. Microgrids not only guarantee a sustainable source of power, it also enables local entrepreneurship.

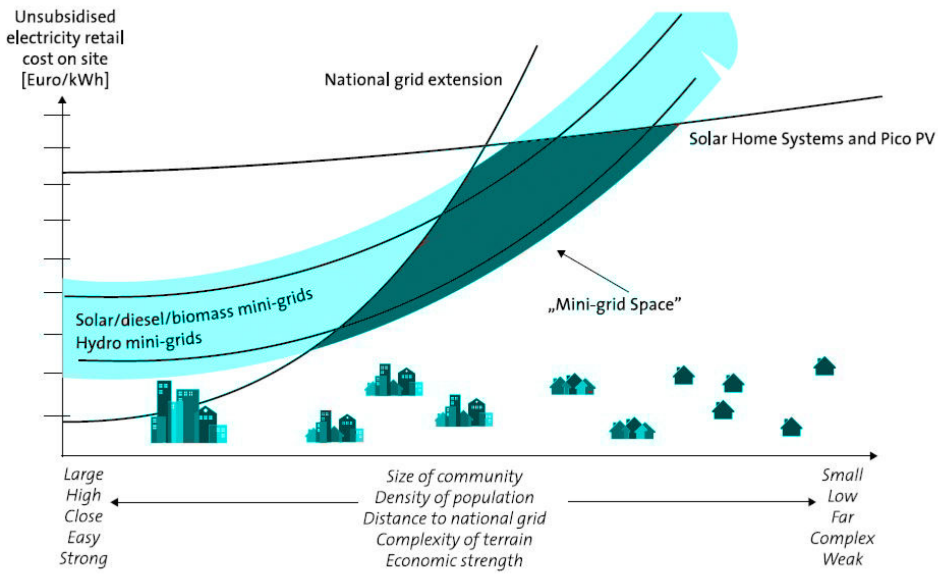

Figure 8.3: Cost of electricity as a function of the size of the communication and rural electrification technology [3]

8.3. Competitive Position and Maturity of the Technology

The technologies involved in the microgrid system are enumerated in the the technology tree illustrated in Figure 8.4. All of these processes are either technologies or skills necessary for the implementation of bipolar DC microgrids. These attributes are used to construct a business case.

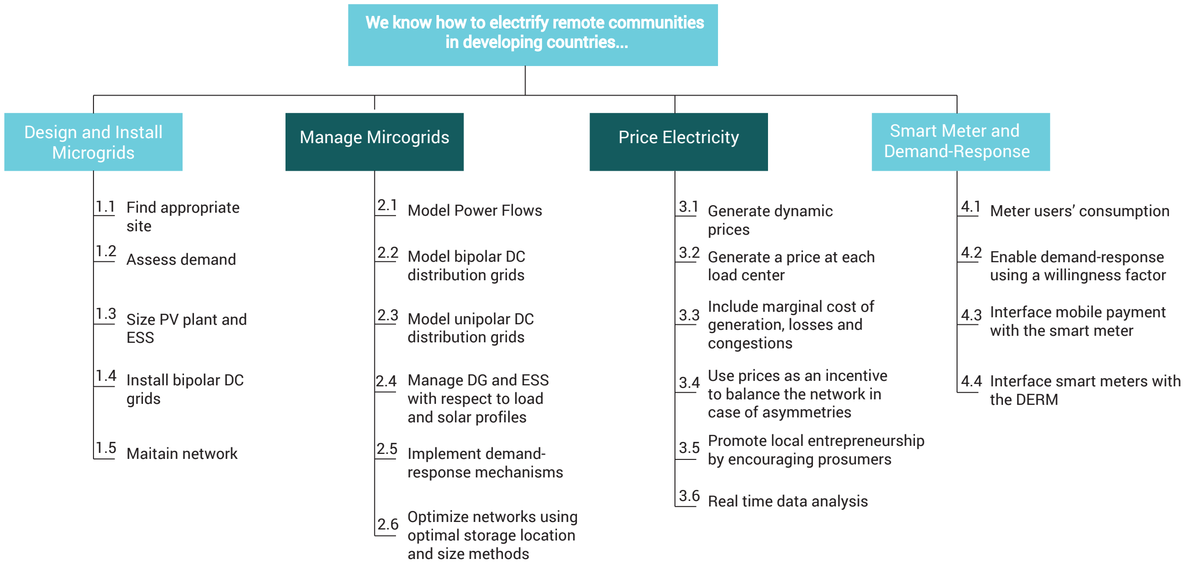

Figure 8.4: Technology tree of the proposed electrification solution. The necessary technologies and skills required for the implementation are divided in four main categories.

Classifying the different technologies and skills relevant to the implementation of bipolar DC microgrids allows for the assessment of the competitive position and maturity of each of them. Table 8.1 and 8.2 show the attributes associated to each of these skills. They relate them to the strategic impact with respect to the market competitiveness, in Figures E.2 and E.3 the attributes are explained.

Strategic Impact	Clear Leader	Strong	Favorable	Tenable	Weak
Base			1.2, 1.3, 1.5		
Key	2.3	2.1, 2.4, 4.1, 4.2, 4.3	4.3, 4.4	1.1	
Pacing	2.6, 3.2, 3.3	2.5, 3.1, 3.5	3.6		
Emerging	1.4, 2.2, 3.4				

Table 8.1: Competitive position of the bipolar DC microgrid system

Strategic Impact	Embryonic	Growth	Mature	Aging
Base			1.2, 1.3, 1.4	
Key		2.3, 4.2,	2.1, 2.4, 4.1, 4.3, 4.4	
Pacing	2.6, 3.6	2.5, 3.1, 3.2, 3.3, 3.5		
Emerging		1.4, 2.2, 3.4		

Table 8.2: Technological maturity of the system.

From Table 8.1, it can be seen that none of the applications are considered weak in comparison to the competition. Only one skill, the identification of appropriate site, is listed in the tenable category. Indeed, no methods have been developed allowing for site selection. Some competing companies already developed tools to select most suitable locations for the implementation of microgrids by considering population density and generation capacity [118]. Note that the rest of the skills relevant to the design and installation of microgrids are evaluated as basic and favorable. During the development of the solution no special attention has been given to these skills, however they should not be a problem in the future. Interfacing mobile payment with smart meters and smart meters with the DERM are key aspects necessary for the collection of revenues and operation of the network, these attributes are listed as favorable. The key assets of the solution, namely microgrids management and pricing mechanisms are either clear leaders or strong. These skills are the main competing advantages differentiating us from the competition. In comparison to competing technologies the DERM developed includes advanced management of DC networks in a bipolar configurations including both demand-side management and system optimization using ESS. The methods used to developed a pricing mechanisms has never been implemented in DC distribution grids. It reflects fare prices to the user by considering network constraints.

Considering the maturity of the attributes part of the technology tree, it can be concluded that most of the technologies and skills are mature or growing. Consequently, most are ready to be implemented. Only two skills are evaluated as embryonic, namely the optimal sizing and siting of ESS and the analysis of real time data. More efforts should be given to these before the commercialization of the solution.

9

THE RURAL ELECTRIFICATION MARKET

This chapter provides some insights about rural electrification. Africa and Asia are the two continents with the lowest rate of electrification. As of now companies and organizations have undertaken many projects in these areas. Some where succesful while other failed. It seems that project funded by public organizations or governments are not sustainable and often stop before their completion. However, it appears that governmental support and an appropriate framework for rural electrification are key to the success of projects. In Africa, Kenya and Tanzania are promoting and gaining in experience with regards to rural electrification, the same applies to India.

9.1. MICROGRID MARKET FOR RURAL ELECTRIFICATION

The remote power system market is expected to boom in the upcoming years as shown in Figure 9.1. The market is divided in four main segments: industrial activities related to commodity extraction, islands, village electrification and remote military applications. The Navigant Research program estimates that the market will grow from $10.9 billion toady to $196.5 billion in 2024, a 20-fold increase. It is expected that the largest contribution to the market will occur in the Asia-Pacific regions followed by the Middle-Eastern/African regions [4]. The amount of people that do not have access to electricity in African and Asian countries is shown in Figure 9.2a and 9.2b. In several reports it is highlighted that an interesting market trend is village electrification which could represent around 35% of the remote microgrid market share [119].

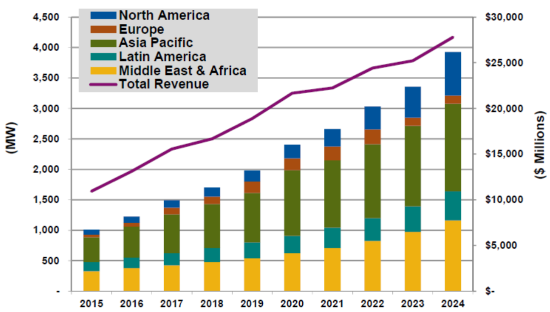

Figure 9.1: Predicted remote microgrid market in terms of installed capacity and revenues [4].

Most of the people living off-grid are poor, a study estimates that there is around 47 million households in Africa and Asia with no access to electricity but benefiting from an annual income of $3,650-18,250. These households are identified as an addressable market for the deployment of off-grid solutions. Note that there are far more households that do not have access to electricity, however their income is deemed insufficient to purchase electricity [5].

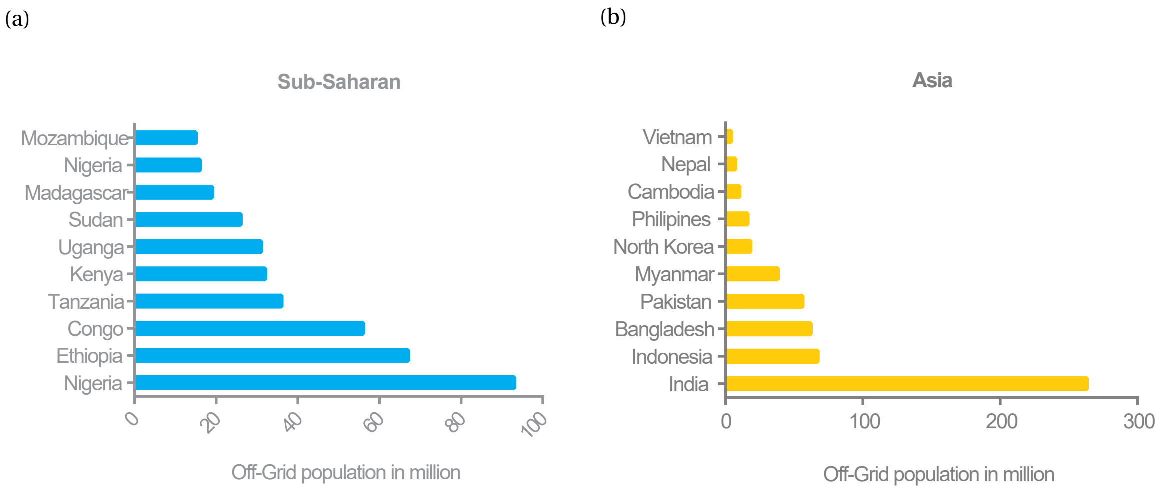

Figure 9.2: Off-grid population in million per country in Sub-Sahara and Asia [5].

9.1.1. AFRICA

Africa can offer huge investment opportunities in the sector of rural electrification. Out of the 1.1 billion in sub-Saharan countries around 600 million do not have a stable access to electricity. Moreover, the population is predicted to explode [120]. The demand is expected to rise from 423 terawatt-hours to 1570 terawatt-hours in 2040, half of the European Union in 2010. In his study Castellano *et al.* expect the electrification rate to increase from 34% in 2010 to 71% in 2040 [121]. It suggests that the demand for decentralized system will considerably rise. The potential market in African countries is mainly village electrification, however there is a need to access to energy in the mining industry, large agricultural farmlands and manufacturing centers [120].

It can be concluded that there is a large demand for rural electrification. However, the economic case of remote microgrids is often neglected and the size of the opportunity are underestimated. It appears that investment considerations are not well understood and government policies promoting rural electrification are non-existent or weak. Most of the laws support grid connection and grid expansion. As result the attractiveness for investors is low as they are forced to operate in a poor infrastructure. In addition, low income levels and low energy consumption patterns are not attractive for large companies which claim that such network are likely to be non-profitable [120]. In spite of these challenges, smaller companies such as Powerhive or SteamaCo have proved that the margins and opportunities are promising. Furthermore, publicly funded projects have not proved to be sustainable, in many cases funding is not renewed. It follows that project are often not completed or not maintained [122].

Kenya and Tanzania are the most mature rural electrification markets in Africa with a peak capacity average of respectively 1 MW and 600 kW. Both government have high targets for rural electrification. Kenya's electrification rate for 2017, 2022 and 2030 are 40%, 60% and 100%. In Tanazania the goals for 2021, 2030 and 2040 are 22%, 50% and 100%. Note that both countries host a special agency for rural electrification [123]. Kenya and Tanzania have one of the highest population of sub-saharan countries, it is expected that access to electricity occurs a higher rate in areas with high population densities [124]

9.1.2. ASIA

Together with the slowing population growth rate, the booming economy has let to a decline of 212 million people living off-grid since the beginning of the century [125]. However, the electrification is still low in comparison to developed country. In India almost 50% of the population, 80 million households, do not have access to electricity while South Asia accounts for 37% of the world's population without access to electricity. Pakistan has the lowest electrification rate in the continent and the electrification rate in India is highly unbalanced from one state to another.

In India the government strongly support off-grid system over grid expansion. The government recognizes that microgrids is the solution to access to energy, recent policy developments support the deployment of microgrids by creating an enabling condition for investment and service providers. Although these policies highlight the importance of rural electrification, their impact is still small compared to the rate of electrification. The main barrier to the deployment of microgrids is the access to finance at the right terms. Subsidies from the government exist but it is often not enough to encourage private investors who consider that the market has high risks [126]. A similar situation is observed in Bangladesh where the rate of electrification is one of the lowest on the continent. There has been an increase in the electrification of rural areas but mainly though the expansion of the distribution and transmission grid. However, households connected to the grid is still low, the cost of getting connected to the electricity network is too high [125]. Initiatives towards rural electrification were also taken in Myanmar which has recently completed an ambitious national electrification plan in 2015 similarly to the Philippines which aim to achieve a 90% electrification by 2017 [127].

9.2. PRIVATE SECTOR PARTICIPATION

Despite the benefits of microgrids in an effort to enable both rural electrification and the development of local economies, the deployment of microgrids is still low and their contribution to rural electrification is small. In some countries, the public sector has participated in the penetration of off-grid solutions through public fundings and policies, however these solutions have not been conclusive enough to alleviate energy poverty. Additionally, the poor understanding of the technology, its operation and maintenance often lead to the failure of these projects [128]. On the other hand, the role of the private sector in energy access projects is promising. As opposed to the public sector for which availability of resources is limited, the private sector has a larger amount of capital to finance these projects [7]. Moreover, private companies have the technical skills necessary to implement, operate and maintain microgrids.

Although implementing solutions to increase the electrification rate is often motivated by social concerns, similarly to any other investment the viability and return on investment is measured by the private sector. The low income of households without access to electricity and the instability of developing countries result in high risk investments. The risks vary for each country but are mainly associated to policy certainty, transparency and the complexity of the regulatory infrastructure from the governments and organizations. According to Williams *et al.* the barriers to the deployment of microgrids for the private sector are the following [7]:

1. Financial: For a business the investment risks and secure stream of revenues are the main contributor to investment decisions. The case of microgrid for rural electrification are high risks and potentially show low expected returns. In rural communities the ability to pay for electricity is limited and often seasonal. Thus, energy payment can be problematic and the purchasing power may not be constant throughout the year [7]. Additionally, the energy demand in these areas is low in comparison to urban areas. Consequently, paying back for a high system cost is even more challenging, even though the price of RE is decreasing rapidly. Uncertainty of energy consumption is a risk for project developers. Consequently, interest rates are high which amplifies the challenge of distributing electricity at an affordable cost [129]. The instability of the market is even higher in developing countries where regulations and policies are uncertain [7].

2. Institutional and Policy: A stable institutional framework and national/state policies are essential to encourage the private sector to invest in high risks microgrid projects for which profitability is low.

In order to do so, the electricity sector and local utilities should be open to oligopoly. Thus, policies should help define the relationship between the public and private sector. Additionally, these regulations should be shaped to increase social welfare rather than commercial motives [130]. On top of enabling access to energy rural electrification should be seen as a way to develop communities' economy and social development. As mentioned before, the purchasing power of local communities is low, consequently energy tariffs should allow for the private companies' return on investment and subsidies should be implemented to increase affordability. The energy market in many developing nations is unprofitable [131]. Additionally, in these countries regulations are often subject to change and not clear which increases the uncertainty of the private sector. Lastly, the cultural gap between private companies and the local communities is often large. The solutions proposed are not always in alignment with communities' expectation resulting in a low local acceptance with poor payments, low collection rates and electricity theft [7, 132].

3. Technical: Microgrids for rural electrification are subject to different constraint in comparison to urban distribution networks or distribution in developing countries. In rural communities, population distribution is an important parameter that should be considered by the project developer. In some cases, loads can be highly dispersed which result in larger distances and higher system costs. These technical challenges should be taken in consideration before the implementation of the project [133]. Moreover, microgrids are designed according to the local demand which makes the system more sensible to load variations. Microgrids are independent systems, the vulnerability to the variability of demand is higher when compared to national or interconnected grids. Access to electricity often lead to the development of the local economy, the grid is thus subject to expand over time at a higher rate than urban areas. Consequently, microgrids should be flexible and should take in consideration the network expansion. These factors lead to a high degree of complexity with regards to sizing and management of DG. An additional technical aspect that should be taken into account to guarantee reliability is maintenance. In rural areas the local population do not have the technical skills to maintain, repair and operate the network [132, 134]. The remoteness of these locations is challenging, in case of failure technical support can take a long time and associate costs are high.

9.2.1. PRIVATE SECTOR ACTORS

Table 9.1 and 9.2 show the major private actors involved in the deployment of microgrids in Africa and Asia. Note that these are companies providing either the infrastructure or management tools of microgrids. Governmental and organizational actors are not involved in these tables as they change for each country. In Africa, most of the projects lead by these companies are either located in Kenya or Tanzania. In Asia, most prominent companies are focusing on the rural electrification of India. It can be concluded that there are no clear leader in the field of microgrids. Companies differ with respect to the business plan, revenue models and sizes (pico-, mini- and micro- grids). Some, such as Mera Gao Power, are focused on ultra low cost systems to provide communities with basic needs such as LED lighting. Others such as, Powerhive, seems to focus on more advanced full solution (infrastructure, operation, maintenance and payment). Many of these solutions rely on AC microgrids. It is worth mentioning that bipolar DC microgrid have not been implemented in the context of rural electrification.

Africa	
Companies	**Description**
powerhive	Powerhive provides AC microgrids, smart meters and management services including the network operation and mobile payment. The company is present in Africa, mainly in Kenya. The company focuses on large-scale local grid projects. It now targets the Asian market, more specifically Myanmar, India and the Philippines.
STEAMACO	Steamaco is a company that specializes in the electricity retail for remote areas in Africa using smart meters and data monitoring. The company is active in Kenya and Tanzania, their project are rather medium scale local grids.
PowerGen RENEWABLE ENERGY	Powergen provides AC microgrids, maintenance services and a pay-as-you-go service. So far the company is present in Kenya and Tanzania with medium scale local grids. The partnership with Steamaco ensures monitoring services and phone payment.
devergy developing energy	Devergy provides DC microgrids, smart meters and management services including the network operation and mobile payment. The company is present in Tanzania.
FRES foundation RURAL ENERGY SERVICES	FRES provides AC hybrid microgrids as well as SHS. The company is present in Africa, mainly in Mali, South Africa, Burkina Faso, Uganda and Guinea Bissau. It uses a monthly fee-for-service to charge its users.

Table 9.1: Major private actors developing and implementing microgrids/mini-grids solution for African's rural areas.

Asia	
Companies	**Description**
GRAMPOWER	Gram power has a three stream of products: smart metering, smart microgrids and smart energy monitoring. Their smart microgrid technologies is a full solution for rural electrification in either single or three phase configuration. The business model is based on prepayment of energy. The company develops projects in India.
OMC	OMC is present on two markets: remote telecom installations and communities. The company offers starter kits for community entrepreneurs with appliances ranging from LED lighting to electrical vehicles. A flat price is charged per battery delivered in the network. The company not only focuses on rural electrification but also on the social and local economy development using microgrids. Projects are rather large scale local grids, all based in India.
मेरा गाँव पावर MGP lighting lives	Mera Gao Power implements ultra low cost DC microgrids for relatively small communities and the poorest states of India. Appliances such LED lighting or cell phone chargers are rented to the consumers. Phone payment is used as a payment method.
orb energy	Orbs reaches both urban and rural markets. The company proposes both solar grid-tied and off-grid solution. Orb is present in different continents. Rural electrification projects are in West and East Africa as well as India.

Table 9.2: Major private actors developing and implementing microgrids/mini-grids solution for Asian's rural areas.

10

Business Model and Time Planning

Using the status of rural electrification in the world in Chapter 9, a business plan is proposed for the implementation of the bipolar DC microgrid, DERM, smart meter and pricing mechanism presented in Chapter 8. First a review of the business and revenue models adopted for remote microgrids is presented. Second the business canvas with detailed information is provided before discussing the goals of this business case.

10.1. Review of Business and Revenue Model for Rural Electrification

10.1.1. Business Models

As presented in the previous section, the microgrid market for rural electrification is a niche. Consequently, there is no clear understanding of what is the most appropriate business and revenue models. The business models adopted by the private sectors vary depending on location and scale of the project. In Africa, payment using mobile phones has been used for SHS and microgrids. The technology is less developed in India. The scale and cost of the microgrid also determines the type of business model. For example the model developed for larger networks such as Powerhive is different that smaller and ultra low cost solutions of Mera Gao. The literature on the business models dedicated for microgrids in the context of rural electrification is rather poor. Palit and Sarangi presents three business models used by Husk Power for India [135, 136]:

1. Built - Owned - Operated - Maintained (BOOM) Company is the owner and responsible for the construction of the microgrids, its operation and its maintenance in the entire chain of development. It requires dedicated staff and overhead is high as well as the investment.

2. Built - Operated - Maintained (BOM) The microgrid is built, operated and maintained by the company responsible for the project. The ownership is shared with local entrepreneurs. The company gets a rental fee and the operation is left to the entrepreneurs. It reduces the operational tasks for the company and promote entrepreneurship. However, the investment costs are still high.

3. Built - Maintained (BM) The plant is built and maintained by the company but owned and operated by local entrepreneurs. The company is a technology provider.

Recently the Anchor-Business-Community Model (ABC Model) has been given a lot of attention. This model follows the BOOM approach where a private operator builds, manages and operates the network. Generally funding is obtained from private investors, loans and in some cases from the government. The goals of this model is to improve viability, reduce risks for private power producers and improve companies' ability to access finance. As can be seen in Figure 10.1a, customer are divided in three groups [3, 6, 7, 137]. Anchors are customer with large and predictable loads, generally requiring electricity for most of the day. Anchor customers guarantee a constant inflow of revenues for the project developer, they secure the operation of the microgrid. Typically anchor loads are located near to communities and can be telecom tower, petrol stations, agro-processing units, retail chains or mining companies. Business customers have smaller load and rely on electricity supply for the operation of their business (e.g. shops). Electricity is critical, however unlike anchors bankability and revenue security cannot be supported by this customer segment. Last, community customers are generally households with smaller and variable loads. The community customer segment is seen as a top-up to the revenues from the the other two segments, little revenue are collected from end-users.

(a)

(b)

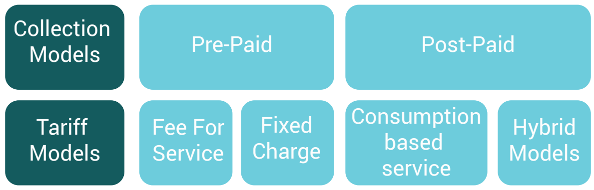

Figure 10.1: 10.1a: ABC model for rural electrification via microgrids, distinction of the three customer segments [6]. 10.1b: Revenue models relevant for rural electrification [7].

10.1.2. REVENUE MODELS

Four mains revenue models were identified in the context of rural electrification [7]. Establishing what is the most appropriate revenue model is essential to secure revenue streams throughout project's lifetime. Revenue models for microgrids fall in two categories: energy consumption based tariff and maximum power consumption. In the energy consumption based model, the user is charged with respect to the amount of energy that has been consumed. This model is the fairest in the sense that consumers only pay for what they have consumed, the tariff is not affected by the consumption of other loads. If this method is adopted it inherently means that each demand center should be equipped with a meter which increases the overall system cost. Under the fixed charge model, consumer pay a fixed amount per month which in most cases allow them to consume a maximum power. Compared with the consumption based tariff, this tariff helps the consumer controlling its budget. Some argues that this model is more appropriate to microgrids since costs are mainly fixed costs [138]. Another model is the fee-for-service model widely used for SHS. Under this tariff a leasing agreement between the provider and consumer is established, the maintenance service is also included. In such a way consumers do not need a large capital to purchase the technology. Similarly to SHS, the cost structure of microgrids is most fixed cost. Consequently, this model could also apply to microgrids. Finally, there are hybrid revenue models combining fixed charges with consumption based tariff. Users pay a fixed tariff enabling them to consume up to a maximum amount of energy, if more is consumed another tariff for each kWh is applied. This system ensure that the fixed cost of the system are met. Additionally consumers that consume less do not subsidize intensive consumers [7].

Collection of revenue can be an issue in developing countries where financial resources are low, furthermore collection can be logistical and technical challenge. The revenue and collection model should secure revenue streams. Pre-paid methods can be implemented through the use of by interfacing the consumers payment with their meter. Revenues are collected prior to consumption, the client is disconnected if he exceeds his credit. Such system reduce the complexity of billing and its helps consumers limiting their energy expenditure. On the other the post payment method is riskier, the revenue stream is not secured [7].

10.2. Business and Revenue Model for Bipolar DC Microgrids

Key Partners

Capital is required to finance the project, the first partner segment is thus investors. Depending on the country where the system is implemented some subsidies or loans can be obtained from the government. However, public founding is often not sufficient enough to finance such projects. Private investors such as venture companies should be approached. The second partner segment are the suppliers. Microgrids are complex system composed of many electrical components. The companies involved in the conception of microgrids are power, storage, PV panels and communication companies. Equipment has to be purchased from them as their technology is already mature and do not require further development. The third partner segment are companies responsible for the manufacturing of the smart meters. Note that these companies could also be the companies in charge of supplying the system's components. Lastly, local organization with experiences in rural electrification should be approached to coordinate the implementation of the project. Past experiences suggest that cultural differences can be a barrier to the success of rural electrification.

Key Activities

The value chain are the activities that a company performs in order to deliver a product or service. In this case, the company is responsible for the rural electrification project throughout its lifetime. Its roles are listed here:

1. Customer identification: Communities with anchor loads nearby are identified. A feasibility study is performed to assess the viability of the project.
2. System engineering: Design of the microgrid system, it mainly includes resources and demand assessment, sizing of the solar plant and ESS and distribution cables as well as other electrical components. It also involves the development of the DERM, control and communication protocols.
3. Installation: Upon ordering and receiving the electrical components necessary for the installation of the system, the company installs the microgrid. In case additional infrastructure is needed, local companies are contacted. Once installed testing is undertaken to ensure that the system is safe and operating under normal conditions.
4. Operation and maintenance: Once the system is installed, the company is responsible for the operation of the project throughout its lifetime. It ensures that the microgrid is operating correctly, it optimizes the microgrid over time (e.g. expanding the network and increasing the generation and storage capacity) and it collects revenues. Increasing the capacity can either be done by purchasing additional solar panels or motivating local entrepreneurs to purchase their own PV panels under the condition that the two parties agree to a deal. Upon the purchase of a solar panel, entrepreneurs should benefit from a reduction of their monthly fee.

Hybrid Revenue Model

The implementation of microgrids is motivated by social incentives, namely providing electricity to increase the social welfare of communities in remote locations. Generation and ESS should thus be sized with respect to the demand in an attempt to generate enough electricity so that demand is matched at all times. As seen in Chapter 4, 5 and 6 in a network where the capacity of both storage and PV panels is enough to satisfy the demand at any time and if distribution lines are sized according to the distribution of load centers, the price of electricity will be zero. Non-zero prices only appears when the supply cannot match the demand or when a congestion is occurring in one of the transmission lines. The cost structure of microgrids based on RE is mainly composed of fixed cost. Operating cost are relatively low given that the energy is supplied by solar panels rather than diesel generators for which the operating cost is large and fluctuate with the ever changing cost of fuel. If the microgrid is sized appropriately the price of electricity should be zero at all times, it follows that implementing a revenue model based on consumption does not make sense as investment cost are not recovered.

An hybrid model that combines a fixed tariff and consumption based tariff is the most suitable revenue model. The fixed tariff accounts for the infrastructure (e.g. PV panels, ESS, electrical components) and maintenance. It is important to note that this tariff does not dictate the maximum energy that can be consumed by a load center. The energy consumed by load centers is priced using the locational pricing mechanism of the DERM. Therefore, if the network is size appropriately the consumption based tariff will be zero and consumers should only pay a monthly fee representing their cost of connection. However, in cases where supply cannot match demand or congestion occurs in some part of the network consumers are charged for their consumption based on the electricity tariff as well as the fixed tariff.

It is important to set the fixed tariff in such a way that it doesn't penalize small consumer or make energy inaccessible when the prices of electricity are not zero. In order to do so, load centers should be identified and categorized according to their expected demand. For example, an agricultural site for which the consumption of energy is intensive due to water pumping activities should have their fixed tariff higher than shops or households. Fixed cost should be calculated as a function of the demand in order to increase affordability for low income community members. Larger consumption is often related to an economic activity, consequently these members have a higher purchasing power. Moreover, the prices of electricity are set using the smart meter and willingness indicators. Therefore, the electricity market is not regulated by the grid operator but by the community. This mechanism causes electricity prices to be in agreement with the income of community members.

In order guarantee the collection of revenue, a pre- payment system should be adopted where users purchase credits from their phone and load it to their meters. Monthly fixed tariff should be deducted on a monthly basis and consumption tariff should be deducted when the electricity prices are higher than zero.

Customer Segments

The literature suggests that the ABC Model is adapted to the implementation of microgrids for rural electrification [139]. Moreover it correlates with the revenue model described above for which fixed prices are assigned according to the consumption of demand center. The role of anchors load is primordial to recover the initial capital of the microgrids, their fixed tariff should be the highest in the network to guarantee electricity affordability for households. The presence of anchor loads is a requirement, rural villages should be selected on the amount of anchor loads and businesses. Therefore, the three customer segments are anchors (large loads from industrial or agricultural activities), businesses (medium loads of shops) and households (small loads). Figure 10.2 shows an approximation of energy expenses for each customer segments based on the fixed tariff proportional to their monthly demand and the demand based tariff at times when there is a shortage of electricity or congestion in the network.

Developing the local economy by encouraging entrepreneurship is an important factor that should be incorporated in the business plan to ensure the sustainability of the project. The pricing mechanism developed is not only used for revenue collection, as demonstrated in Chapter 4 it can results in negative prices under certain conditions. In case of asymmetrical loading of the network, consumers can earn money by changing the poles between which their loads are connected. Furthermore, the DERM support prosumers. A customer can become a prosumer if an agreement is reached with the project manager. The benefits of purchasing PV panels is a reduction of the fixed tariff and an income based on the amount of energy produced.

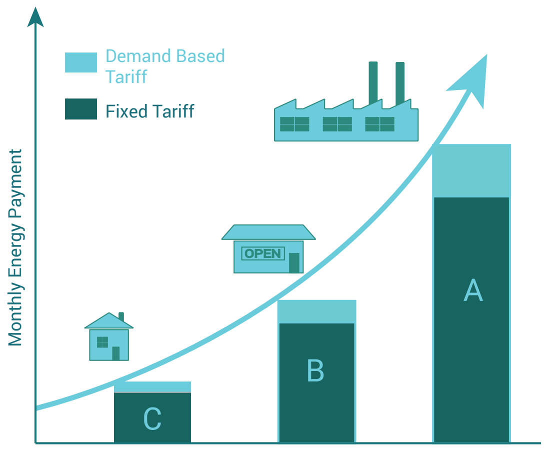

Figure 10.2: Shows the energy expenses according to each customer segments. Note the importance of anchor loads which are the main contributor to revenue collection. The revenue from households is minimal in comparison. This graph is not on scale, it is just used to illustrate the differences and the price structure. Given that the system is sized accordingly, the demand based tariff should be rather low and most income is from the fixed fee.

10.3. TIME PLANNING

Time planning is key to the success of a company, a series of small goals should be planned to achieve an end-goal. Here, the end-goal is to provide electricity to a large portion of the population with no access to electricity in both Africa and Asia.

STEP 1: PILOT PROJECT

Given that the bipolar DC microgrid is a relatively new system and unproven in larger scale, it is of vital importance to showcase its reliability and technical advantages with a robust, working prototype. The most important aspect in this step is to obtain the capital necessary to build the pilot project. Big companies should be approached and show interest in the technology. Thus, finding the right partner is believed to be key to the launch of this technology into the market. The main purpose of this partnership is to finance the implementation of a bipolar DC microgrids for rural electrification.

The main goal of this first project is to gain experience and understand the challenges associated with the technical operation of a bipolar DC microgrid and its impact on the local community. This step will help towards the maturing of the system. Additionally, it is a social experiment that aims to understand how local actors accept the solution. On top of the bipolar configuration of the microgrid, the novelty is the pricing mechanisms and the demand-response enables by the smart meters and willingness indicators to purchase electricity. Such system has never been tested before, consequently it is hard to anticipate how local actors will interact with the system.

From Chapter 9 it can be concluded that the landscape is an important factor for success. The presence of governmental policies and local organizations to promote rural electrification favors the development of projects thanks to subsidies and a framework supporting the private sectors. The countries benefiting from this support are principally Kenya, Tanzania and India. As a matter of fact, most of the private companies and electrification projects are lead in these countries. Kenya has been selected for the implementation of a pilot project. The country has set a goal under the Kenya 30 Vision that aims to improve the legal framework to support the development of electricity projects.

Although the competition is the highest in this area (e.g. Powerhive and Powergen) the amount of unelectrified communities is large enough to enable all businesses to develop in parallel. Following the ABC Model the

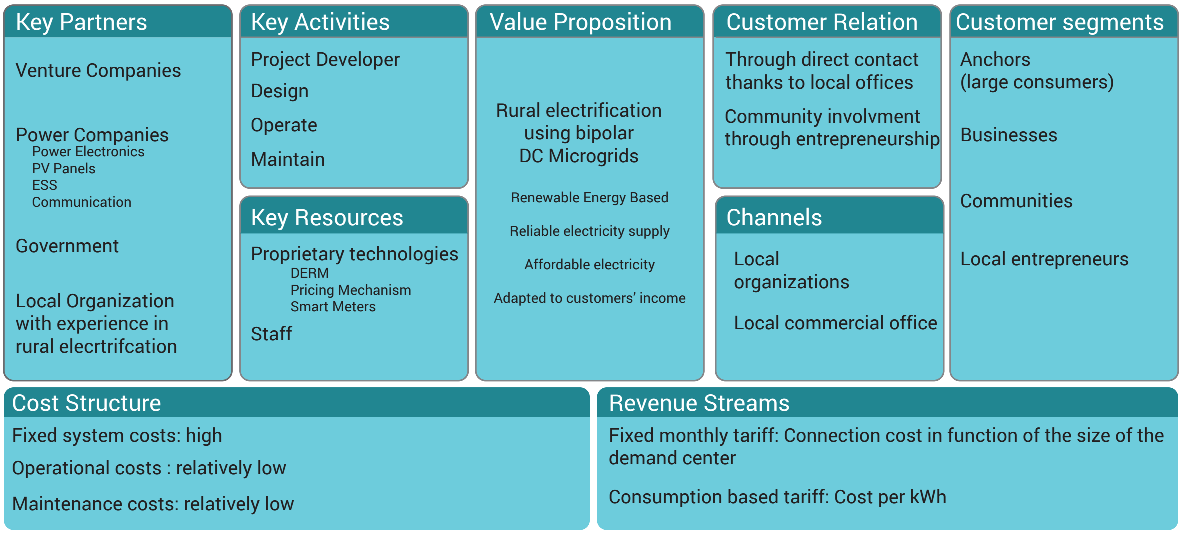

Figure 10.3: Business canvas of the bipolar DC microgrids for rural electrification.

pilot project should be implemented in a rural area where there is at least one anchor load, telecom towers seem to be a good candidate. In Kenya, out of 225 off-grid telecom towers that the main operator, Safaricom, owns, 47 were assessed to be a candidate to bring access to electricity to communities [139]. Note that these towers are now all operated using diesel generators, the associated costs are very expensive. Switching to solar energy would be at the benefit of the communication companies. The area to be electrified should be kept small, around 300 people (50-75 households) and local businesses should be present.

This step is critical for success; enough care should be taken so that the prototype can be fully developed in time. This is seen as the short-term vision. It is estimated that a robust design could take up to 2 years to develop and implement.

STEP 2: REGIONAL AND NATIONAL SCALE

Given that the concept is validated, microgrids provide a reliable source of power at a tariff affordable to the community, it becomes possible to enter the market at a regional level. More villages should be selected in the same region to increase social acceptance. It is also easier to obtain regulatory and other approval if the projects are implemented in the same region. From an operational point of view, it is easier to operate and maintain microgrids if they are located close to each other. Once multiple microgrids are operating in the same region, it is expected that the interest for bipolar DC microgrids will grow. The electrification plan can expand to the national level. This step is designed for a medium-term vision, it could take up to 5 years to implement multiple microgrids at suitable sites in Kenya. Depending on the success of the project, the electrification plan could be extended to the neighbor country, Tanzania where the governmental interest for rural electrification is growing.

STEP 3: TARGETING NEW MARKETS

As explained in Chapter 9, Asia's market for rural electrification is big. The plan is to open local offices facilitating the implementation of bipolar DC microgrids in India. The country interested in promoting rural electrification using policies.

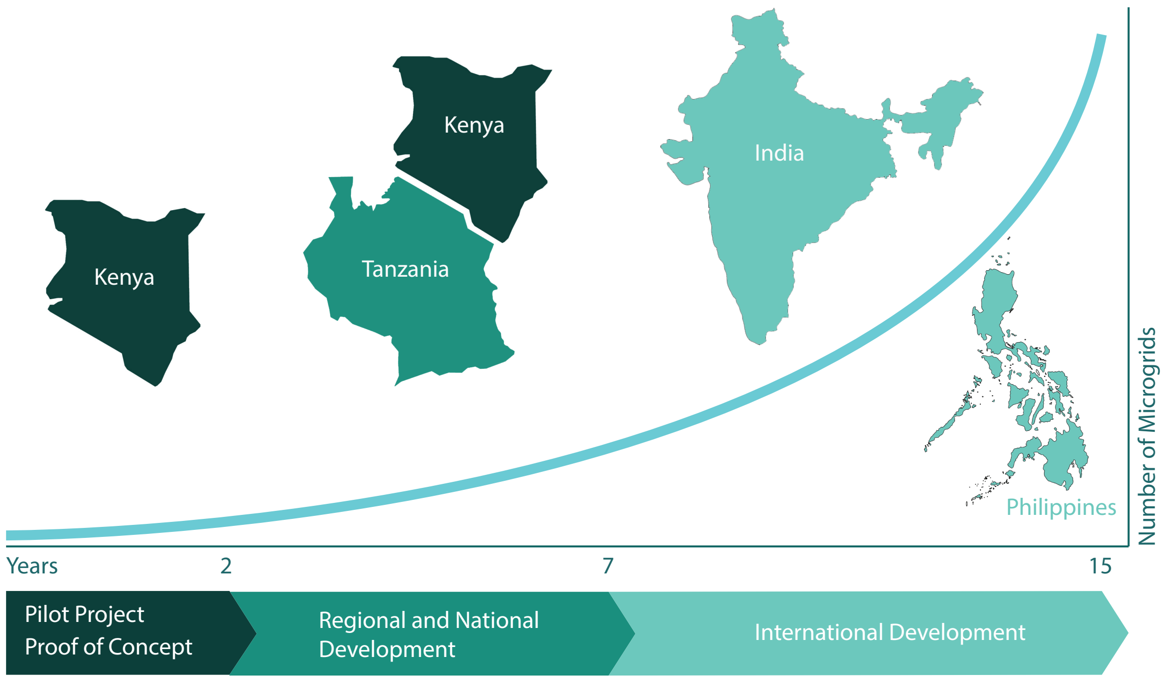

Figure 10.4: Time planning and deployment strategy of bipolar DC microgrids for rural electrification of Africa and Asia.

III

Appendices

A

Supplementary Information for Chapter 3

A.1. OPF FORMULATION

Objective Function

$$
\begin{aligned}
\text{Step 1 \& 3:} \quad & \max \sum_{(m,n,s)\in\mathcal{L}} p^{\mathrm{S}}_{m,n,s} \cdot \Pi^{\mathrm{S}}_{m,n,s} \cdot \Delta t \\
\text{Step 2:} \quad & \max \sum_{(m,n,s)\in\mathcal{L}} p^{\mathrm{S}}_{m,n,s} \cdot \Pi^{\mathrm{S}}_{m,n,s} \cdot \Delta t + \epsilon * \mid u_m - u^*_m \mid
\end{aligned}
$$

Subject to the Power Flow Model

$$
\begin{aligned}
& i_{m,n} = G_{m,n}(u_m - u_n) && \forall (m,n) \in \mathcal{G} \\
& i_m = \sum_{n|(m,n)\in\mathcal{G}} i_{m,n} - \sum_{n|(m,n)\in\mathcal{G}} i_{n,m} && \forall m \in \mathcal{N} \\
& i^{\mathrm{S}}_{m,n} = \sum_{s|(m,n,s)\in\mathcal{S}} i^{\mathrm{S}}_{m,n,s} && \forall (m,n) \in \mathcal{P} \\
& i_m = \sum_{n|(n,m)\in\mathcal{P}} i^{\mathrm{S}}_{n,m} - \sum_{n|(n,m)\in\mathcal{P}} i^{\mathrm{S}}_{m,n} && \forall m \in \mathcal{N} \\
\text{Step 1:} \quad & p^{\mathrm{S}}_{m,n,s} = i^{\mathrm{S}}_{m,n,s} \cdot (u_m - u_n) && \forall (m,n,s) \in \mathcal{S} \\
\text{Step 2 \& 3:} \quad & p^{\mathrm{S}}_{m,n,s} = i^{\mathrm{S}*}_{m,n,s}(u_m - u_n) + i^{\mathrm{S}}_{m,n,s}\left(u^*_m - u^*_n\right) - i^{\mathrm{S}*}_{m,n,s}\left(u^*_m - u^*_n\right) && \forall (m,n,s) \in \mathcal{S}
\end{aligned}
$$

Subject to Network and ESS Constraints

$$
\begin{aligned}
& U_{\min} \le u_m \le U_{\max} && \forall m \in \mathcal{N}_+ \\
& U_{\min} \le -u_m \le U_{\max} && \forall m \in \mathcal{N}_- \\
& U_{\mathrm{N},\min} \le u_m \le U_{N,\max} && \forall m \in \mathcal{N}_{\mathrm{N}} \\
& I_{m,n,\min} \le i_{m,n} \le I_{m,n,\max} && \forall (m,n) \in \mathcal{G} \\
& I^{\mathrm{S}}_{m,n,s,\min} \le i^{\mathrm{S}}_{m,n,s,k} \le I^{\mathrm{S}}_{m,n,s,\max} && \forall (m,n,s) \in \mathcal{S} \\
& P^{\mathrm{S}}_{m,n,s,k,\min} \le p^{\mathrm{S}}_{m,n,s,k} \le P^{\mathrm{S}}_{m,n,s,k,\max} && \forall (m,n,s) \in \mathcal{S}
\end{aligned}
$$

A.2. EXAMPLES INPUTS AND OUTPUTS

Inputs	Generation Units[W]				Loads [W]			
	$p^S_{0,8,4}$	$p^S_{4,0,0}$	$p^S_{7,3,3}$	$p^S_{3,11,7}$	$p^S_{1,9,5}$	$p^S_{5,1,1}$	$p^S_{6,2,2}$	$p^S_{2,10,6}$
$\Pi^S_{m,n,s}$ [$/W]	2	2	5	5	0	0	0	0
Case 1	-300 – 0	-300 – 0	-300 – 0	-300 – 0	100	100	100	100
Case 2	-300 – 0	-300 – 0	-300 – 0	-300 – 0	100	100	100	100
Case 3	-300 – 0	-300 – 0	-300 – 0	-300 – 0	100	100	100	200

Table A.1: Case 1, 2 and 3: Sources and their respective limits. Generators are given a negative range of operation while loads are fixed (lower and upper limits are equal) to a positive value.

Inputs	Branch current[A]			Conductance [Ω^{-1}]		
	$I_{4,5,max}$	$I_{5,6,max}$	$I_{6,7,max}$	$G_{4,5}$	$G_{5,6}$	$G_{6,7}$
Case 1	Inf	Inf	Inf	0.100	0.025	0.100
Case 2	Inf	0.2	Inf	0.100	0.100	0.100
Case 3	Inf	0.2	Inf	0.100	0.100	0.100
	$I_{0,1,max}$	$I_{1,2,max}$	$I_{2,3,max}$	$G_{0,1}$	$G_{1,2}$	$G_{2,3}$
Case 1	Inf	Inf	Inf	0.100	0.025	0.100
Case 2	Inf	Inf	Inf	0.100	0.100	0.100
Case 3	Inf	Inf	Inf	0.100	0.100	0.100
	$I_{8,9,max}$	$I_{9,10,max}$	$I_{10,11,max}$	$G_{8,9}$	$G_{9,10}$	$G_{10,11}$
Case 1	Inf	Inf	Inf	0.100	0.025	0.100
Case 2	Inf	Inf	Inf	0.100	0.100	0.100
Case 3	Inf	Inf	Inf	0.100	0.100	0.100

Table A.2: Case 1, 2 and 3: Lines' conductances and respective current limits set to either infinity or a specific value to force congestions.

Inputs	Generation Units[W]			Loads [W]				
	$p^{S}_{0,7,5}$	$p^{S}_{3,0,0}$	$p^{S}_{6,10,4}$	$p^{S}_{1,8,6}$	$p^{S}_{4,1,1}$	$p^{S}_{5,2,2}$	$p^{S}_{5,2,3}$	$p^{S}_{2,9,7}$
$\Pi^{S}_{m,n,s}$[$/W]	2	2	5	0	0	0	0	0
Case 4.1	-300 – 0	-200 – 0	-1000 – 0	100	100	100	100	100
Case 4.2	-300 – 0	-200 – 0	-1000 – 0	100	100	100	101	100

Table A.3: Case 4.1 and 4.2: Sources and their respective limits. Generators are given a negative range of operation while loads are fixed (lower and upper limits are equal) to a positive value.

Inputs	Branch current[A]			Conductance [Ω^{-1}]		
	$I_{3,4,max}$	$I_{4,5,max}$	$I_{5,6,max}$	$G_{3,4}$	$G_{4,5}$	$G_{5,6}$
Case 4.1	Inf	Inf	Inf	0.100	0.100	0.100
Case 4.2	Inf	Inf	Inf	0.100	0.100	0.100
	$I_{0,1,max}$	$I_{1,2,max}$	–	$G_{0,1}$	$G_{1,2}$	–
Case 4.1	Inf	Inf	–	0.100	0.100	–
Case 4.2	Inf	Inf	–	0.100	0.100	–
	$I_{7,8,max}$	$I_{8,9,max}$	$I_{9,10,max}$	$G_{7,8}$	$G_{8,9}$	$G_{9,10}$
Case 4.1	Inf	Inf	Inf	0.100	0.100	0.100
Case 4.2	Inf	Inf	Inf	0.100	0.100	0.100

Table A.4: Case 4.1 and 4.2: Lines' conductances and respective current limits set to either infinity or a specific value to force congestions.

Outputs	Branch Current [A]			Node Voltage [V]				LMP [$/Wh]			
	$i_{3,4}$	$i_{4,5}$	$i_{5,6}$	u_3	u_4	u_5	u_6	λ^{I}_{3}	λ^{I}_{4}	λ^{I}_{5}	λ^{I}_{6}
Case 4.1	0.56	0.27	-0.31	360.00	354.44	351.73	354.80	2856.2	2913.3	2947.2	2931.9
Case 4.2	0.56	0.27	-0.31	360.00	354.44	351.73	354.83	2856.2	2913.3	2947.2	2931.9
	$i_{0,1}$	$i_{1,2}$	–	u_0	u_1	u_2	–	λ^{I}_{0}	λ^{I}_{1}	λ^{I}_{2}	–
Case 4.1	-0.29	-0.29	–	0.00	2.82	5.70	–	106.7	44.4	0.0	–
Case 4.2	-0.28	-0.28	–	0.00	2.85	5.77	–	106.7	44.4	0.0	–
	$i_{7,8}$	$i_{8,9}$	$i_{9,10}$	u_7	u_8	u_9	u_{10}	λ^{I}_{7}	λ^{I}_{8}	λ^{I}_{9}	λ^{I}_{10}
Case 4.1	-0.27	0.02	0.31	-342.74	-340.00	-340.17	-343.25	-578.8	-584.2	-573.7	-558.4
Case 4.2	-0.27	0.02	0.31	-342.71	-340.00	-340.21	-343.31	-578.8	-584.2	-573.7	-558.4

Table A.5: Case 4.1 and 4.2: Outputs of simulations with branch, node currents and corresponding LMP formulated in terms of current for each node for which a source is connected to.

Inputs	Generation Units[W]				Loads [W]	
	$p^S_{0,6,3}$	$p^S_{3,0,0}$	$p^S_{4,1,1}$	$p^S_{1,7,4}$	$p^S_{5,2,2}$	$p^S_{2,8,5}$
$\Pi^S_{m,n,s}$[\$/W]	2	2	5	5	0	0
Case 5.1	-300 – 0	-300 – 0	-300 – 0	-300 – 0	100	100
Case 5.2	-300 – 0	-300 – 0	-300 – 0	-300 – 0	101	100

Table A.6: Case 5.1 and 5.2: Sources and their respective limits. Generators are given a negative range of operation while loads are fixed (lower and upper limits are equal) to a positive value.

Inputs	Branch current[A]			Conductance [Ω^{-1}]		
	$I_{3,4,max}$	$I_{4,5,max}$	$I_{3,5,max}$	$G_{3,4}$	$G_{4,5}$	$G_{3,5}$
Case 5.1	Inf	Inf	0.1	0.100	0.100	0.100
Case 5.2	Inf	Inf	0.1	0.100	0.100	0.100
	$I_{0,1,max}$	$I_{1,2,max}$	$I_{0,2,max}$	$G_{0,1}$	$G_{1,2}$	$G_{0,2}$
Case 5.1	Inf	Inf	0.1	0.100	0.100	0.100
Case 5.2	Inf	Inf	0.1	0.100	0.100	0.100
	$I_{6,7,max}$	$I_{7,8,max}$	$I_{6,8,max}$	$G_{6,7}$	$G_{7,8}$	$G_{6,8}$
Case 5.1	Inf	Inf	0.1	0.100	0.100	0.100
Case 5.2	Inf	Inf	0.1	0.100	0.100	0.100

Table A.7: Case 5.1 and 5.2: Lines' conductances and respective current limits set to either infinity or a specific value to force congestions.

Outputs	Branch Current [A]			Node Voltage [V]			LMP [\$/Wh]		
	$i_{3,4}$	$i_{4,5}$	$i_{3,5}$	u_3	u_4	u_5	λ^I_3	λ^I_4	λ^I_5
Case 5.1	-0.08	0.18	0.10	359.21	360.00	358.21	-718.4	-1800.0	-2903.8
Case 5.2	-0.08	0.18	0.10	359.18	360.00	358.18	-718.4	-1800.2	-2904.6
	$i_{0,1}$	$i_{1,2}$	$i_{0,2}$	u_0	u_1	u_2	λ^I_0	λ^I_1	λ^I_2
Case 5.1	0.00	0.00	0.00	0.00	0.00	0.00	0.0	0.0	0.0
Case 5.2	0.003	-0.003	0	0.00	-0.03	0	0.0	0.1	-0.1
	$i_{6,7}$	$i_{7,8}$	$i_{6,8}$	u_6	u_7	u_8	λ^I_6	λ^I_7	λ^I_7
Case 5.1	0.08	-0.18	-0.10	-359.21	-360.00	-358.21	718.4	1800.0	2903.8
Case 5.2	0.08	-0.18	-0.10	-359.21	-360.00	-358.21	718.4	1799.8	2903.3

Table A.8: Case 5.1 and 5.2: Outputs of simulations with branch, node currents and corresponding LMP formulated in terms of current for each node for which a source is connected to.

B

Supplementary Information for Chapter 4

B.1. OPF FORMULATION

Objective Function

$$\text{Step 1 \& 3:} \quad \max \sum_{k} \sum_{(m,n,s)\in\mathcal{L}} p^{\mathrm{S}}_{m,n,s,k} \cdot \Pi^{\mathrm{S}}_{m,n,s} \cdot \Delta t \qquad \forall k \in \mathcal{K}$$

$$\text{Step 2:} \quad \max \sum_{k} \sum_{(m,n,s)\in\mathcal{L}} p^{\mathrm{S}}_{m,n,s,k} \cdot \Pi^{\mathrm{S}}_{m,n,s} \cdot \Delta t + \epsilon \cdot | u_{m,k} - u^*_{m,k} | \qquad \forall k \in \mathcal{K}$$

Subject to the Power Flow Model

$$\begin{aligned}
& i_{m,n,k} = G_{m,n}(u_{m,k} - u_{n,k}) && \forall (m,n) \in \mathcal{G}, \quad k \in \mathcal{K} \\
& i_{m,k} = \sum_{n|(m,n)\in\mathcal{G}} i_{m,n,k} - \sum_{n|(m,n)\in\mathcal{G}} i_{n,m,k} && \forall m \in \mathcal{N}, \quad k \in \mathcal{K} \\
& i^{\mathrm{S}}_{m,n,k} = \sum_{s|(m,n,s)\in\mathcal{S}} i^{\mathrm{S}}_{m,n,s,k} && \forall (m,n) \in \mathcal{P}, \quad k \in \mathcal{K} \\
& i_{m,k} = \sum_{n|(n,m)\in\mathcal{P}} i^{\mathrm{S}}_{n,m,k} - \sum_{n|(n,m)\in\mathcal{P}} i^{\mathrm{S}}_{m,n,k} && \forall m \in \mathcal{N}, \quad k \in \mathcal{K} \\
\text{Step 1:} \quad & p^{\mathrm{S}}_{m,n,s,k} = i^{\mathrm{S}}_{m,n,s,k} \cdot (u_{m,k} - u_{n,k}) && \forall (m,n,s) \in \mathcal{S}, \quad k \in \mathcal{K} \\
\text{Step 2 \& 3:} \quad & p^{\mathrm{S}}_{m,n,s,k} = i^{\mathrm{S}^*}_{m,n,s,k}(u_{m,k} - u_{n,k}) + i^{\mathrm{S}}_{m,n,s,k}\left(u^*_{m,k} - u^*_{n,k}\right) - i^{\mathrm{S}^*}_{m,n,s,k}\left(u^*_{m,k} - u^*_{n,k}\right) && \forall (m,n,s) \in \mathcal{S}, \quad k \in \mathcal{K}
\end{aligned}$$

Subject to the Battery Model

$$\begin{aligned}
& e^{\mathrm{S}}_{m,n,s,k_0} = 0 && \forall (m,n,s) \in \mathcal{F}, \quad k \in \mathcal{K} \\
& e^{\mathrm{S}}_{m,n,s,k} = e^{\mathrm{S}}_{m,n,s,k-1} + p^{\mathrm{S,charge}}_{m,n,s,k-1} * \eta^{\mathrm{ESS}}_{m,n,s} * \Delta t + p^{\mathrm{S,discharge}}_{m,n,s,k-1} * \frac{1}{\eta^{\mathrm{ESS}}_{m,n,s}} * \Delta t && \forall (m,n,s) \in \mathcal{F}, \quad k \in \mathcal{K} \\
& p^{\mathrm{S}}_{m,n,s,k} = p^{\mathrm{S,charge}}_{m,n,s,k} + p^{\mathrm{S,discharge}}_{m,n,s,k} && \forall (m,n,s) \in \mathcal{F}, \quad k \in \mathcal{K}
\end{aligned}$$

Subject to Network and ESS Constraints

$$\begin{aligned}
& U_{\min} \le u_{m,k} \le U_{\max} && \forall m \in \mathcal{N}_+, \quad k \in \mathcal{K} \\
& U_{\min} \le -u_{m,k} \le U_{\max} && \forall m \in \mathcal{N}_-, \quad k \in \mathcal{K} \\
& U_{\mathrm{N,min}} \le u_{m,k} \le U_{N,\mathrm{max}} && \forall m \in \mathcal{N}_{\mathrm{N}}, \quad k \in \mathcal{K} \\
& I_{m,n,\min} \le i_{m,n,k} \le I_{m,n,\max} && \forall (m,n) \in \mathcal{G}, \quad k \in \mathcal{K} \\
& I^{\mathrm{S}}_{m,n,s,\min} \le i^{\mathrm{S}}_{m,n,s,k} \le I^{\mathrm{S}}_{m,n,s,\max} && \forall (m,n,s) \in \mathcal{S}, \quad k \in \mathcal{K} \\
& P^{\mathrm{S}}_{m,n,s,k,\min} \le p^{\mathrm{S}}_{m,n,s,k} \le P^{\mathrm{S}}_{m,n,s,k,\max} && \forall (m,n,s) \in \mathcal{S}, \quad k \in \mathcal{K} \\
& E^{\mathrm{ESS}}_{m,n,s,\min} \le e^{\mathrm{S}}_{m,n,s,k} \le E^{\mathrm{ESS}}_{m,n,s,\max} && \forall (m,n,s) \in \mathcal{F}, \quad k \in \mathcal{K} \\
& p^{\mathrm{S,charge}}_{m,n,s,k} \ge 0 && \forall (m,n,s) \in \mathcal{F}, \quad k \in \mathcal{K} \\
& p^{\mathrm{S,discharge}}_{m,n,s,k} \le 0 && \forall (m,n,s) \in \mathcal{F}, \quad k \in \mathcal{K}
\end{aligned}$$

B.2. EXAMPLES INPUTS AND OUTPUTS

(a) (b)

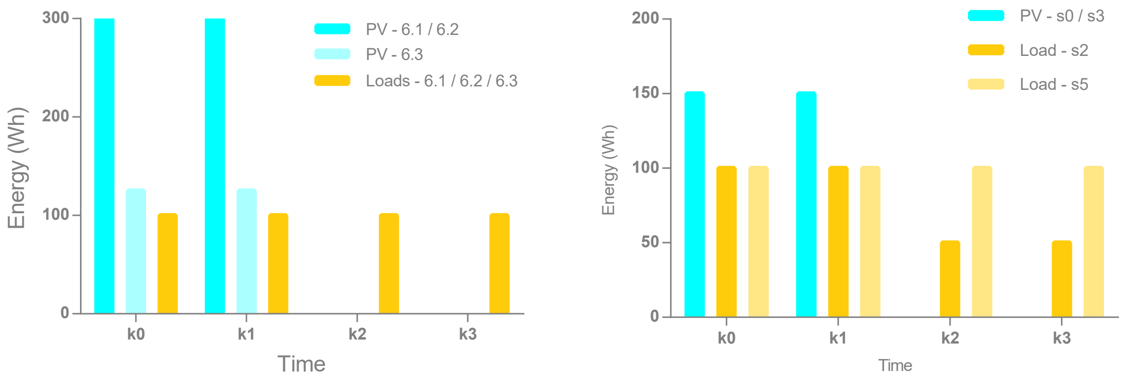

Figure B.1: Irradiance and load profiles for cases 6.1, 6.2 & 6.3 (B.1a) and case 7 (B.1b).

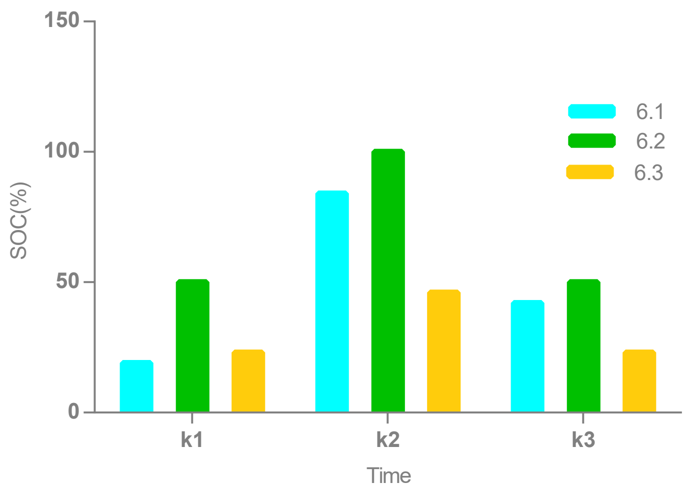

Figure B.2: Case 6.1, 6.2 and 6.3: State of charge of the storage unit.

k	Cases	Generation Units[W]				Loads [W]		ESS [Wh]	η
		$p^S_{0,8,4,k}$	$p^S_{4,0,0,k}$	$p^S_{5,1,1,k}$	$p^S_{1,9,5,k}$	$p^S_{7,3,3,k}$	$p^S_{3,10,6,k}$	$E^S_{6,2,2,\max}$	η
$k0$	Case 6.1	-300 – 0	-300 – 0	-300 – 0	-300 – 0	0 – 100	0 – 100	250	0.95
	Case 6.2	-300 – 0	-300 – 0	-300 – 0	-300 – 0	0 – 100	0 – 100	50	0.95
	Case 6.3	-300 – 0	-125 – 0	-300 – 0	-300 – 0	0 – 100	0 – 100	100	0.95
		$p^S_{0,8,4,k}$	$p^S_{4,0,0,k}$	$p^S_{5,1,1,k}$	$p^S_{1,9,5,k}$	$p^S_{7,3,3,k}$	$p^S_{3,10,6,k}$	$E^S_{6,2,2,\max}$	η
$k1$	Case 6.1	-300 – 0	-300 – 0	-300 – 0	-300 – 0	0 – 100	0 – 100	250	0.95
	Case 6.2	-300 – 0	-300 – 0	-300 – 0	-300 – 0	0 – 100	0 – 100	50	0.95
	Case 6.3	-300 – 0	-125 – 0	-300 – 0	-300 – 0	0 – 100	0 – 100	100	0.95
		$p^S_{0,8,4,k}$	$p^S_{4,0,0,k}$	$p^S_{5,1,1,k}$	$p^S_{1,9,5,k}$	$p^S_{7,3,3,k}$	$p^S_{3,10,6,k}$	$E^S_{6,2,2,\max}$	η
$k2$	Case 6.1	0	0	-300 – 0	-300 – 0	0 – 100	0 – 100	250	0.95
	Case 6.2	0	0	-300 – 0	-300 – 0	0 – 100	0 – 100	50	0.95
	Case 6.3	0	0	-300 – 0	-300 – 0	0 – 100	0 – 100	100	0.95
		$p^S_{0,8,4,k}$	$p^S_{4,0,0,k}$	$p^S_{5,1,1,k}$	$p^S_{1,9,5,k}$	$p^S_{7,3,3,k}$	$p^S_{3,10,6,k}$	$E^S_{6,2,2,\max}$	η
$k3$	Case 6.1	0	0	-300 – 0	-300 – 0	0 – 100	0 – 100	250	0.95
	Case 6.2	0	0	-300 – 0	-300 – 0	0 – 100	0 – 100	50	0.95
	Case 6.3	0	0	-300 – 0	-300 – 0	0 – 100	0 – 100	100	0.95

Table B.1: Case 6.1, 6.2 and 6.3: Sources and their respective limits. Generators are given a negative range of operation while loads are fixed (lower and upper limits are equal) to a positive value.

Outputs		Generation Units[W]				Generation Units [A]			
		$p^{S}_{4,0,0,k}$	$p^{S}_{5,1,1,k}$	$p^{S}_{6,2,2,k}$	$p^{S}_{7,3,3,k}$	$i^{S}_{4,0,0,k}$	$i^{S}_{5,1,1,k}$	$i^{S}_{6,2,2,k}$	$i^{S}_{7,3,3,k}$
Case 6.1	k0	-153.50	0.00	55.23	100.00	-0.45	0.00	0.15	0.29
	k1	-274.10	0.00	169.78	100.00	-0.80	0.00	0.50	0.30
	k2	0.00	0.00	-100.20	100.00	0.00	0.00	-0.29	0.29
	k3	0.00	0.00	-100.20	100.00	0.00	0.00	-0.29	0.29
Case 6.2	k0	-127.20	0.00	26.32	100.00	-0.37	0.00	0.08	0.29
	k1	-127.20	0.00	26.32	100.00	-0.37	0.00	0.08	0.29
	k2	0.00	-76.47	-23.75	100.00	0.00	-0.21	-0.06	0.28
	k3	0.00	-76.47	-23.75	100.00	0.00	-0.21	-0.06	0.28
Case 6.3	k0	-125.00	0.00	24.30	100.00	-0.35	0.00	0.07	0.28
	k1	-125.00	0.00	24.30	100.00	-0.35	0.00	0.07	0.28
	k2	0.00	0.00	-21.93	21.91.00	0.00	0.00	-0.06	0.06
	k3	0.00	0.00	-21.93	21.91.00	0.00	0.00	-0.06	0.06
		$p^{S}_{0,8,4,k}$	$p^{S}_{1,9,5,k}$	$p^{S}_{3,10,6,k}$	–	$i^{S}_{0,8,4,k}$	$i^{S}_{1,9,5,k}$	$i^{S}_{3,10,6,k}$	–
Case 6.1	k0	-100.20	0.00	100.00	–	-0.29	0.00	0.29	–
	k1	-99.75	0.00	100.00	–	-0.29	0.00	0.29	–
	k2	0.00	-100.30	100.00	–	0.00	-0.28	0.29	–
	k3	0.00	-100.30	100.00	–	0.00	-0.28	0.29	–
Case 6.2	k0	-100.30	0.00	100.00	–	-0.29	0.00	0.29	–
	k1	-100.30	0.00	100.00	–	-0.29	0.00	0.29	–
	k2	0.00	-100.20	100.00	–	0.00	-0.28	0.28	–
	k3	0.00	-100.00	100.00	–	0.00	-0.28	0.28	–
Case 6.3	k0	-100.46	0.00	0.00	–	-0.29	0.00	0.29	–
	k1	-100.46	0.00	0.00	–	-0.29	0.00	0.29	–
	k2	0.00	0.00	0.00	–	0.00	0.00	0.00	–
	k3	0.00	0.00	0.00	–	0.00	0.00	0.00	–

Table B.2: Case 6.1, 6.2 and 6.3: Outputs of simulations with generation level of each source in terms of power and current.

k	Generation Units[W]			Loads [W]		ESS [Wh]		η	
	$p^{\mathrm{S}}_{0,7,3,k}$	$p^{\mathrm{S}}_{3,0,0,k}$	$p^{\mathrm{S}}_{6,10,6,k}$	$p^{\mathrm{S}}_{2,9,5,k}$	$p^{\mathrm{S}}_{5,2,2,k}$	$E^{\mathrm{S}}_{1,8,5\mathrm{max}}$	$E^{\mathrm{S}}_{4,1,1,\mathrm{max}}$	$\eta^{\mathrm{ESS}_{1,8,5}}$	$\eta^{\mathrm{ESS}_{4,1,1}}$
$k0$	-150 – 0	-150 – 0	0 – 100	0 – 100	100 – 0	25	25	0.95	0.95
	$p^{\mathrm{S}}_{0,8,4,k}$	$p^{\mathrm{S}}_{4,0,0,k}$	$p^{\mathrm{S}}_{5,1,1}$	$p^{\mathrm{S}}_{1,9,5,k}$	$p^{\mathrm{S}}_{7,3,3,k}$	$E^{\mathrm{S}}_{1,8,5\mathrm{max}}$	$E^{\mathrm{S}}_{4,1,1,\mathrm{max}}$	$\eta^{\mathrm{ESS}_{1,8,5}}$	$\eta^{\mathrm{ESS}_{4,1,1}}$
$k1$	-150 – 0	-150 – 0	0 – 100	0 – 100	100 – 0	25	25	0.95	0.95
	$p^{\mathrm{S}}_{0,8,4,k}$	$p^{\mathrm{S}}_{4,0,0,k}$	$p^{\mathrm{S}}_{5,1,1}$	$p^{\mathrm{S}}_{1,9,5,k}$	$p^{\mathrm{S}}_{7,3,3,k}$	$E^{\mathrm{S}}_{1,8,5\mathrm{max}}$	$E^{\mathrm{S}}_{4,1,1,\mathrm{max}}$	$\eta^{\mathrm{ESS}_{1,8,5}}$	$\eta^{\mathrm{ESS}_{4,1,1}}$
$k2$	0	0	-500 – 0	0 – 100	0 – 25	25	25	0.95	0.95
	$p^{\mathrm{S}}_{0,8,4,k}$	$p^{\mathrm{S}}_{4,0,0,k}$	$p^{\mathrm{S}}_{5,1,1}$	$p^{\mathrm{S}}_{1,9,5,k}$	$p^{\mathrm{S}}_{7,3,3,k}$	$E^{\mathrm{S}}_{1,8,5\mathrm{max}}$	$E^{\mathrm{S}}_{4,1,1,\mathrm{max}}$	$\eta^{\mathrm{ESS}_{1,8,5}}$	$\eta^{\mathrm{ESS}_{4,1,1}}$
$k3$	0	0	-500 – 0	0 – 100	0 – 25	25	25	0.95	0.95

Table B.3: Case 7: Sources and their respective limits. Generators are given a negative range of operation while loads are fixed (lower and upper limits are equal) to a positive value.

	Generation Units[W]			Generation Units [A]		
	$p^{\mathrm{S}}_{3,0,0,k}$	$p^{\mathrm{S}}_{4,1,1,k}$	$p^{\mathrm{S}}_{5,2,2,k}$	$i^{\mathrm{S}}_{4,0,0,k}$	$i^{\mathrm{S}}_{5,1,1,k}$	$i^{\mathrm{S}}_{6,2,2,k}$
k0	-100.30	0.00	100.00	-0.29	0.00	0.29
k1	-100.34	0.00	100.00	-0.29	0.00	0.29
k2	0.00	14.31	50.00	0.00	0.04	0.15
k3	0.00	14.32	50.00	0.00	0.04	0.15
	$p^{\mathrm{S}}_{0,7,3,k}$	$p^{\mathrm{S}}_{0,8,4,k}$	$p^{\mathrm{S}}_{2,9,5,k}$	$i^{\mathrm{S}}_{0,7,3,k}$	$i^{\mathrm{S}}_{0,8,4,k}$	$i^{\mathrm{S}}_{2,9,5,k}$
k0	-125.50	25.00	100.00	-0.37	0.07	0.29
k1	-101.67	1.32	100.00	-0.30	0.00	0.29
k2	0.00	-11.87	79.83	0.00	-0.03	0.22
k3	0.00	-11,87	79.83	0.00	-0.03	0.22
	$p^{\mathrm{S}}_{6,10,6,k}$	–	–	$i^{\mathrm{S}}_{6,10,6,k}$	–	–
k0	0.00	–	–	0.00	–	–
k1	0.00	–	–	0.00	–	–
k2	-132.42	–	–	0.15	–	–
k3	-132.42	–	–	0.15	–	–

Table B.4: Case 7: Outputs of simulations with generation level of each source in terms of power and current.

C

Supplementary Information for Chapter 5

C.1. OPF FORMULATION

Objective Function

$$\max \sum_{k} \sum_{(m,n,s)\in\mathcal{L}} p^{\mathrm{S}}_{m,n,s,k} \cdot \Pi^{\mathrm{S}}_{m,n,s} \cdot \Delta t + \sum_{m,n,s\in\mathcal{V}} s^{\mathrm{ESS}}_{m,n,s} \cdot \Pi^{\mathrm{ESS}}_{m,n,s} \qquad \forall k \in \mathcal{K}$$

Subject to the Power Flow Model

$$i_{m,n,k} = G_{m,n}(u_{m,k} - u_{n,k}) \qquad \forall (m,n) \in \mathcal{G}, \quad k \in \mathcal{K}$$
$$i_{m,k} = \sum_{n|(m,n)\in\mathcal{G}} i_{m,n,k} - \sum_{n|(m,n)\in\mathcal{G}} i_{n,m,k} \qquad \forall m \in \mathcal{N}, \quad k \in \mathcal{K}$$
$$i^{\mathrm{S}}_{m,n,k} = \sum_{s|(m,n,s)\in\mathcal{S}} i^{\mathrm{S}}_{m,n,s,k} \qquad \forall (m,n) \in \mathcal{P}, \quad k \in \mathcal{K}$$
$$i_{m,k} = \sum_{n|(n,m)\in\mathcal{P}} i^{\mathrm{S}}_{n,m,k} - \sum_{n|(n,m)\in\mathcal{P}} i^{\mathrm{S}}_{m,n,k} \qquad \forall m \in \mathcal{N}, \quad k \in \mathcal{K}$$
$$p^{\mathrm{S}}_{m,n,s,k} = i^{\mathrm{S}}_{m,n,s,k} \cdot (u_{m,k} - u_{n,k}) \qquad \forall (m,n,s) \in \mathcal{S}, \quad k \in \mathcal{K}$$

Subject to the Battery Model

$$e^{\mathrm{S}}_{m,n,s,k_0} = 0 \qquad \forall (m,n,s) \in \mathcal{B}, \quad k \in \mathcal{K}$$
$$e^{\mathrm{S}}_{m,n,s,k} = e^{\mathrm{S}}_{m,n,s,k-1} + p^{\mathrm{S,charge}}_{m,n,s,k-1} * \eta^{\mathrm{ESS}}_{m,n,s} * \Delta t + p^{\mathrm{S,discharge}}_{m,n,s,k-1} * \frac{1}{\eta^{\mathrm{ESS}}_{m,n,s}} * \Delta t \qquad \forall (m,n,s) \in \mathcal{F}, \quad k \in \mathcal{K}$$
$$p^{\mathrm{S}}_{m,n,s,k} = p^{\mathrm{S,charge}}_{m,n,s,k} + p^{\mathrm{S,discharge}}_{m,n,s,k} \qquad \forall (m,n,s) \in \mathcal{F}, \quad k \in \mathcal{K}$$

Subject to the Battery Sizing and Placement Model

$$E^{\mathrm{S}}_{m,n,s,\min} \le e^{\mathrm{S}}_{m,n,s,k} \qquad \forall (m,n,s) \in \mathcal{V}, \quad k \in \mathcal{K}$$
$$s^{\mathrm{ESS}}_{m,n,s} \ge e^{\mathrm{S}}_{m,n,s,k} \qquad \forall (m,n,s) \in \mathcal{V}, \quad k \in \mathcal{K}$$
$$s^{\mathrm{ESS}}_{m,n,s} \le S^{\mathrm{S}}_{m,n,s,\max} \cdot b_{m,n,s} \qquad \forall (m,n,s) \in \mathcal{V}, \quad k \in \mathcal{K}$$
$$s^{\mathrm{ESS}}_{m,n,s} \ge S^{\mathrm{S}}_{m,n,s,\min} \cdot b_{m,n,s} \qquad \forall (m,n,s) \in \mathcal{V}, \quad k \in \mathcal{K}$$
$$e^{\mathrm{S}}_{m,n,s,k} = e^{\mathrm{S}}_{m,n,s,k-1} + b_{m,n,s} \cdot p^{\mathrm{S,charge}}_{m,n,s,k-1} * \eta_{m,n,s} * \Delta t + b_{m,n,s} \cdot p^{\mathrm{S,discharge}}_{m,n,s,k-1} * \frac{1}{\eta_{m,n,s}} * \Delta t \qquad \forall (m,n,s) \in \mathcal{V}, \quad k \in \mathcal{K}$$
$$p^{\mathrm{S}}_{m,n,s,k} = b_{m,n,s} \cdot p^{\mathrm{S,charge}}_{m,n,s,k} + b_{m,n,s} \cdot p^{\mathrm{S,discharge}}_{m,n,s,k} \qquad \forall (m,n,s) \in \mathcal{V}, \quad k \in \mathcal{K}$$

Subject to Network and ESS Constraints

$$U_{\min} \le u_{m,k} \le U_{\max} \qquad \forall m \in \mathcal{N}_{+}, \quad k \in \mathcal{K}$$
$$U_{\min} \le -u_{m,k} \le U_{\max} \qquad \forall m \in \mathcal{N}_{-}, \quad k \in \mathcal{K}$$
$$U_{\mathrm{N},\min} \le u_{m,k} \le U_{N,\max} \qquad \forall m \in \mathcal{N}_{\mathrm{N}}, \quad k \in \mathcal{K}$$
$$I_{m,n,\min} \le i_{m,n,k} \le I_{m,n,\max} \qquad \forall (m,n) \in \mathcal{G}, \quad k \in \mathcal{K}$$
$$I^{\mathrm{S}}_{m,n,s,\min} \le i^{\mathrm{S}}_{m,n,s,k} \le I^{\mathrm{S}}_{m,n,s,\max} \qquad \forall (m,n,s) \in \mathcal{S}, \quad k \in \mathcal{K}$$
$$P^{\mathrm{S}}_{m,n,s,k,\min} \le p^{\mathrm{S}}_{m,n,s,k} \le P^{\mathrm{S}}_{m,n,s,k,\max} \qquad \forall (m,n,s) \in \mathcal{S}, \quad k \in \mathcal{K}$$
$$E^{\mathrm{ESS}}_{m,n,s,\min} \le e^{\mathrm{S}}_{m,n,s,k} \le E^{\mathrm{ESS}}_{m,n,s,\max} \qquad \forall (m,n,s) \in \mathcal{B}, \quad k \in \mathcal{K}$$
$$p^{\mathrm{S,charge}}_{m,n,s,k} \ge 0 \qquad \forall (m,n,s) \in \mathcal{B}, \quad k \in \mathcal{K}$$
$$p^{\mathrm{S,discharge}}_{m,n,s,k} \le 0 \qquad \forall (m,n,s) \in \mathcal{B}, \quad k \in \mathcal{K}$$

C.2. EXAMPLES INPUTS AND OUTPUTS

Inputs	Branch current[A]			Conductance [Ω^{-1}]		
	$I_{4,5,max}$	$I_{5,6,max}$	$I_{6,7,max}$	$G_{4,5}$	$G_{5,6}$	$G_{6,7}$
Case 8.1	Inf	Inf	Inf	0.50	0.50	0.50
Case 8.2	Inf	Inf	Inf	0.50	0.50	0.50
Case 8.3	Inf	Inf	Inf	0.50	0.50	0.50
Case 9.1	Inf	Inf	Inf	0.50	0.50	0.50
Case 9.2	Inf	Inf	Inf	0.50	0.50	0.50
Case 10	1.5	Inf	Inf	0.50	0.50	0.50
	$I_{0,1,max}$	$I_{1,2,max}$	$I_{2,3,max}$	$G_{0,1}$	$G_{1,2}$	$G_{2,3}$
Case 8.1	Inf	Inf	Inf	0.50	0.50	0.50
Case 8.2	Inf	Inf	Inf	0.50	0.50	0.50
Case 8.3	Inf	Inf	Inf	0.50	0.50	0.50
Case 9.1	Inf	Inf	Inf	0.50	0.50	0.50
Case 9.2	Inf	Inf	Inf	0.50	0.50	0.50
Case 10	1.5	Inf	Inf	0.50	0.50	0.50
	$I_{8,9,max}$	$I_{9,10,max}$	$I_{10,11,max}$	$G_{8,9}$	$G_{9,10}$	$G_{10,11}$
Case 8.1	Inf	Inf	Inf	0.50	0.50	0.50
Case 8.2	Inf	Inf	Inf	0.50	0.50	0.50
Case 8.3	Inf	Inf	Inf	0.50	0.50	0.50
Case 9.1	Inf	Inf	Inf	0.50	0.50	0.50
Case 9.2	Inf	Inf	Inf	0.50	0.50	0.50
Case 10	1.5	Inf	Inf	0.50	0.50	0.50

Table C.1: Case 8.1-10: Lines' conductances and respective current limits set to either infinity or a specific value to force congestions

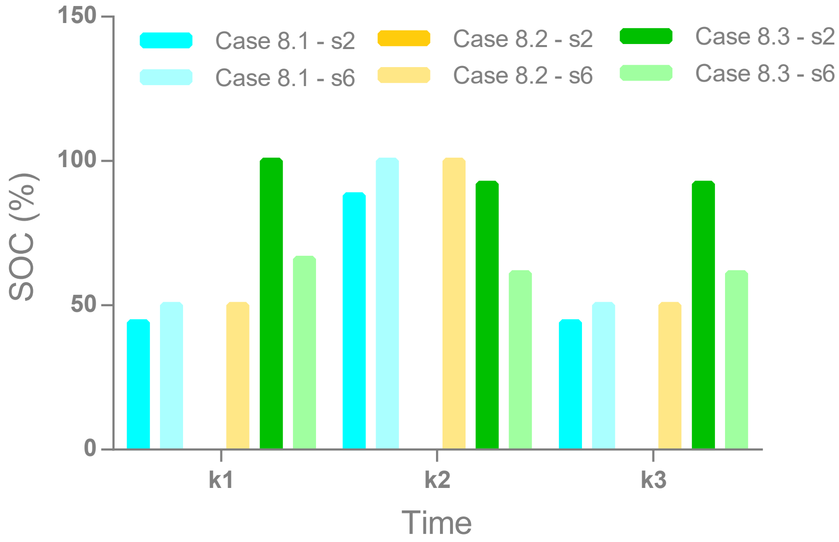

Figure C.1: Case 8.1, 8.2 and 8.3: State of charge of the storage unit.

Outputs		Generation Units[W]				Generation Units [A]			
		$p^S_{4,0,0,k}$	$p^S_{5,1,1,k}$	$p^S_{6,2,2,k}$	$p^S_{7,3,3,k}$	$i^S_{4,0,0,k}$	$i^S_{5,1,1,k}$	$i^S_{6,2,2,k}$	$i^S_{7,3,3,k}$
Case 8.1	k0	-538.22	0.00	278.27	250.00	-1.50	0.00	0.79	0.71
	k1	-538.22	0.00	278.27	250.00	-1.50	0.00	0.79	0.71
	k2	0.00	0.00	-251.14	250.00	0.00	0.00	-0.74	0.74
	k3	0.00	0.00	-251.14	250.00	0.00	0.00	-0.74	0.74
Case 8.2	k0	-250.74	0.00	0.00	250.00	-0.70	0.00	0.00	0.70
	k1	-250.74	0.00	0.00	250.00	-0.70	0.00	0.00	0.70
	k2	0.00	-252.92	0.00	250.00	0.00	-0.70	0.00	0.70
	k3	0.00	-252.92	0.00	250.00	0.00	-0.70	0.00	0.70
Case 8.3	k0	-633.96	0.00	617.11	0.00	-1.76	0.00	1.76	0.00
	k1	-200.00	0.00	-52.47	250.00	-0.58	0.00	-0.15	0.74
	k2	0.00	0.00	0.00	0.00	0.00	0.00	0.00	0.00
	k3	0.00	0.00	-504.48	500.00	0.00	0.00	-1.47	1.47
		$p^S_{0,8,4,k}$	$p^S_{1,9,5,k}$	$p^S_{2,10,6,k}$	$p^S_{3,11,7,k}$	$i^S_{0,8,4,k}$	$i^S_{1,9,5,k}$	$i^S_{2,10,6,k}$	$i^S_{3,11,7,k}$
Case 8.1	k0	-537.96	0.00	278.03	250.00	-1.49	0.00	0.79	0.71
	k1	-537.96	0.00	278.03	250.00	-1.49	0.00	0.79	0.71
	k2	0.00	0.00	-250.92	250.00	0.00	0.00	-0.70	0.71
	k3	0.00	0.00	-250.92	250.00	0.00	0.00	-0.70	0.71
Case 8.2	k0	-527.29	0.00	263.15	250.00	-1.46	0.00	0.75	0.72
	k1	-527.29	0.00	263.16	250.00	-1.46	0.00	0.75	0.72
	k2	0.00	-13.41	-237.50	250.00	0.00	-0.04	-0.66	0.69
	k3	0.00	-13.41	-237.50	250.00	0.00	-0.04	-0.66	0.69
Case 8.3	k0	-406.87	0.00	404.61	0.00	-1.13	0.00	1.13	0.00
	k1	-200.00	-24.51	-27.85	250.00	-0.56	-0.07	-0.08	0.70
	k2	0.00	0.00	0.00	0.00	0.00	0.00	0.00	0.00
	k3	0.00	-167.33	-337.31	500.00	0.00	-0.46	-0.94	1.41

Table C.2: Case 8.1, 8.2 & 8.3: Outputs of simulations with generation level of each source in terms of power and current.

Outputs		Generation Units[W]				Generation Units [A]			
		$p^S_{4,0,0,k}$	$p^S_{4,0,1,k}$	$p^S_{5,1,2,k}$	$p^S_{5,1,3,k}$	$p^S_{6,2,4,k}$	$p^S_{6,2,5,k}$	$p^S_{7,3,6,k}$	$p^S_{7,3,7,k}$
Case 9.1	k0	-868.40	0.00	50.00	29.26	100.00	136.29	250.00	277.44
	k1	-868.84	0.00	50.00	29.18	100.00	137.68	250.00	276.56
	k2	0.00	0.00	50.00	-26.35	100.00	-123.68	250.00	-249.97
	k3	0.00	0.00	50.00	-26.40	100.00	-123.58	250.00	-250.02
Case 9.2	k0	-873.90	0.00	50.00	0.00	100.00	0.00	250.00	443.64
	k1	-873.90	0.00	50.00	0.00	100.00	0.00	250.00	443.64
	k2	0.00	0.00	50.00	0.00	100.00	0.00	250.00	-400.39
	k3	0.00	0.00	50.00	0.00	100.00	0.00	250.00	-400.39
		$p^S_{0,8,8,k}$	$p^S_{0,8,9,k}$	$p^S_{1,9,10,k}$	$p^S_{1,9,11,k}$	$p^S_{2,10,12,k}$	$p^S_{2,10,13,k}$	$p^S_{3,11,14,k}$	$p^S_{3,11,15,k}$
Case 9.1	k0	-870.15	0.00	50.00	0.00	100.00	165.66	250.00	277.40
	k1	-870.59	0.00	50.00	0.00	100.00	165.89	250.00	276.60
	k2	0.00	0.00	50.00	0.00	100.00	-150.07	250.00	-249.99
	k3	0.00	0.00	50.00	0.00	100.00	-150.06	250.00	-250.00
Case 9.2	k0	-873.90	0.00	50.00	0.00	100.00	0.00	250.00	443.64
	k1	-873.90	0.00	50.00	0.00	100.00	0.00	250.00	443.64
	k2	0.00	0.00	50.00	0.00	100.00	0.00	250.00	-400.39
	k3	0.00	0.00	50.50	0.00	100.00	0.00	250.00	-400.39

Table C.3: Case 9.1, 9.2 & 9.3: Outputs of simulations with generation level of each source in terms of power and current.

Outputs		Generation Units[W]							
		$p^S_{4,0,0,k}$	$p^S_{4,0,1,k}$	$p^S_{5,1,2,k}$	$p^S_{5,1,3,k}$	$p^S_{6,2,4,k}$	$p^S_{6,2,5,k}$	$p^S_{7,3,6,k}$	$p^S_{7,3,7,k}$
Case 10	k0	-398.98	0.00	50.00	0.00	50.00	0.00	50.00	239.36
	k1	-398.98	0.00	50.00	0.00	50.00	0.00	50.00	239.37
	k2	-540.00	0.00	200.00	0.00	200.00	0.00	200.00	-66.55
	k3	-540.00	0.00	300.00	0.00	300.00	0.00	300.00	-365.51
		$p^S_{0,8,8,k}$	–	$p^S_{1,9,9,k}$	–	$p^S_{2,10,10,k}$	–	$p^S_{3,11,10,k}$	–
Case 10	k0	-149.42	–	50.00	–	50.00	–	50.00	–
	k1	-149.42	–	50.00	–	50.00	–	50.00	–
	k2	-540.00	–	200.00	–	200.00	–	133.45	–
	k3	-540.00	–	300.00	–	234.63	–	0.00	–

Table C.4: Case 10: Outputs of simulations with generation level of each source in terms of power and current.

D

Supplementary Information for Chapter 6

Figure D.1: Satellite imagery of Godiba's microgrid. Houses are represented in red, the PV plant in blue, the agricultural site in green, the health center in black, the shop in yellow and the school in purple.

House 1			House 2			House 3		
Load	Index	Connection	Load	Index	Connection	Load	Index	Connection
Light	s6	$\mathcal{N}_+ / \mathcal{N}_N$	Light	s11	$\mathcal{N}_+ / \mathcal{N}_N$	Light	s16	$\mathcal{N}_N / \mathcal{N}_-$
Radio	s7	$\mathcal{N}_+ / \mathcal{N}_N$	Radio	s12	$\mathcal{N}_+ / \mathcal{N}_N$	Radio	s17	$\mathcal{N}_N / \mathcal{N}_-$
Fan	s8	$\mathcal{N}_N / \mathcal{N}_-$	Fan	s13	$\mathcal{N}_+ / \mathcal{N}_N$	Fan	s18	$\mathcal{N}_N / \mathcal{N}_-$
Light	s9	$\mathcal{N}_N / \mathcal{N}_-$	Light	s14	$\mathcal{N}_N / \mathcal{N}_-$	Light	s19	$\mathcal{N}_+ / \mathcal{N}_N$
Phone	s10	$\mathcal{N}_N / \mathcal{N}_-$	Phone	s15	$\mathcal{N}_N / \mathcal{N}_-$	Phone	s20	$\mathcal{N}_+ / \mathcal{N}_N$

House 4			House 5			House 6		
Load	Index	Connection	Load	Index	Connection	Load	Index	Connection
Light	s30	$\mathcal{N}_+ / \mathcal{N}_N$	Light	s35	$\mathcal{N}_+ / \mathcal{N}_N$	Light	s40	$\mathcal{N}_+ / \mathcal{N}_N$
Radio	s31	$\mathcal{N}_+ / \mathcal{N}_N$	Radio	s36	$\mathcal{N}_+ / \mathcal{N}_N$	Radio	s41	$\mathcal{N}_+ / \mathcal{N}_N$
Fan	s32	$\mathcal{N}_N / \mathcal{N}_-$	Fan	s37	$\mathcal{N}_N / \mathcal{N}_-$	Fan	s42	$\mathcal{N}_+ / \mathcal{N}_N$
Light	s33	$\mathcal{N}_N / \mathcal{N}_-$	Light	s38	$\mathcal{N}_N / \mathcal{N}_-$	Light	s43	$\mathcal{N}_+ / \mathcal{N}_N$
Phone	s34	$\mathcal{N}_N / \mathcal{N}_-$	Phone	s39	$\mathcal{N}_N / \mathcal{N}_-$	Phone	s44	$\mathcal{N}_N / \mathcal{N}_-$

House 7			House 8			House 9		
Load	Index	Connection	Load	Index	Connection	Load	Index	Connection
Light	s45	$\mathcal{N}_+ / \mathcal{N}_N$	Light	s50	$\mathcal{N}_+ / \mathcal{N}_N$	Light	s60	$\mathcal{N}_+ / \mathcal{N}_N$
Radio	s45	$\mathcal{N}_+ / \mathcal{N}_N$	Radio	s51	$\mathcal{N}_+ / \mathcal{N}_N$	Radio	s61	$\mathcal{N}_N / \mathcal{N}_-$
Fan	s47	$\mathcal{N}_N / \mathcal{N}_-$	Fan	s52	$\mathcal{N}_+ / \mathcal{N}_N$	Fan	s62	$\mathcal{N}_N / \mathcal{N}_-$
Light	s48	$\mathcal{N}_N / \mathcal{N}_-$	Light	s53	$\mathcal{N}_N / \mathcal{N}_-$	Light	s63	$\mathcal{N}_N / \mathcal{N}_-$
Phone	s49	$\mathcal{N}_N / \mathcal{N}_-$	Phone	s54	$\mathcal{N}_N / \mathcal{N}_-$	Phone	s64	$\mathcal{N}_N / \mathcal{N}_-$

House 10			–
Load	Index	Connection	
Light	s65	$\mathcal{N}_+ / \mathcal{N}_N$	
Radio	s66	$\mathcal{N}_+ / \mathcal{N}_N$	
Fan	s67	$\mathcal{N}_+ / \mathcal{N}_N$	
Light	s68	$\mathcal{N}_N / \mathcal{N}_-$	
Phone	s69	$\mathcal{N}_N / \mathcal{N}_-$	

Table D.1: Sources with corresponding indexes and connection for each house. The demand is the same in all case studies.

PV Plant			Agriculture			Shop		
Load	Index	Connection	Load	Index	Connection	Load	Index	Connection
PV Panels	s0	$\mathcal{N}_+/\mathcal{N}_-$	Irrigation Pump	s3	$\mathcal{N}_+/\mathcal{N}_-$	Light	s21	$\mathcal{N}_+/\mathcal{N}_N$
ESS	s1	$\mathcal{N}_+/\mathcal{N}_-$	Water Pump	s4	$\mathcal{N}_+/\mathcal{N}_-$	Fan	s22	$\mathcal{N}_+/\mathcal{N}_N$
Generator	s2	$\mathcal{N}_+/\mathcal{N}_-$	Generator	s4	$\mathcal{N}_+/\mathcal{N}_-$	Fridge	s23	$\mathcal{N}_N/\mathcal{N}_-$
–	–	–	–	–	–	Light	s24	$\mathcal{N}_+/\mathcal{N}_N$

School			Health Center		
Load	Index	Connection	Load	Index	Connection
Computer	s25	$\mathcal{N}_+/\mathcal{N}_N$	Light	s55	$\mathcal{N}_+/\mathcal{N}_N$
Fan	s26	$\mathcal{N}_+/\mathcal{N}_N$	Fridge	s56	$\mathcal{N}_+/\mathcal{N}_N$
Light	s27	$\mathcal{N}_N/\mathcal{N}_-$	Water Pump	s57	$\mathcal{N}_N/\mathcal{N}_-$
Fan	s28	$\mathcal{N}_N/\mathcal{N}_-$	Light	s58	$\mathcal{N}_N/\mathcal{N}_-$
PV Panel	s29	$\mathcal{N}_N/\mathcal{N}_-$	PV Panel	s59	$\mathcal{N}_+/\mathcal{N}_N$

Table D.2: Case 1 and 3: Sources with corresponding indexes and connection for each house.

PV Plant			Agriculture			Shop		
Load	Index	Connection	Load	Index	Connection	Load	Index	Connection
PV Panels	s0	$\mathcal{N}_+/\mathcal{N}_-$	Irrigation Pump	s3	$\mathcal{N}_+/\mathcal{N}_-$	Light	s21	$\mathcal{N}_+/\mathcal{N}_N$
Generator	s2	$\mathcal{N}_+/\mathcal{N}_-$	Water Pump	s4	$\mathcal{N}_+/\mathcal{N}_-$	Fan	s22	$\mathcal{N}_+/\mathcal{N}_N$
ESS	s70	$\mathcal{N}_+/\mathcal{N}_N$	Generator	s4	$\mathcal{N}_+/\mathcal{N}_-$	Fridge	s23	$\mathcal{N}_N/\mathcal{N}_-$
ESS	s71	$\mathcal{N}_N/\mathcal{N}_-$	–	–	–	Light	s24	$\mathcal{N}_+/\mathcal{N}_N$

School			Health Center		
Load	Index	Connection	Load	Index	Connection
Computer	s25	$\mathcal{N}_+/\mathcal{N}_N$	Light	s55	$\mathcal{N}_+/\mathcal{N}_N$
Fan	s26	$\mathcal{N}_+/\mathcal{N}_N$	Fridge	s56	$\mathcal{N}_+/\mathcal{N}_N$
Light	s27	$\mathcal{N}_N/\mathcal{N}_-$	Water Pump	s57	$\mathcal{N}_N/\mathcal{N}_-$
Fan	s28	$\mathcal{N}_N/\mathcal{N}_-$	Light	s58	$\mathcal{N}_N/\mathcal{N}_-$
PV Panel	s29	$\mathcal{N}_N/\mathcal{N}_-$	PV Panel	s59	$\mathcal{N}_+/\mathcal{N}_N$

Table D.3: Case 2: Sources with corresponding indexes and connection for each house.

Installation	Load Type	Power [W]	Hrs/Day	No. in use	$\pi^{S}_{m,n,s}$ [$/Wh]	Watt-hrs/Day
Domestic	Low-energy light	20	6	2	0.75	240
	Radio	10	3	1	0.25	30
	Fan	30	4	1	0.50	120
	Phone charging	5	3	1	0.50	15
	Total	10 houses				**4,050**
Shop	Low-energy light	20	6	2	0.75	240
	Fan	30	8	1	0.50	240
	Fridge	600	24	1	2.00	14,400
	Total	1 shop				**14,880**
Agriculture	Water pump	750 / 8000	5 / 3	1	2.00	3,750 / 24,000
	Irrigation pump	1500 / 8000	3 / 3	1	2.00	4,500 / 24,000
	Total	1 site				**8,250 / 48,000**
School	Low-energy light	20	4	2	0.75	160
	Fan	30	4	2	0.50	240
	Computer	300	4	1	0.75	1,200
	Total	1 school				**1,600**
Health center	Low-energy light	20	4	4	0.75	320
	Fridge	600	24	1	2.00	14,400
	Water pump	3000 / 0	3 / 0	1	2.00	9,000 / 0
	Total	1 center				**23,720 / 14,720**

Table D.4: Estimated electricity demand for all case studies [8].

Purpose	Generator Type	No. in use	$\eta^{S}_{m,n,s}$	Capacity [W]	$\pi^{S}_{m,n,s}$ [$/Wh]	Capacity [Wh]	$\eta^{ESS}_{m,n,s}$
PV Plant	PV	100	0.15	$Irr \cdot 0.15 \cdot 100$	0.00	–	–
	Diesel Generator	1	–	20,000	1.00	–	–
	ESS	–	–	–	–	14,000	0.95
Agriculture	Diesel Generator	1	–	4,000	1.00	–	–
School	PV	2	0.15	$Irr \cdot 0.15 \cdot 2$	0.00	–	–
Health Center	PV	2	0.15	$Irr \cdot 0.15 \cdot 2$	0.00	–	–

Table D.5: Case Study 1: Microgrid's generators with parameters and marginal cost of operation

Connection	Sources	LMP [$/Wh]																
		k0	k1	k2	k3	k4	k5	k6	k7	k8	k9	k10	k11	k12	k13	k14	k15	k16
$\mathcal{N}_+ / \mathcal{N}_-$	$\lambda^{\text{P}}_{27,54}$	1.000	1.000	1.000	1.000	1.000	1.000	1.000	1.000	0	0	0	0	0.006	0.008	0.011	0.002	0.002
	$\lambda^{\text{P}}_{44,71}$	1.000	1.000	1.000	1.000	1.000	1.000	1.000	0.999	0	0	0	0	0.000	0.000	0.000	0.000	0.000
$\mathcal{N}_+ / \mathcal{N}_N$	$\lambda^{\text{P}}_{2,56}$	0.997	0.997	0.997	0.997	0.997	0.997	0.997	1.008	0	0	0	0	1.993	1.991	1.988	-0.519	-0.520
	$\lambda^{\text{P}}_{4,58}$	0.998	0.998	0.998	0.998	0.998	0.998	0.998	1.009	0	0	0	0	1.996	1.995	1.994	-0.521	-0.521
	$\lambda^{\text{P}}_{7,61}$	0.999	0.999	0.999	0.999	0.999	0.999	0.999	1.009	0	0	0	0	1.998	1.998	1.997	-0.521	-0.522
	$\lambda^{\text{P}}_{10,64}$	1.000	1.000	1.000	1.000	1.000	1.000	1.000	1.010	0	0	0	0	2.000	2.000	1.999	-0.522	-0.522
	$\lambda^{\text{P}}_{11,65}$	0.998	0.998	0.998	0.998	0.998	0.998	0.998	1.008	0	0	0	0	1.995	1.994	1.993	-0.521	-0.521
	$\lambda^{\text{P}}_{13,67}$	0.998	0.998	0.998	0.998	0.998	0.998	0.998	1.008	0	0	0	0	1.994	1.993	1.990	-0.520	-0.521
	$\lambda^{\text{P}}_{14,68}$	0.997	0.997	0.997	0.997	0.997	0.997	0.997	1.007	0	0	0	0	1.992	1.990	1.987	-0.519	-0.520
	$\lambda^{\text{P}}_{19,73}$	0.997	0.997	0.997	0.997	0.997	0.997	0.997	1.008	0	0	0	0	1.993	1.992	1.989	-0.520	-0.520
	$\lambda^{\text{P}}_{20,74}$	0.997	0.997	0.997	0.997	0.997	0.997	0.997	1.008	0	0	0	0	1.993	1.992	1.989	-0.520	-0.520
	$\lambda^{\text{P}}_{21,75}$	0.997	0.997	0.997	0.997	0.997	0.997	0.997	1.008	0	0	0	0	1.995	1.995	1.992	-0.520	-0.521
	$\lambda^{\text{P}}_{23,77}$	0.997	0.997	0.997	0.997	0.997	0.997	0.997	1.008	0	0	0	0	2.000	2.000	2.000	-0.521	-0.521
	$\lambda^{\text{P}}_{24,78}$	0.998	0.998	0.998	0.998	0.998	0.998	0.998	1.008	0	0	0	0	1.998	1.997	1.996	-0.521	-0.521
	$\lambda^{\text{P}}_{26,80}$	0.998	0.998	0.998	0.998	0.998	0.998	0.998	1.008	0	0	0	0	1.998	1.998	1.997	-0.521	-0.521
$\mathcal{N}_N / \mathcal{N}_-$	$\lambda^{\text{P}}_{29,2}$	1.008	1.008	1.008	1.008	1.008	1.008	1.008	0.996	0	0	0	0	-2.086	-2.081	-2.056	0.499	0.499
	$\lambda^{\text{P}}_{31,4}$	1.008	1.008	1.008	1.008	1.008	1.008	1.008	0.997	0	0	0	0	-2.090	-2.085	-2.061	0.499	0.500
	$\lambda^{\text{P}}_{34,7}$	1.009	1.009	1.009	1.009	1.009	1.009	1.009	0.997	0	0	0	0	-2.092	-2.088	-2.065	0.500	0.500
	$\lambda^{\text{P}}_{37,10}$	1.008	1.008	1.008	1.008	1.008	1.008	1.008	0.997	0	0	0	0	-2.092	-2.088	-2.064	0.500	0.500
	$\lambda^{\text{P}}_{38,11}$	1.009	1.009	1.009	1.009	1.009	1.009	1.009	0.997	0	0	0	0	-2.091	-2.087	-2.064	0.500	0.501
	$\lambda^{\text{P}}_{40,13}$	1.008	1.008	1.008	1.008	1.008	1.008	1.008	0.997	0	0	0	0	-2.089	-2.084	-2.059	0.499	0.500
	$\lambda^{\text{P}}_{41,14}$	1.008	1.008	1.008	1.008	1.008	1.008	1.008	0.997	0	0	0	0	-2.087	-2.082	-2.057	0.499	0.499
	$\lambda^{\text{P}}_{46,19}$	1.009	1.009	1.009	1.009	1.009	1.009	1.009	0.997	0	0	0	0	-2.089	-2.085	-2.060	0.499	0.500
	$\lambda^{\text{P}}_{47,20}$	1.009	1.009	1.009	1.009	1.009	1.009	1.009	0.997	0	0	0	0	-2.089	-2.084	-2.060	0.499	0.500
	$\lambda^{\text{P}}_{48,21}$	1.009	1.009	1.009	1.009	1.009	1.009	1.009	0.998	0	0	0	0	-2.092	-2.087	-2.062	0.499	0.500
	$\lambda^{\text{P}}_{50,23}$	1.011	1.011	1.011	1.011	1.011	1.011	1.011	0.999	0	0	0	0	-2.096	-2.092	-2.068	0.500	0.501
	$\lambda^{\text{P}}_{51,24}$	1.010	1.010	1.010	1.010	1.010	1.010	1.010	0.998	0	0	0	0	-2.094	-2.089	-2.065	0.500	0.501
	$\lambda^{\text{P}}_{53,26}$	1.009	1.009	1.009	1.009	1.009	1.009	1.009	0.998	0	0	0	0	-2.093	-2.089	-2.065	0.500	0.501

Table D.6: Case Study 1: LMP from $k0$ to $k16$ with respect to sources' connection types for a DC microgrid without optimal placement and sizing of ESS.

Connection	Sources	LMP [$/Wh]																
		k17	k18	k19	k20	k21	k22	k23	k24	k25	k26	k27	k28	k29	k30	k31	k32	k33
$\mathcal{N}_+ / \mathcal{N}_-$	$\lambda^{\mathrm{P}}_{27,54}$	0.001	0.750	1.000	1.000	1.000	1.000	1.000	1.000	1.000	1.000	1.000	1.000	1.000	1.000	1.000	0.000	0.000
	$\lambda^{\mathrm{P}}_{44,71}$	0.000	0.744	0.995	0.995	0.995	0.995	0.995	0.995	0.995	0.995	0.995	0.995	0.995	0.995	0.995	0.000	0.000
$\mathcal{N}_+ / \mathcal{N}_N$	$\lambda^{\mathrm{P}}_{2,56}$	-0.786	0.750	1.009	1.009	1.009	1.009	1.009	1.009	1.009	1.009	1.009	1.009	1.009	1.009	1.009	0.000	0.000
	$\lambda^{\mathrm{P}}_{4,58}$	-0.787	0.751	1.010	1.010	1.010	1.010	1.010	1.010	1.010	1.010	1.010	1.010	1.010	1.010	1.010	0.000	0.000
	$\lambda^{\mathrm{P}}_{7,61}$	-0.788	0.751	1.010	1.010	1.010	1.010	1.010	1.010	1.010	1.010	1.010	1.010	1.010	1.010	1.010	0.000	0.000
	$\lambda^{\mathrm{P}}_{10,64}$	-0.788	0.752	1.011	1.011	1.011	1.011	1.011	1.011	1.011	1.011	1.011	1.011	1.011	1.011	1.011	0.000	0.000
	$\lambda^{\mathrm{P}}_{11,65}$	-0.787	0.750	1.009	1.009	1.009	1.009	1.009	1.009	1.009	1.009	1.009	1.009	1.009	1.009	1.009	0.000	0.000
	$\lambda^{\mathrm{P}}_{13,67}$	-0.786	0.750	1.009	1.009	1.009	1.009	1.009	1.009	1.009	1.009	1.009	1.009	1.009	1.009	1.009	0.000	0.000
	$\lambda^{\mathrm{P}}_{14,68}$	-0.786	0.750	1.008	1.008	1.008	1.008	1.008	1.008	1.008	1.008	1.008	1.008	1.008	1.008	1.008	0.000	0.000
	$\lambda^{\mathrm{P}}_{19,73}$	-0.786	0.749	1.008	1.008	1.008	1.008	1.008	1.008	1.008	1.008	1.008	1.008	1.008	1.008	1.008	0.000	0.000
	$\lambda^{\mathrm{P}}_{20,74}$	-0.786	0.750	1.009	1.009	1.009	1.009	1.009	1.009	1.009	1.009	1.009	1.009	1.009	1.009	1.008	0.000	0.000
	$\lambda^{\mathrm{P}}_{21,75}$	-0.787	0.750	1.008	1.008	1.008	1.008	1.008	1.008	1.008	1.008	1.008	1.008	1.008	1.008	1.008	0.000	0.000
	$\lambda^{\mathrm{P}}_{23,77}$	-0.787	0.750	1.008	1.008	1.008	1.008	1.008	1.008	1.008	1.008	1.008	1.008	1.008	1.008	1.008	0.000	0.000
	$\lambda^{\mathrm{P}}_{24,78}$	-0.787	0.750	1.009	1.009	1.009	1.009	1.009	1.009	1.009	1.009	1.009	1.009	1.009	1.009	1.009	0.000	0.000
	$\lambda^{\mathrm{P}}_{26,80}$	-0.787	0.750	1.009	1.009	1.009	1.009	1.009	1.009	1.009	1.009	1.009	1.009	1.009	1.009	1.009	0.000	0.000
$\mathcal{N}_N / \mathcal{N}_-$	$\lambda^{\mathrm{P}}_{29,2}$	0.748	0.750	0.993	0.993	0.993	0.993	0.993	0.993	0.993	0.993	0.993	0.993	0.993	0.993	0.993	0.000	0.000
	$\lambda^{\mathrm{P}}_{31,4}$	0.749	0.750	0.993	0.993	0.993	0.993	0.993	0.993	0.993	0.993	0.993	0.993	0.993	0.993	0.993	0.000	0.000
	$\lambda^{\mathrm{P}}_{34,7}$	0.750	0.750	0.993	0.993	0.993	0.993	0.993	0.993	0.993	0.993	0.993	0.993	0.993	0.993	0.993	0.000	0.000
	$\lambda^{\mathrm{P}}_{37,10}$	0.750	0.750	0.993	0.993	0.993	0.993	0.993	0.993	0.993	0.993	0.993	0.993	0.993	0.993	0.993	0.000	0.000
	$\lambda^{\mathrm{P}}_{38,11}$	0.750	0.750	0.993	0.993	0.993	0.993	0.993	0.993	0.993	0.993	0.993	0.993	0.993	0.993	0.993	0.000	0.000
	$\lambda^{\mathrm{P}}_{40,13}$	0.749	0.750	0.993	0.993	0.993	0.993	0.993	0.993	0.993	0.993	0.993	0.993	0.993	0.993	0.993	0.000	0.000
	$\lambda^{\mathrm{P}}_{41,14}$	0.748	0.750	0.993	0.993	0.993	0.993	0.993	0.993	0.993	0.993	0.993	0.993	0.993	0.993	0.993	0.000	0.000
	$\lambda^{\mathrm{P}}_{46,19}$	0.749	0.750	0.993	0.993	0.993	0.993	0.993	0.993	0.993	0.993	0.993	0.993	0.993	0.993	0.993	0.000	0.000
	$\lambda^{\mathrm{P}}_{47,20}$	0.749	0.750	0.993	0.993	0.993	0.993	0.993	0.993	0.993	0.993	0.993	0.993	0.993	0.993	0.993	0.000	0.000
	$\lambda^{\mathrm{P}}_{48,21}$	0.750	0.750	0.994	0.994	0.994	0.994	0.994	0.994	0.994	0.994	0.994	0.994	0.994	0.994	0.994	0.000	0.000
	$\lambda^{\mathrm{P}}_{50,23}$	0.751	0.752	0.995	0.995	0.995	0.995	0.995	0.995	0.995	0.995	0.995	0.995	0.995	0.995	0.995	0.000	0.000
	$\lambda^{\mathrm{P}}_{51,24}$	0.750	0.751	0.994	0.994	0.994	0.994	0.994	0.994	0.994	0.994	0.994	0.994	0.994	0.994	0.994	0.000	0.000
	$\lambda^{\mathrm{P}}_{53,26}$	0.750	0.751	0.994	0.994	0.994	0.994	0.994	0.994	0.994	0.994	0.994	0.994	0.994	0.994	0.994	0.000	0.000

Table D.7: Case Study 1: LMP from $k17$ to $k33$ with respect to sources' connection types for a DC microgrid without optimal placement and sizing of ESS.

Connection	Sources	LMP [\$/Wh]														
		k34	k35	k36	k37	k38	k39	k40	k41	k42	k43	k44	k45	k46	k47	k48
$\mathcal{N}_+ / \mathcal{N}_-$	$\lambda^{\mathrm{P}}_{27,54}$	2.000	2.000	2.000	0.000	0.000	0.001	0.001	0.001	0.000	0.001	0.000	0.001	0.000	0.000	0.000
	$\lambda^{\mathrm{P}}_{44,71}$	0.000	0.000	0.000	0.000	0.000	0.000	0.000	0.000	0.000	0.000	0.000	0.000	0.000	0.000	0.000
$\mathcal{N}_+ / \mathcal{N}_N$	$\lambda^{\mathrm{P}}_{2,56}$	2.003	2.003	2.003	0.000	0.000	-0.522	-0.522	-0.786	0.000	-0.262	0.000	-0.261	0.000	0.000	0.000
	$\lambda^{\mathrm{P}}_{4,58}$	2.000	2.000	2.000	0.000	0.000	-0.523	-0.523	-0.787	0.000	-0.262	0.000	-0.262	0.000	0.000	0.000
	$\lambda^{\mathrm{P}}_{7,61}$	1.996	1.996	1.996	0.000	0.000	-0.524	-0.524	-0.788	0.000	-0.262	0.000	-0.262	0.000	0.000	0.000
	$\lambda^{\mathrm{P}}_{10,64}$	2.000	2.000	2.000	0.000	0.000	-0.524	-0.524	-0.788	0.000	-0.263	0.000	-0.262	0.000	0.000	0.000
	$\lambda^{\mathrm{P}}_{11,65}$	1.994	1.994	1.994	0.000	0.000	-0.523	-0.523	-0.787	0.000	-0.262	0.000	-0.262	0.000	0.000	0.000
	$\lambda^{\mathrm{P}}_{13,67}$	1.997	1.997	1.997	0.000	0.000	-0.523	-0.523	-0.786	0.000	-0.262	0.000	-0.261	0.000	0.000	0.000
	$\lambda^{\mathrm{P}}_{14,68}$	1.995	1.995	1.995	0.000	0.000	-0.523	-0.523	-0.786	0.000	-0.262	0.000	-0.261	0.000	0.000	0.000
	$\lambda^{\mathrm{P}}_{19,73}$	1.990	1.990	1.990	0.000	0.000	-0.523	-0.523	-0.786	0.000	-0.262	0.000	-0.261	0.000	0.000	0.000
	$\lambda^{\mathrm{P}}_{20,74}$	1.992	1.992	1.992	0.000	0.000	-0.523	-0.523	-0.786	0.000	-0.262	0.000	-0.261	0.000	0.000	0.000
	$\lambda^{\mathrm{P}}_{21,75}$	1.989	1.989	1.990	0.000	0.000	-0.523	-0.523	-0.787	0.000	-0.262	0.000	-0.261	0.000	0.000	0.000
	$\lambda^{\mathrm{P}}_{23,77}$	1.993	1.993	1.993	0.000	0.000	-0.523	-0.524	-0.787	0.000	-0.262	0.000	-0.262	0.000	0.000	0.000
	$\lambda^{\mathrm{P}}_{24,78}$	1.993	1.993	1.993	0.000	0.000	-0.523	-0.524	-0.787	0.000	-0.262	0.000	-0.262	0.000	0.000	0.000
	$\lambda^{\mathrm{P}}_{26,80}$	1.995	1.995	1.995	0.000	0.000	-0.524	-0.524	-0.787	0.000	-0.262	0.000	-0.262	0.000	0.000	0.000
$\mathcal{N}_N / \mathcal{N}_-$	$\lambda^{\mathrm{P}}_{29,2}$	1.920	1.919	1.918	0.000	0.000	0.498	0.498	0.748	0.000	0.250	0.000	0.249	0.000	0.000	0.000
	$\lambda^{\mathrm{P}}_{31,4}$	1.915	1.913	1.912	0.000	0.000	0.499	0.499	0.749	0.000	0.250	0.000	0.250	0.000	0.000	0.000
	$\lambda^{\mathrm{P}}_{34,7}$	1.913	1.911	1.910	0.000	0.000	0.500	0.500	0.750	0.000	0.251	0.000	0.250	0.000	0.000	0.000
	$\lambda^{\mathrm{P}}_{37,10}$	1.912	1.910	1.909	0.000	0.000	0.500	0.500	0.750	0.000	0.250	0.000	0.250	0.000	0.000	0.000
	$\lambda^{\mathrm{P}}_{38,11}$	1.913	1.912	1.911	0.000	0.000	0.500	0.500	0.750	0.000	0.250	0.000	0.250	0.000	0.000	0.000
	$\lambda^{\mathrm{P}}_{40,13}$	1.915	1.913	1.912	0.000	0.000	0.499	0.499	0.749	0.000	0.250	0.000	0.250	0.000	0.000	0.000
	$\lambda^{\mathrm{P}}_{41,14}$	1.913	1.912	1.911	0.000	0.000	0.499	0.499	0.748	0.000	0.250	0.000	0.249	0.000	0.000	0.000
	$\lambda^{\mathrm{P}}_{46,19}$	1.909	1.907	1.906	0.000	0.000	0.499	0.499	0.749	0.000	0.250	0.000	0.250	0.000	0.000	0.000
	$\lambda^{\mathrm{P}}_{47,20}$	1.911	1.909	1.908	0.000	0.000	0.499	0.499	0.749	0.000	0.250	0.000	0.250	0.000	0.000	0.000
	$\lambda^{\mathrm{P}}_{48,21}$	1.909	1.907	1.906	0.000	0.000	0.500	0.500	0.750	0.000	0.250	0.000	0.250	0.000	0.000	0.000
	$\lambda^{\mathrm{P}}_{50,23}$	1.914	1.912	1.911	0.000	0.000	0.500	0.501	0.751	0.000	0.251	0.000	0.251	0.000	0.000	0.000
	$\lambda^{\mathrm{P}}_{51,24}$	1.912	1.910	1.909	0.000	0.000	0.500	0.500	0.750	0.000	0.251	0.000	0.250	0.000	0.000	0.000
	$\lambda^{\mathrm{P}}_{53,26}$	1.913	1.911	1.910	0.000	0.000	0.500	0.500	0.750	0.000	0.251	0.000	0.250	0.000	0.000	0.000

Table D.8: Case Study 1: LMP from $k34$ to $k48$ with respect to sources' connection types for a DC microgrid without optimal placement and sizing of ESS.

Location	Load	Sources	$p^S_{m,n,s,k}$ [\$/Wh]										
			k0	k1	k2	k3	k4	k5	k6	k7	k8	k9	k10
PV Plant	PV Panel	$p^S_{44,71,0}$	–	–	–	–	–	–	–	-625.00	-3050.00	-965.78	-8837.50
	ESS	$p^S_{44,71,1}$	–	–	–	–	–	–	–		1967.43	–	7231.98
	Generator	$p^S_{44,71,2}$	-497.91	-497.91	-497.91	-497.91	-497.91	-497.91	-497.91	–	–	–	–
Agriculture	Irr. Pump	$p^S_{27,54,3}$	–	–	–	–	–	–	–	–	–	–	–
	Pump	$p^S_{27,54,4}$	–	–	–	–	–	–	–	–	–	–	750.00
	Diesel	$p^S_{27,54,5}$	-705.35	-705.35	-705.35	-705.35	-705.35	-705.35	-705.35	-553.24	–	–	–
House 1	Light	$p^S_{29,2,6}$	–	–	–	–	–	–	–	–	–	–	–
	Radio	$p^S_{29,2,7}$	–	–	–	–	–	–	–	–	–	–	–
	Fan	$p^S_{2,56,8}$	–	–	–	–	–	–	–	–	–	–	–
	Light	$p^S_{2,56,9}$	–	–	–	–	–	–	–	–	–	–	–
	Phone	$p^S_{2,56,10}$	–	–	–	–	–	–	–	–	–	–	–
House 2	Light	$p^S_{31,4,11}$	–	–	–	–	–	–	–	–	–	–	–
	Radio	$p^S_{31,4,12}$	–	–	–	–	–	–	–	–	–	–	–
	Fan	$p^S_{31,4,13}$	–	–	–	–	–	–	–	–	–	–	–
	Light	$p^S_{4,58,14}$	–	–	–	–	–	–	–	–	–	–	–
	Phone	$p^S_{4,58,15}$	–	–	–	–	–	–	–	–	–	–	–
House 3	Light	$p^S_{7,61,16}$	–	–	–	–	–	–	–	–	–	–	–
	Radio	$p^S_{7,61,17}$	–	–	–	–	–	–	–	–	–	–	–
	Fan	$p^S_{7,61,18}$	–	–	–	–	–	–	–	–	–	–	–
	Light	$p^S_{34,7,19}$	–	–	–	–	–	–	–	–	–	–	–
	Phone	$p^S_{34,7,20}$	–	–	–	–	–	–	–	–	–	–	–
Shop	Light	$p^S_{37,10,21}$	–	–	–	–	–	–	–	–	–	–	–
	Fan	$p^S_{37,10,22}$	–	–	–	–	–	–	–	–	–	–	–
	Fridge	$p^S_{10,64,23}$	600.00	600.00	600.00	600.00	600.00	600.00	600.00	600.00	600.00	600.00	600.00
	Light	$p^S_{37,10,24}$	–	–	–	–	–	–	–	–	–	–	–
School	Comp	$p^S_{38,11,25}$	–	–	–	–	–	–	–	–	–	–	–
	Fan	$p^S_{38,11,26}$	–	–	–	–	–	–	–	–	–	–	–
	Light	$p^S_{11,65,27}$	–	–	–	–	–	–	–	–	–	–	–
	Fan	$p^S_{11,65,28}$	–	–	–	–	–	–	–	–	–	–	–
	PV	$p^S_{11,65,29}$	–	–	–	–	–	–	–	-12.50	-61.00	-119.00	-176.75
Hoouse 4	Light	$p^S_{40,13,30}$	–	–	–	–	–	–	–	–	–	–	–
	Radio	$p^S_{40,13,31}$	–	–	–	–	–	–	–	–	–	–	–
	Fan	$p^S_{13,67,32}$	–	–	–	–	–	–	–	–	–	–	–
	Light	$p^S_{13,67,33}$	–	–	–	–	–	–	–	–	–	–	–
	Phone	$p^S_{13,67,34}$	–	–	–	–	–	–	–	–	–	–	–

Table D.9: Case Study 1: Economic dispatch for a bipolar DC microgrid without optimal storage for sources $s0$-$s34$ from $k0$-$k10$.

Location	Load	Sources	$p^S_{m,n,s,k}$ [$/Wh]										
			k0	k1	k2	k3	k4	k5	k6	k7	k8	k9	k10
House 5	Light	$p^S_{41,14,35}$	–	–	–	–	–	–	–	–	–	–	–
	Radio	$p^S_{41,14,36}$	–	–	–	–	–	–	–	–	–	–	–
	Fan	$p^S_{14,68,37}$	–	–	–	–	–	–	–	–	–	–	–
	Light	$p^S_{14,68,38}$	–	–	–	–	–	–	–	–	–	–	–
	Phone	$p^S_{14,68,39}$	–	–	–	–	–	–	–	–	–	–	–
House 6	Light	$p^S_{46,19,40}$	–	–	–	–	–	–	–	–	–	–	–
	Radio	$p^S_{46,19,41}$	–	–	–	–	–	–	–	–	–	–	–
	Fan	$p^S_{46,19,42}$	–	–	–	–	–	–	–	–	–	–	–
	Light	$p^S_{46,19,43}$	–	–	–	–	–	–	–	–	–	–	–
	Phone	$p^S_{19,73,44}$	–	–	–	–	–	–	–	–	–	–	–
House 7	Light	$p^S_{47,20,45}$	–	–	–	–	–	–	–	–	–	–	–
	Radio	$p^S_{47,20,46}$	–	–	–	–	–	–	–	–	–	–	–
	Fan	$p^S_{20,74,47}$	–	–	–	–	–	–	–	–	–	–	–
	Light	$p^S_{20,74,48}$	–	–	–	–	–	–	–	–	–	–	–
	Phone	$p^S_{20,74,49}$	–	–	–	–	–	–	–	–	–	–	–
House 8	Light	$p^S_{48,21,50}$	–	–	–	–	–	–	–	–	–	–	–
	Radio	$p^S_{48,21,51}$	–	–	–	–	–	–	–	–	–	–	–
	Fan	$p^S_{48,21,52}$	–	–	–	–	–	–	–	–	–	–	–
	Light	$p^S_{21,75,53}$	–	–	–	–	–	–	–	–	–	–	–
	Phone	$p^S_{21,75,54}$	–	–	–	–	–	–	–	–	–	–	–
Health	Light	$p^S_{50,23,55}$	–	–	–	–	–	–	–	–	–	–	–
	Fridge	$p^S_{50,23,56}$	600.00	600.00	600.00	600.00	600.00	600.00	600.00	600.00	600.00	600.00	600.00
	Pump	$p^S_{23,77,57}$	–	–	–	–	–	–	–	–	–	–	–
	Light	$p^S_{23,77,58}$	–	–	–	–	–	–	–	–	–	–	–
	PV	$p^S_{50,23,59}$	–	–	–	–	–	–	–	-12.50	-61.00	-119.00	-176.75
House 9	Light	$p^S_{51,24,60}$	–	–	–	–	–	–	–	–	–	–	–
	Radio	$p^S_{24,78,61}$	–	–	–	–	–	–	–	–	–	–	–
	Fan	$p^S_{24,78,62}$	–	–	–	–	–	–	–	–	–	–	–
	Light	$p^S_{24,78,63}$	–	–	–	–	–	–	–	–	–	–	–
	Phone	$p^S_{24,78,64}$	–	–	–	–	–	–	–	–	–	–	–
House 10	Light	$p^S_{53,26,65}$	–	–	–	–	–	–	–	–	–	–	–
	Radio	$p^S_{53,26,66}$	–	–	–	–	–	–	–	–	–	–	–
	Fan	$p^S_{53,26,67}$	–	–	–	–	–	–	–	–	–	–	–
	Light	$p^S_{53,26,68}$	–	–	–	–	–	–	–	–	–	–	–
	Phone	$p^S_{26,80,69}$	–	–	–	–	–	–	–	–	–	–	–

Table D.10: Case Study 1: Economic dispatch for a bipolar DC microgrid without optimal storage for sources $s35$-$s69$ from $k0$-$k10$.

Location	Load	Sources	$p^{S}_{m,n,s,k}$ [\$/Wh]										
			k11	k12	k13	k14	k15	k16	k17	k18	k19	k20	k21
PV Plant	PV Panel	$p^{S}_{44,71,0}$	-3478.19	-2284.02	-2367.45	-4750.05	-3419.95	-3419.97	-4025.00	-1350.00	-37.50	–	
	ESS	$p^{S}_{44,71,1}$	1923.75	227.51	–	227.51	227.51	227.51	2703.65	–	-1046.38	-1084.51	-1084.51
	Generator	$p^{S}_{44,71,2}$	–	–	–	–	–	–	–	–	–	–	–
Agriculture	Irr. Pump	$p^{S}_{27,54,3}$	–	–	–	1500.00	1500.00	1500.00	–	–	–	–	–
	Pump	$p^{S}_{27,54,4}$	750.00	750.00	750.00	750.00	–	–	–	–	–	–	–
	Diesel	$p^{S}_{27,54,5}$	–	–	–	–	–	–	–	–	-119.43	-120.31	-120.31
House 1	Light	$p^{S}_{29,2,6}$	–	–	–	–	–	–	–	20.00	–	–	–
	Radio	$p^{S}_{29,2,7}$	–	–	–	–	–	–	–	–	–	–	–
	Fan	$p^{S}_{2,56,8}$	–	–	–	–	30.00	30.00	–	–	–	–	–
	Light	$p^{S}_{2,56,9}$	–	–	–	–	–	–	–	18.75	–	–	–
	Phone	$p^{S}_{2,56,10}$	–	–	–	–	–	–	–	–	–	–	–
House 2	Light	$p^{S}_{31,4,11}$	–	–	–	–	–	–	–	–	–	–	–
	Radio	$p^{S}_{31,4,12}$	–	–	–	–	–	–	–	–	–	–	–
	Fan	$p^{S}_{31,4,13}$	–	–	30.00	30.00	30.00	30.00	–	–	–	–	–
	Light	$p^{S}_{4,58,14}$	–	–	–	–	–	–	–	–	–	–	–
	Phone	$p^{S}_{4,58,15}$	–	–	–	–	–	–	–	–	–	–	–
House 3	Light	$p^{S}_{7,61,16}$	–	–	–	–	–	–	–	–	–	–	–
	Radio	$p^{S}_{7,61,17}$	–	–	–	–			–	–	–	–	–
	Fan	$p^{S}_{7,61,18}$	–	–	–	–	30.00	30.00	–	–	–	–	–
	Light	$p^{S}_{34,7,19}$	–	–	–	–	–	–	–	–	–	–	–
	Phone	$p^{S}_{34,7,20}$	–	–	–	–	–	–	–		–	–	–
Shop	Light	$p^{S}_{37,10,21}$	–	–	–	–	–	–	–	20.00	–	–	–
	Fan	$p^{S}_{37,10,22}$	30.00	30.00	30.00	30.00	30.00	–	–	–	–	–	–
	Fridge	$p^{S}_{10,64,23}$	600.00	445.19	523.98	600.00	600.00	600.00	600.00	600.00	600.00	600.00	600.00
	Light	$p^{S}_{37,10,24}$	–	–	–	–	–	–	–	20.00	–	–	–
School	Comp	$p^{S}_{38,11,25}$	–	–		300.00	300.00	300.00	155.25	–	–	–	–
	Fan	$p^{S}_{38,11,26}$	–	–	30.00	30.00	12.22	–	–	–	–	–	–
	Light	$p^{S}_{11,65,27}$	–	–	–	–	–	–	40.00	–	–	–	–
	Fan	$p^{S}_{11,65,28}$	–	–	–	–	30.00	30.00	–	–	–	–	–
	PV	$p^{S}_{11,65,29}$	-212.79	-253.50	-257.50	-235.25	–	–	–	-27.00	-0.75	–	–
Hoouse 4	Light	$p^{S}_{40,13,30}$	–	–	–	–	–	–	–	–	–	–	–
	Radio	$p^{S}_{40,13,31}$	–	–	–	–	–	–	–	–	–	–	–
	Fan	$p^{S}_{13,67,32}$	–	–	–	–	30.00	30.00	–	–	–	–	–
	Light	$p^{S}_{13,67,33}$	–	–	–	–	–	–	–	–	–	–	–
	Phone	$p^{S}_{13,67,34}$	–	–	–	–	–	–	–	–	–	–	–

Table D.11: Case Study 1: Economic dispatch for a bipolar DC microgrid without optimal storage for sources $s0$-$s34$ from $k11$-$k21$.

Location	Load	Sources	$p^S_{m,n,s,k}$ [$/Wh]										
			k11	k12	k13	k14	k15	k16	k17	k18	k19	k20	k21
	Light	$p^S_{41,14,35}$	–	–	–	–	–	–	–	20.00	–	–	–
	Radio	$p^S_{41,14,36}$	–	–	–	–	–	–	–	–	–	–	–
House 5	Fan	$p^S_{14,68,37}$	–	–	–	–	30.00	30.00	–	–	–	–	–
	Light	$p^S_{14,68,38}$	–	–	–	–	–	–	–	20.00	–	–	–
	Phone	$p^S_{14,68,39}$	–	–	–	–	–	–	–	–	–	–	–
	Light	$p^S_{46,19,40}$	–	–	–	–	–	–	–	10.83	–	–	–
	Radio	$p^S_{46,19,41}$	–	–	–	–	–	–	–	–	–	–	–
House 6	Fan	$p^S_{46,19,42}$	–	–	30.00	30.00	30.00	30.00	–	–	–	–	–
	Light	$p^S_{46,19,43}$	–	–	–	–	–	–	–	7.99	–	–	–
	Phone	$p^S_{19,73,44}$	–	–	–	–	–	–	–	–	–	–	–
	Light	$p^S_{47,20,45}$	–	–	–	–	–	–	–	–	–	–	–
	Radio	$p^S_{47,20,46}$	–	–	–	–	–	–	–	–	–	–	–
House 7	Fan	$p^S_{20,74,47}$	–	–	–	–	30.00	30.00	–	–	–	–	–
	Light	$p^S_{20,74,48}$	–	–	–	–	–	–	–	20.00	–	–	–
	Phone	$p^S_{20,74,49}$	–	–	–	–	–	–	–	–	–	–	–
	Light	$p^S_{48,21,50}$	–	–	–	–	–	–	–	–	–	–	–
	Radio	$p^S_{48,21,51}$	–	–	–	–	–	–	–	–	–	–	–
House 8	Fan	$p^S_{48,21,52}$	–	–	30.00	30.00	30.00	27.51	–	–	–	–	–
	Light	$p^S_{21,75,53}$	–	–	–	–	–	–	–	20.00	–	–	–
	Phone	$p^S_{21,75,54}$	–	–	–	–	–	–	–	–	–	–	–
	Light	$p^S_{50,23,55}$	–	–	–	–	–	–	–	–	–	–	–
	Fridge	$p^S_{50,23,56}$	600.00	600.00	600.00	600.00	600.00	600.00	600.00	600.00	600.00	600.00	600.00
Health	Pump	$p^S_{23,77,57}$	–	470.48	552.34	758.50	–	–	–	–	–	–	–
	Light	$p^S_{23,77,58}$	–	–	–	–	–	–	–	–	–	–	–
	PV	$p^S_{50,23,59}$	-221.75	–	–	–	-191.00	-139.50	-80.50	-27.00	-0.75	–	–
	Light	$p^S_{51,24,60}$	–	–	–	–	–	–	–	–	–	–	–
	Radio	$p^S_{24,78,61}$	–	–	–	–	–	–	–	–	–	–	–
House 9	Fan	$p^S_{24,78,62}$	–	–	–	–	30.00	30.00				–	–
	Light	$p^S_{24,78,63}$	–	–	–	–				20.00		–	–
	Phone	$p^S_{24,78,64}$	–	–	–	–	–	–	–	–	–	–	–
	Light	$p^S_{53,26,65}$	–	–	–	–	–	–	–	–	–	–	–
	Radio	$p^S_{53,26,66}$	–	–	–	–	–	–	–	–	–	–	–
House 10	Fan	$p^S_{53,26,67}$	–		30.00	30.00	6.85	–	–	–	–	–	–
	Light	$p^S_{53,26,68}$	–	–	–	–	–	–	–	–	–	–	–
	Phone	$p^S_{26,80,69}$	–	–	–	–	–	–	–	–	–	–	–

Table D.12: Case Study 1: Economic dispatch for a bipolar DC microgrid without optimal storage for sources $s35$-$s69$ from $k11$-$k21$.

Location	Load	Sources	$p^{S}_{m,n,s,k}$										
			k22	k23	k24	k25	k26	k27	k28	k29	k30	k31	k32
PV Plant	PV Panel	$p^{S}_{44,71,0}$	–	–	–	–	–	–	–	–	–	-750.00	-1082.57
	ESS	$p^{S}_{44,71,1}$	-1084.51	-1084.51	-1084.51	-1084.51	-1084.51	-1084.51	-1084.51	-1084.51	-1084.51	-324.06	–
	Generator	$p^{S}_{44,71,2}$	–	–	–	–	–	–	–	–	–	–	–
Agriculture	Irr. Pump	$p^{S}_{27,54,3}$	–	–	–	–	–	–	–	–	–	–	–
	Pump	$p^{S}_{27,54,4}$	–	–	–	–	–	–	–	–	–	–	–
	Diesel	$p^{S}_{27,54,5}$	-120.31	-120.31	-120.31	-120.31	-120.31	-120.31	-120.31	-120.31	-120.31	-105.64	–
House 1	Light	$p^{S}_{29,2,6}$	–	–	–	–	–	–	–	–	–	–	–
	Radio	$p^{S}_{29,2,7}$	–	–	–	–	–	–	–	–	–	–	–
	Fan	$p^{S}_{2,56,8}$	–	–	–	–	–	–	–	–	–	–	–
	Light	$p^{S}_{2,56,9}$	–	–	–	–	–	–	–	–	–	–	–
	Phone	$p^{S}_{2,56,10}$	–	–	–	–	–	–	–	–	–	–	–
House 2	Light	$p^{S}_{31,4,11}$	–	–	–	–	–	–	–	–	–	–	–
	Radio	$p^{S}_{31,4,12}$	–	–	–	–	–	–	–	–	–	–	–
	Fan	$p^{S}_{31,4,13}$	–	–	–	–	–	–	–	–	–	–	–
	Light	$p^{S}_{4,58,14}$	–	–	–	–	–	–	–	–	–	–	–
	Phone	$p^{S}_{4,58,15}$	–	–	–	–	–	–	–	–	–	–	–
House 3	Light	$p^{S}_{7,61,16}$	–	–	–	–	–	–	–	–	–	–	–
	Radio	$p^{S}_{7,61,17}$	–	–	–	–	–	–	–	–	–	–	–
	Fan	$p^{S}_{7,61,18}$	–	–	–	–	–	–	–	–	–	–	–
	Light	$p^{S}_{34,7,19}$	–	–	–	–	–	–	–	–	–	–	–
	Phone	$p^{S}_{34,7,20}$	–	–	–	–	–	–	–	–	–	–	–
Shop	Light	$p^{S}_{37,10,21}$	–	–	–	–	–	–	–	–	–	–	–
	Fan	$p^{S}_{37,10,22}$	–	–	–	–	–	–	–	–	–	–	–
	Fridge	$p^{S}_{10,64,23}$	600.00	600.00	600.00	600.00	600.00	600.00	600.00	600.00	600.00	600.00	600.00
	Light	$p^{S}_{37,10,24}$	–	–	–	–	–	–	–	–	–	–	–
School	Comp	$p^{S}_{38,11,25}$	–	–	–	–	–	–	–	–	–	–	–
	Fan	$p^{S}_{38,11,26}$	–	–	–	–	–	–	–	–	–	–	–
	Light	$p^{S}_{11,65,27}$	–	–	–	–	–	–	–	–	–	–	–
	Fan	$p^{S}_{11,65,28}$	–	–	–	–	–	–	–	–	–	–	–
	PV	$p^{S}_{11,65,29}$	–	–	–	–	–	–	–	–	–	-12.50	-61.00
Hoouse 4	Light	$p^{S}_{40,13,30}$	–	–	–	–	–	–	–	–	–	–	–
	Radio	$p^{S}_{40,13,31}$	–	–	–	–	–	–	–	–	–	–	–
	Fan	$p^{S}_{13,67,32}$	–	–	–	–	–	–	–	–	–	–	–
	Light	$p^{S}_{13,67,33}$	–	–	–	–	–	–	–	–	–	–	–
	Phone	$p^{S}_{13,67,34}$	–	–	–	–	–	–	–	–	–	–	–

Table D.13: Case Study 1: Economic dispatch for a bipolar DC microgrid without optimal storage for sources $s0$-$s34$ from $k22$-$k32$.

Location	Load	Sources	$p^S_{m,n,s,k}$										
			k22	k23	k24	k25	k26	k27	k28	k29	k30	k31	k32
House 5	Light	$p^S_{41,14,35}$	–	–	–	–	–	–	–	–	–	–	–
	Radio	$p^S_{41,14,36}$	–	–	–	–	–	–	–	–	–	–	–
	Fan	$p^S_{14,68,37}$	–	–	–	–	–	–	–	–	–	–	–
	Light	$p^S_{14,68,38}$	–	–	–	–	–	–	–	–	–	–	–
	Phone	$p^S_{14,68,39}$	–	–	–	–	–	–	–	–	–	–	–
House 6	Light	$p^S_{46,19,40}$	–	–	–	–	–	–	–	–	–	–	–
	Radio	$p^S_{46,19,41}$	–	–	–	–	–	–	–	–	–	–	–
	Fan	$p^S_{46,19,42}$	–	–	–	–	–	–	–	–	–	–	–
	Light	$p^S_{46,19,43}$	–	–	–	–	–	–	–	–	–	–	–
	Phone	$p^S_{19,73,44}$	–	–	–	–	–	–	–	–	–	–	–
House 7	Light	$p^S_{47,20,45}$	–	–	–	–	–	–	–	–	–	–	–
	Radio	$p^S_{47,20,46}$	–	–	–	–	–	–	–	–	–	–	–
	Fan	$p^S_{20,74,47}$	–	–	–	–	–	–	–	–	–	–	–
	Light	$p^S_{20,74,48}$	–	–	–	–	–	–	–	–	–	–	–
	Phone	$p^S_{20,74,49}$	–	–	–	–	–	–	–	–	–	–	–
House 8	Light	$p^S_{48,21,50}$	–	–	–	–	–	–	–	–	–	–	–
	Radio	$p^S_{48,21,51}$	–	–	–	–	–	–	–	–	–	–	–
	Fan	$p^S_{48,21,52}$	–	–	–	–	–	–	–	–	–	–	–
	Light	$p^S_{21,75,53}$	–	–	–	–	–	–	–	–	–	–	–
	Phone	$p^S_{21,75,54}$	–	–	–	–	–	–	–	–	–	–	–
Health	Light	$p^S_{50,23,55}$	–	–	–	–	–	–	–	–	–	–	–
	Fridge	$p^S_{50,23,56}$	600.00	600.00	600.00	600.00	600.00	600.00	600.00	600.00	600.00	600.00	600.00
	Pump	$p^S_{23,77,57}$		–	–	–	–	–	–	–	–	–	–
	Light	$p^S_{23,77,58}$		–	–	–	–	–	–	–	–	–	–
	PV Panel	$p^S_{50,23,59}$	–	–	–	–	–	–	–	–	–	-12.50	-61.00
House 9	Light	$p^S_{51,24,60}$	–	–	–	–	–	–	–	–	–	–	–
	Radio	$p^S_{24,78,61}$	–	–	–	–	–	–	–	–	–	–	–
	Fan	$p^S_{24,78,62}$	–	–	–	–	–	–	–	–	–	–	–
	Light	$p^S_{24,78,63}$	–	–	–	–	–	–	–	–	–	–	–
	Phone	$p^S_{24,78,64}$	–	–	–	–	–	–	–	–	–	–	–
House 10	Light	$p^S_{53,26,65}$	–	–	–	–	–	–	–	–	–	–	–
	Radio	$p^S_{53,26,66}$	–	–	–	–	–	–	–	–	–	–	–
	Fan	$p^S_{53,26,67}$	–	–	–	–	–	–	–	–	–	–	–
	Light	$p^S_{53,26,68}$	–	–	–	–	–	–	–	–	–	–	–
	Phone	$p^S_{26,80,69}$	–	–	–	–	–	–	–	–	–	–	–

Table D.14: Case Study 1: Economic dispatch for a bipolar DC microgrid without optimal storage for sources $s35$-$s69$ from $k22$-$k32$.

Location	Load	Sources	$p^S_{m,n,s,k}$										
			k33	k34	k35	k36	k37	k38	k39	k40	k41	k42	k43
PV Plant	PV Panel	$p^S_{44,71,0}$	-965.78	-10605.00	-4126.99	-7200.00	-1107.53	-11641.99	-1699.01	-1699.03	-1318.12	-1605.15	-45.00
	ESS	$p^S_{44,71,1}$	–	3405.00	-3073.01	–	26.32	9985.74	26.32	26.32	-3.23	-87.85	-1689.85
	Generator	$p^S_{44,71,2}$	–	–	–	–	–	–	–	–	–	–	–
Agriculture	Irr. Pump	$p^S_{27,54,3}$	–	8000.00	2230.94	2292.99	–	–	–	–	–	–	–
	Pump	$p^S_{27,54,4}$	–	2142.95	8000.00	8000.00	–	–	–	–	–	–	–
	Diesel	$p^S_{27,54,5}$	–	-4000.00	-4000.00	-4000.00	–	–	–	–	–	–	–
House 1	Light	$p^S_{29,2,6}$	–	–	–	–	–	–	–	–	–	20.00	20.00
	Radio	$p^S_{29,2,7}$	–	–	–	–	–	–	–	–	–	–	10.00
	Fan	$p^S_{2,56,8}$	–	–	–	–	30.00	30.00	30.00	30.00	–	–	–
	Light	$p^S_{2,56,9}$	–	–	–	–	–	–	–	–	–	20.00	20.00
	Phone	$p^S_{2,56,10}$	–	–	–	–	–	–	–	–	–	–	–
House 2	Light	$p^S_{31,4,11}$	–	–	–	–	–	–	–	–	–	20.00	20.00
	Radio	$p^S_{31,4,12}$	–	–	–	–	–	–	–	–	–	–	–
	Fan	$p^S_{31,4,13}$	–	–	–	–	30.00	30.00	30.00	30.00	–	–	–
	Light	$p^S_{4,58,14}$	–	–	–	–	–	–	–	–	–	20.00	20.00
	Phone	$p^S_{4,58,15}$	–	–	–	–	–	–	–	–	–	–	–
House 3	Light	$p^S_{7,61,16}$	–	–	–	–	–	–	–	–	–	20.00	20.00
	Radio	$p^S_{7,61,17}$	–	–	–	–	–	–	–	–	–	–	10.00
	Fan	$p^S_{7,61,18}$	–	–	–	–	30.00	30.00	30.00	30.00	–	–	–
	Light	$p^S_{34,7,19}$	–	–	–	–	–	–	–	–	–	20.00	20.00
	Phone	$p^S_{34,7,20}$	–	–	–	–	–	–	–	–	–		
Shop	Light	$p^S_{37,10,21}$	–	–	–	–	–	–	–	–	–	20.00	20.00
	Fan	$p^S_{37,10,22}$	–	–	–	–	30.00	30.00	30.00	2.47		30.00	
	Fridge	$p^S_{10,64,23}$	600.00	599.35	599.27	599.22	600.00	600.00	600.00	600.00	600.00	600.00	600.00
	Light	$p^S_{37,10,24}$	–	–	–	–	–	–	–	–	–	20.00	20.00
School	Comp	$p^S_{38,11,25}$	–	–	–	–		300.00	300.00	300.00	155.25	–	–
	Fan	$p^S_{38,11,26}$	–	–	–	–	30.00	30.00	21.54	–	–	–	–
	Light	$p^S_{11,65,27}$	–	–	–	–	–	–	–	–	40.00	40.00	40.00
	Fan	$p^S_{11,65,28}$	–	–	–	–	30.00	30.00	30.00	30.00	–	–	–
	PV Panel	$p^S_{11,65,29}$	-119.00	-176.75	-221.75	-253.50	-257.50	-7.95	–	–	–	–	–
House 4	Light	$p^S_{40,13,30}$	–	–	–	–	–	–	–	–	–	20.00	20.00
	Radio	$p^S_{40,13,31}$	–	–	–	–	–	–	–	–	–	–	5.11
	Fan	$p^S_{13,67,32}$	–	–	–	–	30.00	30.00	30.00	30.00	–	–	–
	Light	$p^S_{13,67,33}$	–	–	–	–	–	–	–	–	–	20.00	20.00
	Phone	$p^S_{13,67,34}$	–	–	–	–	–	–	–	–	–		

Table D.15: Case Study 1: Economic dispatch for a bipolar DC microgrid without optimal storage for sources $s0$-$s34$ from $k33$-$k43$.

Location	Load	Sources	$p^S_{m,n,s,k}$										
			k33	k34	k35	k36	k37	k38	k39	k40	k41	k42	k43
House 5	Light	$p^S_{41,14,35}$	–	–	–	–	–	–	–	–	–	20.00	20.00
	Radio	$p^S_{41,14,36}$	–	–	–	–	–	–	–	–	–	–	10.00
	Fan	$p^S_{14,68,37}$	–	–	–	–	30.00	30.00	30.00	30.00	–	–	–
	Light	$p^S_{14,68,38}$	–	–	–	–	–	–	–	–	–	20.00	20.00
	Phone	$p^S_{14,68,39}$	–	–	–	–	–	–	–	–	–	–	–
House 6	Light	$p^S_{46,19,40}$	–	–	–	–	–	–	–	–	–	20.00	20.00
	Radio	$p^S_{46,19,41}$	–	–	–	–	–	–	–	–	–	–	–
	Fan	$p^S_{46,19,42}$	–	–	–	–	30.00	30.00	30.00	30.00	–	–	–
	Light	$p^S_{46,19,43}$	–	–	–	–	–	–	–	–	–	20.00	20.00
	Phone	$p^S_{19,73,44}$	–	–	–	–	–	–	–	–	–	–	–
House 7	Light	$p^S_{47,20,45}$	–	–	–	–	–	–	–	–	–	20.00	20.00
	Radio	$p^S_{47,20,46}$	–	–	–	–	–	–	–	–	–	–	–
	Fan	$p^S_{20,74,47}$	–	–	–	–	30.00	30.00	30.00	30.00	–	–	–
	Light	$p^S_{20,74,48}$	–	–	–	–	–	–	–	–	–	20.00	20.00
	Phone	$p^S_{20,74,49}$	–	–	–	–	–	–	–	–	–	–	–
House 8	Light	$p^S_{48,21,50}$	–	–	–	–	–	–	–	–	–	20.00	20.00
	Radio	$p^S_{48,21,51}$	–	–	–	–	–	–	–	–	–	–	–
	Fan	$p^S_{48,21,52}$	–	–	–	–	30.00	30.00	30.00	30.00	–	–	–
	Light	$p^S_{21,75,53}$	–	–	–	–	–	–	–	–	–	20.00	20.00
	Phone	$p^S_{21,75,54}$	–	–	–	–	–	–	–	–	–	–	–
Health	Light	$p^S_{50,23,55}$	–	–	–	–	–	–	–	–	–	–	–
	Fridge	$p^S_{50,23,56}$	600.00	600.00	600.00	600.00	600.00	600.00	600.00	600.00	600.00	600.00	600.00
	Pump	$p^S_{23,77,57}$	–	–	–	–	–	–	–	–	–	–	–
	Light	$p^S_{23,77,58}$	–	–	–	–	–	–	–	–	–	–	–
	PV Panel	$p^S_{50,23,59}$	-119.00	-176.75	-221.75	-253.50	-255.78	-235.25	-191.00	-139.50	-80.50	-27.00	-0.75
House 9	Light	$p^S_{51,24,60}$	–	–	–	–	–	–	–	–	–	20.00	20.00
	Radio	$p^S_{24,78,61}$	–	–	–	–	–	–	–	–	–	–	10.00
	Fan	$p^S_{24,78,62}$	–	–	–	–	30.00	30.00	30.00	30.00	–	–	–
	Light	$p^S_{24,78,63}$	–	–	–	–	–	–	–	–	–	20.00	20.00
	Phone	$p^S_{24,78,64}$	–	–	–	–	–	–	–	–	–	–	–
House 10	Light	$p^S_{53,26,65}$	–	–	–	–	–	–	–	–	–	20.00	20.00
	Radio	$p^S_{53,26,66}$	–	–	–	–	–	–	–	–	–	–	–
	Fan	$p^S_{53,26,67}$	–	–	–	–	30.00	30.00	2.49	–	–	–	–
	Light	$p^S_{53,26,68}$	–	–	–	–				–		20.00	20.00
	Phone	$p^S_{26,80,69}$	–	–	–	–	–	–	–	–	–	–	–

Table D.16: Case Study 1: Economic dispatch for a bipolar DC microgrid without optimal storage for sources $s35$-$s69$ from $k33$-$k43$.

Location	Load	Sources	$p^S_{m,n,s,k}$				
			k44	k45	k46	k47	k48
PV Plant	PV Panel	$p^S_{44,71,0}$	–	–	–	–	–
	ESS	$p^S_{44,71,1}$	-1922.19	-1869.31	-1780.56	-1730.41	-1206.13
	Generator	$p^S_{44,71,2}$	–	–	–	–	–
Agriculture	Irr. Pump	$p^S_{27,54,3}$	–	–	–	–	–
	Pump	$p^S_{27,54,4}$	–	–	–	–	–
	Diesel	$p^S_{27,54,5}$	–	–	–	–	–
House 1	Light	$p^S_{29,2,6}$	20.00	20.00	20.00	20.00	–
	Radio	$p^S_{29,2,7}$	10.00	10.00	–	–	–
	Fan	$p^S_{2,56,8}$	–	–	–	–	–
	Light	$p^S_{2,56,9}$	20.00	20.00	20.00	20.00	–
	Phone	$p^S_{2,56,10}$	5.00	5.00	5.00	–	–
House 2	Light	$p^S_{31,4,11}$	20.00	20.00	20.00	20.00	–
	Radio	$p^S_{31,4,12}$	10.00	10.00	–	–	–
	Fan	$p^S_{31,4,13}$	–	–	–	–	–
	Light	$p^S_{4,58,14}$	20.00	20.00	20.00	20.00	–
	Phone	$p^S_{4,58,15}$	5.00	5.00	5.00	–	–
House 3	Light	$p^S_{7,61,16}$	20.00	20.00	20.00	20.00	–
	Radio	$p^S_{7,61,17}$	10.00	10.00	–	–	–
	Fan	$p^S_{7,61,18}$	–	–	–	–	–
	Light	$p^S_{34,7,19}$	20.00	20.00	20.00	20.00	–
	Phone	$p^S_{34,7,20}$	5.00	5.00	5.00	–	–
Shop	Light	$p^S_{37,10,21}$	20.00	20.00	20.00	20.00	–
	Fan	$p^S_{37,10,22}$	–	–	–	–	–
	Fridge	$p^S_{10,64,23}$	600.00	600.00	600.00	600.00	600.00
	Light	$p^S_{37,10,24}$	20.00	20.00	20.00	20.00	–
School	Comp	$p^S_{38,11,25}$	–	–	–	–	–
	Fan	$p^S_{38,11,26}$	–	–	–	–	–
	Light	$p^S_{11,65,27}$	40.00	–	–	–	–
	Fan	$p^S_{11,65,28}$	–	–	–	–	–
	PV Panel	$p^S_{11,65,29}$	–	–	–	–	–
House 4	Light	$p^S_{40,13,30}$	20.00	20.00	20.00	20.00	–
	Radio	$p^S_{40,13,31}$	10.00	10.00	–	–	–
	Fan	$p^S_{13,67,32}$	–	–	–	–	–
	Light	$p^S_{13,67,33}$	20.00	20.00	20.00	20.00	–
	Phone	$p^S_{13,67,34}$	5.00	5.00	5.00	–	–

Table D.17: Case Study 1: Economic dispatch for a bipolar DC microgrid without optimal storage for sources $s0$-$s34$ from $k44$-$k48$.

Location	Load	Sources	$p^{S}_{m,n,s,k}$				
			k44	k45	k46	k47	k48
House 5	Light	$p^{S}_{41,14,35}$	20.00	20.00	20.00	20.00	–
	Radio	$p^{S}_{41,14,36}$	10.00	10.00	–	–	–
	Fan	$p^{S}_{14,68,37}$	–	–	–	–	–
	Light	$p^{S}_{14,68,38}$	20.00	20.00	20.00	20.00	–
	Phone	$p^{S}_{14,68,39}$	5.00	5.00	5.00	–	–
House 6	Light	$p^{S}_{46,19,40}$	20.00	20.00	20.00	20.00	–
	Radio	$p^{S}_{46,19,41}$	10.00	10.00	–	–	–
	Fan	$p^{S}_{46,19,42}$	–	–	–	–	–
	Light	$p^{S}_{46,19,43}$	20.00	20.00	20.00	20.00	–
	Phone	$p^{S}_{19,73,44}$	5.00	5.00	5.00		–
House 7	Light	$p^{S}_{47,20,45}$	20.00	20.00	20.00	20.00	–
	Radio	$p^{S}_{47,20,46}$	10.00	10.00	–	–	–
	Fan	$p^{S}_{20,74,47}$	–	–	–	–	–
	Light	$p^{S}_{20,74,48}$	20.00	20.00	20.00	20.00	–
	Phone	$p^{S}_{20,74,49}$	5.00	5.00	5.00		–
House 8	Light	$p^{S}_{48,21,50}$	20.00	20.00	20.00	20.00	–
	Radio	$p^{S}_{48,21,51}$	10.00	7.38	–	–	–
	Fan	$p^{S}_{48,21,52}$	–	–	–	–	–
	Light	$p^{S}_{21,75,53}$	20.00	20.00	20.00	20.00	–
	Phone	$p^{S}_{21,75,54}$	5.00	5.00	5.00		–
Health	Light	$p^{S}_{50,23,55}$	20.00	20.00	20.00	20.00	–
	Fridge	$p^{S}_{50,23,56}$	600.00	600.00	600.00	600.00	600.00
	Pump	$p^{S}_{23,77,57}$	–	–	–	–	–
	Light	$p^{S}_{23,77,58}$	60.00	60.00	60.00	60.00	–
	PV Panel	$p^{S}_{50,23,59}$	–	–	–	–	–
House 9	Light	$p^{S}_{51,24,60}$	20.00	20.00	20.00	20.00	–
	Radio	$p^{S}_{24,78,61}$	10.00	10.00	–	–	–
	Fan	$p^{S}_{24,78,62}$	–	–	–	–	–
	Light	$p^{S}_{24,78,63}$	20.00	20.00	20.00	20.00	–
	Phone	$p^{S}_{24,78,64}$	5.00	5.00	5.00		–
House 10	Light	$p^{S}_{53,26,65}$	20.00	20.00	20.00	20.00	–
	Radio	$p^{S}_{53,26,66}$	10.00	–	–	–	–
	Fan	$p^{S}_{53,26,67}$	–	–	–	–	–
	Light	$p^{S}_{53,26,68}$	20.00	20.00	20.00	20.00	–
	Phone	$p^{S}_{26,80,69}$	5.00	5.00	5.00	–	–

Table D.18: Case Study 1: Economic dispatch for a bipolar DC microgrid without optimal storage for sources $s35$-$s69$ from $k44$-$k48$.

Connection	Sources	LMP [$/Wh]		
		k34	k35	k36
$\mathcal{N}_+ / \mathcal{N}_-$	$\lambda^{\mathrm{P}}_{27,54}$	2.000	2.000	2.000
	$\lambda^{\mathrm{P}}_{44,71}$	0.000	0.000	0.000
$\mathcal{N}_+ / \mathcal{N}_N$	$\lambda^{\mathrm{P}}_{2,56}$	0.0071	0.0071	0.0071
	$\lambda^{\mathrm{P}}_{4,58}$	0.0027	0.0027	0.0027
	$\lambda^{\mathrm{P}}_{7,61}$	0.0002	0.0002	0.0002
	$\lambda^{\mathrm{P}}_{10,64}$	0.0006	0.0007	0.0007
	$\lambda^{\mathrm{P}}_{11,65}$	0.0000	0.0000	0.0000
	$\lambda^{\mathrm{P}}_{13,67}$	0.0021	0.0021	0.0021
	$\lambda^{\mathrm{P}}_{14,68}$	0.0010	0.0010	0.0010
	$\lambda^{\mathrm{P}}_{15,69}$	0.0019	0.0019	0.0019
	$\lambda^{\mathrm{P}}_{19,73}$	-0.0032	-0.0032	-0.0032
	$\lambda^{\mathrm{P}}_{20,74}$	-0.0015	-0.0015	-0.0015
	$\lambda^{\mathrm{P}}_{21,75}$	-0.0035	-0.0035	-0.0035
	$\lambda^{\mathrm{P}}_{23,77}$	-0.0011	-0.0011	-0.0011
	$\lambda^{\mathrm{P}}_{24,78}$	-0.0016	-0.0016	-0.0016
	$\lambda^{\mathrm{P}}_{26,80}$	-0.0007	-0.0007	-0.0007
$\mathcal{N}_N / \mathcal{N}_-$	$\lambda^{\mathrm{P}}_{29,2}$	-0.2167	-0.2167	-0.2167
	$\lambda^{\mathrm{P}}_{31,4}$	-0.0813	-0.0813	-0.0813
	$\lambda^{\mathrm{P}}_{34,7}$	-0.0200	-0.0200	-0.0200
	$\lambda^{\mathrm{P}}_{37,10}$	-0.0265	-0.0266	-0.0266
	$\lambda^{\mathrm{P}}_{38,11}$	0.0117	0.0117	0.0117
	$\lambda^{\mathrm{P}}_{40,13}$	-0.0430	-0.0430	-0.0430
	$\lambda^{\mathrm{P}}_{41,14}$	0.1031	0.1031	0.1031
	$\lambda^{\mathrm{P}}_{42,15}$	0.1786	0.1786	0.1786
	$\lambda^{\mathrm{P}}_{46,19}$	0.0415	0.0415	0.0415
	$\lambda^{\mathrm{P}}_{47,20}$	0.0345	0.0345	0.0345
	$\lambda^{\mathrm{P}}_{48,21}$	0.0321	0.0321	0.0321
	$\lambda^{\mathrm{P}}_{50,23}$	0.0059	0.0059	0.0058
	$\lambda^{\mathrm{P}}_{51,24}$	0.0092	0.0092	0.0092
	$\lambda^{\mathrm{P}}_{53,26}$	-0.0038	-0.0038	-0.0038

Table D.19: Case Study 2: LMP from $k34$ to $k36$ with respect to sources' connection types for a DC microgrid without optimal placement and sizing of ESS.

E

SUPPLEMENTARY INFORMATION FOR CHAPTER 8, 9, 10

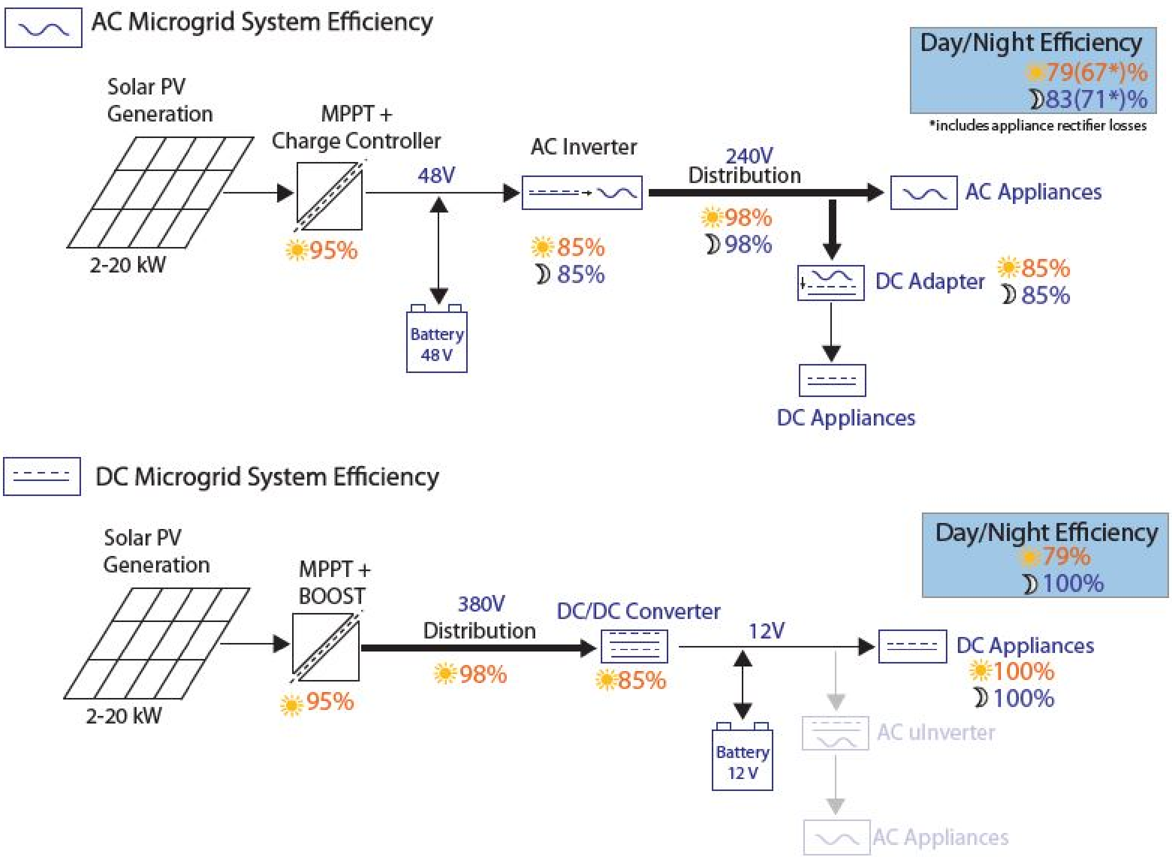

Figure E.1: Day and night efficienct comparison of AC and DC microgrids.

Strategic Impact	Characteristics	Time of impact
Base	• Essential to be in the business • Widely exploited by competitors • Little strategic impact	Yesterday
Key	• Well embodied in products and processes • High strategic impact	Today
Pacing	• Under experimentation by some competitors • Strategic impact likely to be high	Tomorrow
Emerging	• At earlier research stage, or emerging in other industries • Strategic impact unknown, but promising	Future (?)

Figure E.2: Definitions of the attributes defining the strategic impact of the a technology.

Competitive position	Characteristics
Clear leader	Sets the pace and direction of technological development and recognised for such in the industry
Strong	Able to express independent technical actions and set new directions
Favourable	Able to sustain technological competitiveness in general and/or leadership in technical niches
Tenable	Unable to set independent course; continually in catch-up mode
Weak	Unable to sustain quality of technical outputs versus competitors; short-term fire-fighting focus

Figure E.3: Definitions of the attrinutes defining the competitive position of a technology.

Bibliography

[9] T. Dragicevic, J. Vasquez, J. Guerrero, and D. Škrlec, *Advanced LVDC Electrical Power Architectures and Microgrids,* IEEE Electrification Magazine **2**, 54 (2014).

[10] A. T. Elsayed, A. A. Mohamed, and O. A. Mohammed, *DC microgrids and distribution systems: An overview,* Electric Power Systems Research **119**, 407 (2015).

[11] M. Guarnieri, *The Alternating Evolution of DC Power Transmission,* IEEE Industrial Electronics Magazine , 60 (2013).

[12] D. M. Larruskain, I. Zamora, a. J. Mazón, O. Abarrategui, and J. Monasterio, *Transmission and Distribution Networks : AC versus DC,* IEEE Power Engineering Society General Meeting , 1 (2007).

[13] L. Mackay, T. Hailu, G. R. Chandra Mouli, L. Ramırez-Elizondo, J. Ferreira, and P. Bauer, *From DC Nano- and Microgrids Towards the Universal DC Distribution System – A Plea to Think Further Into the Future,* 2015 IEEE Power & Energy Society General Meeting , 1 (2015).

[14] E. Rodriguez-Diaz, J. C. Vasquez, and J. M. Guerrero, *Intelligent DC Homes in Future Sustainable Energy Systems: When efficiency and intelligence work together,* IEEE Consumer Electronics Magazine **5**, 74 (2016).

[1] E. Rodriguez, M. Savaghebi, J. Vasquez, M. Josep, E. Rodriguez-diaz, and J. Guerrero, *An Overview of Low Voltage DC Distribution Systems for Residential Applications,* in *Proceedings of the 5th IEEE International Conference on Consumer Electronics, Berlin 2015* (2015).

[15] B. Fortenbery, *DC Power for Improved Data Center Efficiency,* Power (2007).

[16] K. Techakittiroj and V. Wongpaibool, *Co-existance between AC-distribution and DC-distribution: In the view of appliances,* 2009 International Conference on Computer and Electrical Engineering, ICCEE 2009 **1**, 421 (2009).

[17] G. Makarabbi, V. Gavade, R. Panguloori, and P. Mishra, *Compatibility and performance study of home appliances in a DC home distribution system,* 2014 IEEE International Conference on Power Electronics, Drives and Energy Systems, PEDES 2014 (2014), 10.1109/PEDES.2014.7042151.

[18] L. Mackay, L. Ramırez-Elizondo, and P. Bauer, *DC ready devices - Is redimensioning of the rectification components necessary?* Proceedings of the 16th International Conference on Mechatronics, Mechatronika 2014 , 1 (2014).

[19] L. Mackay, T. Hailu, L. Ramirez-elizondo, and P. Bauer, *Towards a DC Distribution System – Opportunities and Challenges,* in *DC Microgrids (ICDCM), 2015 IEEE First International Conference on DC Microgrids* (2015) pp. 215–220.

[20] USB 3.0 Promoter Group, *Universal Serial Bus Type-C Cable and Connector Specification*, Tech. Rep. (USB 3.0 Promoter Group, 2014).

[21] J. J. Justo, F. Mwasilu, J. Lee, and J. W. Jung, *AC-microgrids versus DC-microgrids with distributed energy resources: A review,* Renewable and Sustainable Energy Reviews **24**, 387 (2013).

[22] M. Davoudi, V. Cecchi, and J. R. Aguero, *Investigating the ability of meshed distribution systems to increase penetration levels of Distributed Generation,* Conference Proceedings - IEEE SOUTHEASTCON (2014), 10.1109/SECON.2014.6950661.

[23] G. Celli, F. Pilo, G. Pisano, V. Allegranza, R. Cicoria, a. Iaria, E. J. Coster, J. M. a. Myrzik, W. L. Kling, J. Ren, M. Kezunovic, K. Guan, M. Choi, S. Lee, L. SeongIl, M. D. I. Clerico, F. Cazzato, and F. Marmeggi, *Modeling and simulation tools for teaching protective relaying design and application for the smart grid,* Transmission and Distribution Exposition Conference: 2008 IEEE PES Powering Toward the Future, PIMS 2008 , 1 (2012).

[24] J. R. Aguero, *Improving the efficiency of power distribution systems through technical and non- losses reduction,* IEEE PES Transmission and Distribution Conference and Exposition (T&D) , 1 (2012).

[25] M. C. Alvarez-Herault, N. Doye, C. Gandioli, N. Hadjsaid, and P. Tixador, *Meshed distribution network vs reinforcement to increase the distributed generation connection,* Sustainable Energy, Grids and Networks **1**, 20 (2015).

[26] A. Colmenar-Santos, C. Reino-Rio, D. Borge-Diez, and E. Collado-Fernández, *Distributed generation: A review of factors that can contribute most to achieve a scenario of DG units embedded in the new distribution networks,* Renewable and Sustainable Energy Reviews **59**, 1130 (2016).

[27] P. Järventausta, S. Repo, A. Rautiainen, and J. Partanen, *Smart grid power system control in distributed generation environment,* Annual Reviews in Control **34**, 277 (2010).

[28] B. Q. Fu, A. Hamidi, A. Nasiri, V. Bhavaraju, and S. B. Krstic, *The Role of Energy Storage in a Microgrid Concept,* IEEE Electrification Magazine , 21 (2014).

[29] D. J. Becker and B. J. Sonnenberg, *DC microgrids in buildings and data centers,* INTELEC, International Telecommunications Energy Conference (Proceedings) (2011), 10.1109/INTLEC.2011.6099725.

[2] G. Byeon, T. Yoon, S. Oh, and G. Jang, *Energy management strategy of the DC distribution system in buildings using the EV service model,* IEEE Transactions on Power Electronics **28**, 1544 (2013).

[30] P. Salonen, T. Kaipia, P. Nuutinen, P. Peltoniemi, and J. Partanen, *An LVDC Distribution System Concept,* NORPIE, Nordic Workshop on Power and Industrial Electroncis , 7 (2008).

[31] J. Lago and M. L. Heldwein, *Operation and control-oriented modeling of a power converter for current balancing and stability improvement of DC active distribution networks,* IEEE Transactions on Power Electronics **26**, 877 (2011).

[32] Y. Gu, W. Li, and X. He, *Analysis and Control of Bipolar LVDC Grid With DC Symmetrical Component Method,* IEEE Transactions on Power Systems **31**, 685 (2015).

[33] G. T. Heydt, B. H. Chowdhury, M. L. Crow, D. Haughton, B. D. Kiefer, F. Meng, and B. R. Sathyanarayana, *Pricing and control in the next generation power distribution system,* IEEE Transactions on Smart Grid **3**, 907 (2012).

[34] S. Borenstein, M. Jaske, and A. Rosenfeld, *Dynamic Pricing, Advanced Metering, and Demand Response in Electricity Markets,* Energy , 1 (2002).

[35] L. Mackay, A. Dimou, R. Guarnotta, G. Morales-espania, L. Ramirez-elizondo, and P. Bauer, *Optimal Power Flow in Bipolar DC Distribution Grids with Asymmetric Loading,* in *IEEE ENERGYCON 2016*, 3 (2016) p. 5.

[36] J. Carpentier, *Contribution à l'étude du dispatching économique,* Bulletin de la Société Française des Électriciens **3** (1962).

[37] M. Cain, R. O'Neill, and A. Castillo, *History of Optimal Power Flow and Formulations,* Federal Energy Regulatory Commission. . . . , 1 (2012).

[38] M. Bachtiar Nappu, A. Arief, and R. C. Bansal, *Transmission management for congested power system: A review of concepts, technical challenges and development of a new methodology,* Renewable and Sustainable Energy Reviews **38**, 572 (2014).

[39] H. Liu, L. Tesfatsion, and A. Chowdhury, *Locational marginal prices for restructured wholesale power markets,* Journal of Energy Markets , 1 (2009).

[40] R. E. Bohn, R. E. Bohn, M. C. Caramanis, M. C. Caramanis, F. C. Schweppe, and F. C. Schweppe, *Optimal pricing in electrical networks over space and time,* Rand Journal of Economics **15**, 360 (1984).

[41] T. J. Overbye, X. Cheng, and Y. Sun, *A comparison of the AC and DC power flow models for LMP calculations,* System Sciences, 2004. Proceedings of the 37th Annual Hawaii International Conference on **00**, 9 pp. (2004).

[42] T. Orfanogianni and G. Gross, *A general formulation for LMP evaluation,* IEEE Transactions on Power Systems **22**, 1163 (2007).

[43] F. C. Schweppe, M. C. Caramanis, R. D. Tabors, and R. E. Bohn, *Spot pricing of electricity*, kluwer aca ed. (The Kluwer International Series in Engineering and Computer Science, 2013).

[44] E. Litvinov, *Design and operation of the locational marginal prices-based electricity markets,* IET Generation, Transmission & Distribution **4**, 315 (2010).

[45] S. P. Holland and E. T. Mansur, *The Short-Run Effects of Time-Varying Prices in Competitive Electricity Markets The Short-Run Effects of Time-Varying Prices in Competitive Electricity Markets*, Tech. Rep. May (Center for the Study of Energy Markets, 2006).

[46] N. G. Singhal and K. W. Hedman, *An integrated transmission and distribution systems model with distribution-based LMP (DLMP) pricing,* 45th North American Power Symposium, NAPS 2013 (2013), 10.1109/NAPS.2013.6666935.

[47] R. Viral and D. K. Khatod, *Optimal planning of distributed generation systems in distribution system: A review,* Renewable and Sustainable Energy Reviews **16**, 5146 (2012).

[48] J. A. Momoh, Y. Xia, and G. D. Boswell, *An approach to determine Distributed Generation (DG) benefits in power networks,* 40th North American Power Symposium, NAPS2008 (2008), 10.1109/NAPS.2008.5307395.

[49] E. Ntakou and M. Caramanis, *Enhanced Convergence Rate of Inequality Constraint Shadow Prices in PMP Algorithm Cleared Distribution Power Markets,* in *2016 American Control Conference* (2016) pp. 1433–1439.

[50] H. Yuan, F. Li, Y. Wei, and J. Zhu, *Novel Linearized Power Flow and Linearized OPF Models for Active Distribution Networks with Application in Distribution LMP,* IEEE Transactions on Smart Grid **3053**, 1 (2016).

[51] M. Farivar and S. Low, *Branch Flow Model: Relaxations and Convexification-Part I,* IEEE Transactions on Power Systems **28**, 2554 (2013), arXiv:arXiv:1204.4865v2 .

[52] G. M. Lewis, *Estimating the value of wind energy using electricity locational marginal price,* Energy Policy **38**, 3221 (2010).

[53] P. Lamaina, D. Sarno, P. Siano, A. Zakariazadeh, and R. Romano, *A model for wind turbines placement within a distribution network acquisition market,* IEEE Transactions on Industrial Informatics **11**, 210 (2015).

[54] D. Gautam and M. Nadarajah, *Influence of distributed generation on congestion and LMP in competitive electricity market,* World Academy of Science, Engineering and Technology **39**, 822 (2009).

[55] N. Kumar, P. Dutta, and L. Xie, *Optimal DG placement for congestion mitigation and social welfare maximization,* NAPS 2011 - 43rd North American Power Symposium (2011), 10.1109/NAPS.2011.6024841.

[56] B. H. Chowdhury and F. Meng, *Economics of grid-tied customer-owned photovoltaic power generation,* IEEE Power and Energy Society General Meeting , 1 (2012).

[57] R. Arghandeh and R. Broadwater, *Distributed energy storage control for optimal adoption of solar energy in residential networks,* International Conference on Nuclear Engineering, Proceedings, ICONE **5**, 489 (2012).

[58] B. R. Sathyanarayana and G. T. Heydt, *Sensitivity-based pricing and optimal storage utilization in distribution systems,* IEEE Transactions on Power Delivery **28**, 1073 (2013).

[59] S. Weckx, R. D'hulst, and J. Driesen, *Locational pricing to mitigate voltage problems caused by high PV penetration,* Energies **8**, 4607 (2015).

[60] A. Castillo and D. F. Gayme, *Profit maximizing storage allocation in power grids,* Proceedings of the IEEE Conference on Decision and Control , 429 (2013).

[61] R. Li, Q. Wu, and S. S. Oren, *Distribution locational marginal pricing for optimal electric vehicle charging management,* IEEE Transactions on Power Systems **29**, 203 (2014).

[62] R. Srinivasa Rao, S. V. L. Narasimham, M. Ramalinga Raju, and A. Srinivasa Rao, *Optimal network reconfiguration of large-scale distribution system using harmony search algorithm,* IEEE Transactions on Power Systems **26**, 1080 (2011).

[63] J. Sun and L. Tesfatsion, *DC Optimal Power Flow Formulation and Solution Using QuadProgJ,* ISU Economics Working Paper No. 06014 , 1 (2010).

[64] J. A. Momoh, Y. Xia, and G. D. Boswell, *Locational marginal pricing for real and reactive power,* IEEE Power and Energy Society 2008 General Meeting: Conversion and Delivery of Electrical Energy in the 21st Century, PES (2008), 10.1109/PES.2008.4596865.

[65] S. Lee, W. Kim, and B. H. Kim, *Performance Comparison of Optimal Power Flow Algorithms for LMP Calculations of the Full Scale Korean Power System,* Journal of Electrical Engineering and Technology **10**, 109 (2015).

[66] A. Castillo, P. Lipka, J.-P. Watson, S. S. Oren, and R. P. O'Neill, *A Successive Linear Programming Approach to solving the IV-ACOPF,* IEEE Transactions on Power Systems , 1 (2015).

[67] J. Lavaei, S. Member, and S. H. Low, *Zero Duality Gap in Optimal Power Flow Problem,* IEEE Transactions on Power Systems **27**, 92 (2012).

[68] J. A. Momoh, *Electric Power System Applications of Optimization*, 2nd ed. (CRC Press, 2013) arXiv:arXiv:1011.1669v3 .

[69] C. Chen, S. Member, A. Atamtürk, and S. S. Oren, *Bound Tightening for the Alternating Current Optimal Power Flow Problem,* IEEE Transactions on Power Electronics , 1 (2015).

[70] H. Zhang and V. Vittal, *A Relaxed AC Optimal Power Flow Model Based on a Taylor Series,* Innovative Smart Grid Technologies - Asia (ISGT Asia), IEEE , 5 (2013).

[71] D. K. Molzahn, S. Member, J. T. Holzer, B. C. Lesieutre, S. Member, and C. L. Demarco, *Implementation of a Large-Scale Optimal Power Flow Solver Based on Semide fi nite Programming,* IEEE Transactions on Power Systems **28**, 3987 (2013).

[72] D. Kirschen and G. Strbac, *The Electrical Engineering Handbook* (Wiley, 2005) pp. 787–803.

[73] A. Wood, B. Wollenberg, and G. Shebleeacute, *Power Generation, Operation and Control*, 3rd ed. (Wiley, 2013) p. 656.

[74] K. Purchala, L. Meeus, D. Van Dommelen, and R. Belmans, *Usefulness of DC Power Flow for Active Power Flow Analysis,* Power Engineering Society General Meeting , 454 (2005).

[75] F. Li and R. Bo, *DCOPF-based LMP simulation: Algorithm, comparison with ACOPF, and sensitivity,* IEEE Transactions on Power Systems **22**, 1475 (2007).

[76] V. N. Bharatwaj, A. R. Abhyankar, and P. R. Bijwe, *Iterative DCOPF model using distributed slack bus,* in *Power and Energy Society General Meeting* (2012) pp. 1–7.

[77] P. A. Ruiz, J. M. Foster, A. Rudkevich, and M. C. Caramanis, *On fast transmission topology control heuristics,* IEEE Power and Energy Society General Meeting , 1 (2011).

[78] P. L. Joskow and J. Tirole, *Transmission Rights and Market Power on Electric Power Networks I : Financial Rights,* CEPR Discussion Papers , 1 (1998).

[79] California-ISO, *Shift Factors : Methodology and Example Why are Shift Factors Important to the Allocation Process ?* (2005).

[80] M. Matcha and S. Kumari, *LMP Calculation wutg Distributed Loos using GA based DCOPF,* Journal of Electrical Systems **8**, 292 (2012).

[81] A. Abirami and T. R. Manikandan, *Analysis of Locational Marginal Pricing Approach for a Deregulated Electricity Market,* International Journal of Trend in Research and Development **3**, 26 (2016).

[82] F. Meng and B. H. Chowdhury, *Distribution LMP-based economic operation for future Smart Grid,* 2011 IEEE Power and Energy Conference at Illinois, PECI 2011 (2011), 10.1109/PECI.2011.5740485.

[83] F. Li, *Fully reference-independent LMP decomposition using reference-independent loss factors,* Electric Power Systems Research **81**, 1995 (2011).

[84] Y. F. Y. Fu and Z. L. Z. Li, *Different models and properties on LMP calculations,* 2006 IEEE Power Engineering Society General Meeting , 1 (2006).

[85] F. Meng, D. Haughton, B. Chowdhury, M. L. Crow, and G. T. Heydt, *Distributed generation and storage optimal control with state estimation,* IEEE Transactions on Smart Grid **4**, 2266 (2013).

[86] F. Li, R. Bo, and W. Zhang, *Comparison of different LMP calculations in power market simulation,* 2006 International Conference on Power System Technology, POWERCON2006 , 1 (2007).

[87] R. Wiget and G. Andersson, *Optimal power flow for combined AC and multi-terminal HVDC grids based on VSC converters,* IEEE Power and Energy Society General Meeting , 1 (2012).

[88] H. W. H. Wang and M. Redfern, *The advantages and disadvantages of using HVDC to interconnect AC networks,* Universities Power Engineering Conference (UPEC), 2010 45th International , 4 (2010).

[89] R. Wiget and G. Andersson, *DC optimal power flow including HVDC grids,* 2013 IEEE Electrical Power and Energy Conference, EPEC 2013 , 1 (2013).

[90] H. Ambriz-Pérez, E. Acha, and C. R. Fuerte-Esquivel, *High voltage direct current modelling in optimal power flows,* International Journal of Electrical Power and Energy Systems **30**, 157 (2008).

[91] W. Feng, S. Member, L. A. Tuan, L. B. Tjernberg, S. Member, A. Mannikoff, and A. Bergman, *A New Approach for Benefit Evaluation of Multiterminal VSC - HVDC Using A Proposed Mixed AC / DC Optimal Power Flow,* IEEE Transactions on Power Delivery **29**, 432 (2014).

[92] T. Saravanan, G. Saritha, and V. Srinivasan, *Optimal Power Flow Using Particle Swarm Optimization,* Middle-East Journal of Scientific ... **20**, 1554 (2014).

[93] R. Wiget, *Combined AC and Multi-Terminal HVDC Grids – Optimal Power Flow Formulations and Dynamic Control,* Ph.D. thesis, ETH Zurich (2015).

[94] J. A. Taylor, *Convex Optimization of Power Systems* (Cambridge University Press, 2015).

[95] L. Gan and S. H. Low, *Optimal Power Flow in Direct Current Networks,* IEEE Transactions on Power Systems **29**, 2892 (2014).

[96] R. Asad and A. Kazemi, *A novel distributed optimal power sharing method for radial dc microgrids with different distributed energy sources,* Energy **72**, 291 (2014).

[97] L. Mackay, M. Imhof, R. Wiget, and G. Andersson, *Voltage dependent pricing in DC distribution grids,* PowerTech (POWERTECH), 2013 IEEE Grenoble , 1 (2013).

[98] J. Beerten, S. Cole, and R. Belmans, *A sequential AC/DC power flow algorithm for networks containing multi-terminal VSC HVDC systems,* IEEE PES General Meeting, PES 2010 , 1 (2010).

[99] R. P. O'Neill, P. M. Sotkiewicz, B. F. Hobbs, M. H. Rothkopf, and W. R. Stewart, *Efficient market-clearing prices in markets with nonconvexities,* European Journal of Operational Research **164**, 269 (2005).

[100] T. Wu, M. Rothleder, Z. Alaywan, and A. D. Papalexopoulos, *Pricing Energy and Ancillary Services in Integrated Market Systems by an Optimal Power Flow,* IEEE Transactions on Power Systems **19**, 339 (2004).

[101] S. Stoft, *IEEE Power and Energy Magazine*, 1 (IEEE PRESS, 2003) arXiv:ISBN 0-471-15040-1 .

[102] F. Li, J. Pan, and H. Chao, *Marginal Loss Calculation in Competitive Electrical Energy Markets,* IEEE International Conference on Electric Utility Deregulation and Power Technologies , 205 (2004).

[103] J. Sustman, *The Hidden Cost of LMP: Marginal Losses | EnergyCentral.net,* (2003).

[104] *GAMS — The Solver Manuals,* (2016).

[105] S. Gill, I. Kockar, and G. W. Ault, *Dynamic Optimal Power Flow for Active Distribution Networks,* Power Systems, IEEE Transactions on **29**, 121 (2014).

[106] R. S. Balog, W. W. Weaver, and P. T. Krein, *The load as an energy asset in a distributed DC smartgrid architecture,* IEEE Transactions on Smart Grid **3**, 253 (2012).

[107] A. S. a. Awad, T. H. M. El-Fouly, and M. M. a. Salama, *Optimal Distributed Generation Allocation and Load Shedding for Improving Distribution System Reliability,* Electric Power Components and Systems **42**, 576 (2014).

[108] K. Singh, V. K. Yadav, N. P. Padhy, and J. Sharma, *Congestion management considering optimal placement of distributed generator in deregulated power system networks,* Electric Power Components and Systems **42**, 13 (2014).

[109] M. Nick, R. Cherkaoui, and M. Paolone, *Optimal siting and sizing of distributed energy storage systems via alternating direction method of multipliers,* International Journal of Electrical Power and Energy Systems **72**, 33 (2015).

[110] S. Ghosh, S. Ghoshal, and S. Ghosh, *Optimal sizing and placement of distributed generation in a network system,* International Journal of Electrical Power & Energy Systems **32**, 849 (2010).

[8] R. Sen and S. C. Bhattacharyya, *Off-grid electricity generation with renewable energy technologies inIndia: An application of HOMER,* Renewable Energy **62**, 388 (2014).

[111] G. Venkataramanan and C. Marnay, *A Larger Role for Microgrids,* IEEE Power & Energy Magazine , 78 (2008).

[112] *Rural Electrification with Solar Energy: Microgrids vs. Solar Home Systems,* (2012).

[113] P. A. Madduri, J. Poon, J. Rosa, M. Podolsky, E. Brewer, and S. Sanders, *A scalable DC microgrid architecture for rural electrification in emerging regions,* IEEE Applied Power Electronics Conference and Exposition (APEC) , 703 (2015).

[114] H. Kakigano, Y. Miura, and T. Ise, *Low-voltage bipolar-type dc microgrid for super high quality distribution,* IEEE Transactions on Power Electronics **25**, 3066 (2010).

[115] S. Xue, C. Chen, Y. Jin, Y. Li, B. Li, and Y. Wang, *Protection for DC distribution system with distributed generator,* Journal of Applied Mathematics **2014** (2014), 10.1155/2014/241070.

[116] S. Groh, D. Philipp, B. E. Lasch, H. Kirchhoff, D. Islam, M. R. Khan, S. Chowdhury, and D. M. Kammen, *The Battle of Edison and Westinghouse Revisited : Contrasting AC and DC microgrids for rural electrification Functionality of DC microgrids,* MES-BREG 2014: Innovating Energy Access for Remote Areas: Discovering Untapped Resources , 1 (2014).

[117] G. Byeon, T. Yoon, S. Oh, and G. Jang, *Energy Management Strategy of the DC Distribution System in Buildings Using the EV Service Model,* IEEE Transactions on Power Electronics **28**, 1544 (2013).

[7] N. J. Williams, P. Jaramillo, J. Taneja, and T. S. Ustun, *Enabling private sector investment in microgrid-based rural electrification in developing countries: A review*, Renewable and Sustainable Energy Reviews **52**, 1268 (2015).

[3] M. Franz, N. Peterschmidt, M. Rohrer, and B. Kondev, *Mini-Grid Policy Toolkit*, Tech. Rep. (European Uniion Energy Initiative Partnership Dialogue Facility, Eschborn, 2014).

[118] Powerhive, *A highly scalable, sustainable energy access solution*, Tech. Rep. (Powerhive, 2015).

[4] A. Burger, *20x Growth Forecast in Remote Microgrid and Nanogrid Market - Microgrid Media*, Microgrid Media (2014).

[119] Technavio, *Global remote microgrid market to reach close to US$ 6,000 million by 2019, says Technavio - Discover Market Opportunities | Technavio - Discover Market Opportunities,* (2015).

[5] I. Orlandi, N. Tyabji, J. Chase, M. Wilshire, and B. Vickers, *Off-grid solar market trends report 2016*, Tech. Rep. February (World Bank Group, 2016) arXiv:arXiv:1011.1669v3 .

[120] MicrogridMedia, *The Investment Case for Mini-Grids and Off-Grids in Africa - Microgrid Media,* (2014).

[121] A. Castellano, A. Kendall, M. Nikomarov, and T. Swemmer, *Brighter Africa*, McKinsey & Company Monthly Journal , 4 (2015).

[122] D. Barber, *Micrograds in Africa: Perspectives From WorldWatch Institute and Navigant Research - Microgrid Media,* (2014).

[123] O. Langniß, L. Energie, D. Lecoufle, F. Gmbh, and C. Kg, *Rural Electrification with Renewable Energies in East Africa Rural Electrification in with Renewable Energies in East Africa*, Tech. Rep. (Renewable Energy Cooperation Programme, 2014).

[124] B. J. van Ruijven, J. Schers, and D. P. van Vuuren, *Model-based scenarios for rural electrification in developing countries,* Energy **38**, 386 (2012).

[125] D. Palit, *Solar energy programs for rural electrification: Experiences and lessons from South Asia,* Energy for Sustainable Development **17**, 270 (2013).

[126] Debajit Palit, *Scaling up Micro-grids in India: Connecting the dots - Microgrid Media,* (2014).

[127] REN21, *REN21 Renewables*, Tech. Rep. 3 (REN21, 2015).

[128] S. Daniel and D. Lounsbury, *Microgrids for Rural Electrification : A critical review of best practices based on seven case studies Microgrids for Rural Electrification : A critical review of best practices*, Tech. Rep. (United Nations Foundation, 2014).

[129] B. K. Sovacool, *Expanding renewable energy access with pro-poor public private partnerships in the developing world,* Energy Strategy Reviews **1**, 181 (2013).

[130] C. M. Haanyika, *Rural electrification policy and institutional linkages,* Energy Policy **34**, 2977 (2006).

[131] E. E. Marandu and R. Luteganya, *Implications of tariff laws on private investment: Tanzanian power sector,* Energy for Sustainable Development **9**, 30 (2005).

[132] T. S. Schmidt, N. U. Blum, and R. Sryantoro Wakeling, *Attracting private investments into rural electrification - A case study on renewable energy based village grids in Indonesia,* Energy for Sustainable Development **17**, 581 (2013).

[133] A. Zvoleff, A. S. Kocaman, W. T. Huh, and V. Modi, *The impact of geography on energy infrastructure costs,* Energy Policy **37**, 4066 (2009).

[134] H. Ahlborg and L. Hammar, *Drivers and barriers to rural electrification in Tanzania and Mozambique - Grid extension, off-grid, and renewable energy technologies,* Renewable Energy **61**, 117 (2014).

[135] D. Palit and G. Sarangi, *The mini-grid experience from India*, Tech. Rep. (Global Network on Energy For Sustainability, 2013).

[136] S. C. Bhattacharyya and S. Asia, *Viability of off-grid electricity supply using rice husk : A case study from South Asia,* Biomass and Bioenergy **8**, 44 (2014).

[6] K. Kurz, *The ABC-Model Anchor customers as core clients for mini-grids in emerging economies*, Tech. Rep. March (Deutsche Gesellschaft fur International Zusammenarbeit, 2014).

[137] S. Malawi, *Incubating Innovation for Rural Electrification*, Tech. Rep. i (World Bank, 2013).

[138] ARE, *for Rural Electrification : Hybrid Mini-Grids for Rural Electrification :*, Tech. Rep. (Alliance for Rural Electrification, 2011).

[139] A. Rodríguez Gómez, *From Gap to Opportunity: The A-B-C Telecom Mini-grid Model for East Africa*, Ph.D. thesis, ME3 (2013).